

# IVSS Intersection accidents: Analysis and Prevention

Final Report – Volume 1 (main report)

# IVSS Intersection accidents: Analysis and Prevention

Final Report – Volume 1 (main report)

Kip Smith  
Anna Bjelkemyr  
Jonas Bårgman  
Björn Johansson  
Magdalena Lindman

Title of the report: IVSS Intersection Accidents: Analysis and Prevention, Final Report – Volume 1 (main report)

Reference number (IVSS): AL80 A 2008:73343

ISBN: 978-91-633-5030-6

Authors: Kip Smith, Anna Bjelkemyr, Jonas Bårgman, Björn Johansson, Magdalena Lindman

Publication date: June 30, 2009

Project manager and contact person: Jonas Bårgman, Autoliv Development AB, Vårgårda, Sweden

IVSS contact: Torbjörn Biding, Vågverket, Sweden

Printed: Chalmers Reproservice, Göteborg, Sweden, 2009

# Introduction

Driving in intersections is a task that most people are familiar with and perform on a daily basis. This project was initiated to advance the understanding of driver actions and behavior in intersections as a basis for developing in-vehicle active safety systems. We used several different approaches and were able to extract useful and corroborating results that industry and academia can use to enhance traffic safety by developing active safety systems for cars. The results range from new methods and taxonomies for further research and development to data that can be used in the design of strategies for warnings and interventions in in-vehicle active safety systems. This report contains a set of results I hope will be a welcome contribution to the research community in better understanding driving in intersections.

The project was funded partially by the Swedish government (via IVSS – see next page) and partly by the Swedish automotive industry. As the project manager I would like to thank all participating partners for their valuable contributions, with special thanks to the principle investigator, professor Kip Smith, for his devotion to the project and large contribution to this report. I would also like to thank IVSS for their funding and support. I know the knowledge gained by the partners due to this project are being and will be used in many direct and indirect ways.

*Jonas Bärghman*

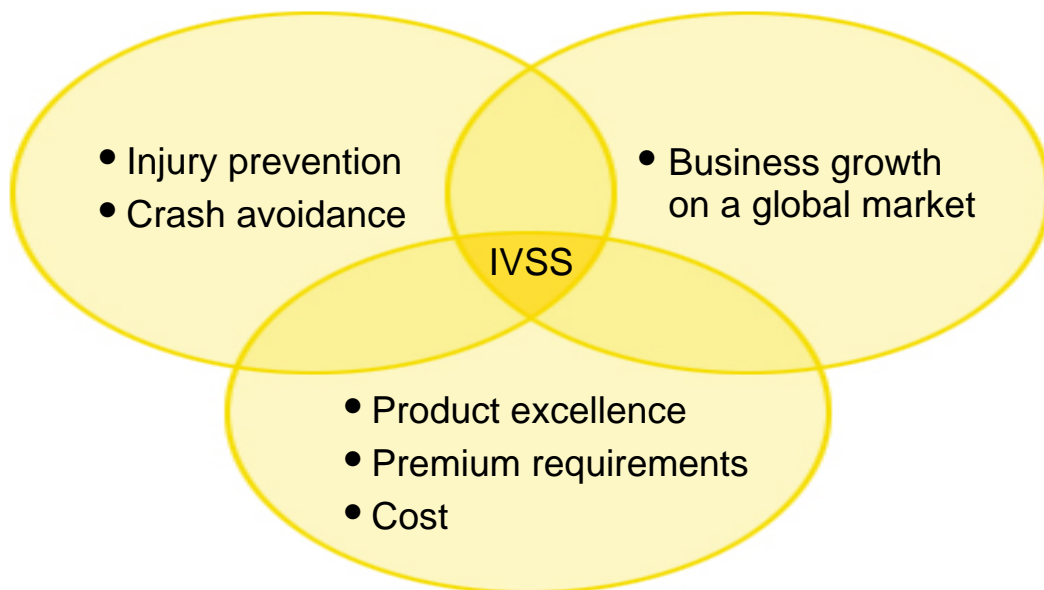
Project manager, Autoliv Development AB



# The IVSS Program

The IVSS program was set up to stimulate research and development for the road safety of the future. The end result will probably be new, smart technologies and new IT systems that will help reduce the number of traffic-related fatalities and serious injuries.

IVSS projects shall meet the following three criteria: road safety, economic growth and commercially marketable technical systems.



**Three interacting components** - for better safety, growth and competitiveness:

## **The human being**

Preventive solutions based on the vehicle's most important component.

## **The road**

Intelligent systems designed to increase security for all road users.

## **The vehicle**

Active safety through pro-active technology.

## Table of Contents

Chapter 1 Summary of Results	1.1
Structure of the chapter and the report	1.1
Partners and acronyms	1.2
The three programs	1.2
Image processing / vehicle trajectory program	1.2
From video to vehicle tracks	1.2
From tracks to trajectories to scenarios	1.2
Encroachment scenarios	1.3
Contextual sensitivity of driver actions	1.3
Simulator program	1.3
Test vehicle program	1.4
Summary of results	1.4
Methods	1.4
2 Getting started	1.4
3 Trajectory extraction from video data	1.4
4 Fundamental definitions and preliminary analyses	1.5
5 Traffic scenarios from the driver's point of view	1.5
Results from Sävenäs and Jung	1.5
6 Observed traffic scenarios at Sävenäs and Jung	1.5
7 Encroachments observed at Sävenäs and Jung	1.6
8 Go / No Go decisions	1.6
Results from simulator studies	1.7
9 Simulations of traffic scenarios at Sävenäs and Jung	1.7
10 Simulated encroachments at Sävenäs and Jung	1.8
11 Ratings of simulated encroachments	1.8
12 Cultural determinants of individual differences in driving style	1.8
Results from the test vehicle	1.9
13 Traffic experienced by the test vehicle	1.9
14 A 5 zone model of characteristic sequences of driver action	1.9
15 Intersection release time	1.10
The convergence of results	1.10
Figures, Chapter 1	1.11
Chapter 2 Getting Started	2.1
Selecting the intersections	2.1

## Table of Contents

Constraints	2.1
Cooperation with Lunds Tekniska Högskola	2.2
Sävenäs	2.2
Jung	2.3
Infrastructure-based equipment	2.3
Lessons learned	2.3
Hardware	2.3
Cameras	2.3
Computers	2.4
GPS synchronization	2.4
Installations	2.4
Sävenäs	2.4
Jung	2.4
Retrofitting the test vehicle	2.5
Environmental sensors	2.5
Video cameras	2.5
Laser radar	2.5
In-vehicle sensors	2.6
Eye/head tracking	2.6
Pedal proximity	2.6
Vehicle dynamics	2.6
Controller area network	2.6
Steering wheel potentiometer	2.6
Fiber optic gyro	2.6
Differential GPS	2.6
Sensor fusion	2.7
Selection of the multi-driver traffic simulator	2.7
Major constraints	2.7
Specification for purchase	2.8
Driver stations	2.8
Vehicle realism	2.8
Data logging	2.9
Two finalists	2.9
End note on the multi-driver simulator	2.9
Upgrade of the driving simulator at SAAB	2.9

## Table of Contents

References	2.10
Figures, Chapter 2	2.11
Chapter 3 Trajectory extraction from video data	3.1
Overview	3.1
Definitions	3.1
Overview of image processing	3.2
Video data	3.2
Coarse image processing	3.2
Fine image processing	3.3
Data format	3.3
Trajectory identification	3.3
Principal trajectories - archetypes of paths	3.3
Track repair	3.4
Quality metric	3.4
Good trajectories	3.4
Splitting	3.5
Merging	3.5
Matching tracks to trajectories	3.5
Distance traveled	3.5
Minimum distance to the center of the intersection	3.5
Crossing the intersection	3.6
Matching the track to a principal trajectory	3.6
Filtering	3.6
Maximum distance from principal trajectory	3.6
Size criterion	3.6
Tracks that become trajectories	3.7
Post-hoc offset correction	3.7
Quality checking	3.7
Result	3.7
Implications	3.7
Correcting the offset	3.8
The model	3.8
The correction	3.8
Additional correction for the secondary road at Sävenäs	3.8

## Table of Contents

Figures, Chapter 3	3.9
Tables, Chapter 3	3.13
Chapter 4 Fundamental definitions and preliminary analyses	4.1
Definitions of traffic scenarios in intersections	4.1
Geometric classification	4.1
Interaction classification	4.1
Traffic scenarios observed at Sävenäs	4.2
Definition of metrics of safety	4.3
Post-encroachment time	4.3
Distance between vehicles	4.3
Time to collision	4.3
Method	4.4
Output	4.4
References	4.4
Figures, Chapter 4	4.5
Tables, Chapter 4	4.8
Chapter 5 Traffic scenarios from the driver's point of view	5.1
Definition of trajectories	5.1
The 6 trajectories at Sävenäs	5.1
The 12 trajectories at Jung	5.2
Scenario classification	5.3
Find red cars	5.3
Check following	5.3
Simple and complex scenarios	5.4
Simple encroachment	5.4
Crossing	5.4
Merging and waiting	5.5
Find most relevant other	5.5
Figures, Chapter 5	5.6
Tables, Chapter 5	5.9
Chapter 6 Observed traffic scenarios at Sävenäs and Jung	6.1
Sävenäs	6.1

## Table of Contents

Scenario counts	6.1
Velocity distributions	6.1
Jung	6.3
Scenario counts	6.3
Velocity distributions	6.3
Figures, Chapter 6	6.5
Tables, Chapter 6	6.8
Chapter 7 Encroachments observed at Sävenäs and Jung	7.1
Post-encroachment time	7.1
PET at Sävenäs	7.2
Probability of PET < .05	7.4
PET at Jung	7.4
Probability of PET < .05	7.6
References	7.6
Figures, Chapter 7	7.7
Tables, Chapter 7	7.18
Chapter 8 Go / No Go decisions	8.1
Introduction	8.1
Previous research on the Go / No Go decision	8.1
Method	8.2
Automated image processing of video data	8.2
The four traffic scenarios	8.2
Minimum velocity marks the decision point	8.2
Lag distance and the decision point	8.3
Post-encroachment distance	8.3
Results	8.3
Distance, time, and apparent velocity at the decision point	8.3
Post-encroachment distance	8.4
Discussion	8.4
References	8.5
Figures, Chapter 8	8.6
Tables, Chapter 8	8.14

## Table of Contents

Chapter 9 Simulations of traffic scenarios at Sävenäs and Jung	9.1
Overview of the simulator experiments	9.1
Experimental protocols	9.2
Experiment 1	9.2
Drivers	9.2
Road circuit and the Sävenäs intersection	9.2
Task and experimental design	9.3
Procedure	9.3
Dependant measures	9.4
Experiment 2	9.4
Drivers	9.4
Road circuit	9.4
Design and task	9.5
Experiment 3	9.5
Drivers	9.5
Road circuit, task, provokers, and projected gap times	9.5
Procedure	9.6
Experiment 4	9.7
Drivers	9.7
Road circuit, task, provokers, and projected gap times	9.7
Procedure	9.7
Experiment 5	9.7
Road circuit, task, and provokers	9.8
Procedure and projected gap times	9.8
Traffic patterns at the simulated intersections	9.8
Experiment 1	9.8
Experiment 2	9.9
Experiment 3	9.10
Experiment 4	9.11
Experiment 5	9.11
Velocity distributions	9.11
Free drives at Sävenäs	9.11
Drives at Sävenäs with provokers	9.13
Discussion	9.13

## Table of Contents

Reference	9.14
Figures, Chapter 9	9.15
Tables, Chapter 9	9.21
Chapter 10 Simulated encroachments at Sävenäs and Jung	10.1
Introduction	10.1
Experiments 1, 2, and 5	10.1
Experiment 3	10.2
Scenario 6xs, LTAP/LD	10.2
Scenario 6xa, LTAP/OD	10.2
The influence of encroachment context	10.3
Experiment 4	10.4
Scenario 6xs, LTAP/LD	10.4
Scenario 6xa, LTAP/OD	10.4
The influence of encroachment context	10.5
The comfort zone	10.5
Figures, Chapter 10	10.5
Tables, Chapter 10	10.13
Chapter 11 Ratings of simulated encroachments	11.1
Summary	11.1
Introduction	11.2
Method	11.3
Participants	11.3
Apparatus	11.3
Stimuli	11.3
Task	11.4
Procedure	11.4
Questionnaires	11.5
Results	11.5
Ratings and driving	11.5
Ratings = F(PET)	11.5
Mean effects, aggregated data	11.6
Differential effects across the range of PET	11.6
Critical values of PET	11.6



## Table of Contents

Implications for the design of active safety systems	11.7
References	11.8
Figures, Chapter 11	11.9
Tables, Chapter 11	11.14
Chapter 12 Cultural determinants of individual differences in driving style	12.1
Materials	12.1
Schwartz value survey	12.1
Driver style questionnaire	12.1
Driver behavior questionnaire	12.1
Correlation analysis	12.1
Implications for the design of active safety systems	12.3
References	12.4
Tables, Chapter 12	12.5
Figures, Chapter 12	12.7
Chapter 13 Traffic experienced by the test vehicle	13.1
The case study	13.1
On the extraction of observations by the image processing system	13.1
Representativeness of the passes	13.2
Velocity of the test vehicle	13.2
The encroachment incident	13.3
Figures, Chapter 13	13.4
Tables, Chapter 13	13.7
Chapter 14 A 5 zone model of characteristic sequences of driver action	14.1
Introduction	14.1
Method	14.2
Participant	14.2
Vehicle	14.2
Route	14.2
Procedure	14.3
Dependent variables	14.3
Heading	14.3
Gaze and head angles	14.3

## Table of Contents

Analyses	14.4
Heading	14.4
Gaze and head angles	14.4
Difference between gaze and head angles	14.4
Acceleration	14.4
Results	14.5
Scenario 1: A right turn from the primary road	14.5
Data	14.5
Heading	14.5
Gaze and head angles	14.5
Acceleration	14.6
Synthesis, the 5 zone model	14.6
Scenarios 2 - 6	14.7
Right turns (Scenarios 1 and 2)	14.7
Left turns (Scenarios 3 and 4)	14.7
Straight ahead passes (Scenarios 5 and 6)	14.7
Turns from the primary road to the secondary road (Scenarios 1 and 3)	14.8
Turns from the secondary road to the primary road (Scenarios 2 and 4)	14.8
Discussion	14.8
Characteristic sequences of driver actions	14.8
Future work	14.9
Implications for the design of active safety systems	14.9
References	14.10
Figures, Chapter 14	14.11
Tables, Chapter 14	14.17
Chapter 15 Intersection release time	15.1
Introduction	15.1
Visual search while driving	15.1
Previous work on visual search in intersections	15.2
A task analysis of visual search in a non-signalized intersection	15.3
Hypotheses regarding the decision about lateral encroachment	15.4
Intersection release distance - Gaze	15.4
Intersection release distance - Head	15.5
Break readiness	15.6

## Table of Contents

Logic	15.6
Method	15.7
Drivers	15.7
Task and setting	15.7
Apparatus	15.7
Procedure	15.8
Synchronizing trajectories	15.8
Dependant variables	15.8
Gazes and time	15.8
Brake readiness	15.9
Results	15.9
Driver 1	15.9
Intersection release distance - Gaze	15.9
Focal distance of gazes on the crossing road	15.9
Expected velocity of traffic	15.10
Intersection Release Distance – Head	15.10
Brake readiness	15.11
Driver 2	15.11
Other drivers	15.11
Discussion	15.11
References	15.12
Figures, Chapter 15	15.14
Chapter 16 Synthesis of results that may inform the design of active safety systems	16.1
Introduction	16.1
Disclaimer	16.1
Contextual factors that may influence the design of active safety systems	16.1
Identification of traffic scenarios	16.1
Velocity as a function of traffic scenario	16.2
Frequency of encroachments as a function of traffic scenario	16.2
A template for active safety system functionality	16.2
System functionality	16.2
The relevance of our work to the template	16.3
Specific results that can be used for preliminary specification of system parameters	16.4
Probability of PET < 5%	16.4

## Table of Contents

Buffer distances	16.4
Ratings of the welcomeness of warnings	16.4
Go/No-Go decisions	16.5
Tables, Chapter 16	16.5



## Chapter 1 - The three programs and summary of results

The overarching goal of the IVSS Intersection project has been to improve traffic safety (i.e. the “Vision Zero” goal) as well as to spur industry growth and competitive advantage. The specific goal was to inform the design of in-vehicle active safety systems for application in intersections. Depending on the implementation, such systems are likely to activate during impending near-crash situations or other incidents. The project has operationalized the concept of a ‘near-crash situation’ with a quantitative metric of encroachment.

Encroachment occurs whenever one vehicle crosses the path of another that has the right of way. We refer to the encroaching vehicle as the ‘provoker’ because the provoker provokes the encroachment incident. The focus of the project was to inform the design of in-vehicle active safety systems that activate (alert or intervene) when they detect impending encroachments in intersections.

The development of in-vehicle active safety systems is expected to promote the growth and competitiveness of the Swedish automotive industry. To these ends, the IVSS Intersections project was built upon a three-legged foundation: (1) image processing of video data of traffic at two monitored intersections (Sävenäs and Jung) looked for and identified encroachments, (2) repeated drives through those intersections by an instrumented test vehicle documented the adaptive nature of ‘normal’ driving at these intersections, and (3) simulations of encroachment in those intersections.

All three programs - Image processing, test Vehicle, and SimulationS - within the IVSS project focused on a pair of intersections. The first was Sävenäs, a three-way intersection with a speed limit of 50 kph in an industrial area 5 km east of Göteborg, Figure 1.1a. The second was Jung, a 70 kph four-way intersection on the E20, 120 northeast of Göteborg, Figure 1.2b. The criteria and process used to select Sävenäs and Jung are discussed in Chapter 2.

A hallmark of the project has been the mutually informative interaction across the programs. The convergence of independently derived results lends credence to the methods and findings. In the course of conducting the research, each of the three programs developed methodologies that can be applied in future projects with similar or other specific aims. This effort has raised the level of competence of all partners at investigating and understanding driver behavior and the constraints on in-vehicle active safety systems in intersections.

### Structure of the chapter and the report

This chapter has three sections. The first defines the three programs within the IVSS Intersections project. The second contains summaries of the results organized chapter by chapter:

- Chapters 2 through 5 discuss methods and preliminary results.
- Chapters 6, 7, and 8 discuss analyses of vehicle trajectory data, velocity distributions, and encroachment incidents observed at the Sävenäs and Jung intersections.
- Chapters 9 through 12 discuss analyses of similar data from the simulator studies and link those analyses to the data from the monitored intersections.
- Chapters 12, 13, and 14 discuss analyses of data from the instrumented test vehicle.

The third section of this chapter summarizes the mutual informative interactions across the three programs.

## Chapter 1 - The three programs and summary of results

The report concludes with a discussion of lessons learned and recommendations for future research. The lessons are presented as a template of functionalities for a potential active safety system designed to alert drivers to impending encroachment in intersections.

### Partners and acronyms

Autoliv - Autoliv Development AB

Chalmers - Department of Mechanical Engineering, Chalmers Technical University

IDA - Department of Information and Computer Science, Cognitive Systems Engineering Laboratory, Linköping University

ISY - Department of Electrical Engineering, Computer Vision Laboratory, Linköping University

SAAB - SAAB Automobile AB (GM Europe)

VCC - Volvo Car Corporation AB

Vägverket - The Swedish Road Administration

### The three programs

#### Image processing / vehicle trajectory program

##### From video to vehicle tracks

Autoliv mounted and maintained a video camera on the side of the Renova building at the Sävenäs intersection. The camera recorded 626 hours of traffic between the hours of 09:00 and 15:00 on days with few shadows from January 2006 to July 2008. Similarly, Autoliv mounted and maintained a pair of video cameras on each of two light standards at the Jung intersection. The four cameras at Jung recorded 95 hours of traffic between the hours of 09:00 and 15:00 on days with few shadows from March 2007 to May 2008.

This data base of video images was analyzed using software written for this project by researchers at ISY. The image processing software, running on a network of computers at the National Supercomputer Center, automatically extracted the tracks of more than 744,000 objects from the video data from Sävenäs and 152,000 from Jung. Each track is a time-series of the locations and inferred size of an object that is likely to be a vehicle.

##### From tracks to trajectories to scenarios

Many analyses were performed on the data sets of vehicle tracks. VCC and Chalmers conducted a series of assessments of the quality of the image processing data and wrote post-processing software that filtered and applied corrections to the observed tracks. The post-processing was designed to increase the likelihood that the detected objects are in fact vehicles. The corrected and filtered tracks are called trajectories.

VCC and Chalmers developed computer algorithms that use combinations of trajectories to classify traffic scenarios in intersections and applied them to the trajectory data from the two intersections. The VCC effort introduced the concept of defining traffic scenarios by the geometry of the trajectories of vehicles that are in an intersection more-or-less simultaneously. The work at Chalmers built upon the foundation laid by VCC to extend the geometric classification of traffic scenarios to account for the driver's point of view.

## Chapter 1 - The three programs and summary of results

### Encroachment scenarios

Both VCC and Chalmers developed quantitative metrics of ‘near-crash situations’ and applied them to the data from the intersections. Once again, the effort by VCC introduced the primary metric used in the project to operationalize the ill-defined concept of ‘near-crash’. This metric is Post-Encroachment Time (PET) and is defined as the minimum temporal separation between a pair of vehicles on crossing paths. The first vehicle is said to ‘encroach’ upon the second when it crosses the path of a second vehicle that has the right of way. The computation of PET considers the location of the vehicles where their trajectories cross and their sizes to provide an estimate of just how ‘near’ the near-crash situation became. The shorter the value of PET, the more threatening the incident.

The initial analysis of PET data from scenarios at Sävenäs found many encroachments with PET values less than a second. As this result does not appear to match observations at Sävenäs, Autoliv and Chalmers took a second look at the data, uncovered the need to apply a correction to the image processing output, applied the correction, and performed a second analysis of encroachments.

### Contextual sensitivity of driver actions

The corrected trajectory data were the basis for an analysis by Autoliv and Chalmers of the distribution of velocity of vehicles at the intersections that provides base lines for characterizing ‘normal’ driving in the intersections. Deviations from these base lines may be critical information for in-vehicle active safety systems. The analysis investigated the influence of traffic scenario on the velocities entering, within, and exiting the intersections. They present evidence for the contextual sensitivity of drivers’ adaptation to traffic scenarios.

Chalmers used the corrected trajectory data to conduct an analysis of the contextual sensitivity of drivers’ decisions to commit an encroachment. This analysis yielded a model that predicts the decision point where most drivers will (not) turn left across another’s path at the intersections. The model defines the contextual influences on the times and distances at which drivers appear to be comfortable with encroachments and lends itself as a basis for implementation in in-vehicle active safety systems.

### **Simulator program**

The second program conducted controlled laboratory experiments that investigated driver behavior in intersections with an emphasis on encroachment. There were two mutually informative series of experiments in a pair of driving simulators. Both revealed the influence of traffic context on driver responses to encroachment.

The experiments conducted at IDA used a desk-top multi-driver simulator. As many as four drivers could drive simultaneously on the same simulated road circuit and interact at its replicas of the Sävenäs or Jung intersections. The experiments tested five alternative approaches to generating encroachments in a simulator environment and eliciting driver responses to them. The tests settled on an approach that appears to have found the right mix of veridicality (adherence to reality) and experimental control of the PET between pairs of vehicles in simulated encroachments.

The program of experiments documented that the average participant drove normally in the simulated intersections but that many did not. It also documented that it is possible to induce most participants to drive normally, to stage encroachments that are (relatively) unexpected, and to elicit spontaneous responses to those encroachments. Thus, the power of these simulation experiments is not in the replication of the real world but in the creation of



## Chapter 1 - The three programs and summary of results

controlled scenarios (e.g., with extremely short PET values) that are both rare and cannot be staged in an actual intersection.

The experiments conducted at SAAB used a high-fidelity fixed-base simulator. The driver sat in an actual passenger car surrounded by a wrap-around projection screen. The experiments manipulated the PET between pair of vehicles in simulated encroachments at Sävenäs and elicited quantitative self-reports from drivers about the acceptability of warnings to them.

### Test vehicle program

The third program collected and analyzed data from the Autoliv instrumented test vehicle during repeated drives through the Sävenäs and Jung intersections. The vehicle was a Volvo V70 equipped with a suite of sensors that gather data about the driver's actions, the vehicle's performance, and the surrounding scene. A four-camera eye-tracking system (SmartEye Pro), a foot-well camera, and pedal proximity sensors provided information about the direction of the driver's gaze and head orientation and anticipatory control actions. CAN-bus logs generated data on velocity, pedal control, steering angle and other dynamic variables. A digital global positioning system recorded data on location and an independent measure of velocity. A cluster of roof-mounted cameras produced an image of the surrounding scene with a combined horizontal field of view of approximately 200°.

Analyses of data from the test vehicle were conducted at Chalmers and Autoliv. The two studies focused on the driver's actions within the context of the traffic scenario and vehicle dynamics. While more than a dozen volunteers drove the test vehicle through the intersections, the studies focused primarily on an extensive data set from one driver. This case study was the basis for the development of a pair of descriptive models that define characteristic sequences of control actions. These models predict how drivers can be expected to respond to evolving traffic conditions in intersections and lend themselves as bases for implementation in in-vehicle active safety systems.

## Summary of results

### Methods

The first section of the report contains four chapters that document the steps taken to enable data collection and the methods that generate and analyze the multiple streams of data.

#### 2 Getting started

Chapter 2 summarizes the work done to get the project started. This work included the selection of the Sävenäs and Jung intersections, the selection of the software for the multi-driver simulator, and the retrofitting of the instrumented test vehicle. The discussion reviews the constraints on the decisions that were made and the time line of the project.

- Selection of Sävenäs and Jung
- Selection of multi-driver simulator

#### 3 Trajectory extraction from video data

Chapter 3 provides an overview of the image processing system developed by ISY for this project. The goals of the image processing program were (1) to develop a method for extracting the temporal and spatial coordinates of vehicles from the pixels of images obtained

## Chapter 1 - The three programs and summary of results

by infrastructure-mounted video cameras and (2) to provide the basic data for analyses of traffic scenarios, driver behavior, and encroachments. These data form the baseline for comparisons with data from the test vehicle and simulator programs.

The chapter reviews methods developed by VCC for analyzing and repairing data generated by the image processing software. The key innovation is the introduction of archetypical vehicle trajectories called ‘principal trajectories’ that are used to determine the trajectory that best fits each track. The chapter also reviews the methods developed by Autoliv and Chalmers for filtering and correcting repaired trajectories.

- Automated extraction of vehicle tracks from video images
- Assignment of tracks to trajectories using principal trajectories
- Repairing and filtering of trajectories

### 4 Fundamental definitions and preliminary analyses

VCC developed the backbone of the data analysis program relatively early in the project. Chapter 4 documents the method for scenario classification based on the geometry of vehicle trajectories, the post-encroachment time (PET) metric, and other metrics. It also presents the results of the initial applications of the classification method to the image processing data from Sävenäs.

- Geometric scenario classification method
- First-stage analysis of data from Sävenäs

### 5 Traffic scenarios from the driver’s point of view

Autoliv and Chalmers build upon the work by VCC to fine-tune the method for scenario classification. Chapter 5 discusses the updated classification system that differentiates scenarios depending upon the driver’s point of view.

- Scenario classification from the driver’s point of view

## **Results from Sävenäs and Jung**

The three chapters in the second section of the report present analyses of the traffic scenarios at Sävenäs and Jung. Data about the base rates of traffic scenarios, of encroachment incidents, and of adaptive velocity control may inform the design and development of in-vehicle active safety systems.

### 6 Observed traffic scenarios at Sävenäs and Jung

Chapter 6 discusses the traffic scenarios and velocity distributions observed at Sävenäs and Jung. The scenario classification system developed by Autoliv and Chalmers was used to count and determine the distribution of scenarios. At Sävenäs, 40% of scenarios were ‘solo’ drives in which one car is in the intersection. By far the most common trajectories though the Sävenäs intersection were (a) the right turn from the north to the west and (b) its return, the left turn from the west to the north. At Jung, only 20% were solo drives. As expected, the most common trajectories were straight drives on the E20.

Contextual sensitivity is a hallmark of skilled human performance. It could also be a characteristic of in-vehicle active safety systems. Specifically, both drivers and in-vehicle active safety systems need to adapt to the changes in the traffic situation. Velocity is a key indicator of adaptive behavior that is readily available to in-vehicle sensors.

## Chapter 1 - The three programs and summary of results

To ascertain situations in which drivers displayed adaptive velocity control, Autoliv and Chalmers conducted statistical tests that examined the cumulative frequency distribution of velocity at 10 meter intervals along all trajectories. Several types of comparison are discussed including the influence of the presence of a potential provokers on the velocity of drivers with the right of way. The analyses defined a key component of ‘normal’ driving behavior through the intersections. Knowledge of normal behavior is essential to the detection of abnormal behavior and to the design of active safety systems.

- Base rate of scenarios at Sävenäs and Jung
- Contextual sensitivity of velocity control

### 7 Encroachments observed at Sävenäs and Jung

Autoliv and Chalmers built upon the work by VCC to fine-tune the application of the PET metric. Encroachment occurs when a provoker crosses the path of a vehicle with the right of way. The fine-tuning considers only cases in which the provoker crosses first. The analyses presented in Chapter 7 applied this refinement to document the base rates of encroachment at Sävenäs and Jung.

An opportunity for encroachment exists when two (or more) cars are in the intersection at the same time, one with the right of way and one that could cross its path. Given the operational definitions of encroachment used in the analyses, 8% of traffic scenarios at Sävenäs provided the opportunity for encroachment. In most scenarios, more than 20% of potential provokers took the opportunity to provoke an encroachment. Encroachment is common at Sävenäs.

The overall rate of encroachment at Jung is more than twice that at Sävenäs. A full 28% of scenarios at Jung provided the opportunity for encroachment and 9% of provokers took the chance. Encroachment at Jung is much too common.

The analyses compare the base rates for encroachment across traffic scenarios and recommend scenarios that deserve special attention when designing active safety systems.

- Distribution of encroachment times and distances at Sävenäs and Jung
- Identification of traffic scenarios with relatively high rates of encroachment

### 8 Go / No Go decisions

Chapter 8 introduces a novel approach to understanding when and where drivers make the decision whether or not to turn left and to encroach upon an approaching car that has the right of way in an unsignalized intersection. The analysis used the data from Sävenäs and Jung to investigate four different left-turn scenarios - where the car with the right of way arrives from the opposite direction, from the lateral direction, from the intended direction (merging), and while making its own left turn. For each scenario, we found the distances between the provoker and the car with the right of way (1) at the time when we can assume the decision to turn (or not) is made and (2) for the resulting encroachments. Logistic regression identified the distances associated with the 50/50 acceptance probabilities for both the decision to turn (encroach) and the outcomes of decisions to encroach for all four scenarios at both intersections. We expected to find wide variability in these distances. Instead, we observed an invariant outcome across the four left-turn scenarios. We argue that tacit knowledge of this invariant may drive the decision of whether or not to turn and encroach and that this knowledge should be made explicit in the design of in-vehicle active safety systems.

- Predictive models of the decision (not) to encroach for four left-turn scenarios

## Chapter 1 - The three programs and summary of results

### Results from simulator studies

The third section of the report presents data from the simulator studies at SAAB and IDA. The discussions focus on the variability of drivers in a simulator, their adaptive behavior in the face of encroachments, and on how they rated the welcomeness of a hypothetical alert to observed encroachments.

#### 9 Simulations of traffic scenarios at Sävenäs and Jung

Chapter 9 describes the five experiments conducted in the multi-driver simulator at IDA. In each of the experiments, volunteers drove repeatedly through replicas of the Sävenäs or Jung intersections.

To ascertain whether encroachment incidents would arise naturally in realistic simulations of the Sävenäs intersection, Experiments 1 and 2 were designed to create as natural a driving environment and experience as we could in the laboratory. We constructed realistic road circuits with intersections that replicated the Sävenäs intersection and flows of traffic that appeared natural. This realism prompted fast but cautious driving by our participants.

Faced with need to satisfy the project's goal of observing encroachment incidents and to overcome drivers' natural caution, we adopted a radically different approach for Experiments 3 and 4. These experiments created driving conditions in which encroachment incidents were frequent and predictable. Participants drove a route in which they had the right of way through each of the replicas of the Sävenäs intersection where they encountered another car. More often than not, that car would turn left across the participant's path. The turns were timed to generate short PET values.

As expected, participants quickly learned to anticipate the starkly unrealistic behavior of the provokers and adapted their driving behavior in response. The nature of this adaptation is the data we were hoping to find. Armed with the expectation of encroachment, drivers slowed to allow the provoker to pass before proceeding through the intersection. The observation that drivers modified their driving to avoid expected encroachment bodes well for the introduction of active safety systems designed to detect and alert drivers to impending encroachments.

The paradigm for Experiment 5 blended the best elements of the previous experiments. As in Experiments 1 and 2, drivers were instructed to explore the simulated world. They crossed the replica of the Jung intersection many times, in all directions, and at their own pace. As in Experiments 3 and 4, drivers occasionally encountered provokers at the intersection. Unlike the provokers in the previous experiments, the presence of provokers at Jung was unpredictable. The drivers' responses to these encroachments are, accordingly, more likely to emulate those by drivers who experience encroachment at real intersections.

The velocities of cars in the simulator experiments were not representative of traffic at Sävenäs. The variability in velocity in the simulator far exceeded that at Sävenäs. It is clear that greater experimental control is needed for this type of experimental setting if replication were to be the goal. The data set from the simulation of Jung is too small to support similar analyses.

- Overview of simulator experiments
- Lack of representativeness: no replication of traffic scenarios, highly variable velocities
- Velocity control in response to predictable encroachments

## Chapter 1 - The three programs and summary of results

### 10 Simulated encroachments at Sävenäs and Jung

Chapter 10 discusses the encroachments observed in the five simulator experiments at IDA. All five were designed to set up opportunities for encroachment. The first two documented that few experimental participants opted to provoke an encroachment. These results led to the redesign of the experiments. The redesign featured cars that were intentionally driven to provoke encroachment. In Experiment 3, the drivers of the provokers were human confederates. The confederates followed a script designed to create encroachments with known and fixed PET values. Software drove the provokers in Experiments 4 and 5. Like the confederates, the software adhered to a script with assigned PET values. In both experiments, the frequent and predicable appearance of provokers created artificial driving conditions.

In all but the first encounter, the observed PET values were greater than the scripted values. This result reveals that the drivers slowed to avoid the encroachments and to cross the intersections well after the provokers. It took only one experience with a provoker for the drivers to expect encroachments to occur and to compensate by modifying their velocity. They adapted their driving so that they defined different comfort zones for the two types of encroachment. The experiments support the conclusion that drivers seek to achieve longer PET times when encroached upon from ahead than from the side.

- Definition of contextual variability in ‘comfort zones’ for encroachment
- Recommendations for thresholds for alerts to potential encroachment

### 11 Ratings of simulated encroachments

The experiments discussed in Chapter 11 were run in SAAB’s fixed-based driving simulator with a 220° view angle. They presented simulated encroachment incidents in a replica of the Sävenäs intersection. In each of the 36 trials, a provoker turned left across the path of a vehicle that had the right of way as it drove straight through the intersection. After each trial, participants rated the welcomeness of hypothetical alerts to the incident they had just experienced.

Repeated measures ANOVA revealed that welcomeness increased monotonically as PET decreased. Alerts to provokers that encroached from the side were more welcome than alerts to provokers that encroached from directly ahead. Participants welcomed alerts more when they were in the vehicle with the right of way than when they were in the provoker.

The significant interaction between driver point of view and encroachment direction may have implications for the design of active safety systems. The analysis indicated that an alert was welcomed significantly less when participants were sitting in a provoking vehicle that turns in front of a vehicle that can be seen by looking straight ahead. It appears that the design of active safety systems may have to accommodate information about the right of way as well as the type of encroachment.

- Contextual sensitivity of the welcomeness of alerts to encroachment
- Quantification of the relationship between encroachment time and the welcomeness of an alert

### 12 Cultural determinants of individual differences in driving style

Chapter 12 presents an analysis of the responses by participants in the IDA experiments to a battery of self-report questionnaires in an attempt to identify factors that might influence the acceptance of active safety systems. The data are consistent with the interpretation that speeders and drivers who are not easily distracted may find it exciting to ‘game the system’

## Chapter 1 - The three programs and summary of results

by pushing an active safety system to the limit where it issues an alert. Alerts may need to be implemented in a manner that precludes their transformation into a behavioral reward for thrill-seekers. The data also suggest that drivers from traditional, fatalistic cultures may find active safety systems superfluous or frivolous. It behooves designers of automotive systems to take into account their cultural bias and not to assume that drivers from other cultures will welcome alerts as they would.

- Information that may influence the international marketing of active safety systems

### Results from the test vehicle

The three chapters of the final section of the report present analyses of data collected using the Autoliv instrumented test vehicle. The analyses in Chapters 13 and 14 focus on an extensive data set from one driver, a 33 year-old female, at Sävenäs. The driver followed a predetermined circuit that took her through the intersection on all six possible trajectories. The analyses in Chapter 15 include the drives taken by 10 additional drivers.

#### 13 Traffic experienced by the test vehicle

Chapter 13 documents the representativeness of the passes made by the test vehicle through the Sävenäs intersection and describes its one encroachment incident. The repeated drives through Sävenäs afforded an assessment of how well the automated trajectory extraction system worked. There are two major findings. First, the trajectory extraction system recovered 87% (193 of 222) of the passes through the intersection made by the test vehicle. The processing appears to have been particularly challenged by the one case in which a high percentage of vehicles have to come to a complete stop. The low recovery rate when the test vehicle entered the intersection from the north on the secondary road may reflect difficulties with the reconciliation of segments of trajectories broken when a vehicle stops.

The chapter includes a first-hand account of the one encroachment experienced by the driver of the test vehicle. This incident was an example of a left-turn across path from the opposite direction (LTAP/OD) with an PET value of 1 second. The PET value would likely have been shorter had the driver not been attentive and braked sharply. We view this incident as a paradigm that illustrates the need for the development of active safety systems.

- Overview of the case study using the test vehicle
- Representativeness of the drives in the case study
- Description of the one experienced encroachment event

#### 14 A 5 zone model of characteristic sequences of driver actions

Chapter 14 develops a model of driver behavior when approaching, entering, and exiting an intersection based upon a case study of one driver at Sävenäs. The model is a template of how we can expect drivers to act in an urban intersection and identifies characteristic sequences of actions that define spatial zones. The three principal parameters used to define the model are the vehicle heading and the driver's gaze and head movements. The analyses indicate that there are more similarities across cases with the same sequence of road types (e.g. primary to secondary road or secondary to primary road) than there are similarities across cases with the same driver intent (e.g. turning right).

- Descriptive model of the contextual dependency of driver actions when approaching, entering, and exiting an intersection
- Templates for expected driver actions - base lines for detecting irregular behavior

## Chapter 1 - The three programs and summary of results

### 15 Intersection release time

The study described in Chapter 15 investigated the gazes and control actions taken by multiple drivers when approaching the Sävenäs intersection on a single trajectory with the right of way. The study introduces a novel metric - intersection release distance - to gauge whether, when, and where a driver assesses the potential for encroachment. The analysis assumes that drivers search the crossing roadway for information about the locations and velocities of other vehicles. Gazes and head rotations directed away from the driver's lane and toward the crossing roadway are diagnostic of an ongoing search. The distance from the center of the intersection where that search ends - the intersection release distance - is diagnostic of the judgment that the path through the intersection is clear. Application of the metric to the data from Sävenäs uncovered characteristic changes in intersection release distance that varied as a function of traffic scenario.

- Descriptive model of the contextual dependency of driver actions when searching for potential provokers
- Templates for expected driver actions - base lines for detecting irregular behavior

### **The convergence of results**

Figure 1.2 shows the programs that form the three-legged foundation for the IVSS Intersections project: Image processing, test Vehicle, and SimulationS. The image processing program provided base line data on trajectories. Analyses of trajectories informed the development of the geometric method for classifying traffic scenarios that is, in turn, a cornerstone for all three programs.

The known trajectories of the drives by the test vehicle provided the opportunity to test the scenario classification algorithm and to document the influence of traffic scenario on data capture. The one encroachment incident experienced by the test vehicle informed the design of the experiments conducted in the simulator studies of encroachment.

Figures

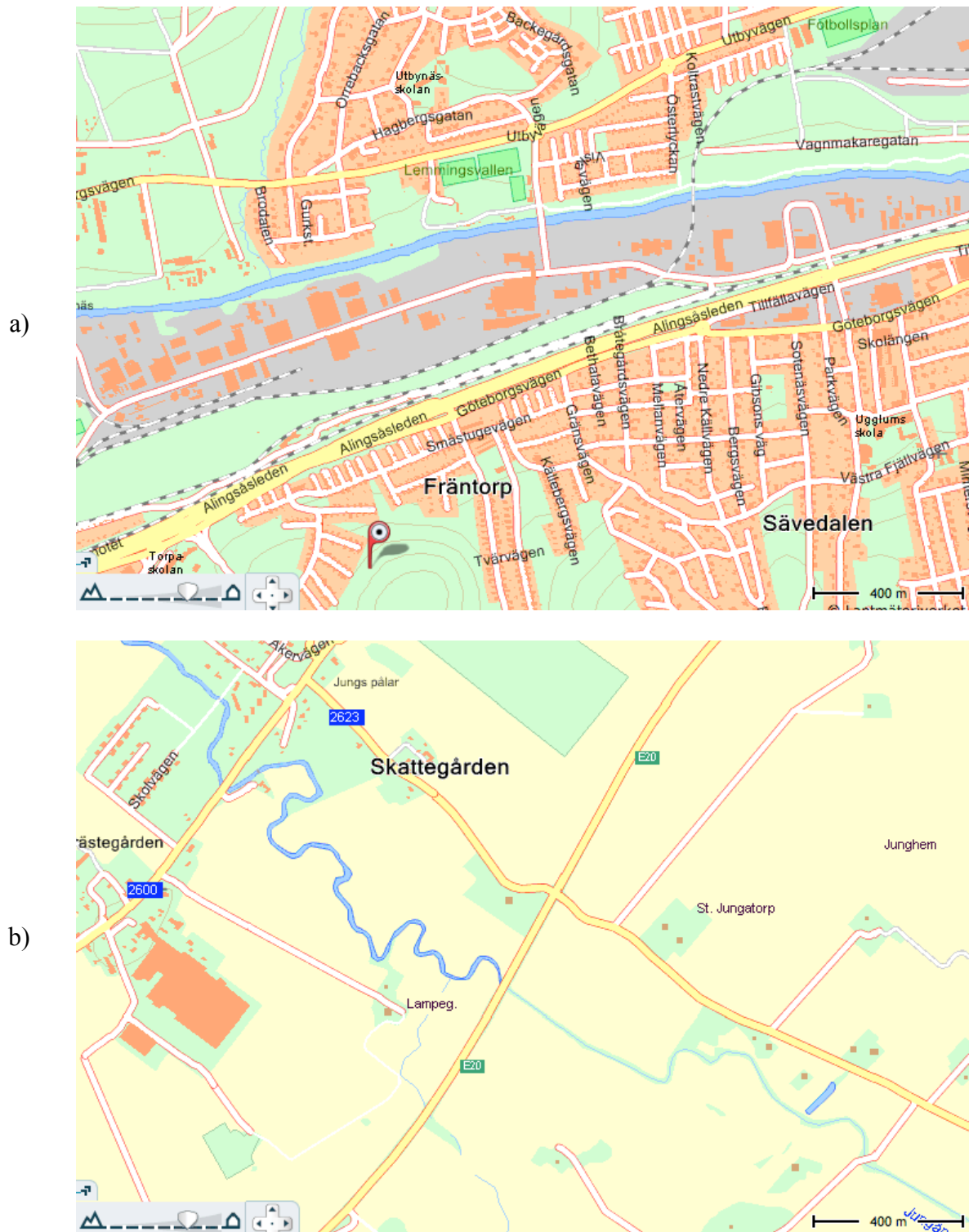


Figure 1.1 Maps showing the locations of the monitored intersections, (a) Sävenäs, (b) Jung.



## Chapter 1 - The three programs and summary of results

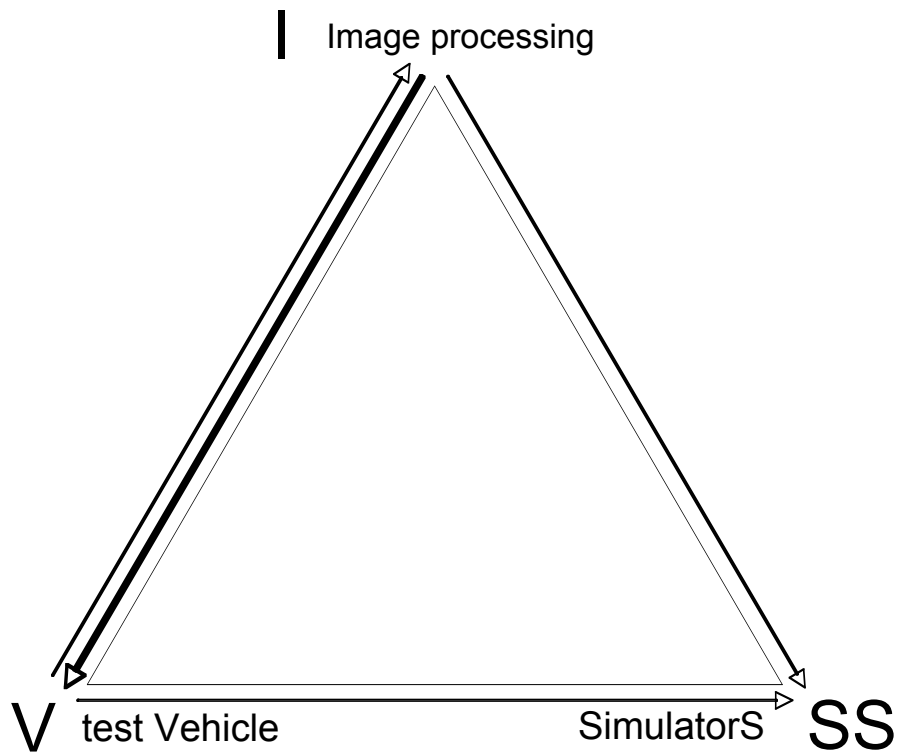


Figure 1.2 The three programs and the convergence of results

## Chapter 2 - Getting Started

This chapter summarizes work done by the partners in the IVSS Intersections project to prepare for data collection and analysis. There were five primary preparatory tasks: (1) Selecting the intersections, (2) Installing infrastructure-based equipment (cameras) at the intersections, (3) Retrofitting the test vehicle, (4) Selecting the multi-driver simulator that was installed at Linköpings universitet, and (5) Upgrading the high-fidelity driving simulator at SAAB. The tasks are shown in the top five rows of the project time line, Figure 2.1, and are discussed in turn.

### Selecting the intersections

Two non-signalized intersections were studied in this project. The first - at Sävenäs, 5 km east of Göteborg - is a 3-way intersection in a semi-rural industrial area with significant traffic flow and a 50 kph speed limit. The second - at Jung 120 km northeast of Göteborg - is a 4-way 70 kph intersection in a fully rural area on the main road from Göteborg to Stockholm (E20). Intersection video acquisition equipment was installed in both intersections.

### Constraints

There were four major constraints on the selection process that settled upon the Sävenäs and Jung intersections: camera stability, ease of access, estimates of relatively high incident rates, and proximity to either Vårgårda or Göteborg.

For the first intersection it was highly desirable to be able to mount the equipment on a building so that the first implementation of the image processing system would not have to deal with the complications of swaying or other extraneous motion. These considerations played heavily in the selection of the Sävenäs intersection. For the second intersection (Jung) it was sufficient that there be accessible high-masts (or buildings) with power available to mount cameras and equipment in the vicinity of the intersection.

The selection process started by contacting Thomas Bergbom of Vägverket Region Väst to obtain a list of intersections in and around Göteborg with accident rates that statistical analysis indicates are significantly high. Vägverket provided a list of approximately 50 intersections. The 15 with the highest accident rates were visited. All were either already being rebuilt, scheduled to be rebuilt in the near future, too large for feasible camera installations, or too complex for parsimonious analysis of traffic scenarios. Accordingly, none of the 15 were selected as the intersections to be studied during the project.

The second approach was to ask traffic (infrastructure) engineers at Vägverket about “good” candidates with relatively high estimated incident rates. This resulted in a list of approximately five intersections. Three of these were considered to have insufficient traffic flow. The final two were the Jung intersection on the E20 and the Rasta intersection on the E20 outside Vårgårda. Both were due for rebuilding, but no fixed date for the start had been set.

The third approach was to find 4-way intersections with relatively high traffic flows on both primary and secondary roads and then apply Vägverket’s Effektsamband 2000 models (algorithms) to those flows. The models use Equations 2.1 to estimate the yearly rate of police-reported accidents as a function of three factors: traffic flow (on primary and secondary roads), intersection type, and speed limit. Figure 2.2 presents the output of model when applied to the data from candidate intersections. The model predicted that the Jung, Vårgårda, and Lilla Edet intersections would have high accident rates.

## Chapter 2 - Getting Started

$$Amt = a * Q_t^b * \left(\frac{Q_s}{Q_t}\right)^c$$
$$Q = Total\_incoming\_ADT$$
$$Q = Indom\_ing\_secondary\_road\_ADT$$
$$a, b, c = Depending\_on\_intersect\_type\_and\_traffic\_environment$$
(2.1)

In summary, all three approaches identified the Jung intersection as a strong candidate for the project. The pragmatic concern of camera stability identified the Sävenäs intersection as a viable candidate for the initial effort.

### Cooperation with Lunds Tekniska Högskola

A fourth approach was considered and tested at Jung. An in-depth meeting was arranged with Prof. Christer Hydén at Lunds Tekniska Högskola (LTH) to gain insight into the Swedish Traffic Conflict Technique (Hydén, 1987). LTH were very helpful and subsequently applied the technique to the Jung intersection but were unable to provide specific guidelines or candidates for the choice of intersections in the Göteborg area. The LTH report about the Jung intersection is attached as Appendix 1.

### Sävenäs

The Sävenäs intersection (WGS84; Lat: 57.7327, Long: 12.0543) was chosen based on its location (5 km east of Göteborg), the ease of access to buildings where cameras could be mounted and remain stable, and statements made by a Vägverket traffic engineer that the intersection was relatively prone to incidents. The estimated traffic flow was approximately 200 vehicles per hour on the main roads (west and north). A to-scale map is shown in Figure 2.3. The intersection lies just north of the railroad tracks where Utfallsgatan meets Lemmingsgatan. As the street names indicate, the Sävenäs intersection is located in a mixed residential-industrial area. Figure 2.4 is an image from the camera mounted on the Renova Combustion Plant on the southwest corner of the intersection. This camera gathered the video data for the project. The view is to the northeast.

While technically a 4-way intersection, the southern roadway is an access road that terminates immediately in a private, industrial-area parking lot. The access road is not shown in the map of Figure 2.3 but can be seen on the right side of the photo, Figure 2.4. Traffic on the access road into and out of the lot is light. Accordingly, throughout this report we have treated the Sävenäs intersection as a 3-way 'T'.

Traffic from the west (Utfallsgatan) and east have the right-of-way. The road from the north (Lemmingsgatan) has a yield sign. The primary traffic flow is from the north (a residential neighborhood) to the west (toward Göteborg) and the return from west to north. The intersection has single lanes in all directions. There is no left-turn pocket lane from the west to the north. The secondary road from the north is sufficiently wide to provide two de-facto lanes, one for turning left and one for turning right. The speed limit on all three roads is 50 kph.

Detailed measurements of the geometry and layout of the intersection and adjacent infrastructure were made using transit and chain. These data supported the development of the model of the intersection used in the simulator studies.

## Chapter 2 - Getting Started

### Jung

The second intersection selected for the project is the high-speed 4-way intersection on the E20 at Jung (RT90; x: 6470296, y: 1343530), 120 km northeast of Göteborg. In keeping with the rural setting, the speed limit on the E20 is 90 kph. Signage directs traffic to slow to 70 kph in the vicinity of the intersection.

Detailed measurements of the geometry and layout of the intersection were made using transit and chain to support the development of the model of the intersection used in the simulator studies. Figure 2.5 shows the resulting map. The Jung intersection is much more complex than the Sävenäs intersection. Both directions of traffic on the secondary crossing road must stop at the E20. There are left-turn pocket lanes and dedicated right-turn lanes from both directions of the E20 to the secondary road. If no vehicle is turning left off the E20, there is room for a vehicle crossing the E20 to cross one direction of traffic, wait in the middle, and then proceed across the other direction of traffic.

A gas station occupies the northwest corner of the intersection. The other three corners are open fields. Cameras were mounted on lampposts on the northwest corner and the southeast corner. In moderate to heavy winds, the lampposts were vulnerable to sway which often compromised the processing of the video data. The data acquisition computer was housed under the sign for the gas station. Cables to the cameras in the southeast corner were run through culverts under the secondary road and suspended over the E20.

Because not all drivers adhered to the 70 kph limit, Vägverket installed speed cameras at Jung during the project. We have not processed data collected after the speed cameras were installed. In the summer of 2008, Vägverket widened the intersection and accidentally severed the cables, terminating data acquisition.

### Infrastructure-based equipment

Both intersections were equipped with cameras and a data acquisition and compression computer. As part of the project, Autoliv developed video acquisition technology and data acquisition and retrieval procedures. That work was initially allocated to LiU-ISY but was transferred in February 2006 to Autoliv.

### Lessons learned

The first step in the process of designing the infrastructure-based equipment was a review of a similar effort in the United States. The SAVME project (Ervin, MacAdam, Vayda, and Anderson, 2001) used video data to track vehicles on a straight road. A limited amount of data were collected at intersections. Discussions with contacts at both the University of Michigan Traffic Research Institute (UMTRI) and the National Highway Traffic Safety Association (NHTSA) developed a list of “lessons learned” that informed the choice of intersections and hardware. The salient lessons were the need for stable camera platform and a reliable source of power.

### Hardware

#### Cameras

Several options for camera hardware were evaluated at Autoliv and ISY. The main factors under consideration were the hardware interface and flexibility in synchronization and video compression. Constraints on the selection of hardware were the length of cable

## Chapter 2 - Getting Started

from the camera to the data-acquisition computer (100+ m) and the needs for high image compression and minimal compression artefacts. Gigabit-Ethernet cameras from Tattile were chosen.

### Computers

A high end workstation was used to acquire and compress video data at both Sävenäs and Jung. The systems were similar but had different peripherals and disc configurations. Separate network cards were used for each camera. Most data transmission relied on standard gigabit Ethernet networks. At Jung, data from the cameras on the far (southeast) corner of the intersection were transmitted using a fiber optic cable suspended over the intersection. A junction box at the computer was the interface between the cable and a standard gigabit Ethernet network.

Disc configuration depended on the number of cameras used. Each camera had one dedicated system disc, one dedicated temporary disc, and an external USB disc. The external discs were used to store the compressed video data. These discs were easily swapped and formed the primary media for data retrieval.

### GPS synchronization

Each computer had an integrated HOPF (<http://www.hopf-time.com/>) GPS time synchronization card and an external GPS antenna. The synchronization card provided a 1Hz signal to an external micro processor that generated a 20Hz signal that was fed to the cameras (+5V). The card made it possible to trigger all cameras in the intersection to collect data at essentially the same time ( $\pm 1\text{ms}$ ) and to record the time from the GPS signal. An identical system was installed in the instrumented vehicle, making it possible to synchronize the infrastructure-based video with data from the test vehicle.

### **Installations**

#### Sävenäs

Initially, two cameras were mounted directly on the Renova Combustion Plant on the southwest corner of the Sävenäs intersection. The building provided a firm anchor eliminating many of the problems associated with camera motion that could compromise the quality of the output from the image processing system. Each camera was placed in weather-proof housing (Pemel TPH5000, [www.pemel.se](http://www.pemel.se)) with integrated climate control (temperature controlled heating/fan).

Relatively early in the project, the decision was made to use only one camera. The camera location is shown in Figure 2.6. Its view of the intersection is shown in Figure 2.4. The second camera had been placed to the west of (behind) the pedestrian overpass shown in Figure 2.6 to provide coverage of traffic approaching the intersection from the west.

A synchronization and power unit were placed in a weather-proof housing less than 1m from the camera. Approximately 65m of cables (power, synchronization and Ethernet in parallel) connected the cameras to the computer. The computer and synchronization units were placed in a heated room inside of the Renova Combustion Plant.

#### Jung

In November 2006, four synchronized cameras were installed at the Jung intersection. Two cameras were mounted on a light mast on the northwest corner near the gas station and two were mounted on a light mast on the southeast corner. Each pair of cameras covered the intersection proper and the roads on the opposite side. Because the

## Chapter 2 - Getting Started

installation involved a partial closing of the E20, it was performed by licensed personnel (SKANSKA Produktion) and at night (22:00-06:00). The computer and synchronization unit was placed adjacent to the computer in a locked and insulated box with a temperature controlled fan.

### Retrofitting the test vehicle

The instrumented vehicle was a 2001 Volvo V70 equipped with a relatively extensive suite of sensors, Table 2.1. Sensors mounted on the car body recorded information about the traffic environment. Sensors inside the cab monitored the driver. Other sensors recorded data about vehicle dynamics. The sensors record data at different sampling frequencies. To facilitate sensor fusion and synchronicity, Autoliv developed a data acquisition system that generates a consistent set of time stamps and enables the data to be visualized and analyzed using commercial software (Matlab).

Table 2.1 The suite of sensors in/on the instrumented vehicle

---

Environment
3 video cameras
Laser radar
Driver
4 camera eye/head tracking system
Food/pedal proximity
Vehicle dynamics
Controller Area Network (CAN)
Steering wheel potentiometer
Fiber Optic Gyro (FOG)
Differential GPS

---

### Environmental sensors

#### Video cameras

Three greyscale cameras were mounted in a tight cluster on the roof of the vehicle to record the visual scene. Each camera has a field-of-view of approximately  $70^\circ$  ( $f = 4.5\text{mm}$  and  $\frac{1}{2}''$  CCD). The cluster forms a semi-circle with a small overlap between adjacent cameras. The combined horizontal field-of-view is approximately  $200^\circ$  centered directly ahead and aligned with a generic driver's head position. The alignment and roof-top location mimic as closely as possible the view seen by the driver. While this minimizes horizontal parallax errors, there is still approximately 500 mm of vertical displacement relative to the driver's head position in vertical direction. This offset produces some vertical parallax error. The video is captured with a resolution of one-quarter VGA (320x240 pixels) at a 25 Hz nominal frame rate. Post-processing merges the images into a single seamless  $200^\circ$  field-of-view image.

#### Laser radar

An IBEO Alasca (<http://www.ibeo-as.com/>) laser scanner scans the forward scene at 20 Hz and produces distance/angle measurements for a field-of-view greater than  $180^\circ$ . Analysis of the distance/angle data proved to be computationally intensive and were not performed for this project.

## Chapter 2 - Getting Started

### **In-vehicle sensors**

#### Eye/head tracking

The vehicle cab was equipped with a 4-camera Smart Eye Pro (Smart Eye, 2004) eye tracking system that captured images of the driver at 60 Hz. This system was the major source of data used to analyze the driver's visual search for information. The key data are the directions of the driver's gaze and head.

The eye-tracker cameras were distributed across the cab from the left door to the right rear-view mirror, Figure 2.7. This wide configuration enabled tracking over a 200° field-of-view. The eye-tracker was configured to generate data using a vehicle-centered coordinate system. Calibration of the cameras used reference markers in the cab. The locations of the markers in the cab was determined with a precision of  $\pm 1$  mm using a Faro Arm (<http://measuring-arms.faro.com/>).

#### Pedal proximity

To obtain information about brake and accelerator readiness, the driver-side foot-well was equipped with sensors that recorded the proximity of the driver's foot to the brake and accelerator pedals. Each pedal was fitted with a light source and a photo sensor that detected light reflected by the driver's shoe whenever it was within approximately 60 mm of the pedal.

### **Vehicle dynamics**

#### Controller area network

Selected data from the vehicle's Controller Area Network (CAN) bus were recorded. CAN is an industry standard for communication between the vehicle's electronic monitors and controllers.

Data on the position of the brake and accelerator pedals complements the pedal proximity data from the driver's foot well. The CAN data indicate how far the pedal is depressed as percentage of its total range of motion. CAN data on the steering wheel angle were recorded but found to be insufficiently accurate to support reliable analyses of vehicle motion. The CAN velocity data correlated strongly with GPS velocity data.

#### Steering wheel potentiometer

Due to the low resolution of the CAN data on the steering wheel angle, an extra sensor was installed. A linear potentiometer was attached to a threaded circular clamp attached to the steering column.

#### Fiber optic gyro (FOG)

a Fiber Optical Gyro (KVH DSP-5000, <http://www.kvh.com/>) measures the yaw rate with very high precision. These data were primarily used in the sensor fusion with the GPS data to extract better positioning, velocity and heading information.

#### Differential GPS

A G12 GPS Receiver from Ashtech was used. The G12 GPS receiver features 12-channel/ 12-satellite operation; each of up to 12 visible satellites can be assigned to a discrete channel for continuous tracking. Each satellite broadcasts almanac and ephemeris data every 30 seconds which will be recorded by G12. The G12 is designed for both stand alone and DGPS operation; when it is in DGPS operation, it will use SWEPOS reference GPS stations (a Swedish Differential GPS correction service). The

## Chapter 2 - Getting Started

G12 uses instantaneous Doppler values from four satellites to compute velocity which makes it independent of the last position fix.

There are many sources of error that affect GPS positioning accuracy (ephemeris data error, satellite clock error, ionosphere, troposphere, multipath and receiver noise in measuring range). Without GPS most of these do not have a significant effect on the precision, while when in Differential mode (as used in this study), most of these errors are to a large extent removed – producing. Multipath error and receiver noise on the other hand are not correlated with the reference base station and is not cancelled by the use of differential GPS. Multipath error is when the information sent from the satellites is being reflected on e.g. buildings in close proximity to the GPS receiver. When the receiver receives the reflected information, it cannot distinguish between this and the “real” signal; however in the G12, integrated Doppler measurements are used to smooth the range measurements and reduce the errors resulting from receiver noise. Since GPS receivers rely on using time of flight measurements on the incoming information, a reflected signal will have the error of the additional distance of time of flight between the receiver and the reflector (building). Multipath errors are also reduced by means of a digital signal processing technique implemented in the hardware and software of the G12 receiver. This technique removes multipath errors for reflected signals with delays of 37 meters or more, almost entirely. Even so, especially in the Sävenäs intersection, there were several large buildings that easily reflect the GPS signal – making it necessary to use additional sensors and sensor fusion for better position estimates. Also, of course GPS cannot operate if it does not have satellite coverage (needs at least 4 satellites visible), which often was the case in the west road in the Sävenäs intersection.

### Sensor fusion

Buildings like those at Sävenäs can occlude the signal from the GPS satellites leading to data ‘dropouts’. To offset this problem, Autoliv developed a sensor fusion algorithm to calculate vehicle position, velocity and heading in the absence of GPS data. Inputs to the algorithm are data from the FOG and CAN bus (vehicle velocity and acceleration). For details on the algorithm, see Ardeshiri et al. (2005).

### Selection of the multi-driver traffic simulator

The fourth preparatory task was the selection and purchase of low-fidelity desk-top multi-driver traffic simulator for use at LiU. The original plan was to conduct experiment and to ‘work the bugs out’ of the system at LiU and then transfer all or part of it to SAAB and/or Chalmers.

### Major constraints

There were three major constraints on the selection of the system. First, it had to support as many as four workstations so that four participants in an experiment could (a) drive four different cars in the same virtual world and (b) interact when they met at intersections. Second, each workstation had to support three monitors displaying a continuous 180° view of the virtual world. The wide angle of view was needed so that the participants could see out the side windows and look down the crossing road at the intersections. Finally, only European providers were considered to facilitate same-day technical support.



## Chapter 2 - Getting Started

### Specification for purchase

This section reproduces the text of the specification for the Multi-Driver Traffic Simulator that was sent to candidate vendors.

The Multi-Driver Traffic Simulator is a research tool for studying drivers' behavior at traffic situations. It is a simulator that allows several drivers to interact in a shared virtual traffic environment. Unlike most existing driving simulators, the emphasis in the traffic simulator is on the realism of traffic dynamics, i.e., how vehicles move relative to each other. The purpose of the MDTS is to allow controlled studies of drivers' behavior in different situations and under different conditions. The physical simulator will consist of at least four driver stations of which ideally at least two are realistic vehicle mock-ups with a large, wide-angle screen, while the rest could be desktop-versions. Since most of the physical equipment is commercially available, the requirement specification is primarily addressing the functionality of the software.

#### Driver stations

Since a majority of intersection conflicts involve more than two vehicles, commonly three or four, there should be a minimum of four driver stations.

To enhance realism of the lab experience, there should be a minimum of two driver stations as realistic mock-ups with large wide-angle screens.

Each subject shall have a unique view of the shared virtual environment from his/her position in the driving seat. Every participant drives a car and sees the world from that car's viewpoint.

To ensure that subjects are able to look at the crossing traffic, each subject shall view the virtual world through the windscreen and all of the front-side windows.

To study complex traffic situations, it should be possible to use as many as four driver cars in experiments.

#### Vehicle realism

To ensure the realism of "normal" driving tasks, there should be accurate timing with minimal delays of all actions taken by the drivers within the virtual world. Driver actions have effects that can be seen by the driver with minimal delay.

The virtual world should have good graphic resolution to reduce the likelihood of adverse influence on performance such as eye strain, dizziness or nausea.

The cars should look, act and feel as much like a passenger vehicle as possible.

Mechanisms used to communicate intent to other drivers should all be fully functional and realistic. These mechanisms include brake lights, headlights with both high and low beams, and turn signals.

The acceleration, brake and steering performance of each vehicle within the virtual world shall be realistic.

A simulated vehicle should not be able to travel outside the roads without realistic consequences.

To make subjects feel as if they are not meeting the same vehicles over and over again, color and/or shape should be used to make the simulated vehicles distinguishable.

## Chapter 2 - Getting Started

### Data logging

The bulleted list below is shown to give an overview of the data to be logged from the experiments.

- Scenario number
- Subject identity
- Timestamp
- Every vehicles' position within the road network as 'x y z h p r'- coordinates using the Swedish standard RT90 coordinate system.
- Vehicle position, relative the intersection, as meters on the road from the intersection point and on which intersection road-branch
- Speed in km/h
- Lateral position
- Usage of directional indicator
- Usage of brake pedal
- Usage of gas pedal
- Acceleration/Deceleration

### **Two finalists**

There were two finalists that met most of the criteria, ST Software (Groningen, The Netherlands) and Oktal (Toulouse, France). Initial license fees for the Oktal system were 50% more than those for ST. All other costs (hardware, support, etc.) and rendering capabilities were comparable. Cost considerations resulted the selection of STSim.

### **End note on the multi-driver simulator**

The STSim software routinely crashes during an experiment in which two or more drivers interact in the same virtual world. The vendor has been unable to fix this bug. This failing greatly reduces the utility of the multi-driver facility. Scenarios involving only one driver run without crashing.

### **Upgrade of the driving simulator at SAAB**

The fifth preparatory task was to upgrade the existing single-car high-fidelity driving simulator at SAAB to support studies of driver behavior (in addition to the development and testing of HMI systems). The plan at the beginning of the project was to enable SAAB to conduct experiments using the same software and presenting the same experimental scenarios as at LiU. The unique contributions at SAAB were to have been the high-fidelity of the simulator, the realism of the driver's in-car experience, and the recording of the driver's gaze and head directions using a 2-camera eye-tracker.

During the course of the project, it was found that it would have been prohibitively time-consuming (and expensive) to retrofit the STSim software (purchased for the LiU simulator) to interface with the actuators in the vehicle in the SAAB simulator. The more cost-effective option was to abandon the idea of installing STSim and to engage a contractor (Pixcode) to upgrade the existing software to present urban traffic scenarios with intersections. In hindsight, given the unreliable performance of the STSim software

## Chapter 2 - Getting Started

and opaqueness of the STSim scenario generator, this decision was definitely the right one to make. The experiment run at SAAB using the Pixcode software presented realistic and accurately-rendered replicas of the Sävénäs intersection that elicited frank responses from participants. The simulator at SAAB is now a top-of-the-line experimental facility for studying driver behavior.

### References

Ardeshiri, T., Kharrazi, S., Sjöberg, J., Bårgman, J., & Lidberg, M. (2005). Sensor Fusion for Vehicle Positioning: Intersection Active Safety Applications. *8th International Symposium on Advanced Vehicle Control*. Taipei: Taiwan.

Hydén, C. (1987). *The development of a method for traffic safety evaluation: The Swedish Traffic Conflict Technique*. Bulletin 70, Institut för trafikteknik, LTH, Lund.

Ervin, R., MacAdam, C. Vayda, A., & Anderson, E. (2001). *Applying the SAVME database of inter-vehicle kinematics to explore the natural driving environment*. Transportation Research Board Paper No. 01-0496.

## Chapter 2 - Getting Started

### Figures

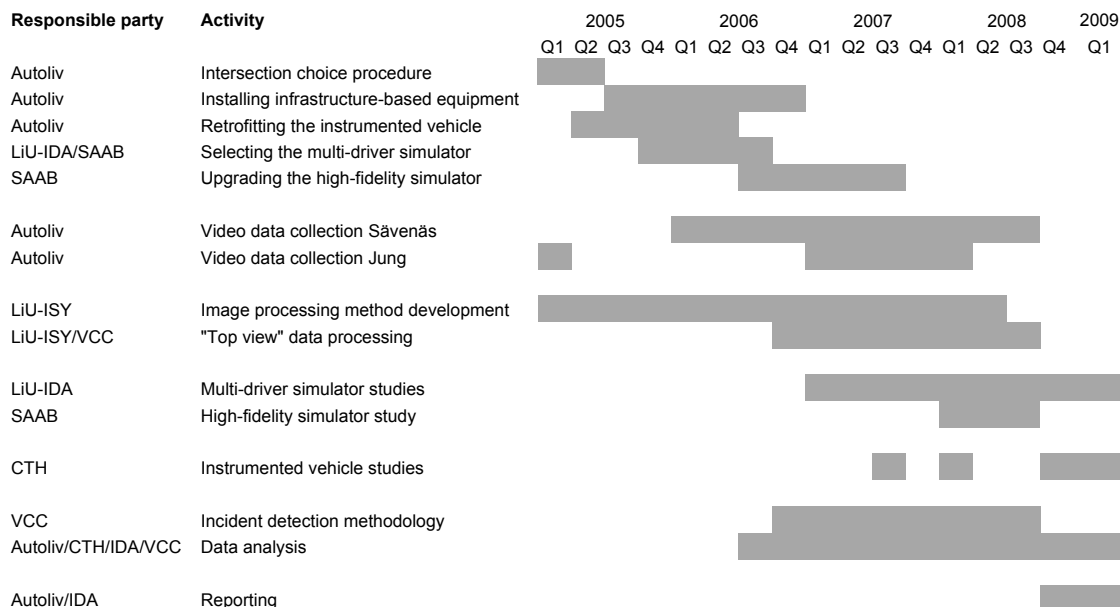


Figure 2.1 The time line for the IVSS project

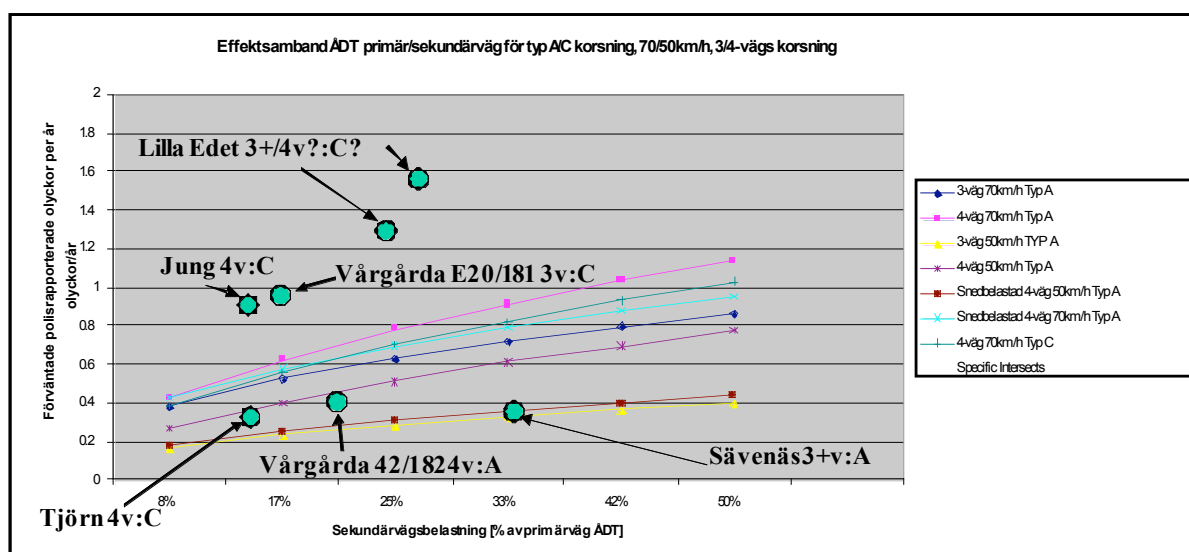


Figure 2.2. Examples of the anticipated number of police reported accidents per year as a function of the intersection type, speed limit and traffic flow on primary and secondary roads.

## Chapter 2 - Getting Started

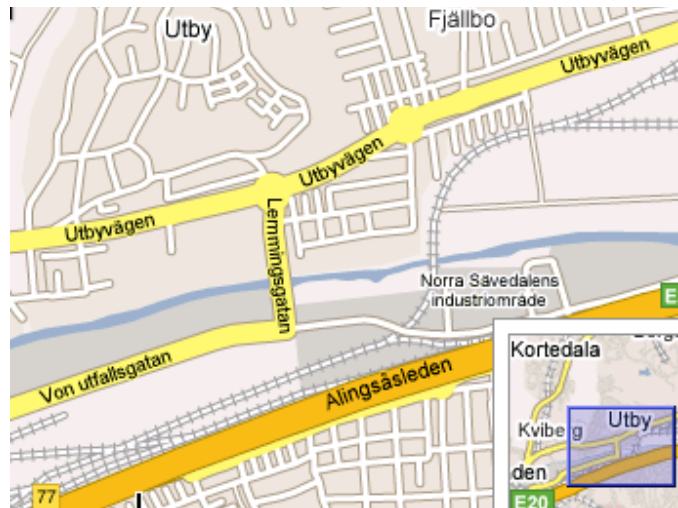


Figure 2.3 The Sävenäs intersection. Traffic from the north must yield to traffic from the east. The primary flow of traffic is from the north to the west and from the west to the north.

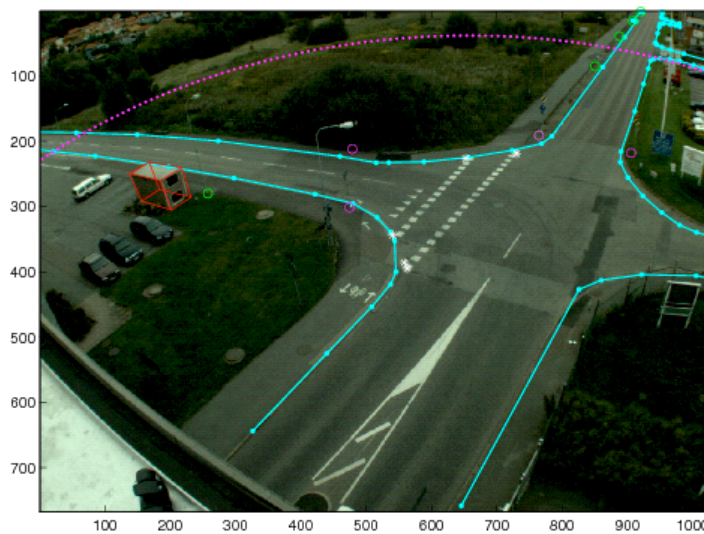


Figure 2.4 The Sävenäs intersection as seen by the camera used to obtain the video data for the image processing analyses. The overlay shows high precision GPS measurements used to calibrate the image processing results and for the design of the simulator model of the intersection.

## Chapter 2 - Getting Started

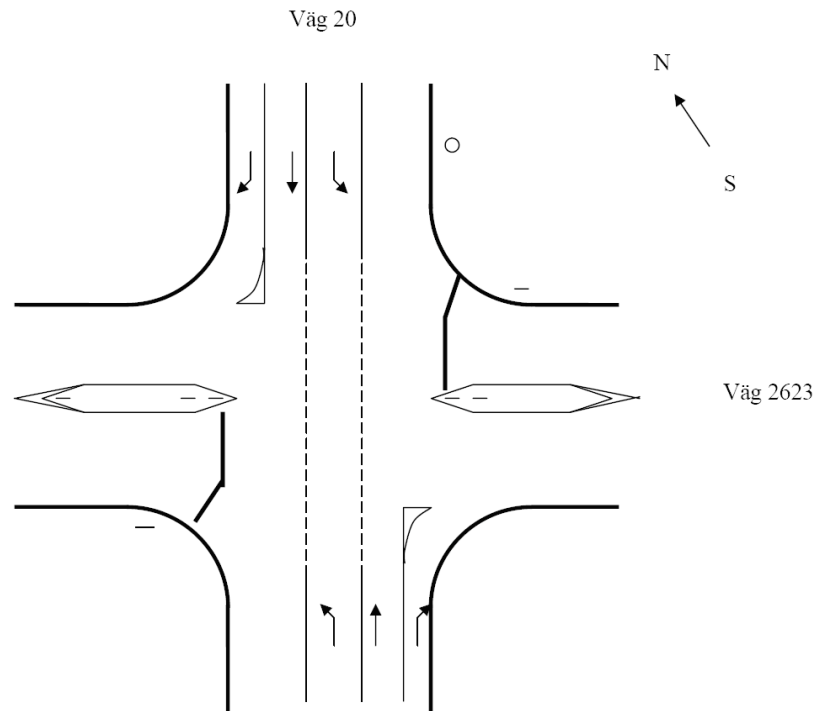


Figure 2.5 Layout of Jung intersection

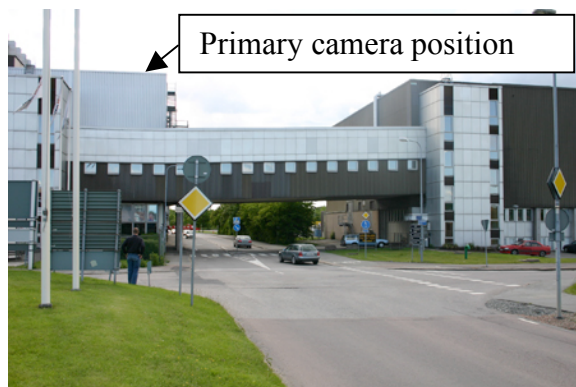


Figure 2.6 Location of the camera on the Renova Combustion Plant on the southwest corner of the Sävsnäs intersection.



Figure 2.7 Locations of the 4 eye-tracking cameras in the cab of the instrumented vehicle.

## Chapter 3 - From Video Images to Vehicle Trajectories

### Overview

This chapter covers the processing steps taken by the image processing system that convert the 2D images captured by the video cameras installed at Sävenäs and Jung into digital records of the 3D trajectories of individual vehicles. The three dimensions are time and the position of the vehicle in Cartesian coordinates (X and Y) measured in meters from the center of the intersection. Trajectories contain {X, Y, T} values at 20 Hz with one line of data for each frame of video in which the vehicle was identified.

The chapter has four sections. The first presents the definitions of terms used throughout this report to describe events in the intersections and the data that capture those events. The second section provides a high-level overview of the automated processing that extracts objects from the video images. The software packages that implement the object extraction were written for this project by the Department of Electrical Engineering, Computer Vision Laboratory, (ISY) at LiU. Their report is attached as Appendix 2 for readers who want more detail about the image processing algorithms. The third section discusses the procedures that identify which objects to identify as valid vehicle trajectories. The final section describes a correction that is made to all tracks generated by the image processing software.

The descriptions in this chapter provide a relatively non-technical, step-by-step account of the process that transforms video images into vehicle trajectories. Table 1 outlines the sequence of steps and provides a map to the discussion here. In Table 1, the temporal sequence of steps is shown from top to bottom. The sequence of artifacts created by during the process starts at the left and moves to the right.

### Definitions

As a vehicle approaches, crosses, and exits the intersection, it defines a PATH. A path is largely an expression of the driver's intent, the rules of the road, and environmental factors. The time-course of a path, defined by its position as a function of time, is its TRAJECTORY. Paths and trajectories exist in the world.

The six paths at Sävenäs are defined by combinations of entry road and exit road, Figure 3.1a. The 12 paths at Jung are defined by the entry direction (south, west, north, east) and action taken in the intersection (left turn, straight, right turn), Figure 3.1b.

Our video cameras made digital recordings of events in the intersections. Contiguous sets of pixels in those recordings contain images of OBJECTS. Objects are digital entities that correspond to events in the world. The time-course of an object is its TRACK. Many of the objects are vehicles and many more are not. The course information processing system extracts objects and their tracks from video data. The trajectory identification system assigns object tracks to vehicle trajectories.

A traffic SCENARIO is a category of paths. The simplest scenarios are 'solo cases' defined by the path taken by one vehicle driving through the intersection alone. Most scenarios are defined by the paths taken by vehicles that are in the intersection during the same span of time. Two systems for classifying scenarios were developed during the course of this project. The classification schemes are discussed in Chapter 5. Each member of a category of scenarios is a CASE.

The problems solved by the coarse image processing system are to identify objects that are likely to be vehicles and to extract a smoothly-varying track for each object. The problem

## Chapter 3 - From Video Images to Vehicle Trajectories

solved by the trajectory identification system is to assess which tracks are likely to be vehicle trajectories. The final process classifies each trajectory as an instance of a traffic scenario.

### Overview of image processing

#### Video data

The video cameras record digital image data and store them in segments of approximately two hours on removable discs with USB connectors. The discs are manually transferred from the intersection acquisition site to a server computer where they can be inspected and processed.

One of the major challenges faced by the developers of the system was to distinguish between a vehicle and the shadow it casts. To minimize shadows and to make them consistent, only the data collected between 11:00 and 14:00 on ‘good days’ were manually extracted for analysis. The relatively high sun angle at midday reduced the length of shadows. A day was judged to be ‘good’ if the ambient lighting was consistent, glare off the roads was low, and the camera lens was clear. The criteria used to classify ‘good’ days were relatively lax to ensure that a large number of tracks were processed. Fleeting shadows caused by small clouds are the primary criterion for rejection on the grounds of inconsistent lighting. Recent rain followed by sun is the primary source of glare off wet roads. Both spiders and birds liked to nest in the camera house, reducing visibility.

The first steps in the image processing rectify lens distortion and compensate for camera motion. Image stabilization was not needed at Sävenäs where the camera was secured to a building but was essential at Jung where the cameras were mounted on tall light standards that swayed in the wind.

#### Coarse image processing

The rectified and stabilized midday images were processed at the National Supercomputer Center running algorithms developed for this project. There were two stages of processing, course and fine tracking. The coarse tracking uses either 12.5% or 25% of the pixels in the original images to speed processing and to obtain first-pass estimates of the  $\{X, Y, T\}$  coordinates of the track of each object. It uses an object’s location in the previous frame (time step) to infer where its location should be in the current frame.

Disentangling sources of occlusion was major challenge to system development. To address this issue, the system discriminates between the background and objects in the foreground. The background (e.g., buildings, trees, and their shadows) remains in the same place across many frames. Objects that move about form the foreground. Most objects are vehicles but some are pedestrians or the shadows of clouds or other sources of confound. The background can occlude foreground objects and foreground objects can occlude each other. For the system to initialize an object, it cannot be occluded by the background or another object. An object is identified by its motion (displacement across frames) and size.

In essence, the tracking system generates a 3D box for each object and finds the size and orientation of the box that best fits the object, frame by frame. Boxes, like vehicles, cast shadows. The optimization of box size and orientation takes the expected length and orientation of shadows into account. The dimensions and orientation of the box are inputs to an extended Kalman filter in the 3D ground plane domain. The filter generates an estimate of the location of the center of the bottom of the box on the ground (road) in the current frame. This estimate and previous estimate constrain the estimate made in the next frame. The sequence of estimates define the  $\{X, Y, T\}$  coordinates of the object’s track.



## Chapter 3 - From Video Images to Vehicle Trajectories

The tracks defined by the coarse image processing are the inputs to the second stage of processing, trajectory identification. Implementation details and remaining challenges are discussed in Appendix 2.

### Fine image processing

The third stage of processing is an optional, fine-grained analysis of object tracks that differs from the coarse processing in two critical ways. First, it uses the entire pixel array (rather than only 25%). Second, it takes as input both the video images and the trajectories identified in the second stage (discussed below). Like the coarse processing, the fine processing uses a Kalman filter to estimate the location of the center of the box that represents a vehicle. Unlike the coarse processing, it uses the trajectory to guide the estimate of the position of the box in the next frame. No new objects are generated. The output is a refined version of the assigned trajectory. The processing is done at the National Supercomputer Center. Implementation details are discussed in Appendix 2.

### Data format

Both the coarse and fine image processing write files in a standard format. Every object is a data structure with vectors of time, location, velocity etc. The format is readable by the commercial software package Matlab© ([www.Mathworks.com](http://www.Mathworks.com)) which is used extensively in the trajectory identification process.

## Trajectory identification

### Principal trajectories - archetypes of paths

Vehicles traveling through an intersection typically follow a distinct path. They enter the intersection within a specific lane on a road. They cross the intersection or turn and then exit the intersection within a specific lane on another road (or the extension of the same road). In a video image, vehicles enter the frame at a specific point, cross the (known location of the) intersection, and exit the frame at another specific point.

Principal trajectories are archetypes of common paths. The six paths at Sävenäs are shown in Figure 3.1a and the twelve paths at Jung in Figure 3.1b. Principal trajectories form the basis for automating a mechanism for winnowing good tracks from bad. For example, the image processing system can have difficulty distinguishing between a vehicle and the shadow cast by a small cloud. Most vehicles roughly follow to one of the principal trajectories. The shadows of clouds do not. An extraneous track can be excluded from subsequent analysis by comparing its track with the set of principal trajectories.

The original implementation of interactive software that defines principal trajectories was written for this project by Volvo Car Corporation (VCC). Their documentation is attached as Appendix 3. The input to the algorithm is a data set of tracks defined by the coarse image processing system. The algorithm identifies the entrance and exit points for every track within the data set. It clusters them to define a small set of entry point and exit points. It prompts the user to draw boxes to identify the entry and exit zones at the end of each road.

After the manual identification, the algorithm identifies all tracks that begin in a given entry zone and end in a given exit zone. The average of these tracks is defined as the principal trajectory for that path. The averaging procedure uses space (distance from the known center of the intersection) rather than time. The output are the  $\{X, Y\}$  coordinates of the most common paths taken by vehicles through the intersection.

## Chapter 3 - From Video Images to Vehicle Trajectories

### Track repair

The tracks generated by the image processing system do not always capture the trajectories by vehicles through the intersection. There are three prominent sources of confound. First, some tracks are generated by objects that are not vehicles (e.g., the shadows of clouds). Second, a vehicle's trajectory can be broken into several pieces and represented by multiple objects and their tracks. Third, an object can be occluded by another object and its track captured by that object. Track capture can occur when a short vehicle passes behind (from the viewpoint of the camera) taller vehicle.

The track repair algorithms identify extraneous tracks and fix broken and captured tracks. There were two steps in this process. The first was to establish quality measures that identify and monitor defective tracks. The second applies the measures to a data set to transform broken or captured tracks into a trajectory that better emulates a principal trajectory. As shown in Table 3.1, these algorithms operate on tracks, not on video data.

### Quality metric

Nine measures of the quality of a track are used to assess the likelihood that a track captures a portion of a vehicle's trajectory. The nine measures are:

- Number of frames (an index of time duration)
- Track length
- Minimum distance to the center of the intersection
- Largest jump (change in X and Y) between frames
- Largest span (the greater of the distances traveled in the X and Y directions)
- Rotation quality (the maximum change in orientation divided by the track length)
- Average distance to the best matching principal trajectory
- Length of track parallel to the matching principal trajectory
- Confidence in the fit to the matching principal trajectory

The measures are summed to form an aggregate quality metric. The larger the value of the metric, the greater the likelihood that the track represents the entire trajectory of a vehicle through the intersection. The value computer for a track is compared to a standard threshold. Objects with tracks that exceed the threshold are assumed to represent a vehicle.

Tracks that meet the threshold are flagged as 'repaired' (even though no repair was needed). Tracks that fall short of the threshold are not immediately deleted. They are flagged as low quality and become available to the track repair algorithms.

### Good trajectories

The first of the automated repair algorithms sorts the low quality tracks to exclude those that are unlikely to represent segments of trajectories. The sorting procedure uses as criteria the median values of the headings of the principal trajectories entering and exiting the intersection. Any object with a track with a heading that deviates from these medians is assumed to be something that will not influence the paths taken by drivers, e.g., a flag, cloud, spider, or bird. These objects are removed from the calculations.

This process risks excluding actual vehicles on non-standard trajectories. The tolerance for deviation from a principal trajectory was set by inspection of the video sequences so that

## Chapter 3 - From Video Images to Vehicle Trajectories

there are few cases where “good” objects were removed. It is likely that “bad” trajectories remain in the dataset.

### Splitting

The second repair algorithm deals with the problem of track capture, cases in which a track appears to jump from one object to another. An example is shown in Figure 3.2. The dark blue vehicle with the yellow track in Figure 3.2a has the right of way and is turning left. The image processing software inferred that it continued straight ahead. What has likely happened in this example is that the image processing ‘lost’ the object corresponding to the turning vehicle when it became occluded by the yielding vehicle that is waiting to turn left. Once it begins the yielding vehicle begins to turn, it is identified as a new object that traces the green track. The image processing software, having lost the original object and finding a new trace, assumes the two should be linked and creates the bizarre trace shown in Figure 3.2a.

The splitting is done by monitoring the deviation from the closest principal trajectory. A track is considered to have jumped when suddenly begins to deviate from a principal trajectory and then the deviation continues to increase. The point where the sudden deviation starts is used as point where the track is split, Figure 3.2b. Tracks that are split are flagged as ‘repaired’. The algorithm is able to handle multiple splits by the same object.

### Merging

The third repair algorithm identifies short segments of tracks that follow a principal trajectory but that fail to meet the criterion for length. The algorithm attempts to merge two or more of these broken tracks to form a more complete track. The process begins by identifying a broken track (as flagged by the quality process). It looks for tracks that (a) begin shortly after that track ends, (b) that might be following the same principal trajectory, and (c) are no further away from the principal trajectory. If a match is found, the two segments are merged using interpolation and flagged as ‘repaired’. The repair shown in Figure 3.2c contains several instances of track merging.

### **Matching tracks to trajectories**

Every repaired track is subjected to a series of tests to determine whether it qualifies as a valid trajectory. If it qualifies, it is compared to the set of principal trajectories to identify which trajectory it best matches. The numerical thresholds used as criteria for the testing and matching were defined by iterative manual analysis.

### Distance traveled

To qualify as a trajectory, the length of a track, at either Sävenäs or Jung, must exceed 30m. This criterion excludes a lot of noisy tracks. The value 30 m was chosen because the distance between the center and western boundary of the camera coverage at Sävenäs. A greater distance would have eliminated many good trajectories on the road to and from Göteborg. As the range of coverage is greater at Jung, tracks shorter than 30 m are likely to be damaged and are viable candidates for exclusion.

### Minimum distance to the center of the intersection

Many tracks terminate before they reach the intersection or begin after exiting the intersection. Figure 3.3a is an example from Sävenäs. This track suggests that object #1960 proceeded south on the secondary road and veered sharply into the oncoming lane before entering the intersection. As this is an extremely unlikely event, a criterion is needed to sort out this type of track. At Sävenäs, the criterion was set to 9 meters from the center of the

## Chapter 3 - From Video Images to Vehicle Trajectories

intersection on the basis of cases like that shown in Figure 3.3b. In this example, object #267 hugged the curb while making a right turn from the secondary road onto the main road. The minimum distance between this track, and others like it, is slightly less than 9 meters. As these tracks appear to be valid trajectories, the criterion can be no greater than 9 meters.

### Crossing the intersection

Due to errors in the image processing, there are many broken tracks that cannot be merged with other broken tracks. At Sävenäs, this is especially common when vehicles on the secondary road yield to vehicles on the primary road. (Stationary objects disturb the Kalman filter.) Figure 3.4a shows an example. Track #275 ends within 9 meters of the center of the intersection but cannot be unambiguously assigned to a trajectory. In contrast, there is not ambiguity about the track #747, Figure 3.4b. Even though a large part of the trajectory is missing, there is no doubt that this object represents a vehicle entering the intersection from the north.

To exclude the former type of track while retaining the latter, it is necessary to set criteria that require a track to cross the intersection. To be considered valid at Sävenäs, a track must be more than 2 meters long on both sides of the center of the intersection. The criterion at Jung is 7 meters to accommodate its greater size.

### Matching the track to a principal trajectory

Repaired tracks that survive these tests are candidate trajectories. A track is assigned a trajectory using the sign and value of the  $\{X, Y\}$  coordinates of its start and end points. For example, consider track #267 of Figure 3.3b. Because the center of the intersection is set to  $\{0, 0\}$ , this track starts at a large positive value of  $Y$  and a near zero value of  $X$ . It ends with a large negative value of  $X$  and a near zero value of  $Y$ . This combination is unique to trajectory 2, Figure 3.1a.

### **Filtering**

Not all valid trajectories can be used in the analyses. There are two additional processing steps that winnow valid trajectories.

### Maximum distance from principal trajectory

The first process filters out trajectories that match a principal trajectory but consistently different from it. Figure 3.5 provides an example of a mismatch to trajectory 1 at Sävenäs. This object is probably a bicycle on the path that runs parallel to trajectory 1. The algorithm computes the average distance between the trajectory and its principal and compares it to a threshold. The threshold is set to 5 meters at both Sävenäs and Jung.

### Size criterion

The second filter is different than all the rest of the procedures described in this chapter. Although trucks are a factor in traffic, the technical limitations of the image processing system made it necessary to remove truck traffic from the analysis. Accordingly, all traffic sequences in the intersections involving a vehicle longer than a criterion are excluded from the analysis. The criterion vehicle length is 5 meters at Sävenäs and 8 meters at Jung. The greater length at Jung reflects the improved resolution of objects by the multiple camera system at Jung. At a later stage of processing discussed in Chapter 5, the scenario classification system developed by Chalmers removes all trajectories when a long vehicle is present.

## Chapter 3 - From Video Images to Vehicle Trajectories

### Tracks that become trajectories

Only 30% of the tracks extracted by the coarse video processing system survived the track repair, matching and filtering processes. The 30% are deemed valid trajectories, are assigned to scenarios, and used in the analyses described in the following chapters. The majority of the 70% that are removed are non-traffic objects like shadows of clouds, and spiders on the camera lens. Some are broken and otherwise irreparable tracks.

### **Post-hoc offset correction**

#### **Quality checking**

Trained technicians conducted an analysis of the accuracy of the tracks generated by the course image processing system. The analysis used the 'Hedvig tool', a video viewer (custom-built for this project) that superimposes vehicle tracks upon replays of the original video sequences. Hedvig supports a wide range of viewing options from frame-by-frame still images to rapid replay the combined track and video images. It also accepts data entry from the user.

The analysis consisted of a frame-by-frame comparison of the tracks from 20 different vehicles, 5 vehicles on each of 4 different days. Hedvig was used to display the original video frames (without their tracks). By using the computer mouse to click on the image, the technician was able to specify the {X, Y} coordinates of the point on the ground below the center of a vehicle. The point was meant to represent 'ground truth'. Generating the ground truth files was labor intensive but highly rewarding.

#### Result

Comparison of the manually specified ground truth files with the tracks generated by the image processing software uncovered a consistent bias with respect to the vehicle's distance from the camera. We call the difference between the manually specified {X, Y} coordinates (ground truth) and those generated by the image processing the 'offset';  $\text{offset} = \text{actual} - \text{calculated}$ . The systematic offset has the following characteristics:

- For tracks moving away from the camera's fixation point, the track is consistently behind the video image of the vehicle. The offset is towards the camera.
- For tracks moving toward the camera's fixation point, the track is consistently in front of the video image of the vehicle. The offset is again towards the camera.
- For both directions of travel, the amplitude of the offset within the intersection is approximately 1m. The amplitude increases with distance from the intersection.
- The magnitude of the bias in the lateral direction (within a lane, Y) is less than in the longitudinal direction (along the path, X).

The offset in locations is sufficiently consistent from frame to frame that it does not appear to introduce a significant bias to the velocity data. Applying an offset correction will, of course, produce a change in the velocities.

#### Implications

The offset shifts each track toward the camera. Computations based upon the tracks will, accordingly, be incorrect. The offset precludes the reliable detection of encroachment when actual vehicle separations are less than 2 m. The tracks are likely to indicate the vehicles collided.

## Chapter 3 - From Video Images to Vehicle Trajectories

The analysis indicated that post-hoc correction was needed to generate tracks that can be relied upon when conducting analyses of trajectory data.

### Correcting the offset

#### The model

A set of post-hoc corrections was generated by finding the best-fit least-squares multiple regression models for the offsets observed on each of the paths through the intersection (6 paths at Sävenäs, 12 at Jung). Predictor variables are the X (E-W) and Y (N-S) coordinates from the image processing data. The response variable is the magnitude of the offset. The model generates beta coefficients for the constant, X, Y, XY, X<sup>2</sup> and Y<sup>2</sup>.

$$\hat{d} = \beta_0 + \beta_1x + \beta_2y + \beta_3xy + \beta_4x^2 + \beta_5y^2 \quad (3.1)$$

The weights differ across the different paths.

#### The correction

The correction procedure applies the beta weights to shift the trajectory data so that the point assigned to the center of the vehicles corresponds better to the actual location of the vehicle.

The first step in the procedure applies the beta weights to the locations specified by the image processing software for each frame of a trajectory,  $\{x_0, y_0\}$ . The output for a frame specifies a value of  $\Delta(d)$ , the best estimate of the correction to the offset. The direction of  $\Delta(d)$  is towards of the camera; its length is the hypotenuse of a triangle that has its sides in the X and Y directions. The correction needs to be in these direction. Accordingly it is necessary to calculate the angle  $\alpha$  between the camera location  $\{x_{cam}, y_{cam}\}$  and the vehicle location:

$$\alpha = \arctan\left(\frac{y_0 - y_{cam}}{x_0 - x_{cam}}\right) \quad (3.2)$$

The second step is then to calculate the components of  $\Delta(d)$  in both the X and Y directions and add them to the original coordinates. The corrected trajectories positions are:

$$\begin{cases} x_1 = x_0 + \hat{d} \cos \alpha \\ y_1 = y_0 + \hat{d} \sin \alpha \end{cases} \quad (3.3)$$

This shift is the only correction required at Jung and along the main road at Sävenäs.

#### Additional correction for the secondary road at Sävenäs

Using Hedvig, it was found that the corrected trajectories along the secondary road at Sävenäs required a second correction. Only those portions of trajectories along the north road at distances greater than 5 m needed the additional correction. None of the trajectories at Jung needed an additional correction.

The oblique viewing angle of the one camera made it difficult to accurately place the 'ground truth' below the vehicle along the secondary road. As a result, the manual procedure systematically misplaced the location systematically to the east (away from the camera). To correct this error, the coordinates of trajectories along the secondary road were shifted by:

$$\Delta N = \begin{cases} 0 & \text{if } y_1 \leq 5 \\ \frac{(y_1 - 5)}{17.5} & \text{if } y_1 > 5 \end{cases} \quad (3.4)$$

### Chapter 3 - From Video Images to Vehicle Trajectories

Once again, it was necessary to extract the components of this shift in the X and Y directions. Because the direction of the main road is not due east-west but is rotated 3° counter clockwise, the direction of the correction is 183° with 0° defined as East. The final coordinates become:

$$\begin{cases} x_2 = x_1 + \Delta N \cos 3^\circ \\ y_2 = y_1 + \Delta N \sin 3^\circ \end{cases} \quad (3.5)$$

#### Figures

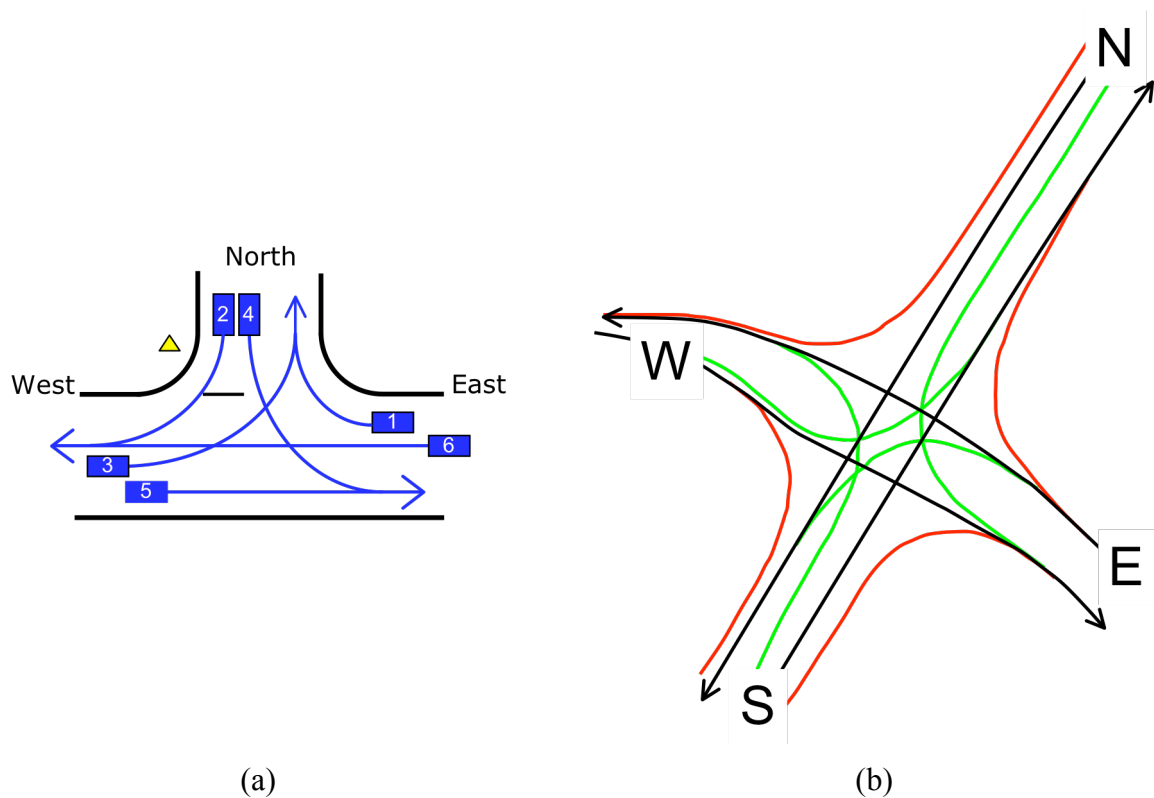


Figure 3.1 The labeling schemes used to define (a) the 6 possible trajectories through the Sävenäs intersection, and (b) the 12 possible trajectories through the Jung intersection. The labels for the trajectories at Jung have two letters. The first letter indicates the cardinal direction of entry into the intersection (N, E, S, W). The second indicates the path taken (L for left turn, shown in green, S for straight, black, and R for right turn, red).

### Chapter 3 - From Video Images to Vehicle Trajectories

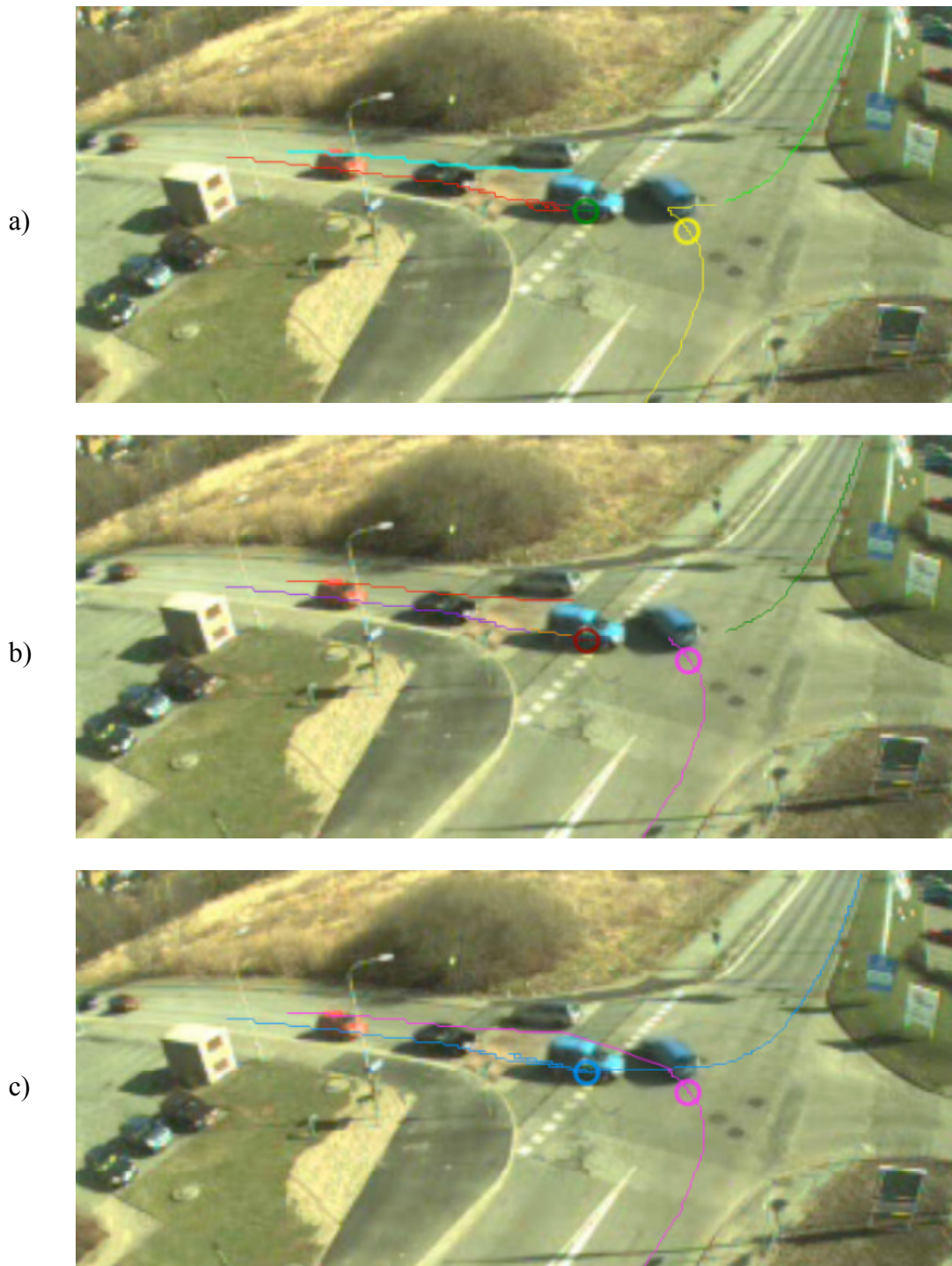


Figure 3.2 An example of automated track repair. The images were created by the software package Hedvig developed for this project. Hedvig superimposes the tracks generated by the image processing system upon the video data captured by the cameras. The circles represent estimates by the coarse image processing system of the current locations of the center of the vehicles. (a) The output from the image processing. The (yellow) track of the vehicle turning left has been captured by the (green) track of the vehicle waiting to turn left. (b) Repaired tracks after automatic splitting. (c) Repaired tracks after automatic splitting and merging.



### Chapter 3 - From Video Images to Vehicle Trajectories

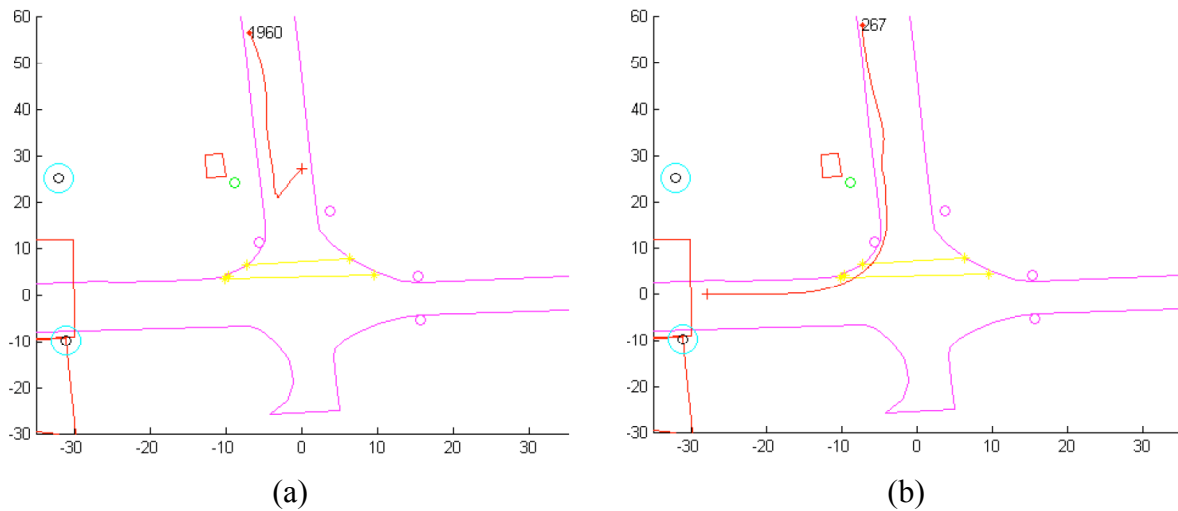


Figure 3.3 Tracks that illustrate the need for a criterion for the minimum distance to the center of the intersection. (a) A track that terminates prior to the intersection cannot be fit to a trajectory and must be excluded. (b) A track that appears to be a valid trajectory is retained. The minimum distance criterion is 9 meters at Sävenäs and **XX** meters at Jung.

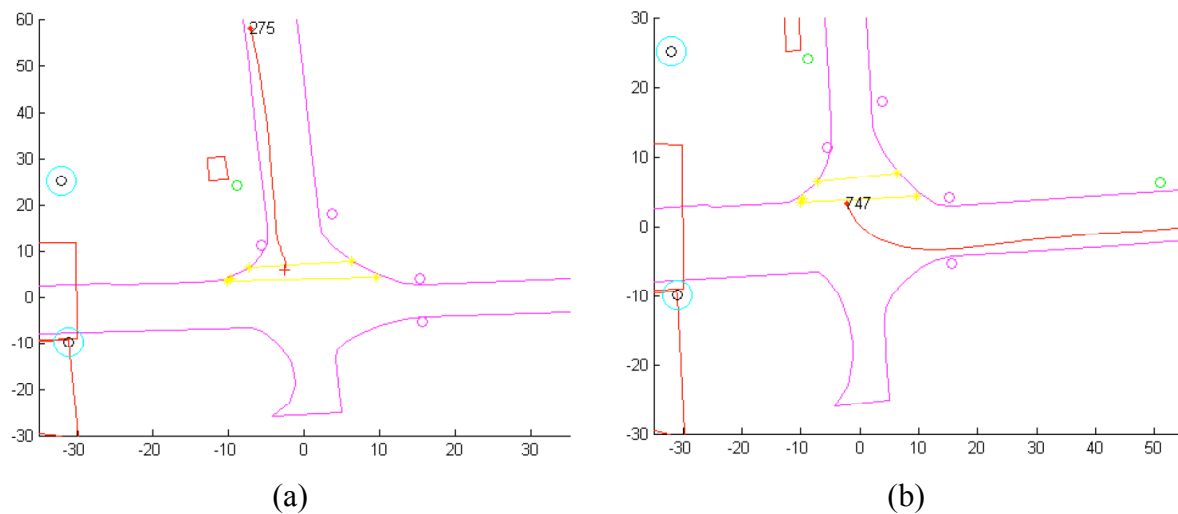


Figure 3.4 Tracks that illustrate why a valid track must cross the intersection. (a) A track that passes the 9 meter criterion but that terminates prior to the intersection. (b) A track that appears to be a valid trajectory. The criteria for the length of a track on both sides of the center point is 2 meters at Sävenäs and 7 meters at Jung.

### Chapter 3 - From Video Images to Vehicle Trajectories

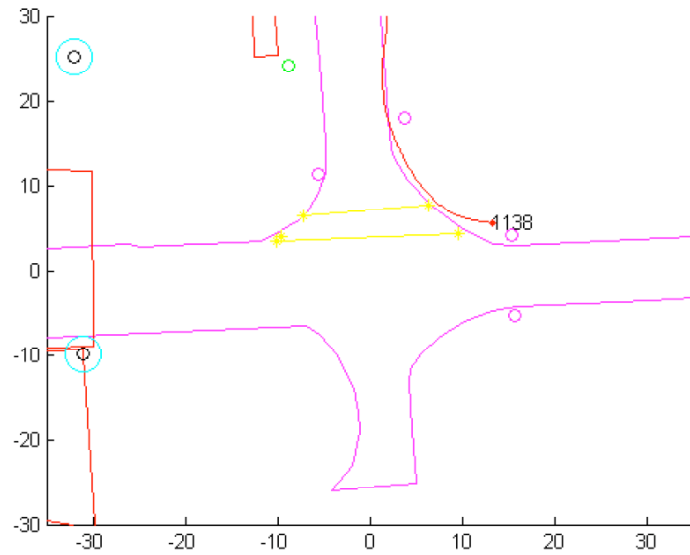


Figure 3.5 A track that parallels a principal trajectory but is consistently far from it. The object that generated this track is probably a bicycle on a bike path. The criterion for the maximum allowable difference between a track and its best matching principal is 5 meters at both Sävenäs and Jung.

### Chapter 3 - From Video Images to Vehicle Trajectories

Table 3.1 Overview of the sequence of input and output that transforms 2D video images into refined 3D {X, Y, T} trajectories of individual vehicles.

	Images	Objects		3D Trajectories				Scenarios
	2D pixels	With 3D tracks	Repaired tracks	Principal	Initial	Valid	Refined	
Video	OUT							
Coarse image processing	IN	OUT						
Trajectory identification								
Principal trajectories		IN		OUT				
Track repair		IN	OUT					
Match track to trajectory			IN	IN	OUT			
Filtering					IN	OUT		
Post-hoc offset correction						IN	OUT	
(Fine image processing)	IN						IN/OUT	
Scenario assignment							IN	OUT

## Chapter 4 - Fundamental definitions and preliminary analyses

### Definitions of traffic scenarios in intersections

This chapter presents and illustrates the application of fundamental methods to classify traffic scenarios and to detect and quantify incidents or accidents. The first-stage analyses in this chapter form the basis for the analyses present in the chapters that follow.

#### Geometric classification

This classification approach provides a general method that can be applied to *any* three- or four-way intersection. It can also—in a logical and straight-forward way—be further developed to meet the requirements of different analysis purposes. The procedure is here presented in two steps: first the geometrical classification concerning the vehicle's trajectory in relation to the physical intersection; and second, the interaction classification that describes that trajectory in relation to other road-users.

The first step in the classification is to define a division of the intersection layout with Zones as shown in Figure 4.1. The image processing data provide the spatial definition of the Sävenäs intersection and hence can be used in the definition of the intersection zones. A bird's eye view of the zones at Sävenäs is depicted in Figure 4.2.

In the next step, a Road Segmentation system is provided. In a typical four-way intersection, with one lane in each direction, it is possible to identify and define entry, exit and central zones. Taking into account traffic dynamics when vehicles are approaching the central part of the intersection, entry lanes are further divided into four zones, whereas exit lanes are represented by two zones as is shown in Figure 4.1.

- Entry zones: A1 to A4, B1 to B4, C1 to C4, D1 to D4
- Exit zones: A, A5, B, B5, C, C5 and D, D5
- Central zone: Z

The Core of the intersection consists of the central zone and four entry and exit zones surrounding it. The nine shaded zones in Figure 4.1 constitute its ideal representation. The length of the lane zones can be easily modified by means of the variable named *bl* (box length, typically set equal to 5-10 meters).

Further, the intersection Center is the region where all four lanes merge together, starting where arriving vehicles begin to turn. In Figure 4.1 it is represented by the central square labeled *Z*. This is the zone where most of the intersecting conflicts may actually happen. Therefore, taking into account the real characteristics of an intersection, the central zone can be further divided into smaller zones. With a higher resolution, it is possible to identify clusters of conflict points and also discover groups of events with similar driving patterns.

Finally, a Trajectory type is identified according to the sequence of zones that a vehicle visits. The zones form the basis for the classification system summarized in Table 4.1. In Table 4.1, all possible legal trajectories have the general sequence: entry zone, central zone, exit zone. Every vehicle that reaches the central zone of an intersection has four possible alternatives: turn right, go straight, turn left or make a U-turn. As there are four possible ways to arrive at the central zone, there are 16 different trajectories. If the object's trajectory does not fulfill these requirements it is classified as 'other'.

#### Interaction classification

A fundamental variable named *interact* is created for each object (vehicle) and then filled in with relevant information related to the characteristics of its interaction with other vehicles.

## Chapter 4 - Fundamental definitions and preliminary analyses

Interactions are observed and analyzed when they occur within the intersection core.

The Number of vehicles (NoV) is defined as the total number of cars per time unit that pass through the intersection (or, depending on the upcoming analysis, by some subset of the intersection defined by an arrangement of predefined zones; for example, the intersection core).

Then, the following categories are identified: the single-car situation, the fundamental two-car situation, and the general multiple-car situation. Cases in the last category can be treated as simultaneous combinations of two-car situations.

Now a Scenario can be defined as an observation of two interacting vehicles, and further classified according to the combination of the trajectories made by those two vehicles. When there is a multiple-vehicle interaction the corresponding number of scenarios is obtained using a simple sum:

$$N_{scenario} = \sum_{i=1}^{n-1} i = \frac{n(n-1)}{2},$$

where  $n$  is the total number of interacting vehicles. A single-car scenario refers to the case in which only one vehicle passes by the intersection.

According to the combination of vehicle paths, the following categories outline the scenarios:

- Crossing; scenario with vehicles with intersecting paths.
- Merging; scenarios with vehicles moving from different to the same direction.
- Splitting; scenarios with vehicles moving from same to different directions.
- Following; scenario with one vehicle behind another vehicle that is moving ahead or waiting.
- Oncoming; scenario with oncoming traffic, none of the parties have the intention to turn and cross over the opposite lane.
- General; any other scenario.

Within each of these categories, specific scenarios can be defined. Crossing-path scenarios, the focus of analyses presented later in this chapter, include the four cases listed in Table 4.2: Left Turn Across Path/Opposite Direction (LTAP/OD), Left Turn Across Path/Lateral Direction (LTAP/LD), Straight Crossing Paths (SCP) and Leaving by Left - Arriving by Right (LL-AR).

### Traffic scenarios observed at Sävenäs

This section presents the results of applying the scenario classification method to the image processing data from Sävenäs. Note that the analyses presented here do not make the selections and delimitations of the data that are made for the second stage of analysis presented in Chapter 7. As discussed there, the second stage analysis excludes interactions with heavy vehicles and restricts the definition of encroachment to the first car in a string of cars when an encroaching vehicle crosses its path. Hence, the data presented here should be interpreted as a holistic description of the complete dataset from Sävenäs.

## Chapter 4 - Fundamental definitions and preliminary analyses

The frequency of the most common trajectories in the Sävenäs dataset are shown in Figure 4.3. As there are very few vehicles driving straight from the south, it is naturally expected to have a minimal number of SCP scenarios.

Table 4.3 presents the distribution of interactions considering the number of interacting vehicles. The single-car scenario was the most frequent type of interaction. Interactions that involved more than 6 vehicles were not identified due to limitations in the extraction of data from the video files.

The number of interactions is clearly affected by the number of objects present in the input data. Figure 4.4 sketches the influence of the omission of objects over the number of identified interactions with different cases of NoV involved. This assessment is useful in estimating the consequences of missing actual objects with usable trajectories that were not correctly extracted from the video files and/or were not classified as appropriate.

The outline scenario-categories are distributed as in Table 4.4. Crossing scenarios represent 13%.

The distribution of interactions classified within crossing-path scenarios are presented in Table 4.5. Leaving by Left/Arriving by Right (LL/AR) represents almost 45% of the interactions.

An illustration of the spatial distribution of all identified encroachment zones in Sävenäs is presented in Figure 4.5. Since the scenarios LTAP/OD, LTAP/LD and LL/AR are the most frequent cases, and recalling that they are mainly characterized by the combinations of trajectories shown in Table 4.5 (see also Figure 4.3); it is natural that the central point of the distribution is somewhat offset (towards the north-west from the central point of the intersection).

### Definition of metrics of safety

In this section, fundamental methods are provided for defining safety indicators using the data from the image processing system. These procedures are based upon established definitions of each measure.

#### Post-encroachment time

Post-encroachment time (PET) is defined as the time measured from the moment in which the first road user leaves a potential collision zone (encroachment zone) to the moment in which the other road user enters this zone (Allen, Shin, & Cooper, 1977).

#### Distance between vehicles

Distance between vehicles (DBV) is the (continuously measured) minimum distance between two vehicles (León Cano & Kovaceva (2008)). It is estimated as the distance between the two closest points corresponding to each vehicle. The computed minimum distance is then used to estimate the approaching speed of two vehicles.

#### Time to collision

Time to collision (TTC) is defined as the extrapolated time until a collision would occur (keeping the heading and speed of both vehicles constant).  $TTC_{min}$  is the minimum TTC in all the interaction (Hayward, 1972)

## Chapter 4 - Fundamental definitions and preliminary analyses

### Method

Several indicators are computed based on the interaction of two vehicles. One vehicle is identified as the subject vehicle (SV) and the other is identified as the interacting vehicle (IV). These can be addressed to any (or combinations) of the classifications described above for directed analysis.

Among the most relevant input parameters are

- Object identifier of the IV
- Interacting time (duration)
- Minimum distance to the IV (considering both vehicles as particles). This is used to estimate the spatial distribution of conflict points within the intersection.

DBV is computed at each interacting time step. For this purpose, the approach of each vehicle silhouette uses simple geometrical shapes that embody the actual vehicle's 2D layout. Then, DBV is simply equal to the minimum distance between those simple shapes as depicted in Figure 4.6.

The calculation of TTC for each position point (time step) is implemented as follows:

1. An extrapolation of the trajectory of each vehicle in the direction of the current heading and with the current speed is done (straight line for each vehicle).
2. A set of time-dependent collision equations are solved in order to find the time at which a collision would occur between the two vehicles. If this time is negative or not real (i.e., the extrapolated trajectories do not produce a collision), TTC is set equal to infinite.

The Computation of PET (single value) follows three main steps as illustrated in Figure 4.7;

1. The intersection point of two crossing trajectories is identified.
2. Both vehicles, whose shapes are approximated with rectangles, are virtually placed on top of each other at the intersection point (using their central points) with their respective headings. The quadrilateral area defined by the sides of the vehicles (or their projection) constitutes the encroachment zone.
3. The interaction is virtually replayed to identify the elapsed time from the moment in which the first vehicle (leaving object, LO) fully leaves the encroachment zone, until the moment in which the second vehicle (arriving object, AO) enters the encroachment zone.

### Output

Limitations in the extraction of data from the video-files significantly influenced the output when applying these methods to the Sävenäs and Jung datasets. For example, the noise in the data associated with large vehicles is one of the arguments for excluding them from the analyses in the chapters that follow. This also forms the argument for not illustrating the output with figures of the complete datasets, as was done in the previous section on traffic scenarios observed at Sävenäs.

### References

Allen, B., Shin, T., Cooper, P. (1977). *Analysis of Traffic Conflicts and Collisions*, Department of Civil Engineering, McMaster University, Hamilton, Ontario - Road and Motor Vehicle Safety Branch, Transport Canada, Ottawa.

## Chapter 4 - Fundamental definitions and preliminary analyses

Hayward, J.C. (1972). *Near-Miss Determination Through Use of a Scale of Danger*, Pennsylvania Transportation and Traffic Safety Center.

León Cano, J., Kovaceva, J. (2008). *Incident Detection at Intersections - Incident Classification and Thresholds*, Department of Applied Physics, Chalmers University of Technology, Göteborg, Sweden.

### Figures

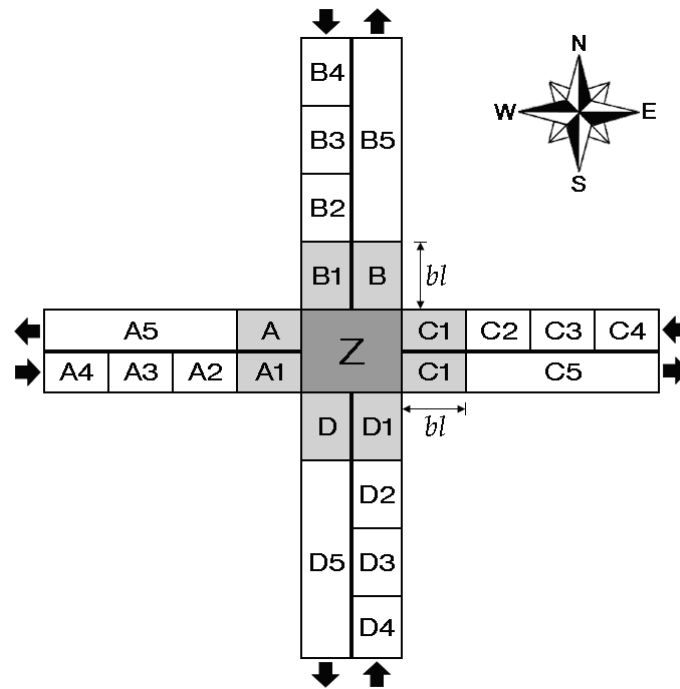


Figure 4.1 Definition of zones for a typical 4-way intersection. The shaded regions constitute the core of the intersection and the arrows indicate the traffic flow directions. The cardinal directions afford direct comparison with the representation of the actual intersection shown in Figure 4.2.



## Chapter 4 - Fundamental definitions and preliminary analyses

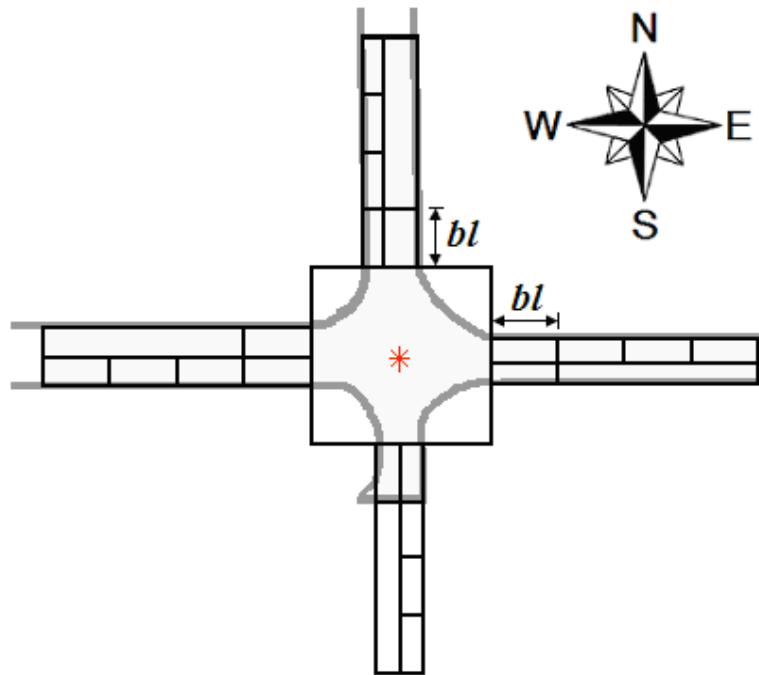


Figure 4.2 Definition of the Zones considering the real size and layout of the Sävenäs intersection. The variable  $bl$  that represents the length of the lane Zones of the core is set equal to 5 meters.

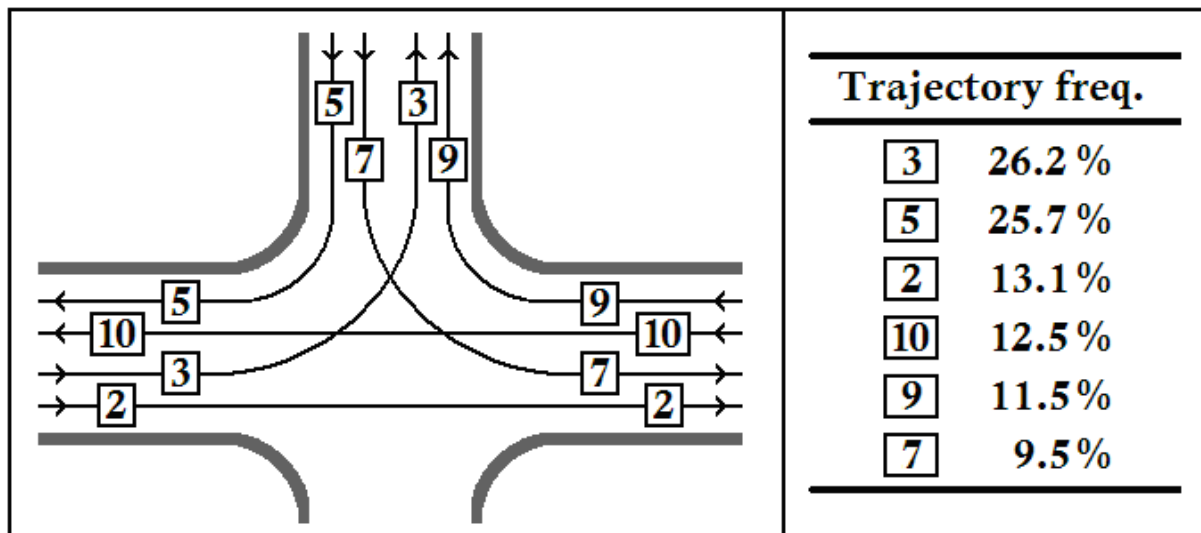


Figure 4.3 Frequencies of the detected—and observed—vehicle trajectories. The frequencies shown here constitute 98.5% of the total number of usable cases. The distribution (in descending order) of the rest of trajectories and their corresponding frequencies are: 15, 0.421%; 1, 0.413%; 13, 0.182%; 8, 0.109%; 4, 0.102%; 14, 0.095%; 11, 0.082%; 6, 0.057%; 12, 0.033%; 16, 0.006%.

## Chapter 4 - Fundamental definitions and preliminary analyses

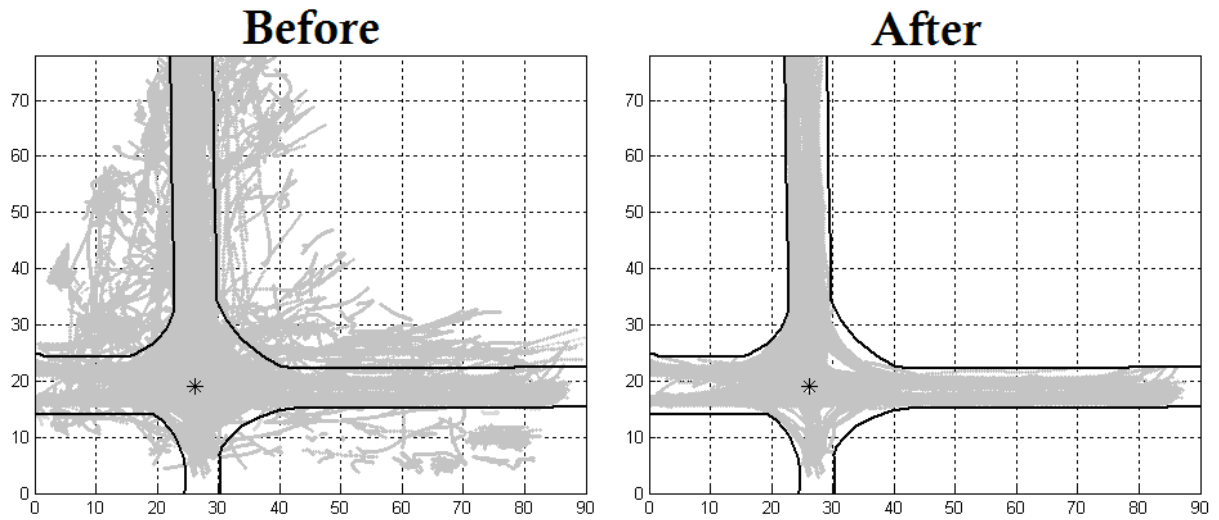


Figure 4.4 Outcome of the trajectory quality-checking procedure. In this example a file that has 2000 objects was pre-processed. A total of 1000 objects with usable trajectories were classified as good enough.

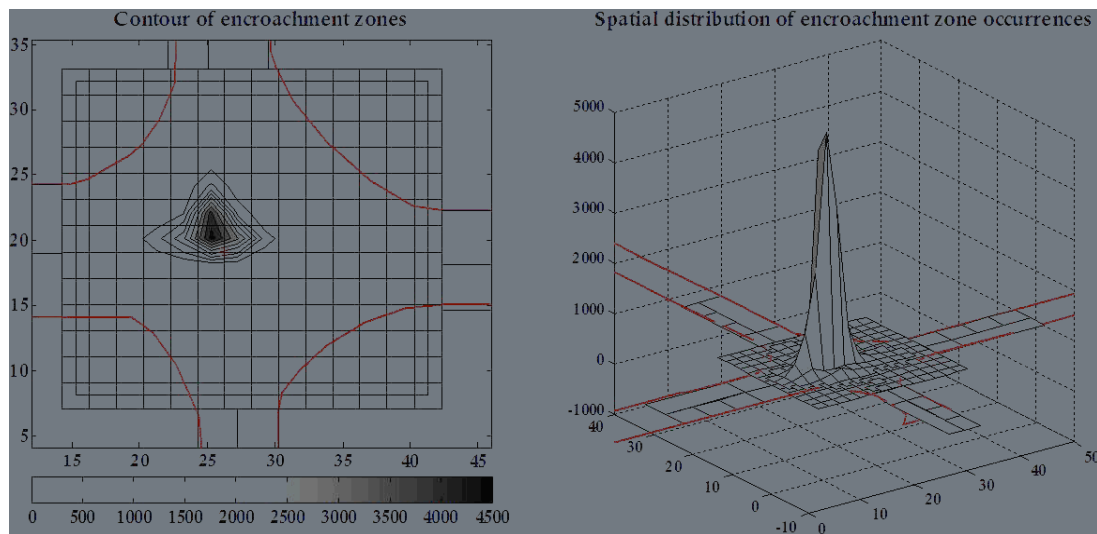


Figure 4.5: Distribution of the occurrences of encroachment zones in Sävenäs. Here, the zone that represents the intersection centre is further divided into a grid of little squares of metres arranged in 13 rows and 14 columns.

## Chapter 4 - Fundamental definitions and preliminary analyses

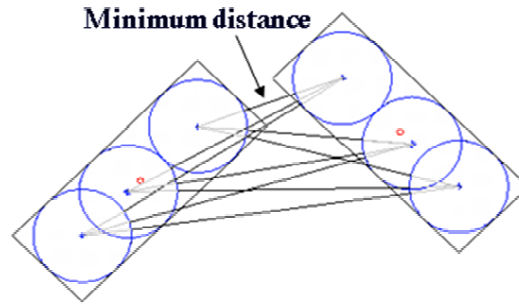


Figure 4.6: Computation of DBV by using arranged sets of circles to represent the vehicles' silhouettes.

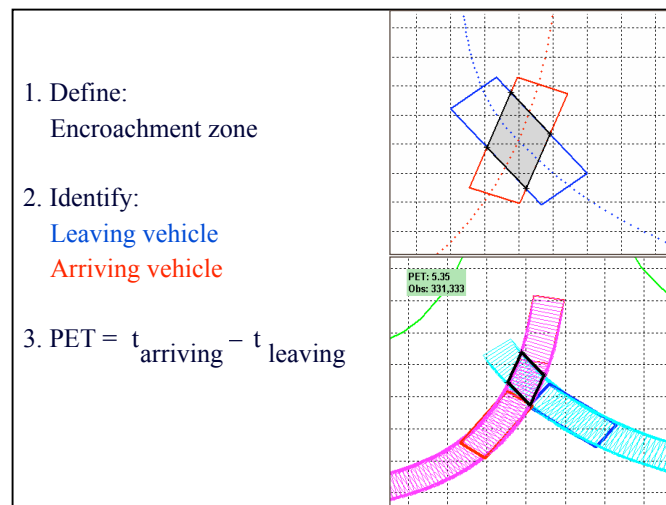


Figure 4.7: Main principle of computation of PET.

### Tables

Table 4.1 Numbering scheme for legal trajectories.

Trajectory ID	Entry	Exit
1	A1	D
2	A1	C
3	A1	A
5	B1	A
6	B1	D
7	B1	C
8	B1	B
9	C1	B
10	C1	A
11	C1	D
12	C1	C
13	D1	C
14	D1	B
15	D1	A
16	D1	D

## Chapter 4 - Fundamental definitions and preliminary analyses

Table 4.2 Scheme and graphical representation of crossing-path scenarios. Notice that an interaction corresponding to a LTAP/OD case can actually be set by four different combinations of trajectories. Refer to Figure 4.1 and Table 4.1 to confirm that the trajectory pairs 3-10, 7-14, 11-2 and 15-6 will be classified as LTAP/OD scenarios.





ID	Crossing path scenarios	
1	Left Turn Across Path/ Opposite Direction LTAP/OD	
2	Left Turn Across Path/ Lateral Direction LTAP/LD	
3	Straight Crossing Paths SCP	
4	Leaving by Left/ Arriving by Right LL/AR	

Table 4.3 Percentage distribution of interactions according to the number of vehicles (NoV) that interact simultaneously.

Number of vehicles in interaction	1	2	3	4	5	6
Percentage of interactions	53.04	33.08	11.19	2.37	0.31	0.01

## Chapter 4 - Fundamental definitions and preliminary analyses

Table 4.4 Distribution of interactions classified within scenario-categories. The computations are based on interactions with  $NoV \geq 2$ .

Scenario	Relative frequency (%)
Crossing	13.09
Merging	13.10
Splitting	16.72
Following	26.07
Oncoming	16.39
General	14.63

Table 4.5 Distribution of interactions classified within crossing-path scenarios. These computations are based on interactions with  $NoV \geq 2$ . The trajectory pairs presented are the most representative combinations of each crossing scenario in Sävenäs

Crossing scenario	Relative frequency (%)	Trajectories
LTAP/OD	34.22	3, 10
LTAP/LD	20.20	7, 10
SCP	0.82	varies
LL/AR	44.76	3, 7

## Chapter 5 - Traffic Scenarios from the Driver's Point of View

The first part of this chapter discusses the classification system developed by Autoliv and Chalmers to characterize traffic scenarios at the Sävenäs and Jung intersections. The second part outlines automated processing steps used to assign trajectories to scenarios.

The system was designed to be used by behavioral scientists studying the control actions taken by drivers approaching, crossing, and exiting intersections. It adopts the perspective of the driver of a target vehicle, called the 'blue car'. Scenarios are defined using the trajectory of the blue car and the trajectories of all other cars within the intersection while the blue car passes through it. Each of the other vehicles is labeled a 'red car'. The system yields a large number of categories and a fine-grained account of the distribution of traffic.

### Definition of trajectories

For each intersection there is a basic set of paths. The principal trajectories discussed in Chapter 3 are the archetypes for members of the set. There are 6 basic paths at Sävenäs and 12 at Jung.

#### The 6 trajectories at Sävenäs

Figure 5.1a shows the assignment of labels to the six possible paths a vehicle can take through the Sävenäs intersection. Vehicles on the main east-west road, on trajectories 5 and 6, have the right-of-way. By law, vehicles entering the intersection from the secondary road, on trajectories 2 and 4, must yield to vehicles arriving from either direction on the primary road. Figure 5.1b shows the scenario where the driver of a car on trajectory 6 can expect the driver of the car on path 4 to yield the right of way.

Because there are 6 paths a car can take through the intersection, there are 6x6 pairs of paths that two cars can take. We use the matrix shown in Table 5.1a to capture the 42 basic cases (6 'solo' cases and 36 two-car cases). The key to the mnemonics for the cell entries is shown in Table 5.2b. The rows represent the trajectories taken by the blue car. The columns represent the trajectories taken by the red car. When there is no red car, there is no interaction. However, as these 'solo' drives through the intersection are common, the first column of the matrix represents cases where there is no red car.

The interaction shown in Figure 5.1b serves as an example to illustrate the use of the matrix and its mnemonics. The interaction involves a blue car on trajectory 6 (East to West with the right of way) and a red car on trajectory 4 (North to East). From the point of view of the blue car, the red car is crossing its path from the side. The corresponding cell is located at the intersection of the row labeled 6 and the column labeled 4. The mnemonic for the interaction is 6xs (blue car on trajectory 6 with a red car crossing (x) from the side (s)). Crossing cases can occur when the red car approaches from either the side (e.g., 4xs), from ahead (e.g., 6xa), or from the direction that the blue car intends to take (e.g., 3xi). Merging cases occur whenever both cars have the same intended direction (e.g., 2ms). 'Following' cases occur along the principle diagonal - where the blue car is behind a red car on the same trajectory - and in those off-diagonal cells where the two vehicles are on different trajectories but approach the intersection from the same direction (e.g., 1fr). In following cases, the lead car can turn right (e.g. 2fr) or left (e.g., 3fl) or continue straight ahead (e.g. 5fc). Finally, there are many cases where the second car is within the intersection but is unlikely to require much consideration. The mnemonics to these cases begin with the letter 'n' to signify that no interaction is likely.

The 42 cells in the basic matrix of Table 5.1 account only for solo drives and interactions between two vehicles. It must be expanded to take into account three additional types of

## Chapter 5 - Traffic Scenarios from the Driver's Point of View

situations. First, there are 36 cases involving a red car that is waiting (to turn) at the intersection. Second, there are an additional 36 where there is more than one red car. Third, 36 more cells are needed to represent cases involving multiple red cars of which at least one is waiting to turn. Table 5.2 shows the additional 108 cells that complete the matrix of scenarios.

There are a total of 150 scenarios in this classification scheme. This combinatoric explosion is a direct result of an attempt to capture the elements of traffic situations that may lead them to differ from the driver's point of view. The three sketches shown in Figure 5.2 build upon the basic crossing from the side scenario of Figure 5.1b (6xs) to illustrate similar situations that may (or may not) differ from the driver's point-of-view. The 150 cases, shown in Tables 5.1 and 5.2, are the focus of discussions in Chapter 7.

### The 12 trajectories at Jung

Figure 5.3a shows the assignment of labels to the 12 possible paths a vehicle can take through the Jung intersection. A different labeling scheme was used for Jung. The first letter indicates the cardinal direction from which the car enters the intersection. The second letter indicates the path it takes through the intersection, turning left, going straight, or turning right. Thus the label NS represents a car from the north traveling straight and WR represents a car from the west turning right. Table 5.3 shows the basic matrix of 12 solo drives and the 12x12 pair of paths that two cars can take.

The labels for scenarios involving two or more cars concatenate the labels for the constituent solo drives. An example is shown in Figure 5.3b. Here the blue car enters the intersection from the south while a red car turns left from the north. The 2-letter label for the blue car is followed by the 2-letter label for the red car. The final letter in the 5-letter string indicates whether the scenario involves crossing (X), merging (M) or waiting (W).

The complete list of scenarios adds another three 12x12 matrixes to account for waiting red cars, multiple red cars, and multiple waiting red cars. The result is a total of 588 traffic scenarios at the 4-way Jung intersection.

### Scenario classification

This section describes the automated processing used at Autoliv and Chalmers to classify each trajectory as (part of) a traffic scenario. In this and other sections of the report, we refer to the vehicle that is the focus of discussion as the 'blue car' and all other vehicles as 'red cars'. When the blue car is the only vehicle within the intersection, its trajectory defines the scenario. When there are red cars present as well, the combination of trajectories defines the scenario.

The valid, filtered trajectories from the image processing system described in Chapter 3 are the input to the classification software. As suggested by the bottom row of Table 3.1, scenario classification can be seen as the final step in the conversion of video images into data that can be used to assess the factors that influence the occurrence of incidents in the intersections.

As discussed in Chapter 3, only 30% of the objects detected by the image processing software survive the process that defines valid trajectories. The scenario classification software defines a scenario only when every vehicle in the intersection has a valid trajectory. This means that every occurrence of an invalid trajectory creates a window in time when no

## Chapter 5 - Traffic Scenarios from the Driver's Point of View

scenarios are defined. Because trucks are filtered out and do not have valid trajectories, none of the scenarios contain a truck. Every vehicle in a scenario is (the size of) a passenger car or small van. In what follows, we use the word 'car' rather than 'vehicle' to underscore this point.

When there are two cars in the intersection at the same time, each car takes its turn as the blue car. The scenario assignment differs according to the perspective of each driver. For example, consider the situation shown in Figure 5.4. Here one car is driving straight through the intersection with the right of way and another with a yield sign. This situation differs dramatically for the two drivers. The driver with the right of way expects to be able to proceed through the intersection without interference from a car that should yield. The driver with the yield sign needs to decide whether or not to yield or to turn in front of the other car. These two different sets of expectations and responsibilities justify classifying the same situation from both perspectives. As a result, there is one scenario assignment for each car. The number of scenarios matches the number of cars with valid trajectories.

A key but arbitrary assumption has been made to enable the classification process. The software considers only cars within a fixed zone around the intersection. The limits used to define the 'intersection' at Sävenäs and Jung are shown in Figures 5.5a and 5.5b, respectively. These limits are arbitrary distances from the center of the intersection. Adoption of a different limits would likely change the resulting assignments of trajectories to scenarios. The limits were influenced by the placement of the cameras and the resulting resolution of the images. Trajectory resolution was best within these limits. The number and locations of red cars in a scenario are determined by the time it takes the blue car to enter and exit the area defined by these limits.

### Find red cars

For each blue car, the first step is to identify all the red cars that are within the intersection for any length of time when it is inside the intersection. Red cars do not need to be within the area for the duration of the blue car's transit. Some red cars may exit the area as the blue car enters. Others may enter as the blue car exits.

When there are no red cars, the blue car is assumed to have been alone in the intersection and is assigned to a 'solo' scenario according to its trajectory. It is counted as an entry in the first column of the scenario matrix, Table 5.1 for Sävenäs and Table 5.3 for Jung. When there are red cars, the algorithm continues.

### Check following

The next factor checked is the criterion for 'following'. A blue car is said to be following a red car when it crosses the center of the intersection less than a fixed number of seconds after the red car and from the same direction. The time required for effective braking led us to fix this parameter at 1.5 seconds. Red cars that remain more than 1.5 seconds ahead of the blue car as they pass through the intersection are considered a 'multiple' car. The path taken by the red car as it leaves the intersection determines which of the possible following cases apply (e.g., either 1fr or 1fc, SSSLF or SSSRF).



## Chapter 5 - Traffic Scenarios from the Driver's Point of View

### Simple and complex scenarios

A thought experiment led us to differentiate between simple and complex scenarios. Imagine you are the driver of the blue car, crossing the intersection with the right of way. In one case, there is a car on the right waiting to cross the intersection after you pass. In another, a line of cars is waiting to cross. Does it matter to you, as the driver of the blue car, whether it is only one car or an entire line that is waiting? We think not. Simple scenarios consist of one or more red cars that are all on the same trajectory or are all waiting on the same road. In contrast, a complex scenario is defined by two or more red cars on different trajectories. Driving through an intersection is made more eventful by the presence of cars coming from multiple directions. The key insight here is that it is not the number of vehicles that ratchets up the complexity but the number of different trajectories.

Accordingly, the next step taken by the automated scenario software is to distinguish between simple and complex scenarios. If there is only one red car (or a stream of red cars on the same trajectory), the case is defined as a simple case. Its cell in the basic matrix is defined by the row for the path taken by the blue car and the column for the path taken by the (leading) red car.

If two or more red cars enter the intersection on different trajectories, then we assume that both cars are potential sources of interest to the driver of the blue car. These 'multiple' cases are classified by checking four criteria in a fixed sequence: encroachment, crossing, merging, waiting, and proximity in time.

#### Simple encroachment

Encroachment is special type of traffic scenario that received a lot of attention during this project. Encroachment occurs whenever the blue car is in the intersection, has the right of way, and a red car crosses its path. Because encroachments are a major source of crashes in intersections, the software gives them the highest priority when sorting cases involving multiple red cars. Figure 5.6a presents an example of encroachment in a case with multiple red cars. In this example a red car is turning left across the path of the blue car as a second car approaches from ahead. The categorization system considers the relative hazard posed by the two cars. Because the hazard posed by the encroachment is likely to be the more salient to the driver the blue car, the case is classified as an instance of encroachment and assigned to the multiple cell corresponding to the path of the encroaching red car (6xsm).

#### Crossing

The second criterion used to sort cases involving multiple red cars is crossing. Like encroachment, crossing traffic is a major source of crashes in intersections. Figure 5.6b presents an example of a crossing scenario with multiple red cars. The case is similar but crucially different from the encroachment shown in Figure 5.6a. In Figure 5.6b, we consider the case from the perspective of the driver making the turn. For the driver of the blue car on path 4, the red car on path 6 is crossing or will soon cross its path. This is an instance of crossing rather than encroachment because the blue car does not have the right of way. A second red car is approaching and merging from the side. Because the hazard posed by the crossing car is likely to be the more salient to the driver the blue car, the case is classified as an instance of crossing and assigned to the multiple cell corresponding to the path of the crossing red car (4xim).

## Chapter 5 - Traffic Scenarios from the Driver's Point of View

### Merging and waiting

The third criterion is merging. If one of the red cars is merging with the blue car so that they will exit the intersection in the same direction, the case is classified as an instance of merging. An example is shown in Figure 5.7a.

The fourth criterion is waiting. A car is defined as waiting for the blue car if its velocity is less than a threshold value (1.5 m/s) at the time that the blue enters the intersection. Waiting red cars, like that shown in Figure 5.7b, are given some priority because their presence is likely to influence to some degree the actions of the driver of the blue car. In cases with multiple red cars, a waiting red car defines the case if the second red car is unlikely to encroach or cross or merge with the blue car. Figure 5.7c presents an example.

### Find most relevant other

The final criterion invokes the construct 'intersection time' which is defined as the time when the distance between the car and the center of the intersection is at its minimum. For cars on straight paths, the intersection time is when they cross the centerline of the intersection. For cars making turns, the intersection time defined by the shortest perpendicular from its path to the center. In cases without encroachment, crossing, merging, or waiting, the software compares the intersection time for the blue car and all the red cars. The case is classified according to the path taken by the red car with the nearest intersection time.

Figures

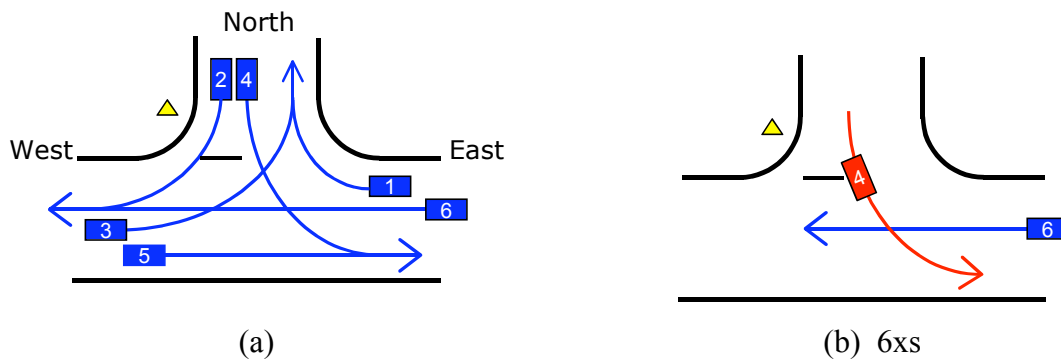


Figure 5.1 (a) The numbering scheme used by the driver-perspective classification system to define the 6 possible trajectories through the Sävenäs intersection. (b) A sample interaction. The blue car is the driver's car and has the right-of-way. The red car is crossing its path from the side. If the red car were to turn in front of the blue car, it would be an instance of 'encroachment'.

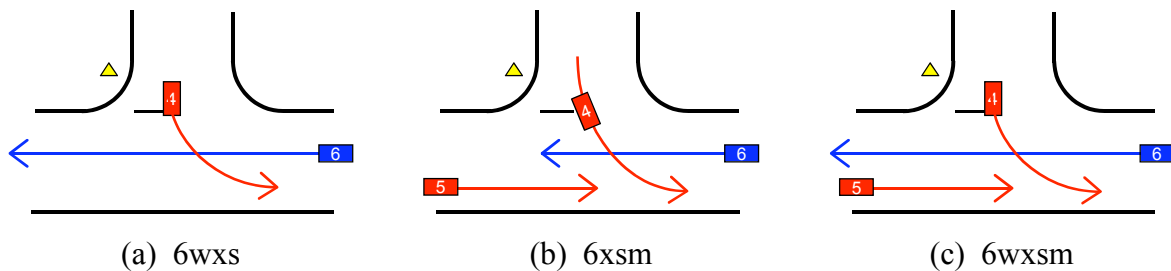


Figure 5.2 Sketches of related traffic situations that may differ from the perspective of the driver of the blue car. In panel (a), a red car waits to turn left (6wxs). In (b), a red car is encroaching from the side and a second red car is approaching from ahead. Because the driver of the blue car is likely to find the encroachment more salient than the approaching car, the encroachment defines the multiple case (6xsm). In (c), a red car waits to turn left and a second red car is approaching from ahead. The waiting car defines the multiple case (6wxsm).

Chapter 5 - Traffic Scenarios from the Driver's Point of View

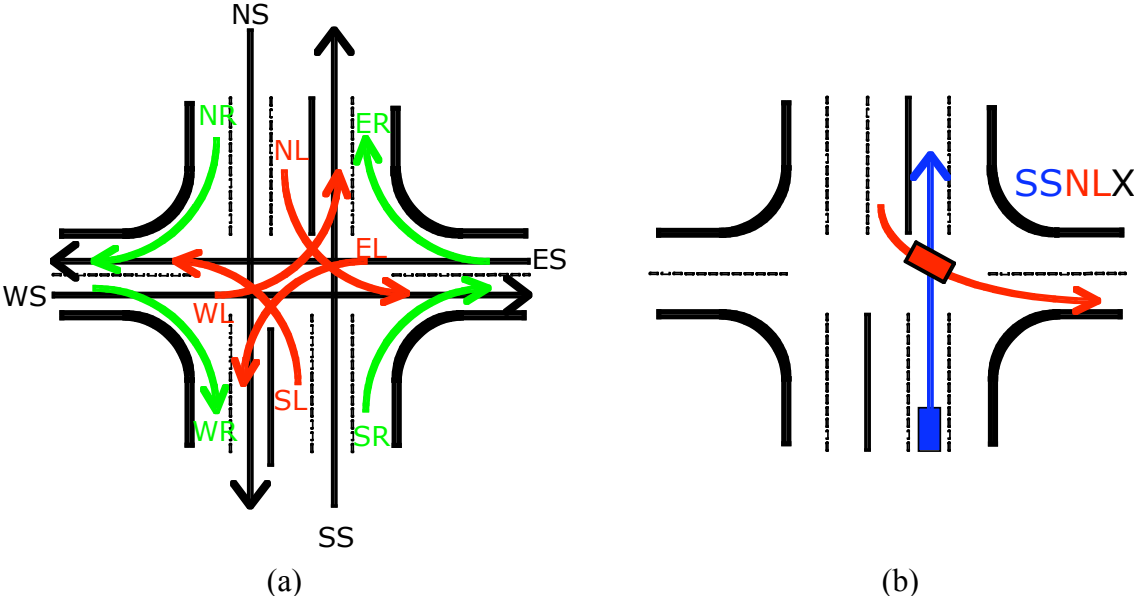


Figure 5.3 (a) The labels for the 12 solo paths at Jung. (b) An example of the concatenation of solo labels to define the label for a two car scenario.

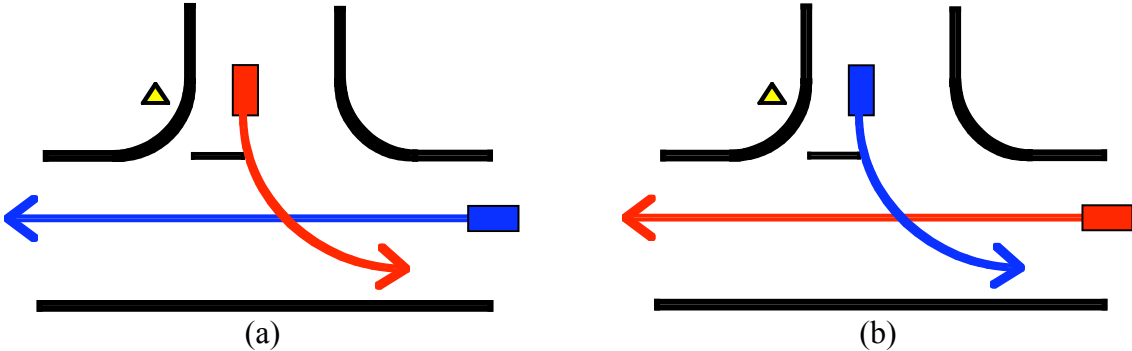


Figure 5.4 Sketches showing how the same encounter can be classified as two different traffic scenarios, (a) from the perspective of the car with the right of way and (b) from the perspective of the yielding car that will turn left.

## Chapter 5 - Traffic Scenarios from the Driver's Point of View

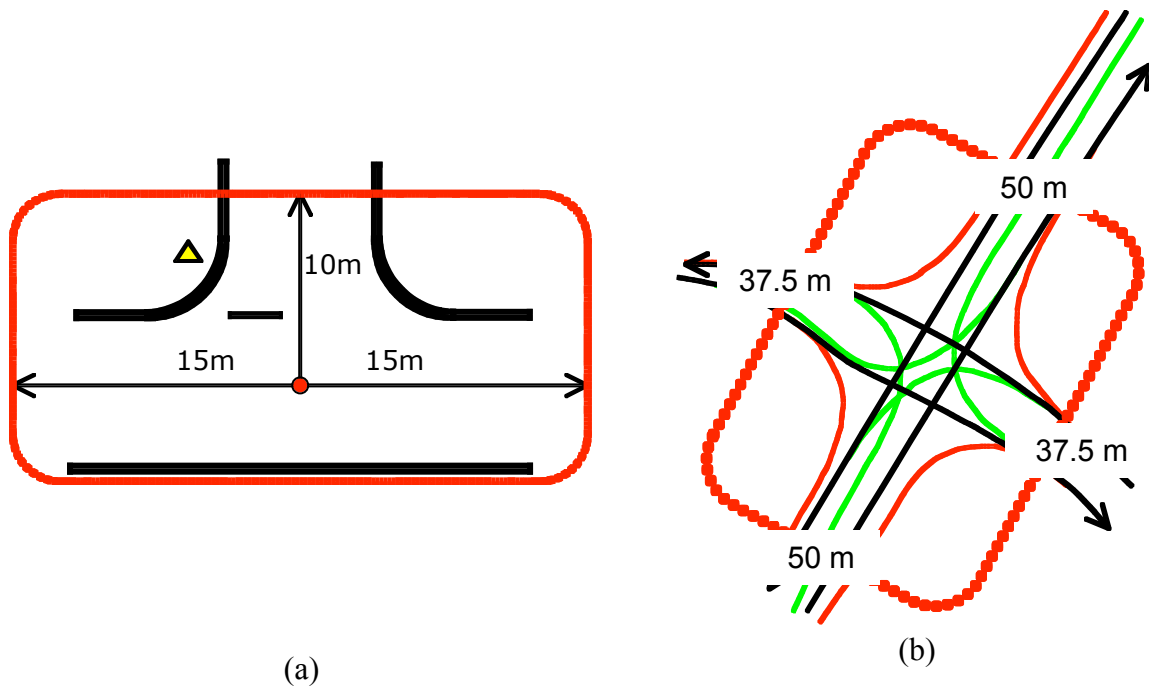


Figure 5.5 The dimensions of the area used to define traffic scenarios at (a) Sävenäs and (b) Jung. Both sketches are oriented with north up. The rotation of the sketch for Jung reflects the actual orientation of the intersection.

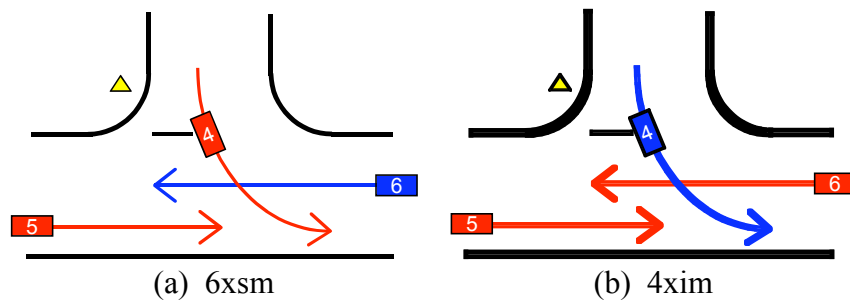


Figure 5.6 Sketches of cases involving multiple red cars at Sävenäs. In panel (a), a red car on path 4 encroaches on the blue car's right of way by crossing from the side. A second red car on path 5 approaches from ahead. The encroachment defines the multiple case (6xsm). In (b), the blue car does not have the right of way. The red car on path 6 crosses from the intended direction. A second red car approaches from the side. The crossing car defines the multiple case (4xim).

## Chapter 5 - Traffic Scenarios from the Driver's Point of View

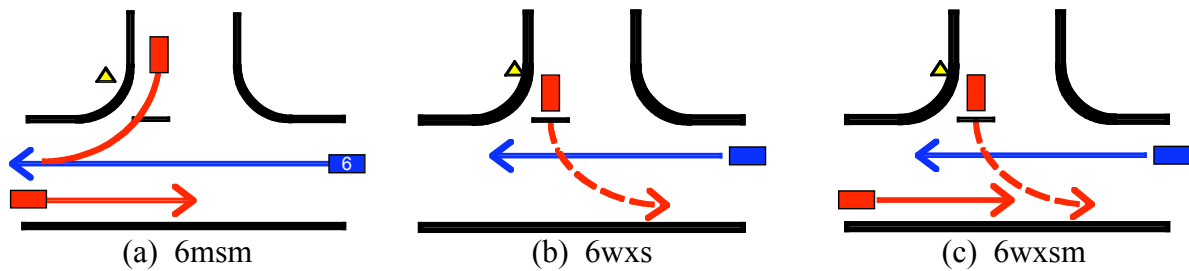


Figure 5.7 Sketches of cases involving merging and waiting red cars. In panel (a), the car on path 2 is merging with the blue car as a second red car approaches from ahead. The merging car defines the multiple case (6msm). In (b) the red car on path 4 waits to turn left (6wxs). In (c), a red car waits to turn left as a second red car approaches from ahead. The waiting car defines the multiple case (6wxsm).

### Tables

Table 5.1 (a) The 6x7 matrix of traffic scenarios at Sävenäs involving one or two cars. Cell entries indicate the mnemonic label use to designate a scenario. The numbers in the first column are the labels for scenarios involving only one (solo) car. (b) The key to the mnemonics of the cell entries. The driver's car is the blue car. The other car is the red car.

Blue		Red							key
		Solo	1	2	3	4	5		
1	1	1fr	1nxir	1ma	1nxil	1nma	1fc	E to N	a (from) ahead c continuing straight ahead f following i (from the) intended direction l (turning to the) left m merging n no interaction likely r (turning to the) right s (from the) side x crossing
2	2	2nms	2fr	2nxil	2fl	2nxis	2ms	N to W	
3	3	3ma	3nxi	3fl	3xi	3fc	3xa	W to N	
4	4	4nxi	4fr	4xs	4fl	4ms	4xi	N to E	
5	5	5nxar	5nxs	5fl	5ms	5fc	5nxac	W to E	
6	6	6fr	6ms	6xa	6xs	6nxa	6fc	E to W	
		E to N N to W W to N N to E W to E E to W							

(a)

(b)

## Chapter 5 - Traffic Scenarios from the Driver's Point of View

Table 5.2 The 3x6x6 matrix of traffic scenarios that account for waiting red cars, multiple red cars, and multiple waiting red cars at Sävenäs. The prefix 'w' signifies waiting, the suffix 'm' multiple.

Blue	Waiting						Multiples						Waiting Multiples						
	1w	2w	3w	4w	5w	6w	1m	2m	3m	4m	5m	6m	1wm	2wm	3wm	4wm	5wm	6wm	
1	1wfr	1wnxir	1wma	1wnxil	1wnma	1wfc	1frm	1nxirm	1mam	1nxilm	1nmam	1fcm	1wfrm	1wnxirm	1wmam	1wnxilm	1wnmam	1wfc	E to N
2	2wnms	2wfr	2wnxil	2wfl	2wnxis	2wms	2nmsm	2frm	2nxilm	2flm	2nxism	2msm	2wnmsm	2wfrm	2wnxilm	2wflm	2wnxism	2wmsm	N to W
3	3wma	3wnxi	3wfl	3wxi	3wfc	3wxa	3mam	3nxim	3flm	3xim	3fcm	3xam	3wmam	3wnxim	3wflm	3wxim	3wfc	3wxam	W to N
4	4wxi	4wfr	4wxs	4wfl	4wms	4wxi	4nxim	4frm	4xsm	4flm	4msm	4xim	4wxim	4wfrm	4wxsm	4wflm	4wmsm	4wxim	N to E
5	5wnxar	5wnxs	5wfl	5wms	5wfc	5wnxac	5nxarm	5nxsm	5flm	5msm	5fcm	5nxacm	5wnxarm	5wnxsm	5wflm	5wmsm	5wfc	5wnxacm	W to E
6	6wfr	6wms	6wxa	6wxs	6wnxa	6wfc	6frm	6msm	6xam	6xsm	6nxam	6fcm	6wfrm	6wmsm	6wxam	6wxs	6wnxam	6wfc	E to W

Table 5.3 The 12 solo traffic scenarios at Jung and the 12x12 matrix of simple traffic scenarios.

	SOLO	S			E			N			W				
		L	S	R	L	S	R	L	S	R	L	S	R		
S	L	SL	SLSLF	SLSSF	SLSRF	SLELX	SLES	SLESM	SLELX	SLNLZ	SLNSX	SLNRM	SLWLX	SLWSX	SLWRZ
	S	SS	SSSLF	SSSSF	SSSRF	SSELX	SSESX	SSERM	SSELX	SSNLX	SSNSZ	SSNRZ	SSWLM	SSWSX	SSWRZ
	R	SR	SRSLF	SRSSF	SRSRF	SRELX	SRESZ	SRRERZ	SRELX	SRNLX	SRNSZ	SRNRZ	SRWLZ	SRWSM	SRWRZ
E	L	EL	ELSLX	ELSSX	ELSRZ	ELELF	ELESF	ELERF	ELELF	ELNLX	ELNSM	ELNRZ	ELWLZ	ELWSX	ELWRM
	S	ES	ESSLM	ESSSX	ESSRZ	ESELF	ESESF	ESERF	ESELF	ESNLX	ESNSX	ESNRM	ESWLX	ESWSZ	ESWRZ
	R	ER	ERSLZ	ERSSM	ERSRZ	ERELF	ERESF	ERERF	ERELF	ERNLZ	ERNSZ	ERNRZ	ERWLM	ERWSZ	ERWRZ
N	L	NL	NLSLZ	NLSSX	NLSRM	NLELX	NLESX	NLERZ	NLELX	NLNLZ	NLNSF	NLNRF	NLWLX	NLWSM	NLWRZ
	S	NS	NSSLX	NSSSZ	NSSRZ	NSELM	NSESX	NSERZ	NSELM	NSNLZ	NSNSF	NSNRF	NSWLX	NSWSX	NSWRM
	R	NR	NRSLM	NRSSZ	NRSRZ	NRELZ	NRESM	NRRERZ	NRELZ	NRNLZ	NRNSF	NRNRF	NRWLZ	NRWSZ	NRWRZ
W	L	WL	WLSLX	WLSSM	WLSRZ	WLELZ	WLESX	WLERM	WLELZ	WLNLX	WLNSX	WLNRF	WLWLZ	WLWSF	WLWRF
	S	WS	WSSLX	WSSSX	WSSRM	WSELX	WSESZ	WSERZ	WSELX	WSNLZ	WSNSX	WSNRZ	WSWLZ	WSWSF	WSWRF
	R	WR	WRSLZ	WRSSZ	WRSRZ	WRELM	WRESZ	WRERZ	WRELM	WRNLZ	WRNSM	WRNRZ	WRWLZ	WRWSF	WRWRF

## Chapter 6 - Observed traffic scenarios at Sävenäs and Jung

This chapter presents counts of traffic scenarios determined by the scenario classification system that takes the driver's perspective on traffic (Chapter 5) and discusses key findings from analyses of the distributions of velocities at the two intersections. The data provide base lines for the distributions of traffic and velocities at Sävenäs and Jung.

### Sävenäs

#### Scenario counts

The counts shown in the cells of the matrix of Table 6.1 summarize the number and relative frequency of observations at Sävenäs. Table 6.2 presents the full accounting for the 6 solo scenarios and the 144 scenarios with traffic. The entries below the matrix present the sums and relative frequencies for each column.

A total of 177,020 observations were classified. Of the 150 cells in the matrix, 7 had no counts and 7 had more than 5,000. While 35 had fewer than 10 observations, 41 had more than 1,000. The distribution of counts is approximately log-normal.

In 40% of the scenarios, there was only one (blue) car. More than half of these cases involved either trajectory 2, the right turn from the north to the west, or the return trajectory 3, the left turn from the west to the north. The least common trajectory by far was trajectory 4, the left turn from north to east. In spite of the three-fold disparity in total counts across cases, the relative frequency of solo cases was approximately 40% for all cases.

Cases involving only one red car accounted for another 40% of the total. Again, more than half of these cases involved trajectories 2 and 3. Not only were these trajectories the most common for solo trips, they also accounted for the most common two-car interactions. By far the most common pairing of trajectories involves two cars on trajectory 3. This scenario occurs when a car entering the intersection from the west is closely followed by a second car and both turn left onto the secondary road. There is no dedicated left-turn pocket lane at Sävenäs.

Of the two-car interactions, only a small percentage involved waiting red cars. Of the waiting cars, the vast majority were on trajectories 2 and 4. These counts represent cars that were respecting the yield sign when there was another car in the intersection. The relative frequency of waiting differed markedly between these trajectories. Less than 10% of cars on trajectory 2 had to wait but nearly 30% of cars on trajectory 4 had to wait. It appears that turning right and merging requires much less yielding than crossing two lanes of traffic to turn left.

Only 20% on the cases were classified as either 'multiples' or 'waiting multiples'. These data support the inference that it is relatively unusual to find three or more cars in the Sävenäs intersection at the same time. The distribution of these cases reveals the source of congestion. By far the most frequent multiple case involves trajectory 3, the left turn from west to north. A car on this trajectory frequently has to wait for a car on trajectory 6 before making its turn. As it waits, a (third) car often pulls up behind it or enters the intersection from another direction. The bottleneck at Sävenäs appears to be the lack of a left-turn lane from the west to the north.

#### Velocity distributions

Figure 6.1 is a graph of the average velocities for solo drives on each of the 6 paths at Sävenäs. The data are plotted at 10 meter intervals starting 30 meters before the center of the



## Chapter 6 - Observed traffic scenarios at Sävenäs and Jung

intersection and ending 20 meters beyond it. The red lines represent right turns, green lines left turns, and black lines passes straight through the intersection. Odd-numbered trajectories are marked by squares and even-numbered trajectories by circles. Trajectories 1 and 3, marked by squares, are turns from the primary road to the secondary road. Trajectories 2 and 4, marked by circles, are turns from the secondary road to the primary road.

Drivers with the right of way who do not turn, marked by the black lines in Figure 6.1, barely slow for the intersection. In contrast, drivers from the second road, marked by circles, slow appreciably before the intersection. This slowing presumably reflects both preparation for turning and the need to check for crossing traffic with the right of way. Drivers who intend to turn from the primary road onto the secondary road slow considerably less. The difference between the driving tasks represented by the two red (or green) curves is the relative direction the driver needs to look to decide whether or not to yield the right of way. For drivers turning from the secondary road the direction is 90° to the either side. For drivers turning from the primary road the direction is straight ahead. It appears that drivers slow less when checking for oncoming traffic than for crossing traffic.

Velocity data for all traffic scenarios with a sufficient number of observations ( $N > 400$ ) were extracted from the image processing data at 6 distances from the center of the intersection (from 30 meters prior to the center to 20 meters after in 10 meter increments). Medians and cumulative frequency distributions were found at each distance. Kolmogorov-Smirnov were tests run on 72 pairs of scenarios (e.g., 6xa vs. 6xs, LTAD/OD vs. LTAD/LD) at each distance to ascertain whether the distributions of velocities differed. Of the total of 408 comparisons with sufficient data, 295 were significantly different after applying the Bonferroni correction for multiple comparisons ( $p < .00012$ ). This finding reveals that the velocity of traffic at Sävenäs responds to the traffic scenario.

Velocities tend to be faster during solo drives than in the presence of traffic (220 of 295 tests). The notable exception is when following another car. Following cases account for all 35 tests that uncovered significantly faster driving in traffic than when without traffic. Figure 6.2 presents two examples of the impact of following on velocity. The magnitude of the difference in average velocity is more than 2 kph during and after the right turn. This suggests that drivers who find themselves 'stuck' behind another car 'compensate' for their 'delay' by accelerating faster than they ordinarily would as soon as they turn away from the car ahead. This latent aggression is seen in every case when a following driver takes a different path through the intersection than the car it has been following. While this finding may not have a direct impact on the design of active safety systems, it is salient in the velocity data at Sävenäs.

As expected, the distributions of velocities for cars that yield the right of way are lower than for cars on identical paths that do not have to yield. As shown in Figure 6.3, the difference can be substantial ( $> 5\text{kph}$ ) when approaching the intersection. The path shown in Figure 6.3 is the left turn from the west to the north. Oncoming cars have the right of way. Drivers who intend to turn and who fail to yield to oncoming vehicles may become the provokers of encroachments. Slowing and yielding transform a potential encroachment into a benign situation. Three pieces of information flag the difference between an impending encroachment and relative safety: (a) knowledge of the driver's intent, (b) detection of an oncoming car with the right of way, and (c) the characteristic differences in velocity profiles.

The velocity data from Sävenäs reveal a third effect of traffic scenario - velocities slow considerably when there are several cars in the intersection. An example is shown in Figure 6.4. The three scenarios are (1) the solo path from west to east on the primary road, (2) the same path in the presence of one car that is waiting to merge from the left, and (3) the same

## Chapter 6 - Observed traffic scenarios at Sävenäs and Jung

drive with one car waiting to merge plus at least one other car. Velocities are essentially identical for the solo drive and the case with one waiting car. They are appreciably lower when there are additional cars in the intersection. This example illustrates how drivers, on average, adapt to traffic complexity. Velocity and traffic complexity can be expected to display an inverse relationship.

### Jung

#### Scenario counts

The counts shown in the cells of the matrix of Table 6.3 summarize the number of observations at Jung. The entries below the matrix present the sums and relative frequencies for each column. Table 6.4 presents the full accounting for the 576 scenarios with traffic. The color scheme highlights blocks of scenarios with similar geometries. All scenarios in the yellow cells involve one or more cars following another. From the perspective of the driver of the blue car, traffic in the blue cells arrives from the right, traffic in the green cells is oncoming, and traffic in the beige cells arrives from the left.

The data set from Jung is both smaller than that from Sävenäs and divided into many more scenarios (588 vs. 150). As a result, there are many scenarios with relatively few cases. A total of 33,824 observations were classified. Of the 576 scenarios with traffic, 157 had no counts and 4 had more than 1,000. While 372 had fewer than 10 observations, 56 had more than 100. The distribution of counts has a strong positive skew. The abundance of zero counts reflects the fact that traffic on the E20 has the right of way and has to wait only when turning left across the other lane of the E20.

Only a fifth of drives through the Jung intersection involved only one car. As expected, by far the most common trajectories represented through traffic on the E20; more than two thirds of all traffic involved trajectories SS (from the south going straight) and NS (from the north going straight). The major source of cross traffic was the road to the east; more than 70% of cars from the east crossed both lanes of the E20. Less than half the traffic from the west crossed both lanes. Traffic engineers may find these observations useful.

In 20% of the scenarios, there was only one (blue) car. Nearly 80% of the solo drives were through traffic on the E20. The least common trajectories both for solo drives and for scenarios with traffic were NL, a left turn off the E20, and its return ER, the right turn onto E20.

Cases involving only one red car accounted for another 30% of the total. Again, more than two thirds of these cases involved through traffic on the E20. The most common pairings of trajectories involved (a) two cars traveling the same direction on the E20 and (b) one car headed south and one headed north. Cars entering the intersection from either the east or west can expect to wait for cross traffic on the E20.

#### Velocity distributions

Figure 6.5 presents graphs of the average velocities for solo drives on the 12 paths at Jung. As in Figure 6.1, the data are plotted at 10 meter intervals starting 30 meters before the center of the intersection and ending 20 meters beyond it. Figure 6.4a plots data for drivers on the E20 with traffic from the south marked by circles and traffic from the north by squares. Figure 6.4b plots data from the secondary road with traffic from the west marked by circles

## Chapter 6 - Observed traffic scenarios at Sävenäs and Jung

and traffic from the east by squares. Red lines represent right turns, green lines left turns, and black lines passes straight through the intersection.

Figure 6.5a reveals that drivers continuing straight through the intersection barely slowed down. Drivers making a turn from the north, shown by squares, decelerated more rapidly than they did from the south. The direction of travel had a greater impact on the average velocity than the type of turn being made.

The average velocity profiles for drivers entering the intersection from the secondary road, Figure 6.5b, are less uniform. All display a distinct minimum value that is presumably associated with the need to stop and check for traffic on the E20 before proceeding. As shown by the red curves in Figure 6.5b, the location of the minimum velocity occurred later for turns to the right and earlier for turn to the left for traffic from west.

The velocity data from Jung were the subject to the same analyses as those from Sävenäs. The only difference was the number that served as the threshold for considering a scenario ( $N > 50$  rather than 400). Adopting the higher threshold would have eliminated most of the interesting comparisons between pairs of scenarios. Of the total of 462 comparisons, only 15 were significantly different after applying the Bonferroni correction for multiple comparisons ( $p < .00011$ ). In all 15 cases where the Kolmogorov-Smirnov test found a significant difference between similar scenarios, the velocity was always higher for the solo drives.

In marked contrast with Sävenäs, this finding reveals that the velocity of traffic at Jung rarely responds to the traffic scenario. There is insufficient data to assess the occurrence of speeding up after following and slowing down prior to yielding. There is, however, ample evidence for an overall lack of contextual sensitivity in the velocity data at Jung. This finding may reflect the nature of the intersection. Most drivers continue straight through the intersection on the E20. They have the right of way and do not adjust their velocities to account for the presence of traffic. Drivers appear to approach the task of driving on a freeway differently than they do driving on a narrow road in an industrial area.

## Chapter 6 - Observed traffic scenarios at Sävenäs and Jung

### Figures

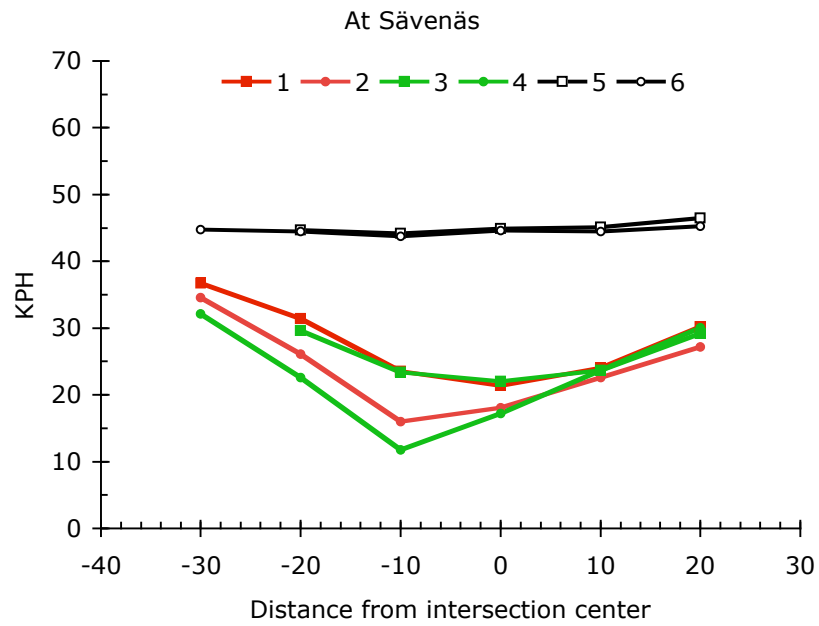


Figure 6.1 Average velocity profiles for each trajectory at Sävenäs.

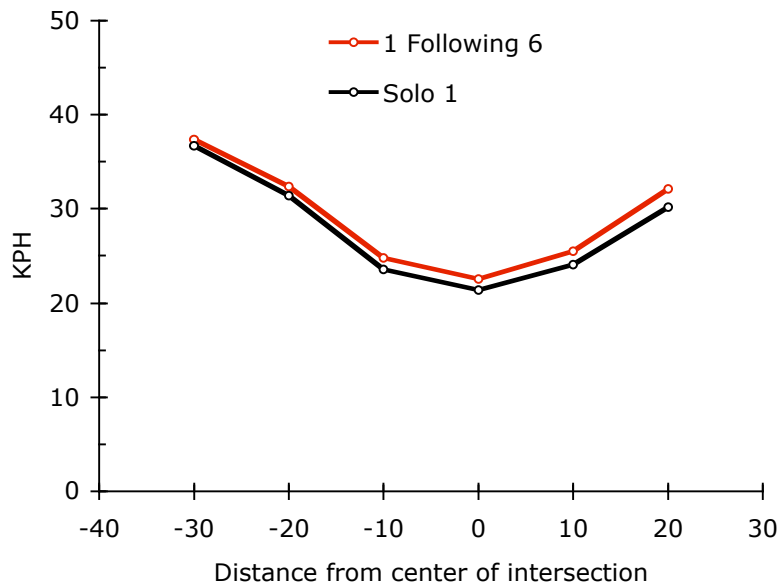


Figure 6.2 Average velocity profiles at Sävenäs for right turns from the primary road to the secondary road when solo and when following a car driving straight through the intersection.

## Chapter 6 - Observed traffic scenarios at Sävenäs and Jung

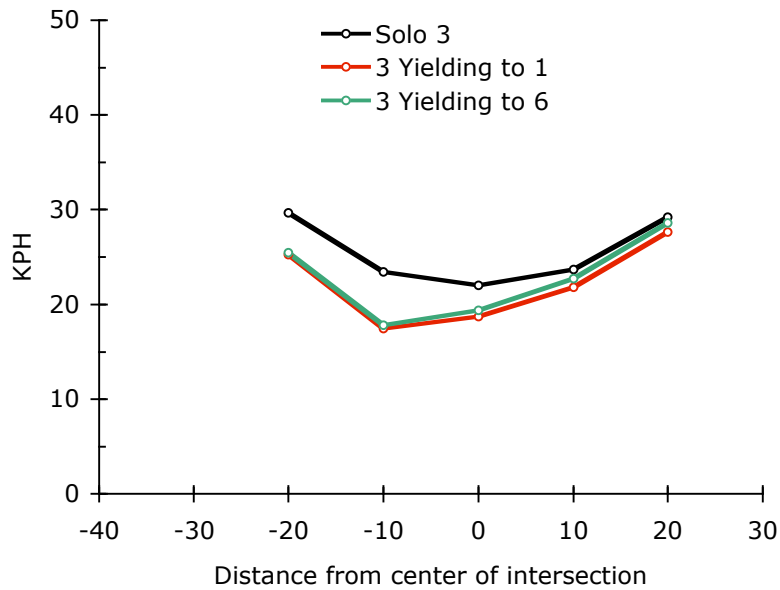


Figure 6.3 Average velocity profiles at Sävenäs for cars turning left turn from the primary road showing the influence of yielding.

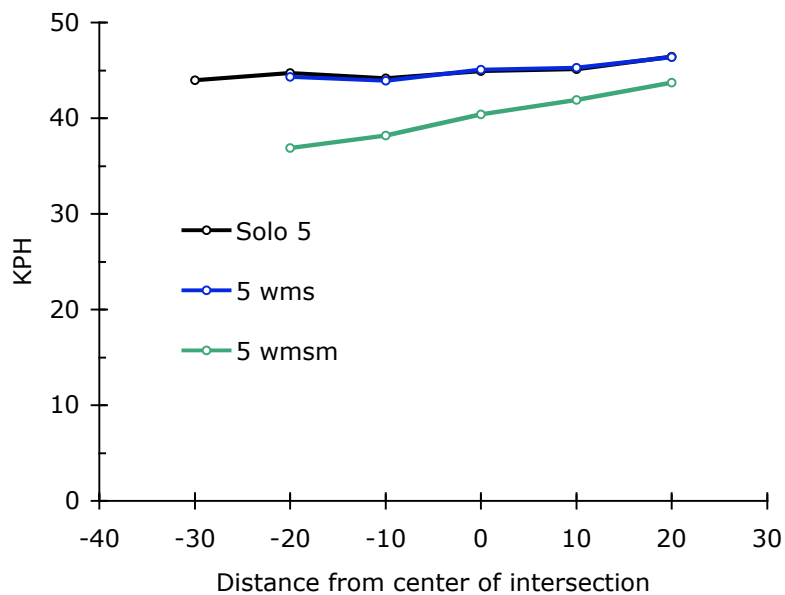


Figure 6.4 Average velocity profiles at Sävenäs for cars crossing the intersection on a straight path showing the differential influence of additional cars when one is waiting to merge.

## Chapter 6 - Observed traffic scenarios at Sävenäs and Jung

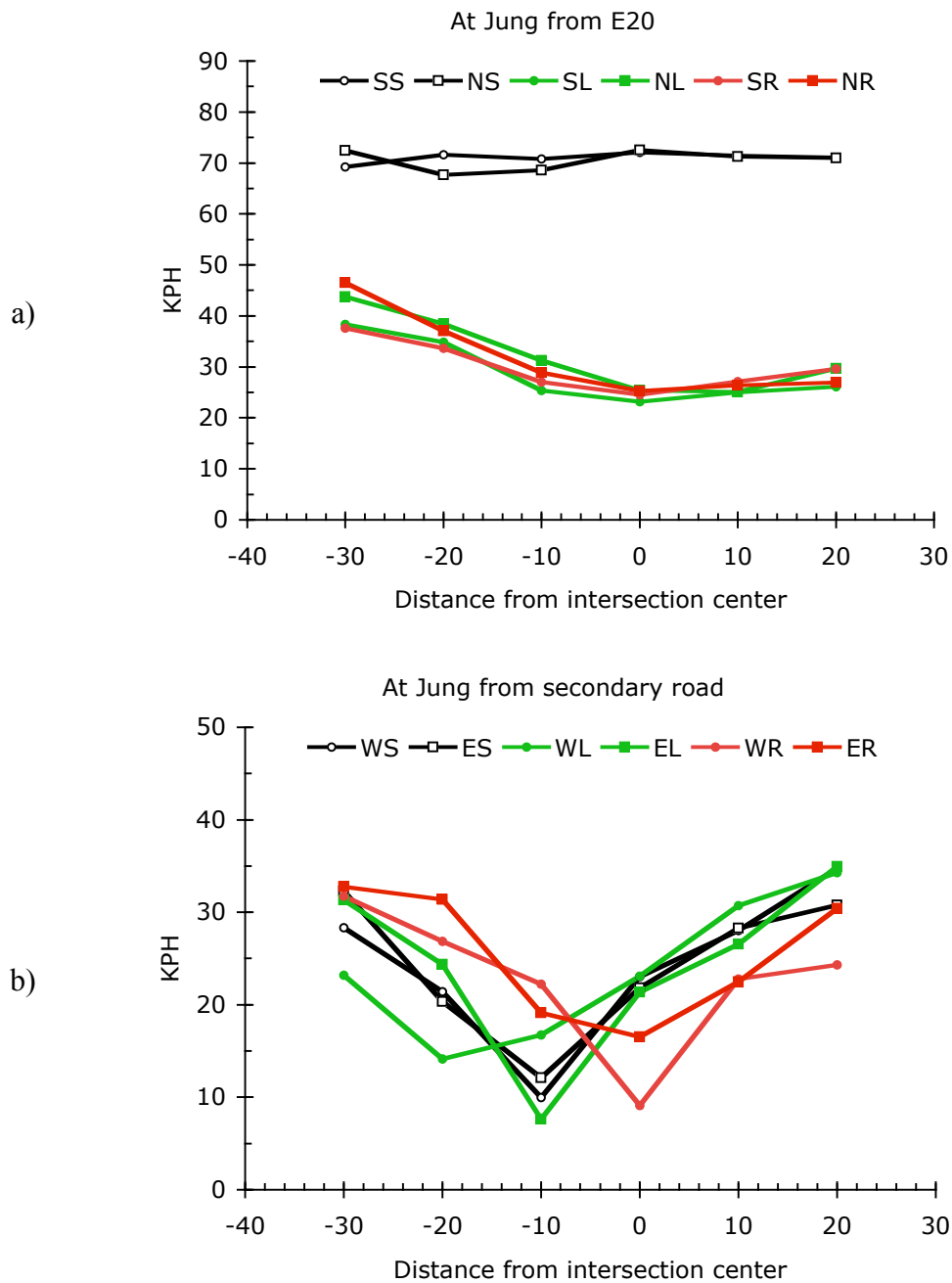


Figure 6.5 Average velocity profiles at Jung for traffic arriving at the intersection on (a) the E20 and (b) the secondary road.

## Chapter 6 - Observed traffic scenarios at Sävenäs and Jung

### Tables

Table 6.1 Summary of the distribution of traffic scenarios observed at Sävenäs

Blue	Counts			Percentages		
	Solo	With Traffic	Total	Solo	By Case	
1	9 645	13 342	22 987	42	13	E to N
2	17 731	26 762	44 492	40	25	N to W
3	16 970	29 625	46 595	36	26	W to N
4	5 443	10 346	15 789	35	9	N to E
5	9 903	14 165	24 068	41	14	W to E
6	10 415	12 674	23 089	45	13	E to W
			177 020			

## Chapter 6 - Observed traffic scenarios at Sävenäs and Jung

Table 6.2 The distribution traffic scenarios at Sävenäs.

Blue	Solo	Red					Waiting						Multiples						Waiting Multiples									
		1	2	3	4	5	6	1w	2w	3w	4w	5w	6w	1m	2m	3m	4m	5m	6m	1wm	2wm	3wm	4wm	5wm		6wm		
1	9645	748	2634	2212	1052	980	352	3	286	443	301	10	3	762	411	1892	188	302	76	2	92	490	101	1	1	E to N		
2	17731	2124	4644	4814	2474	1765	1638	6	129	29	324	5	5	852	3419	895	334	703	2310	4	158	35	87	2	5	N to W		
3	16970	1824	5000	6305	1374	1288	1718	1	123	25	864	6	11	1520	231	2993	1767	117	3082	6	7	77	1274	0	12	W to N		
4	5443	835	1221	1798	1071	703	668	1	85	4	200	0	2	141	25	1836	274	440	968	0	8	29	32	3	2	N to E		
5	9903	1025	2514	2694	594	970	958	5	52	12	520	5	6	318	463	845	726	1246	348	0	53	46	750	13	2	W to E		
6	10415	694	1732	2222	663	1018	545	4	911	420	617	7	4	32	567	1532	384	50	192	0	246	476	358	0	0	E to W		
70107		7250	17745	20045	7228	6724	5879	20	1586	933	2826	33	31	3625	5116	9993	3673	2858	6976	12	564	1153	2602	19	22			
40%		4%	10%	11%	4%	4%	3%	0%	1%	1%	2%	0%	0%	2%	3%	6%	2%	2%	4%	0%	0%	1%	1%	0%	0%			
							64871							5429							32241							4372
							37%							3%							18%							2%

Table 6.3 Summary of the distribution of traffic scenarios observed at Jung.

		SOLO	S			E			N			W			TOTAL	
			L	S	R	L	S	R	L	S	R	L	S	R		
S	L	253	83	135	15	51	131	3	3	521	27	61	162	60	1505	4%
	S	2859	327	3481	149	345	1510	78	121	1081	159	303	1500	415	12328	36%
	R	148	36	140	70	17	56	0	5	150	24	10	136	37	829	2%
E	L	88	45	167	6	20	21	1	9	120	7	12	114	74	684	2%
	S	231	65	682	11	15	147	6	20	676	30	70	68	43	2064	6%
	R	34	5	57	0	5	9	4	1	13	3	7	9	4	151	0%
N	L	29	5	51	0	10	23	0	8	13	1	9	14	2	165	0%
	S	2571	920	919	98	232	1438	19	21	2447	85	440	1219	600	11009	33%
	R	163	112	170	18	21	162	5	5	137	89	12	62	53	1009	3%
W	L	88	67	81	2	8	92	5	6	250	3	17	17	9	645	2%
	S	256	153	511	26	97	69	9	6	564	22	22	125	31	1891	6%
	R	203	49	229	14	100	88	6	2	589	16	18	69	161	1544	5%
		6923	1867	6623	409	921	3746	136	207	6561	466	981	3495	1489	33824	
		20%	6%	20%	1%	3%	11%	0%	1%	19%	1%	3%	10%	4%		



## Chapter 6 - Observed traffic scenarios at Sävenäs and Jung

Table 6.4 The distribution of traffic scenarios at Jung.

		ONE RED CAR													
		L			S			R							
		L	S	R	L	S	R	L	S	R	L	S	R	SUBTOTAL	
S	L	34	114	10	9	48	0	2	117	10	7	38	42	431	4%
	S	257	1827	121	51	238	18	14	847	113	63	207	305	4061	39%
	R	11	83	16	9	24	0	1	67	8	2	16	18	255	2%
E	L	8	32	4	9	15	1	2	75	6	11	21	16	200	2%
	S	25	126	9	7	45	4	2	167	15	15	51	27	493	5%
	R	2	14	0	0	4	1	0	8	1	0	4	2	36	0%
N	L	2	17	0	3	3	0	4	10	1	2	3	1	46	0%
	S	157	839	74	82	246	12	18	1415	72	91	229	164	3399	33%
	R	9	81	8	8	22	3	1	74	20	6	37	29	298	3%
W	L	8	35	2	4	23	1	2	51	3	8	10	5	152	1%
	S	26	136	9	16	49	8	2	165	17	15	53	22	518	5%
	R	23	128	8	20	47	1	1	106	11	9	36	25	415	4%
		562	3432	261	218	764	49	49	3102	277	229	705	656	10304	
		5%	33%	3%	2%	7%	0%	0%	30%	3%	2%	7%	6%		

		MULTIPLE RED CARS													
		L			S			R							
		L	S	R	L	S	R	L	S	R	L	S	R	SUBTOTAL	
S	L	47	21	5	23	43	1	0	404	16	29	65	11	665	6%
	S	62	1649	27	143	570	11	69	226	46	60	482	28	3373	29%
	R	25	57	52	4	10	0	3	83	16	4	57	14	325	3%
E	L	36	135	2	10	2	0	6	45	1	0	78	49	364	3%
	S	39	556	2	2	62	2	16	504	15	43	11	10	1262	11%
	R	3	43	0	3	3	2	1	5	2	7	2	2	73	1%
N	L	1	34	0	5	17	0	4	2	0	4	8	0	75	1%
	S	538	79	23	49	449	3	2	1014	13	166	414	114	2864	25%
	R	74	89	10	4	69	2	4	58	69	2	7	3	391	3%
W	L	58	46	0	2	56	4	4	196	0	6	1	0	373	3%
	S	126	374	17	66	8	1	4	394	5	3	35	3	1036	9%
	R	25	101	6	61	29	5	1	482	5	3	19	95	832	7%
		1034	3184	144	372	1318	31	114	3413	188	327	1179	329	11633	
		9%	27%	1%	3%	11%	0%	1%	29%	2%	3%	10%	3%		

		ONE WAITING RED CAR													
		L			S			R							
		L	S	R	L	S	R	L	S	R	L	S	R	SUBTOTAL	
S	L	2	0	0	6	18	1	1	0	0	8	18	6	60	4%
	S	5	5	1	40	181	23	1	8	0	96	230	59	649	39%
	R	0	0	0	4	10	0	0	0	0	1	14	2	31	2%
E	L	0	0	0	0	3	0	0	0	0	0	1	2	6	0%
	S	1	0	0	3	11	0	0	2	0	2	4	4	27	2%
	R	0	0	0	0	0	1	0	0	0	0	1	0	2	0%
N	L	1	0	0	2	2	0	0	1	0	1	2	0	9	1%
	S	49	1	1	67	240	4	0	14	0	63	159	177	775	46%
	R	2	0	0	5	18	0	0	5	0	1	7	6	44	3%
W	L	0	0	0	2	1	0	0	0	0	0	4	2	9	1%
	S	0	0	0	3	10	0	0	1	0	3	14	6	37	2%
	R	0	0	0	2	5	0	0	1	0	1	4	5	18	1%
		60	6	2	134	499	29	2	32	0	176	458	269	1667	
		4%	0%	0%	8%	30%	2%	0%	2%	0%	11%	27%	16%		

		MULTIPLE RED CARS WITH WAITING													
		L			S			R							
		L	S	R	L	S	R	L	S	R	L	S	R	SUBTOTAL	
S	L	0	0	0	13	22	1	0	0	1	17	41	1	96	3%
	S	3	0	0	111	521	26	37	0	0	84	581	23	1386	42%
	R	0	0	2	0	12	0	1	0	0	3	49	3	70	2%
E	L	1	0	0	1	1	0	1	0	0	1	14	7	26	1%
	S	0	0	0	3	29	0	2	3	0	10	2	2	51	2%
	R	0	0	0	2	2	0	0	0	0	0	2	0	6	0%
N	L	1	0	0	0	1	0	0	0	0	2	1	1	6	0%
	S	176	0	0	34	503	0	1	4	0	120	417	145	1400	42%
	R	27	0	0	4	53	0	0	0	0	3	11	15	113	3%
W	L	1	0	0	0	12	0	0	3	0	3	2	2	23	1%
	S	1	1	0	12	2	0	0	4	0	1	23	0	44	1%
	R	1	0	0	17	7	0	0	0	0	5	10	36	76	2%
		211	1	2	197	1165	27	42	14	1	249	1153	235	3297	
		6%	0%	0%	6%	35%	1%	1%	0%	0%	8%	35%	7%		

## Chapter 7 - Encroachments observed at Sävenäs and Jung

One of the goals of this project was to characterize the occurrence of ‘incidents’ (near-crash situations) at the monitored intersections. As the meaning of ‘incident’ is vague, we resisted the temptation of arbitrary definition. Instead, our approach was to define a quantitative metric that could be applied to traffic scenarios, to apply the metric to the observed scenarios at Sävenäs and Jung, and to report the results. These results presented in this chapter address the following questions:

- What is the distribution of post-encroachment times in the monitored intersections?
- Do the distributions differ across traffic scenarios?
- What is the effect of velocity or roadway width, etc.?

As discussed in Chapter 4, VCC developed the backbone of the PET analysis method. The method was refined by Autoliv and Chalmers in a second stage of analysis. The first section of this chapter discusses the modifications to the original method. The second and third sections of the chapter discuss the application of the refined method to the data from Sävenäs and Jung.

### Post-encroachment time

Figure 7.1 is a sketch of the geometry of a typical situation that can lead to encroachment. The blue car has the right of way. The red car turns left across its path. By failing to yield the right of way, the red car encroaches upon the path of the blue car. When the cars are in close proximity, the driver of the encroaching car can be said to ‘provoke’ the driver of the car with the right of way. We use the word ‘provoker’ when describing an encroaching red car.

Post-encroachment time (PET) is an elapsed time. It is defined as the time (in seconds) between (a) the moment when the first car (the provoker) leaves a potential collision zone (the ‘encroachment zone’) and (b) the moment in which the second car (the blue car) enters this zone. PET is a time measure of the minimum separation between the two vehicles. The smaller the value of PET, the closer the cars. A crash occurs when PET equals zero.

The encroachment zone is shown as a green rhomboid in Figure 7.1. It is defined by the geometry of the paths taken by the two cars. The lengths of the sides of the rhomboid are defined by the widths of the cars and the angle at which they cross.

The two archetypical encroachment scenarios are shown in Figure 7.2. Both involve a provoker that turns left across the path of a car with the right of way. The relative direction of the provokers path distinguishes the two scenarios. In one case the provoker turns left from the opposite direction (LTAP/OD) and the other from the lateral direction (LTAP/LD). Less typical encroachment scenarios involve merging. The provoker turns either left or right and merges onto the path of a car with the right of way.

The modification by Autoliv and Chalmers consider only cases in which the red car turns in front of the blue car, Figure 7.3a. An initial analysis included cases in which the red car turns behind the blue car, Figure 7.3b and, in cases with multiple consecutive vehicles, each red-blue car combination, Figure 7.3c. The refinement counts only the first red car in the line of traffic.

The method reads the trajectory data associated with encroachment scenarios and computes the value of PET for every occurrence. The first step in the algorithm is to identify cases in which a provoker turns left in front of a car that has the right of way when the blue car is within the area used to define the intersection. These areas are shown in Figure 5.5.

## Chapter 7 - Encroachments observed at Sävenäs and Jung

The second step in the algorithm is to identify the point where the trajectories intersect. The intersection point defines the center of the rhomboidal encroachment zone.

The software approximates the size and shape of a car and its direction of travel using a rectangle with a defined center point and a known heading. The rectangle and its heading are generated by the image processing software, Chapter 3, and are stored with the trajectory data. The size and shape of the encroachment zone is defined by virtually placing the center points of the two cars' rectangles on top of each other at the intersection point and with their respective headings. The quadrilateral area defined by the sides of the vehicles (or their projection) constitutes the encroachment zone. The software then finds the times when the first car leaves the encroachment zone and the second car enters the zone. It calculates PET by subtracting the first time from the second.

This analysis presented here considers merging scenarios as well as crossing scenarios. This required a modification of the PET software. The modification addresses the fact that merging paths may or may not cross. The centerlines of the cars' paths may run parallel for a considerable distance. Instead of looking for the intersection point of centerlines, the software finds the initial points where the trajectories are within 2 meters (one car width) of each other. These two points are then used for the superposition of rectangles and the determination of the encroachment zone.

The data used in the analyses are refined trajectories, Table 3.1. Refined trajectories have been filtered to remove extraneous objects and large objects like trucks. They have also been shifted using the post-hoc offset correction. The lack of trucks and the addition of the correction in the refined data set remove spurious incidents that may have been detected initially.

### PET at Sävenäs

There are six pairs of trajectories at Sävenäs that pose the opportunity for encroachment. The two archetypical crossing cases are shown in Figure 7.2. Four additional are shown cases in Figure 7.4. The first three additional cases involve merging; the fourth is a crossing case where both vehicles are turning.

Table 7.1 presents the counts and relative frequencies of observed encroachments for all 6 cases. The counts represent the total number of cases for each scenario in which the red car turned in front of the blue car while the blue car was within the area used to define the intersection, Figure 5.5a. The relative frequencies indicate the percentage of total cases for each scenario that produced an encroachment.

Inspection of Table 7.1 reveals that the most common encroachment scenario at Sävenäs involved a blue car on trajectory 6 (east to west with the right of way) and a red car on trajectory 3 (west to north, the most frequently traveled path). This is the dangerous 'left turn across path from opposite direction' (LTAP/OD) scenario in which the relative directions of motion could produce a high-velocity crash. More than 20% of all observed cases of this scenario produced an encroachment.

Similarly high frequencies of encroachment were observed both for cases with one red car and cases with multiple red cars all 6 encroachment scenarios. Encroachment is common.

Encroachment is most common in merging from the right cases, Figure 7.4b (6ms), involving multiple cars. The typical scenario involves a line of traffic waiting to turn right. In half of observed cases, the lead car appears to have become impatient and decided to merge into the path of a car traveling from east to west.

## Chapter 7 - Encroachments observed at Sävenäs and Jung

Scenarios involving waiting red cars rarely produced encroachment. Often, the waiting car is yielding the right of way rather than provoking. In other cases, the presence of a yielding car on a different trajectory appears to influence the provoker to yield. This may be a manifestation of the social impact of multiple others on driver decision making (e.g., Latané, 1981; Smith, 2008).

There are three additional salient findings at Sävenäs. First, the distributions of observed PET values differ between the two types of left turn across path, Figure 7.2. Second, the presence of multiple cars does not influence the observed value (only their frequency for scenario 6ms, as discussed above). Third, in many merging cases the separation between vehicles is frequently less than 2 seconds. At 50 kph, the distance between the provoker and the blue car that ends up behind it is often less than 30 meters. The data that support these findings are discussed in turn.

Figure 7.5 and similar figures that follow contain two graphs that represent the same data using different units of measurement. Figure 7.5a shows the mean and standard deviations of observed PET values in seconds. In Figure 7.5b, the seconds have been converted into meters using the assumption that the blue car approaches the intersection at the posted speed limit (50 kph at Sävenäs and 70 kph at Jung). The distances represent the expected separation between vehicles during an average encroachment.

Figure 7.5 compares the PET values for the two left turn across path scenarios of Figure 7.2. The means are significantly different,  $t(344) = 5.32$ ,  $p < .001$ , with the average encroachment from the opposite direction being nearer (33.3 m) than from the lateral direction (37.8 m).

A more detailed analysis is afforded by inspection of Figure 7.6. In this figure and others like it, the upper two panels plot the distribution of observed PET values between 0.0 seconds (a crash) and 4.0 seconds (56 meters at 50 kph). The lower panel contains the corresponding cumulative frequency functions. The Kolmogorov-Smirnov statistical test is used to compare the distributions.

The distributions plotted in Figure 7.6 are significantly different,  $D(501, 214) = 0.21$ ,  $p < .001$ . Not only do their means differ but the two sets of data differ. Encroachment times are consistently shorter (shifted to the left) for scenario 6xa (LTAP/OD) than for scenario 6xs (LTAP/LD). When coupled with the higher relative velocities of the two cars in the oncoming case, the shorter PET values make this scenario particularly dangerous. This finding could be used to guide the development of active safety systems.

Similar analyses compared scenarios involving one red car and multiple cars (e.g., comparing 6xa and 6xam) for all 6 encroachment types. None of the comparisons were statistically significant. It appears that the presence of additional cars did not have an appreciable influence on the distribution of PET values.

Figure 7.7 compares the PET values for the three merging scenarios of Figure 7.4a, b, and c. In all three scenarios, the average PET was less than 2 second (28 meters). The most extreme is scenario 6ms, Figure 7.4b, merging from the right. In this scenario the average separation between the merging provoker and the car with the right of way was only 20.5 meters.

The distributions for the merging scenarios are plotted in Figure 7.8. Inspection of these graphs uncovers the ominous finding reported in Table 7.2. The two panels in Table 7.2 reproduce the four quadrants of the layout of Figure 7.4. Cells in the first panel indicate the percentage of observed PET values less than 2.0 seconds (28 meters) and 0.5 seconds (7 meters). Cells in the second panel indicate the percentage of total cases with encroachments at these levels. Fully 22% of all drivers who approach the Sävenäs intersection from the east can expect to end up on the bumper of a car turning right. This unexpectedly high frequency

## Chapter 7 - Encroachments observed at Sävenäs and Jung

makes merging from the right, scenario 6ms, Figure 7.4b, a viable candidate for focusing the development of active safety systems.

### Probability of PET < .05

Because PET can be calculated only after the fact, it does not lend itself to immediate implementation in an active safety system. Nevertheless, observed distributions of PET values can be used to suggest thresholds that delimit 'unacceptably short' PET values from those that drivers might be more willing to tolerate. The location of such thresholds is arbitrary. For the sake of illustration, we have adopted the 5% standard used in many statistical tests and calculated the value of PET two standard deviations below the mean of the observed distributions.

The two graphs of Figure 7.9 show the observed distributions of PET values at Sävenäs for all LTAP/OD and LTAP/LD scenarios. The bold vertical lines are plotted two standard deviations below the mean of the observed distributions, 1.10 seconds (15.2 meters at 50 kph) for LTAP/OD scenarios and 1.15 seconds (16.0 meters) for LTAP/LD scenarios. As only five in every 100 observations is expected to lie beyond this limit (at shorter values of PET), it represents a strict criterion for a low pass filter. An analysis of this type might be useful for designers of systems who seek to reduce false alarms to acceptable levels.

### Jung

There are 28 pairs of trajectories at Jung that pose the opportunity for encroachment. The proliferation, compared to Sävenäs, is due to three features of the four-way intersection. First, traffic on the secondary road can encroach when crossing the primary road (the E20). Second, secondary traffic can encroach on traffic turning left off the E20. Third, secondary traffic can encroach on each other. Figure 7.10 shows half of the encroachment scenarios, the scenarios encountered by blue cars from the south or west. The other half are mirror images from the north and east.

Table 7.3 presents the counts and relative frequencies of observed encroachments for all 28 cases summed over single red cars, multiple red cars, and waiting scenarios. Of the 951 observed encroachments, 359 involved single red cars, 563 multiple red cars, and only 29 waiting cars. Perhaps the most significant finding concerning encroachments at Jung is their frequency. Only 3% of all scenarios with the potential for encroachment actually evolved into an encroachment. The contrast with Sävenäs could not be more striking. It appears that the high velocities on the E20 and its width strongly discourage risk-taking provokers. Speed and intersection size clearly matter.

There are only 5 scenarios with observed frequencies of encroachment greater than 15% at Jung. Three of these have too few observations to support an assessment of the representativeness of the data. The remaining two, NSSLX and WSELX, are both LTAP/OD scenarios. Indeed, fully 67% of the drivers traveling across the E20 from the west who encountered a car turning left from the east experienced encroachment. It appears that the local traffic has not adjudicated the right of way in scenarios involving left turns off the primary road (the E20) and straight drives on the secondary road. The high frequency of encroachment these scenarios could be used to guide the development of active safety systems.

The discussion of Jung encroachments highlights five additional findings. First, there is a profound influence of the direction of encroachment by crossing traffic. Encroachment times

## Chapter 7 - Encroachments observed at Sävenäs and Jung

were shorter when the provoker crosses from the left than from the right. Second, there appears to be an asymmetry in the distribution of PET in the two LTAP/OD scenarios involving pairs of cars driving on the E20. Third, there is a similar asymmetry in the two LTAP/LD scenarios. In both cases the risk is greater for drivers from south than from the north. Fourth, in contrast with Sävenäs, there is only a minor difference in the distributions of PET values for the LTAP/OD and LTAP/LD scenarios. Finally, the number of cars in the intersection appears to strongly influence the distribution of PET values for left-turn merges, Figure 7.4a, at Jung. The data that support these findings are discussed in turn.

The graphs of Figure 7.11 plot the PET values for the two orthogonal scenarios shown in Figure 7.10b. In these scenarios the blue car enters the intersection from either the south or the north and the provoker enters from either the west or the east. The comparison focuses on the relative direction of the provoker's approach. When the provoker crossed the E20 from the left (SSWSX, NSESX), the average value of PET was significantly shorter than when the provoker crossed from the right (SSESX, NSWSX),  $t(434) = 7.61$ ,  $p < .001$ . PET values were shorter when the provoker comes from the far side.

The distributions shown in Figure 7.12 underscore the shifting of values to the left when the provoker crossed from the far side. Not only do their means differ but the two sets of data differ,  $D(183, 270) = 0.39$ ,  $p < .001$ . This finding suggests that it may be appropriate for designers of active safety systems to focus efforts at detecting encroachments from the far (left) side of the highway.

The data plotted in Figures 7.13 and 7.14 reveal a directional asymmetry in the distribution of PET values for LTAP/OD scenarios at Jung. In these scenarios the driver with the right of way and the provoker enter the intersection from opposite directions on the E20. PET values were significantly shorter when the driver with the right of way entered from the south (SSNLX) than from the north (NSSLX),  $t(27) = 2.62$ ,  $p < .01$ . The encroachments were, on average, 12 meters closer. While significant, interpretation of this result is tempered by acknowledgement that there are only 14 cases of drivers from the north turning left at Jung.

An identical asymmetry is seen in the data plotted in Figures 7.15 and 7.16. Here the comparison is of LTAP/LD scenarios. In these scenarios the driver with the right of way enters the intersection on the E20 and the provoker turns left across her path from the near side. PET values were significantly shorter when the driver with the right of way entered from the south (SSELX) than from the north (NSWLX),  $t(69) = 1.43$ ,  $p < .08$ . The encroachments were, on average, 7.5 meters closer. Once again, drivers from the south who encounter an encroachment can expect to experience shorter values of PET than drivers from the north.

The specifics of these two observations are not likely to generalize beyond Jung. Their implications, however, may be universal. The data from Jung point to a contextual influence on the distribution of encroachments. While the data do not identify the factor or factors that produce the asymmetry, there is a strong hint in the list of the total counts of cases in each scenario, Chapter 6, Table 6.4. There were very few left turns from the north, Figures 7.13 and 7.14, and relatively few from the east, Figures 7.15 and 7.16. The PET values were consistently short in scenarios where traffic was relatively uncommon. If much of the traffic on the E20 is local and if local drivers are tacitly aware of the low base rate of left turns, it may be the case that drivers from the south fail to adjust to the rare cases where left turns across their path occur. If this speculation holds at other intersections, knowledge of the base rates of left turns could guide the development of active safety systems.

At Sävenäs there was a significant difference between the distributions of PET values for LTAP/OD and LTAP/LD scenarios. That difference was not seen at Jung. Neither the

## Chapter 7 - Encroachments observed at Sävenäs and Jung

average PET values nor their distributions were significantly different. This finding suggests that the difference seen at Sävenäs may reflect a local contextual variable. A likely candidate is the flip side of the point made just above. The shorter PET times at Sävenäs were associated with left turns on the most common path. Cars with the right of way are relatively uncommon. The common element is the low base of one or the other of the two paths. When traffic is relatively infrequent - when a scenario is unexpected - PET values tend to be shorter.

The final data set discussed here highlights the impact of the number of cars when the provoker merges from the left (NSELX, SSWLX), Figure 7.4a. At Jung, as at Sävenäs, PET values in merging scenarios can be relatively short. As shown in Figure 7.17, the average PET value for scenarios with only one red car is less than 4.4 seconds (85 meters at 70 kph). For scenarios with multiple red cars, the average value of PET is less than 3.6 seconds (68 meters). The difference is significant,  $t(50) = 3.3$ ,  $p < .001$ . The cumulative frequency distributions shown in Figure 7.18 underscore the increased likelihood of encroachment when there are several cars in the intersection. Once again, extrapolation of finding must be tempered by acknowledging the small number of observations.

### Probability of PET < .05

The two graphs of Figure 7.19 show the observed distributions of PET values at Jung for all LTAP/OD and LTAP/LD scenarios and plot lines two standard deviations below the mean, 2.70 seconds (52.5 meters at 70 kph) for LTAP/OD scenarios and 2.91 seconds (56.6 meters) for LTAP/LD scenarios. As only five in every 100 observations is expected to lie beyond this limit (at shorter values of PET), it represents a strict criterion for a low pass filter. An analysis of this type might be useful for designers of systems who seek to reduce false alarms to acceptable levels.

### References

- Latané, B. (1981). The psychology of social impact. *American Psychologist*, 36, 343-356.
- Smith, K. (2008). Immediacy, trust, and remote command and control. *Journal of Cognitive Engineering and Decision Making*. 2 (2), 105-117.

Figures

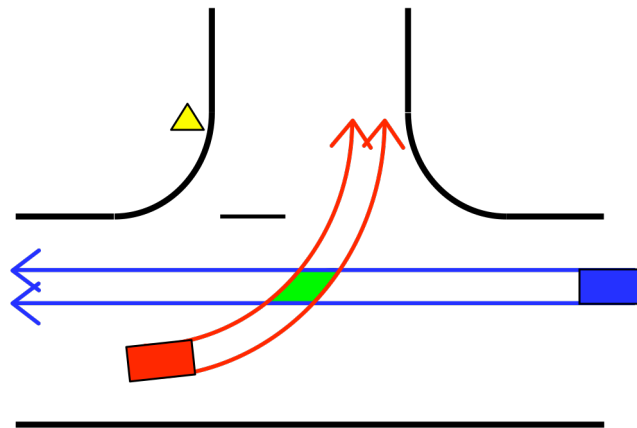


Figure 7.1 A sketch of a typical scenario that can produce an encroachment. The 'encroachment zone' is the green rhomboid.

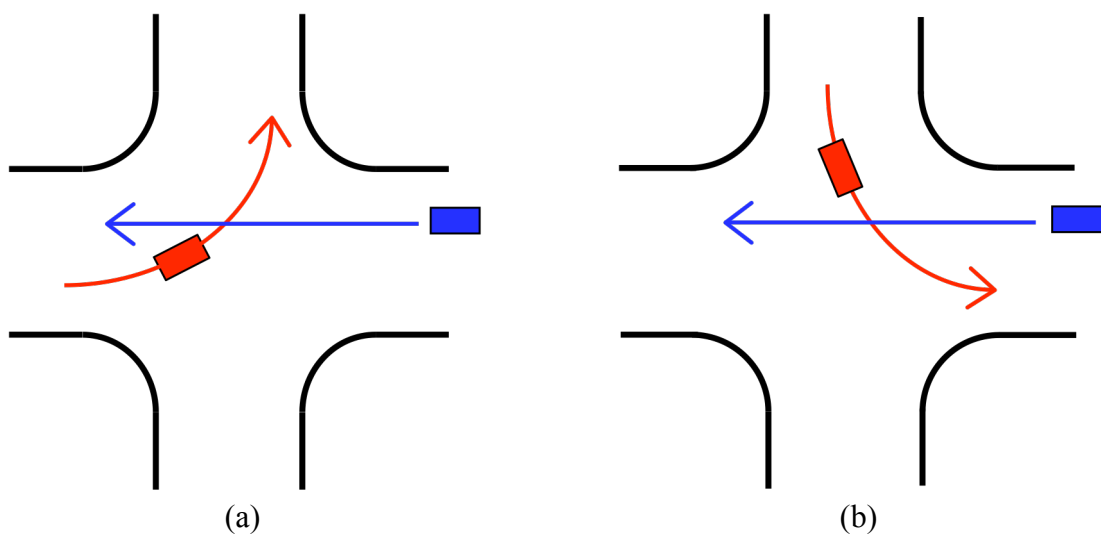


Figure 7.2 Sketches of the two archetypical encroachment scenarios. The blue car has the right of way. The red car encroaches on its path. (a) Left turn across path from the opposite direction (LTAP/OD). (b) Left turn across path from the lateral direction (LTAP/LD).



## Chapter 7 - Encroachments observed at Sävenäs and Jung

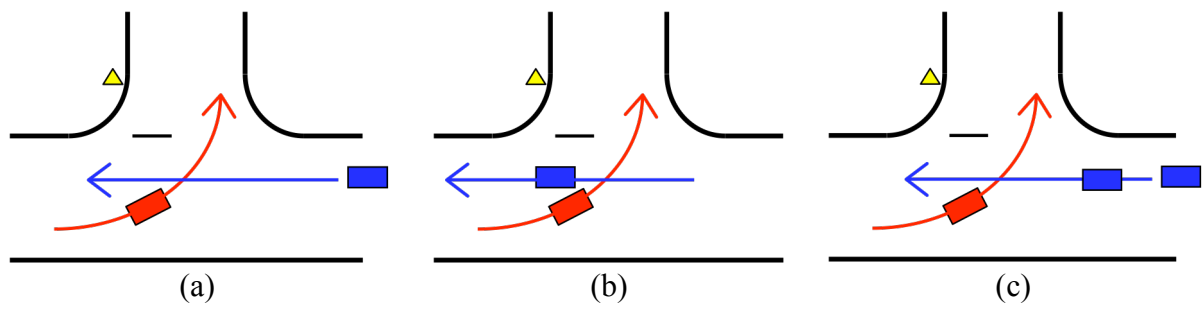


Figure 7.3 (a) The LTAP/OD case considered in these analyses. (b) The additional two-car case counted as an encroachment in the initial analyses. (c) The multiple car case that generated multiple encroachments in the initial analyses.

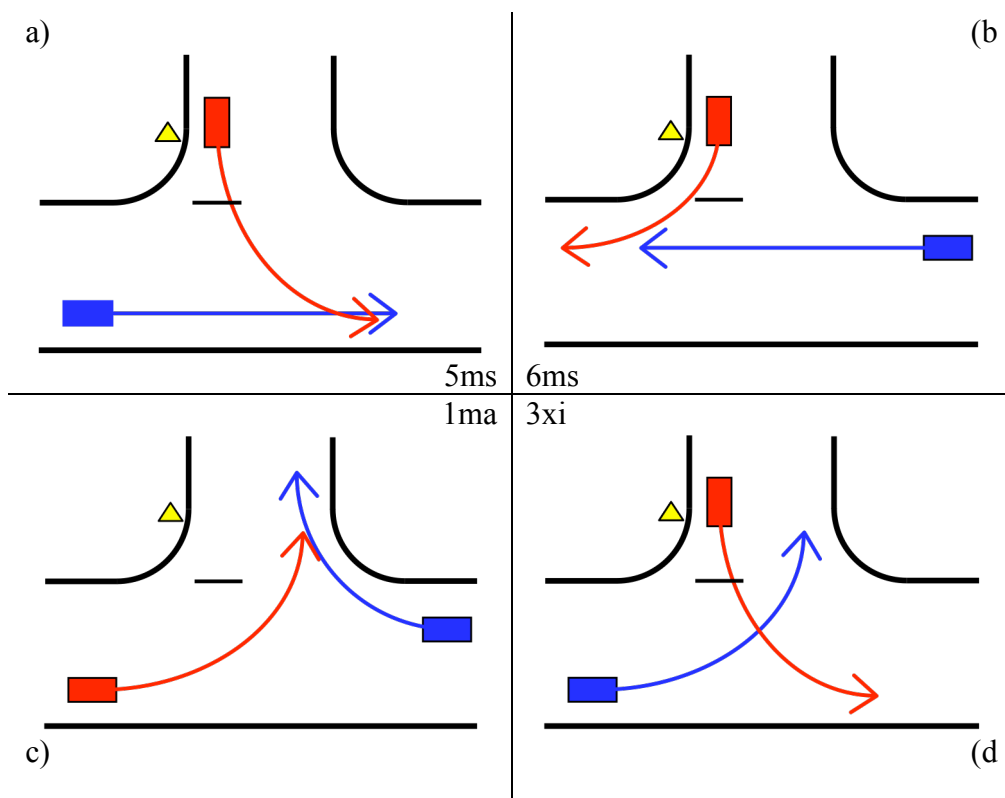


Figure 7.4 The four additional encroachment scenarios at Sävenäs. (a) Merging from the left (5ms), (b) Merging from the right (6ms), (c) Merging together (1ma), and (d) Crossing from the intended direction of travel (3xi).

## Chapter 7 - Encroachments observed at Sävenäs and Jung

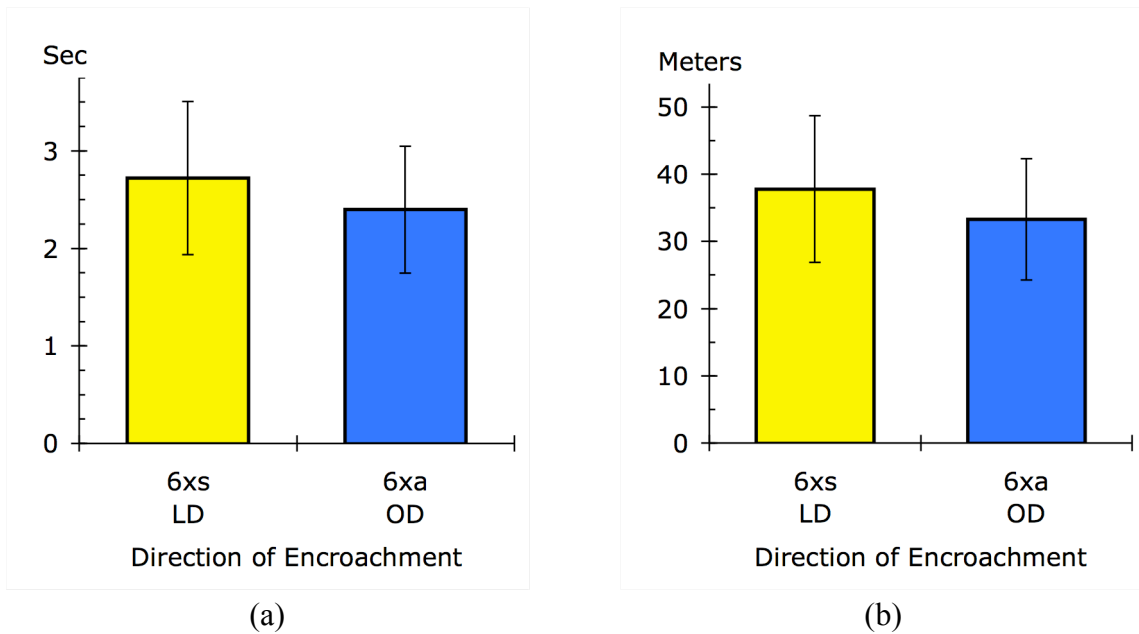


Figure 7.5. Plots comparing observed PET values for LTAP/LD and LTAP/OD cases at Sävenäs. (a) Observed PET values in seconds. (b) The distance traveled during that time at 50 kph.

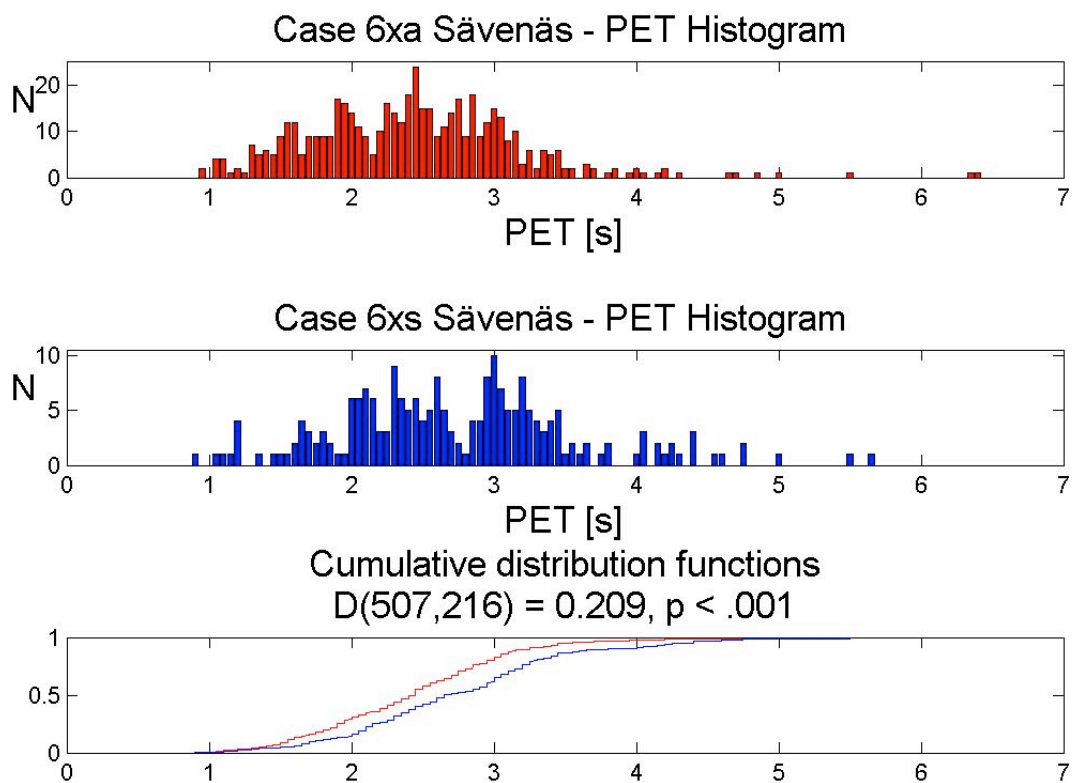


Figure 7.6. Histograms and cumulative distribution functions of observed PET values for LTAP/LD and LTAP/OD cases at Sävenäs.

## Chapter 7 - Encroachments observed at Sävenäs and Jung

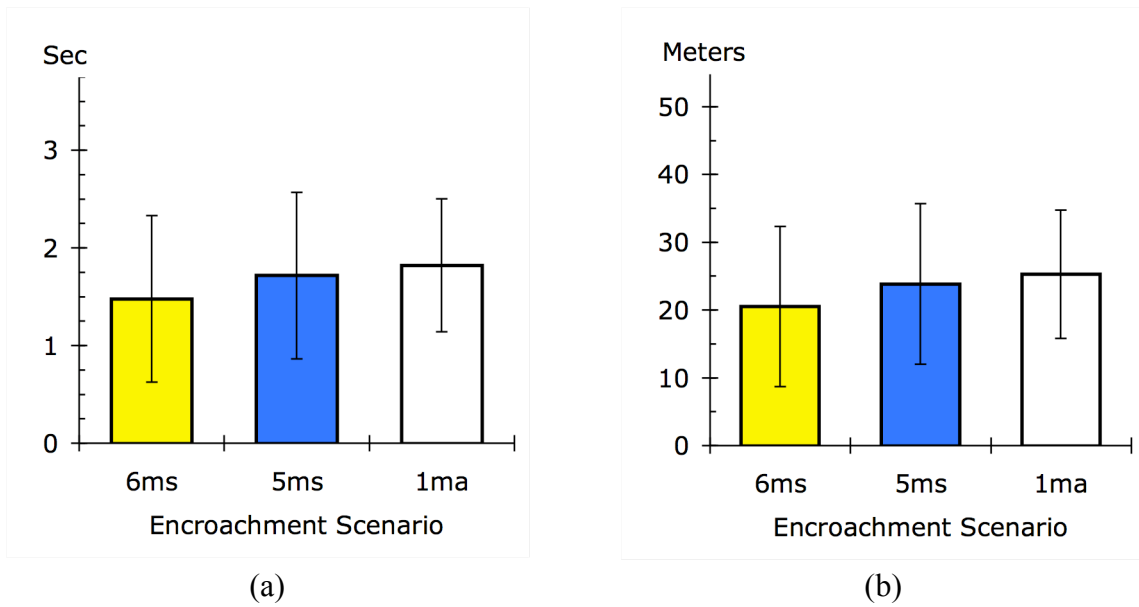


Figure 7.7. Plots showing the mean and standard deviations of observed PET values for 3 merging cases at Sävenäs. (a) Observed PET values in seconds. (b) The distance traveled during that time at 50 kph.

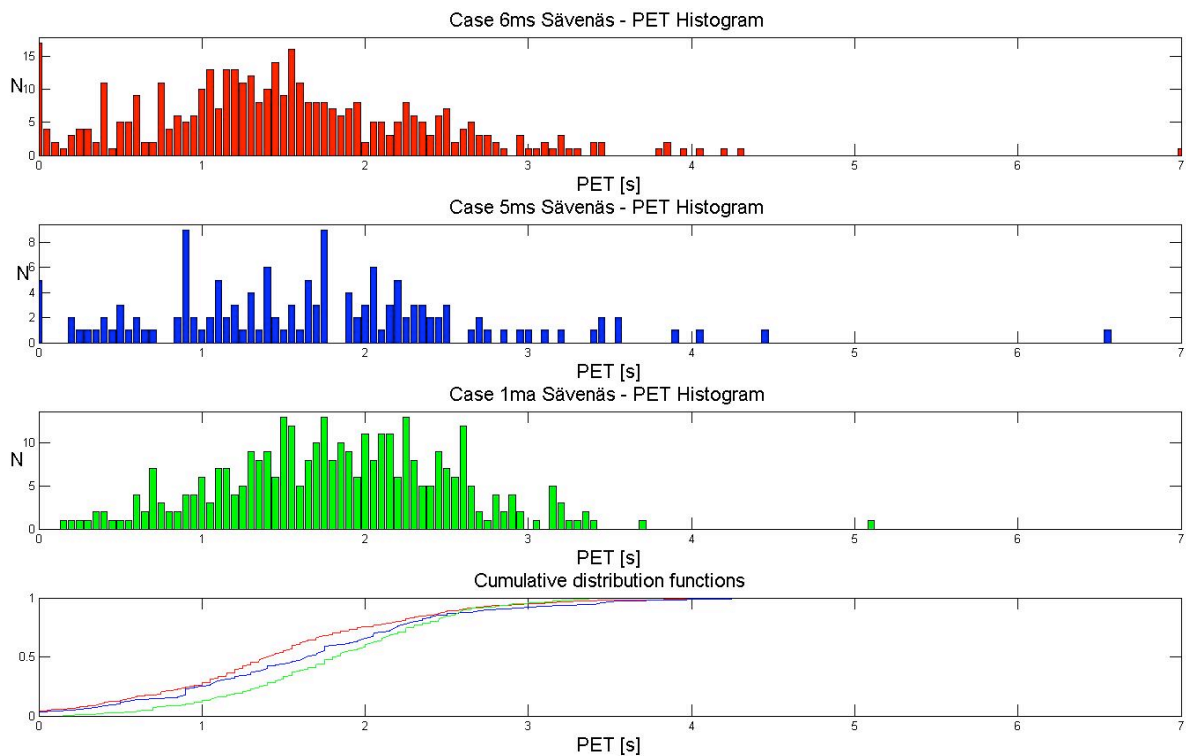


Figure 7.8. Histograms and cumulative distribution functions of observed PET values for 3 merging cases at Sävenäs.

## Chapter 7 - Encroachments observed at Sävenäs and Jung

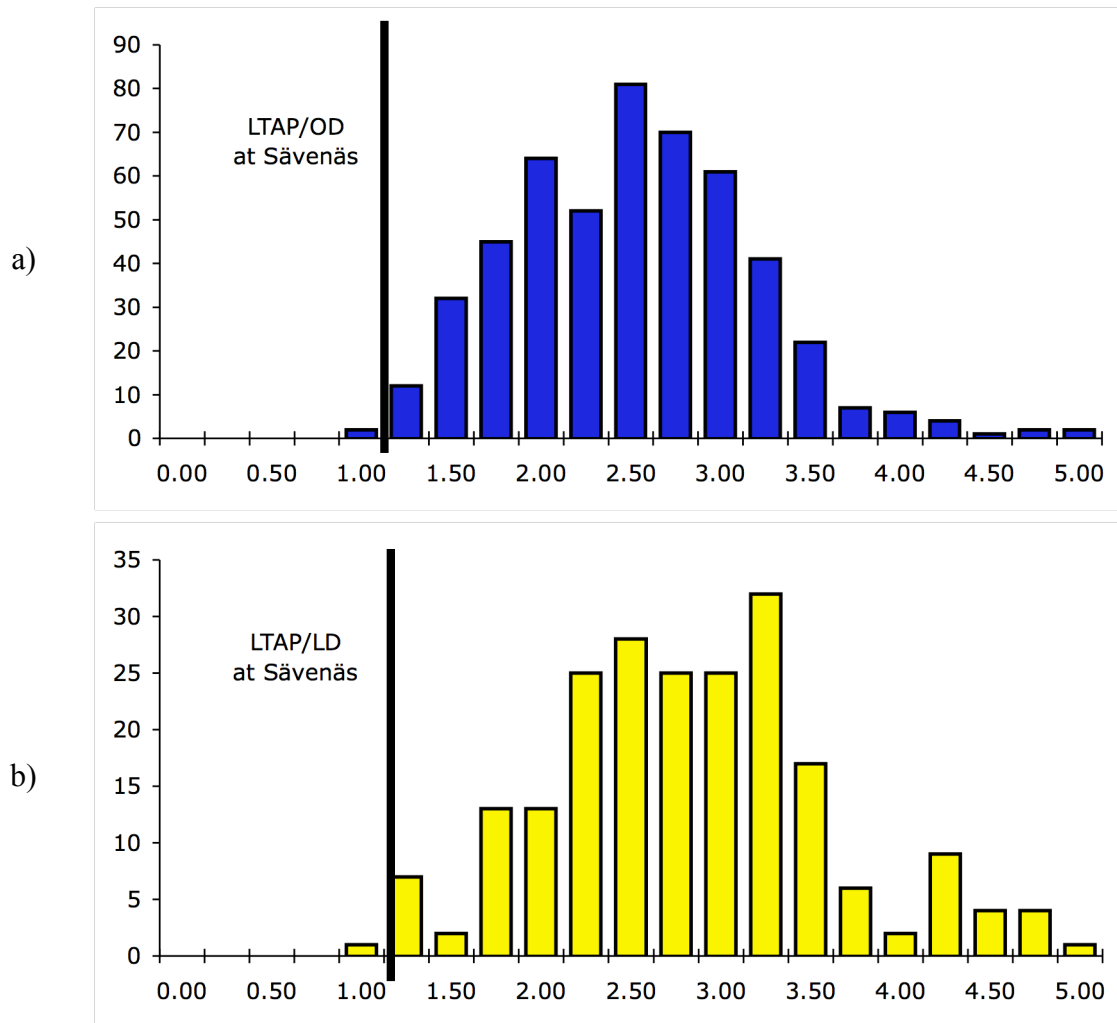


Figure 7.9 Histograms of PET values at Sävenäs showing the location of the 5th percentile of a normal distribution for the (a) all LTAP/OD scenarios and (b) all LTAP/LD scenarios.

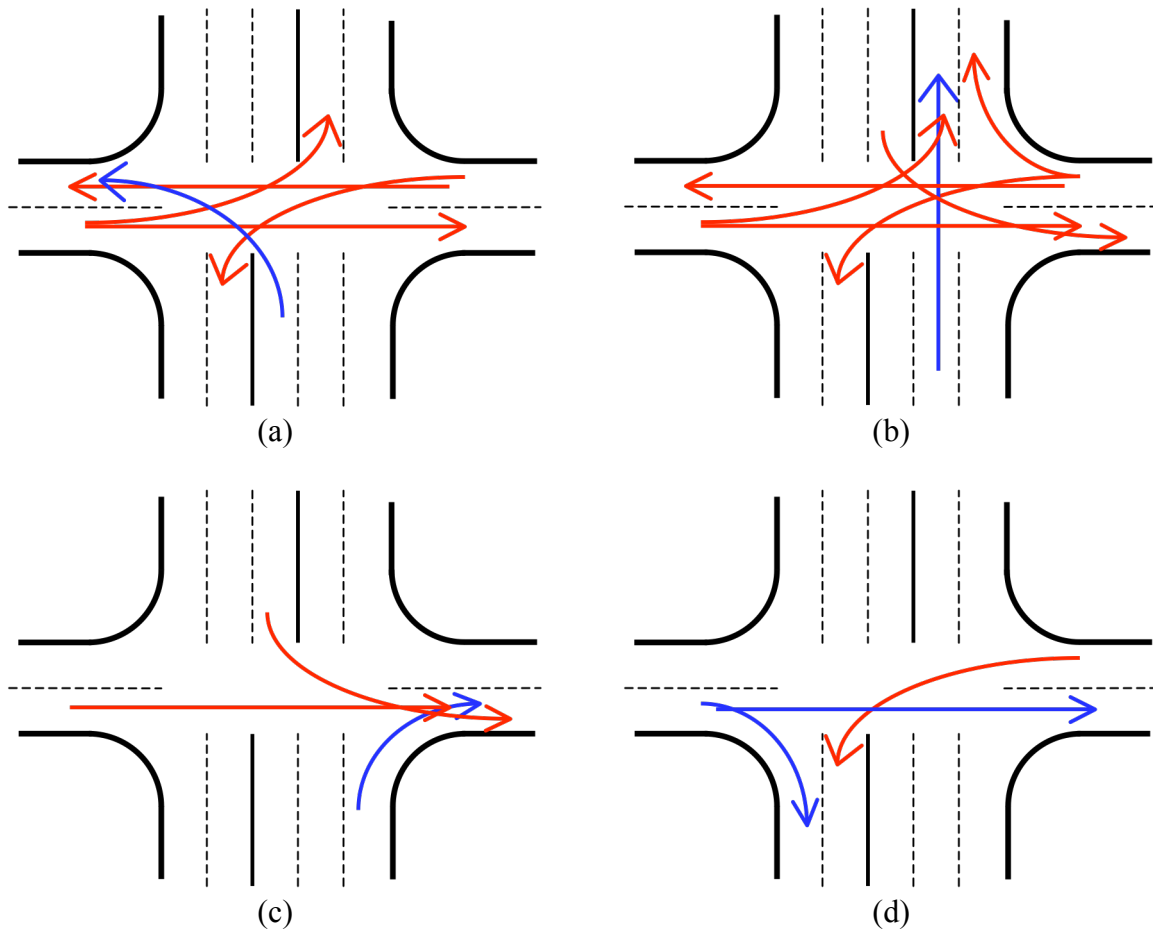


Figure 7.10 Encroachment scenarios at Jung for vehicles with the right of way (blue cars) (a) turning left from the south, (b) proceeding straight from the south, (c) turning right from the south, and (d) on two paths from the west. An identical mirror set exists for traffic from the north and east.

## Chapter 7 - Encroachments observed at Sävenäs and Jung

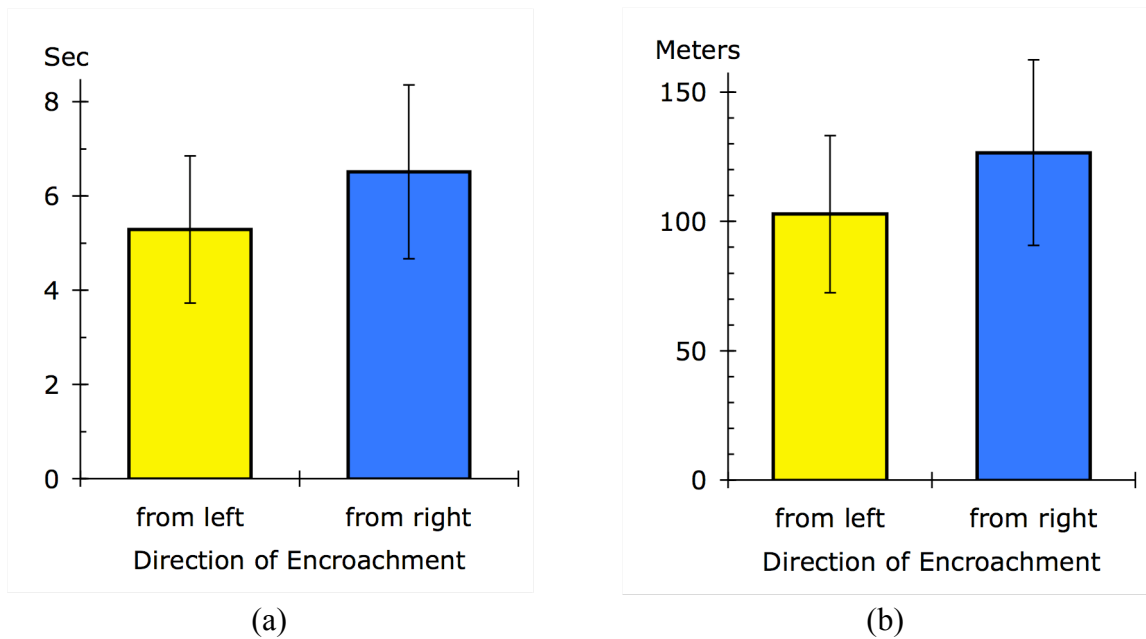


Figure 7.11. Plots showing the influence of the direction of travel the secondary road on observed PET values for crossing cases at Jung. (a) Observed PET in seconds. (b) The distance traveled during that time at 70 kph.

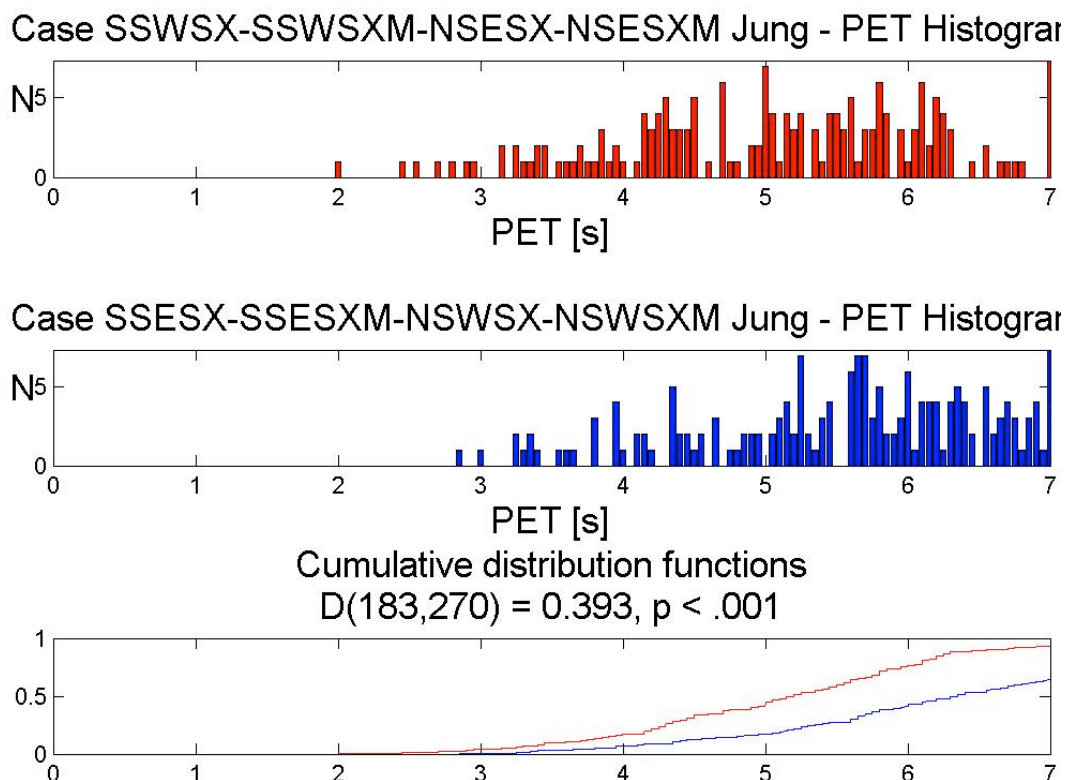


Figure 7.12. Histograms and cumulative distribution functions of observed PET values for traffic crossing the E20.

## Chapter 7 - Encroachments observed at Sävenäs and Jung

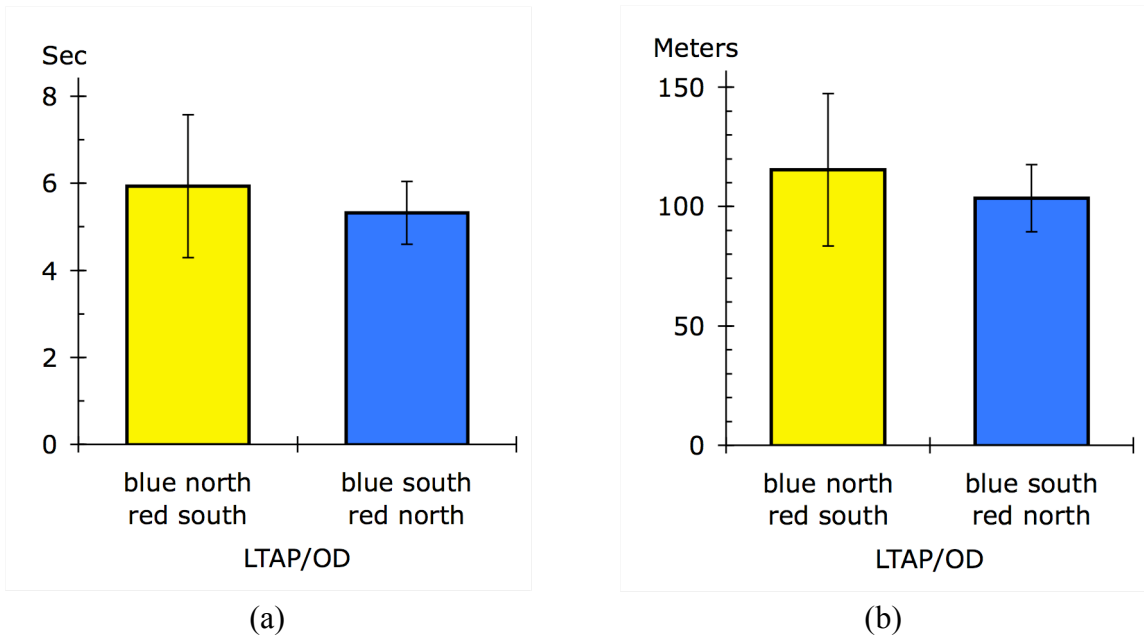


Figure 7.13. Plots showing the influence of the direction of travel on the E20 on observed PET values for LTAP/OD cases at Jung. (a) Observed PET in seconds. (b) The distance traveled during that time at 70 kph.

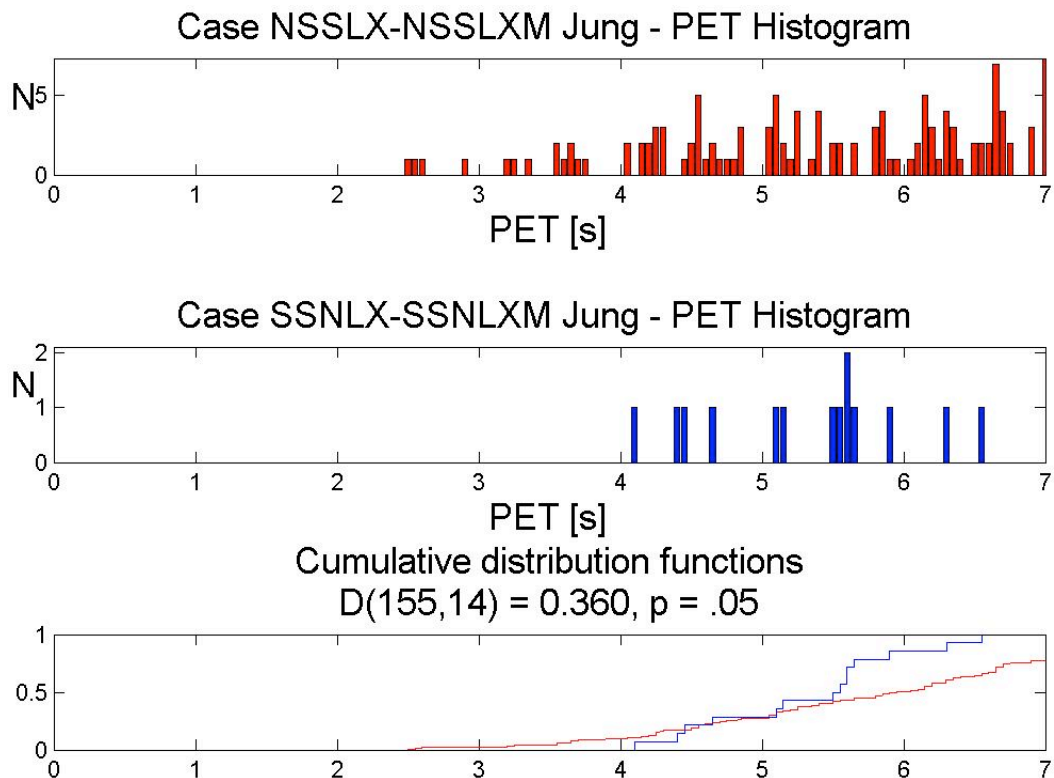


Figure 7.14. Histograms and cumulative distribution functions of observed PET values for LTAP/OD cases at Jung.

## Chapter 7 - Encroachments observed at Sävenäs and Jung

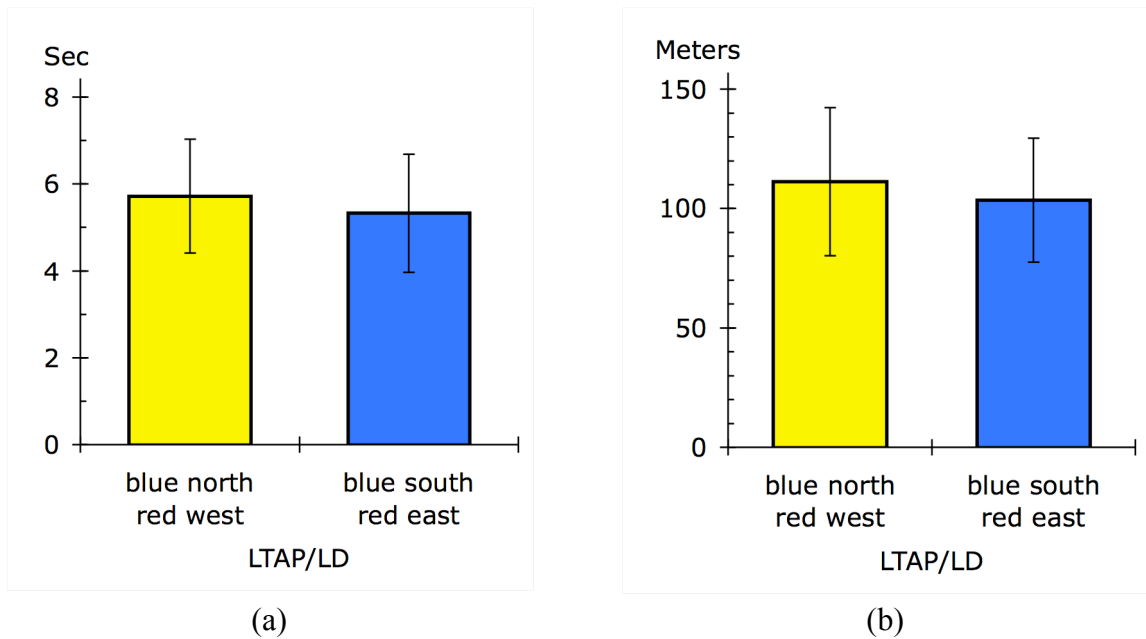


Figure 7.15. Plots showing the influence of the direction of travel on the E20 on observed PET values for LTAP/LD cases at Jung. (a) Observed PET in seconds. (b) The distance traveled during that time at 70 kph.

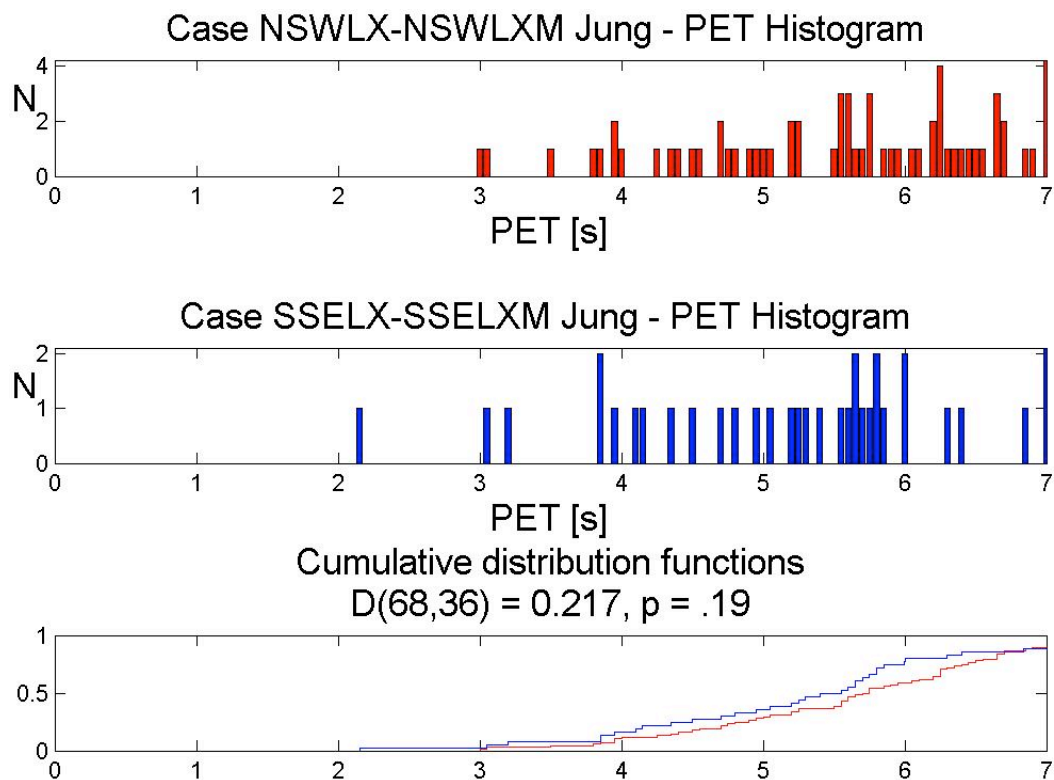


Figure 7.16. Histograms and cumulative distribution functions of observed PET values for LTAP/LD cases at Jung.



## Chapter 7 - Encroachments observed at Sävenäs and Jung

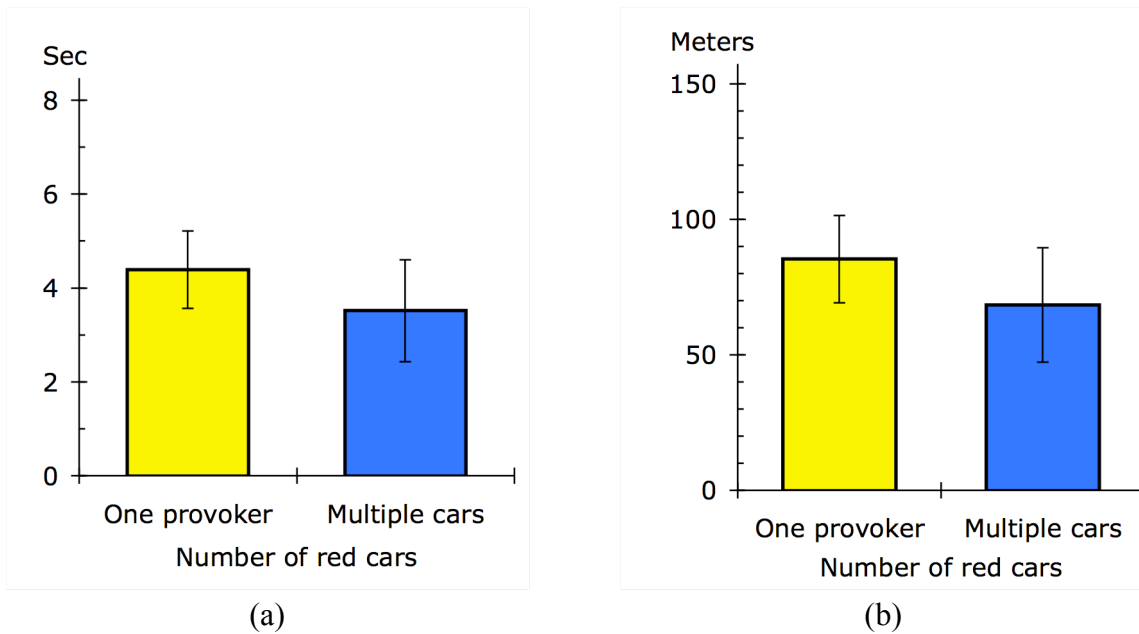


Figure 7.17. Plots showing the influence of the number of cars in the intersection on left turn merges at Sävenäs. (a) Observed PET in seconds. (b) The distance traveled during that time at 70 kph.

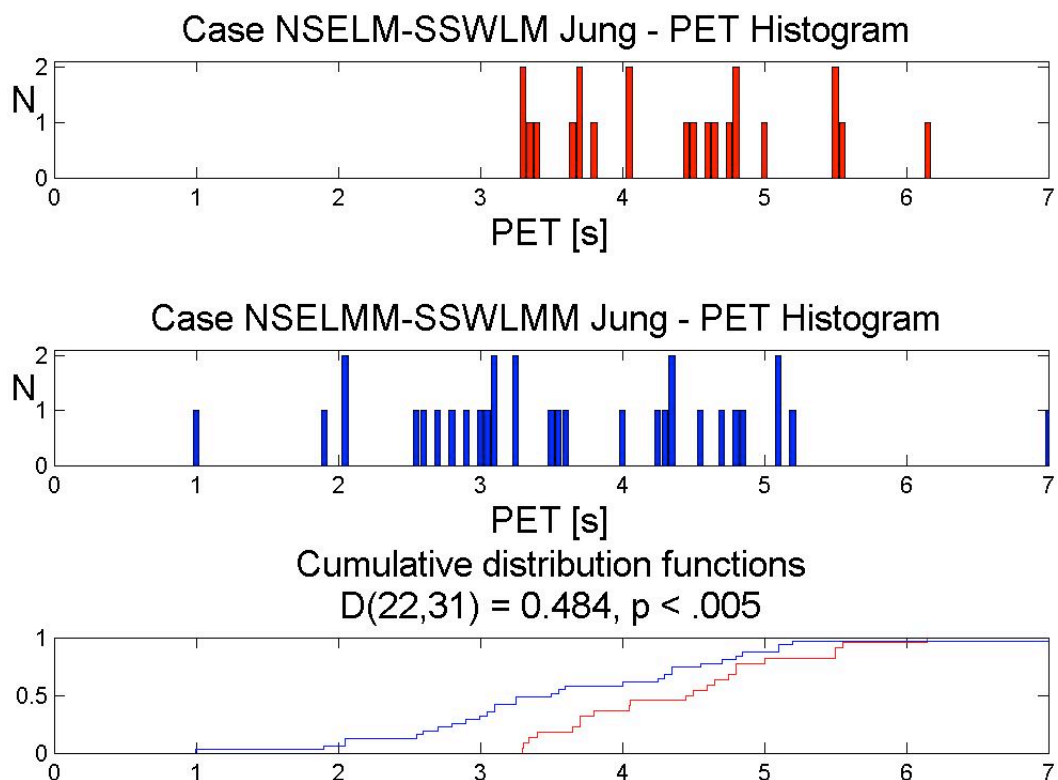


Figure 7.18. Histograms and cumulative distribution functions of observed PET for merging cases at Jung involving one or multiple red cars.

## Chapter 7 - Encroachments observed at Sävenäs and Jung

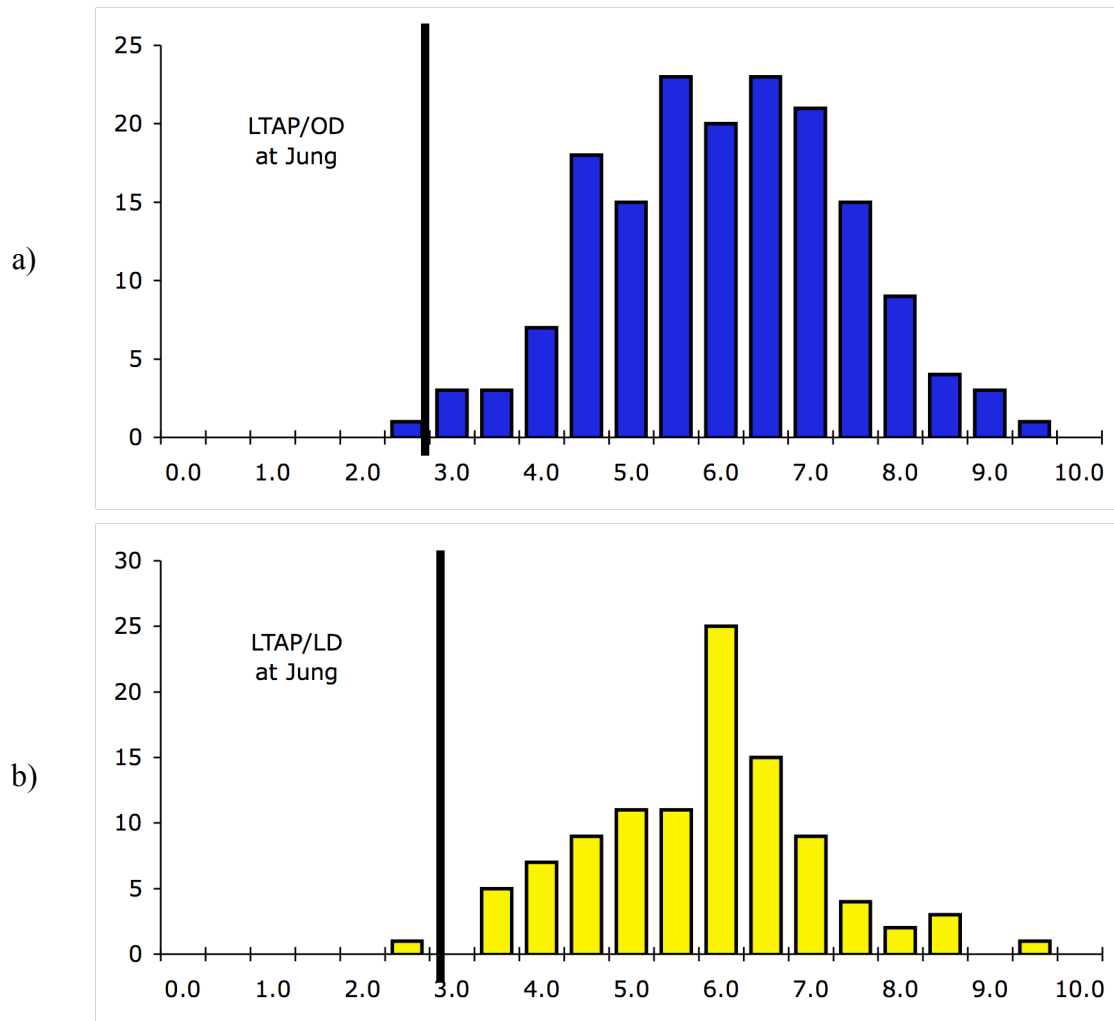


Figure 7.19 Histograms of PET values at Jung showing the location of the 5th percentile of a normal distribution for the (a) all LTAP/OD scenarios and (b) all LTAP/LD scenarios.

## Chapter 7 - Encroachments observed at Sävenäs and Jung

Table 7.1 (a) Counts and (b) relative frequencies of observed encroachments at Sävenäs.

Blue	Solo	One red car						One waiting red car						Multiple red cars						Multiple red cars with waiting						
		1	2	3	4	5	6	1w	2w	3w	4w	5w	6w	1m	2m	3m	4m	5m	6m	1wm	2wm	3wm	4wm	5wm	6wm	
1		344						2						317						3						E to N
2																										N to W
3		370						11						297						31						W to N
4																										N to E
5		139						1						103						5						W to E
6		386	504	214				4	4	0				278	354	149				1	3	2				E to W

Blue	Solo	One red car						One waiting red car						Multiple red cars						Multiple red cars with waiting						
		1	2	3	4	5	6	1w	2w	3w	4w	5w	6w	1m	2m	3m	4m	5m	6m	1wm	2wm	3wm	4wm	5wm	6wm	
1		16%						0%						17%						1%						E to N
2																										N to W
3		27%						1%						17%						2%						W to N
4																										N to E
5		23%						0%						14%						1%						W to E
6		22%	23%	32%				0%	1%	0%				49%	23%	39%				0%	1%	1%				E to W

Table 7.2 Percentage of merging scenarios at Sävenäs with encroachments less than 2.0 and 0.5 seconds.

Separation		% of observed encroachments				% of total cases			
Seconds	Meters	5ms		6ms		5ms		6ms	
		1ma	3xi	1ma	3xi	1ma	3xi	1ma	3xi
> 2.0	> 28	65%	75%	12%	22%	12%	22%	12%	22%
> 0.5	> 7	6%	9%	1%	3%	1%	3%	1%	3%
> 2.0	> 28	60%	4%	10%	1%	10%	1%	10%	1%
> 0.5	> 7	3%	0%	0%	0%	0%	0%	0%	0%

## Chapter 7 - Encroachments observed at Sävenäs and Jung

Table 7.3 (a) Counts and (b) relative frequencies of observed encroachments at Jung.

a)

		S			E			N			W					
		L	S	R	L	S	R	L	S	R	L	S	R			
S	L				1	15					8	19				
	S				0	144	0				15	71				
	R										0	3				
E	L															
	S													0		
	R													3		
N	L				2	3					3	1				
	S				156	31	114				68	136	5			
	R				6	8										
W	L															
	S													65		
	R													15		

915

b)

		S			E			N			W					
		L	S	R	L	S	R	L	S	R	L	S	R			
S	L				2%	11%					13%	12%				
	S				0%	10%	0%				12%	5%				
	R										0%	2%				
E	L															
	S													0%		
	R													43%		
N	L				20%	13%					33%	7%				
	S				17%	13%	8%				15%	11%	1%			
	R				5%	5%										
W	L															
	S													67%		
	R													15%		

3%

## Chapter 8 - Go / No Go Decisions

### Introduction

Intersection crashes involving a vehicle that encroaches upon another's path are over-represented in crash statistics and are frequently fatal (Chan, 2006; McGuin & Brown, 1999). Encroachment scenarios involve a car with the right of way, which we refer to as the 'blue car', and a second car that turns in front of the blue car across or into its path. The car that makes the turn provokes the encroachment. We refer to the encroaching car as the 'provoker' or the 'red car'.

The four basic encroachment scenarios are shown in Figure 8.1. The figures represent the three-way Sävenäs intersection. There are two instances of each type of scenario at the four-way Jung intersection where traffic in both directions of the E20 has the right of way. For example, Figure 8.1a shows the red car turning left across the path of the blue car from the opposite direction (LTAP/OD). At Jung, this type of encroachment can be provoked by a car from the south turning left across the path of a car from the north and by a car from the north turning left across the path of a car from the south.

This chapter presents analyses of data from both Sävenäs and Jung that identify several contextual factors that appear to influence the decision by the driver of the provoker to turn or not to turn. We call this decision the 'Go / No Go decision'. Analyses of the image processing data, Chapter 3, identify the separation (in both time and distance) between the red and blue cars at the time when the decision is assumed to be made. Logistic regression is used to define the separation at which 50% of the drivers of red cars in the scenarios shown in Figure 8.1 decided (not) to turn. We call this point the '50/50 point' for the Go /No Go decision. At shorter distances and times, most drivers do not encroach. At greater distances, most do. We offer the 50/50 point as a criterion for generating expectations for the behavior of drivers in scenarios that have the potential for encroachment. These context-dependent expectations could be used to inform the design of active safety systems that would alert drivers to the encroachment.

### Previous research on the Go / No Go decision

Research on left-turns in intersections is active (e.g., Caird & Hancock, 2002; Chan, 2006, 2007; Davis & Swenson, 2004; Ragland et al., 2006; Yan & Radwan, 2007; Yan, Radwan, & Guo, 2007). Some studies use simulators to study driver actions in near-crash situations (e.g., Caird, Chisholm, Edwards & Creaser, 2007). Most describe on-site observations of traffic and post-hoc analyses using logistic regression to identify the critical distance or critical time when 50% of drivers decide (not to) make the left turn. This study adopts and extends the latter approach. Most of the previous work has used time as the metric of separation (e.g., Tian, et al., 1999). Following Harrell and Spaulding (2001), we prefer to use distance as our principal metric. Information about distance is immediately available to both the driver's eye and to sensors that would inform in-vehicle systems. In contrast, time (e.g., time to contact) requires untenable assumptions about the constancy of velocities.

Many studies of left turns focus on gap acceptance - the situation where a provoker turns through a stream of traffic. The 'gap' is the measure of time or distance between vehicles in the stream. Ragland, et al., (2005) argue that where there is only one blue car and no stream of traffic, the appropriate term is 'lag' - the measure of time or distance between the opportunity for the red car to turn and the arrival of the blue car. In this study, we have studied the lag, not the gap.

## Chapter 8 - Go / No Go Decisions

### Method

#### Automated image processing of video data

The tracks generated by the image processing system, Chapter 3, were culled to eliminate all over-size vehicles, e.g., trucks and buses, to retain our focus on passenger cars. Trajectories and scenarios were defined using the algorithms developed by Autoliv and Chalmers. The time-stamped trajectory data make it possible to identify pairs of cars that were in the intersection at the same time and to identify which car turned left (or not) across the path of another and whether there were additional cars in view.

#### The four traffic scenarios

Separate analyses were conducted for each of the four traffic scenarios sketched in Figure 8.1. In each scenario the blue car has the right of way and the red car is the provoker. The driver of the red car makes the decision (not) to turn and cross the path of the blue car. Figure 8.1a is a left turn across path from the opposite direction (LTAP/OD). The provoker turns from the main road but should yield to the blue car. In the other three scenarios, the provoker turns from the secondary road. At Sävenäs traffic on the secondary road has a yield sign; there are stop signs at Jung for traffic on the secondary road from both the east and west, Figure 5.3. Figure 8.1b represents a left turn left across the right-of-way path from the lateral direction (LTAP/LD). In the crossing scenario shown in Figure 8.1c, both cars are turning left with the blue car turning from the right of way road. There are insufficient data from Jung to support analysis of the crossing scenario. In the merging scenario, Figure 8.1d, both cars intend to travel in the same direction down the right of way road.

#### Minimum velocity marks the decision point

Our analyses take what we believe to be a novel approach to defining the point where the driver of the provoker can be expected to make the decision (not) to encroach. Our premise is that the decision to encroach is made the time when the car's velocity is at its minimum. If the decision is to Go, the car begins to accelerate. If the decision is No Go, deceleration continues. This line of reasoning identifies the inflection point in the average velocity profile at the best estimate for where the average driver makes the decision (not) to Go. We call this point the 'decision point' as it is where we infer the driver of a provoker is likely to make the decision (not) to encroach. The concept of a decision point may be a useful addition to the design of active safety systems. It is an easily definable location with respect to the center of an intersection.

To define the decision points for left turns at Sävenäs and Jung, we extracted the velocity profiles of more than 60,000 left-turning vehicles at Sävenäs and more than 4,000 at Jung. We averaged the profiles for each trajectory and found the distances from the center of the intersection of the velocity minima. These distances are sketched in Figure 8.2. At Sävenäs, the decision point is 8.9 meters from the center of the intersection on both the west and north roads; at Jung the distance ranged from 8.0 to 12.5 meters. The lack of symmetry at Jung is due to the fact that the nominal center of the intersection is offset approximately a meter to the north.

## Chapter 8 - Go / No Go Decisions

### Lag distance and time at the decision point

The separation between a red car at the decision point and oncoming blue car defines the lag at the point where and time when we infer that most drivers make the decision (not) to encroach. The data generated by the image processing system make it possible to compute the lag as functions of both distance and time. We calculated both metrics of lag for all observations of decisions (not) to encroach.

We used logistic regression to calculate the '50/50 point' in the distribution of lag distances and times. This value represents the distance at which 50% of drivers decide to encroach and 50% do not. When separations are greater, most drivers are willing to encroach.

### Post-encroachment distance

Post-encroachment distance is the minimum distance between the provoker and the car with the right of way during the encroachment. As described in Chapters 4 and 5, the computation of post-encroachment considers the location of the cars where their trajectories cross and their dimensions to provide an estimate of just how 'near' the near-crash situation became. Only pairs of vehicles that are within the zones sketched in Figure 5.5 are included in these analyses. (The boundaries are 10 and 15 meters from the center of the intersection at Sävenäs and 37.5 and 50 meters at Jung).

The post-encroachment distance can be calculated only when the provoker's decision was to Go and there was, in fact, an encroachment. It is an estimate of the outcome of the provoker's decision to encroach. The mean of the distribution of post-encroachment distances represents our best estimate for the 'trailing buffer' (Chan, 2007). When the buffer is smaller than this threshold, most people perceive the risk of encroachment as too great.

## Results

Figures 8.3 through 8.6 plot the observed percentages of Go decisions at Sävenäs. The bin widths for the plotted data are 2 meters and 0.10 seconds. The several thousand actual observations are not displayed to avoid visual clutter. Because there are far fewer data at Jung, Figures 8.7 through 8.9 plot the actual observations of Go and No Go decisions. The bin widths for the plotted data are again 2 meters and 0.10 seconds. The smooth lines in the graphs are the best-fitting logistic regression models to the observations. The point midway along the model curve where it crosses the 50th percentile defines the 50/50 point. Tables 8.1 and 8.2 summarize the findings from these figures for Sävenäs and Jung, respectively.

### Distance, time, and apparent velocity at the decision point

The 50/50 point for the separation between the provoker and the car with the right of way varies across the four scenarios. At Sävenäs, the direction of the provoker's approach appears to influence the driver's decision. The distance is much less (54.5 m) for the oncoming scenario (LTAP/OD) than it is for the three cases where the provoker enters from the secondary road ( $66 \pm 3$  m). This directional dependence is not replicated at Jung. It is not possible to ascertain whether the apparent lack of directional dependence at Jung is due to the relatively small sample size or to contextual factors associated with the greater width of the intersection and the higher speeds of traffic on the E20. The width and speed undoubtedly influence the doubling of the observed values.

## Chapter 8 - Go / No Go Decisions

Tables 8.1 and 8.2 also list the 50/50 points for the time between vehicles at the decision point. The ratio of the 50/50 points by distance and time is an estimate of the apparent relative velocity of the two cars at the time when the driver of the provoker decides (not) to encroach. With the exception of the one crossing scenario, the velocities are remarkably uniform at both Sävenäs (40 kph) and Jung (80 kph).

### Post-encroachment distance

We calculated the post-encroachment distance for each observed Go decision for which there was a second vehicle within the zones shown in Figure 5.5. The results might differ if the zones were defined using different boundaries.

The data from all scenarios are distributed normally. The means of the distributions represent our best estimate of the 'trailing buffers' - the outcome of the decision to encroach. They are listed in the bottom rows of Tables 8.1 and 8.2.

We expected to find wide variability in these distances. Instead, we observed a relatively narrow range of outcomes across all four scenarios at Sävenäs ( $52 \pm 6$  meters) and the two crossing scenarios at Jung ( $138 \pm 6$  meters). At both Sävenäs and Jung, the longest buffer is for the LTAP/OD scenario and the shortest for the merging scenario.

### Discussion

These data support the inference that drivers may make contextually sensitive decisions of whether or not to encroach. At both Sävenäs and Jung, the 50/50 points in both time and distance are shorter for the LTAP/OD scenario than in the LTAP/LD scenario. This difference may be explained by the observation that the provoker in the OD scenario often has some velocity heading into the intersection.

With the exception of the Sävenäs crossing scenario, the values of the apparent relative velocity at the decision point are remarkably constant - approximately 40 kph at Sävenäs and 80 kph at Jung. The uniformity of the implied velocities suggests that the drivers in our study may have a shared tacit (unspoken but understood) expectation for the velocity of vehicles at these intersections. Tacit expectations for velocity are a hallmark of ecological psychology and its interpretation of driver behavior (e.g., Caird and Hancock, 2002). Our data strongly support the argument that drivers act as if they are able to extract information about the velocity of traffic directly from the optic flow field. This finding supports the contention that it would be appropriate for designers of active systems to assume that drivers share a tacit expectation for the velocity of traffic.

The values of the trailing buffers are remarkably uniform as well, on the order of 60 meters at Sävenäs and 140 meters at Jung. This internal consistency, if it is found to hold elsewhere, may represent a key finding. It is possible that the drivers of the 11,000+ pairs of vehicles in this study acted as if they knew how much separation they needed to have at the decision point to achieve a fixed trailing buffer. This implies tacit knowledge of an invariant relationship between three parameters: the decision point (the point of minimum velocity), the distance to the car with the right of way at that point, and the expected velocity profiles of both vehicles. All three parameters in this hypothesized invariant relationship are amenable to implementation in in-vehicle active safety systems.



## Chapter 8 - Go / No Go Decisions

### References

- Caird, J. K., Hancock, P. A., (2002). Left turn and gap acceptance accidents. In: Dewar, R. E., Olson, R. (Eds.), Human Factors in Traffic Safety. Lawyers & Judges Publishing, Tucson, AZ, pp. 591-630.
- Caird, J. K., Chisholm, S. L. Edwards, C. J., & Creaser, J. I. (2007). The effect of yellow light onset time on older and younger drivers' perception response time (PRT) and intersection behavior. Transportation Research Part F, 10, 383-396.
- Chan, C.-Y. (2006). Characterization of driving behaviors based on field observation of intersection left-turn across-path scenarios. IEEE Transactions on Intelligent Transportation Systems, 7 (3), 322-331.
- Chan, C.-Y. (2007). An investigation of traffic characteristics and their effects on driver behaviors in intersection crossing-path maneuvers. Proceedings of the 2007 IEEE Intelligent Vehicles Symposium.
- Davis, G. A. & Swenson, T. (2004). A field study of gap acceptance by left-turning drivers. Transportation Research Record, 1899, 71-75.
- Harrell, W. A. & Spaulding, L. M. (2001). Social psychological models of choice behavior and drivers' left turns. Journal of Social Psychology, 141, 714-722.
- McGuin, G. & Brown, D. B. (1999). Characteristics of traffic crashes among young, middle-aged, and older drivers. Accident Analysis and Prevention, 31, 181-198.
- Ragland, D. R., Arroyo, S., Shladover, S. E., Misener, J. A., & Chan, C.-Y. (2006). Gap acceptance for vehicles turning left across on-coming traffic: Implications for intersection decision support design. Proceedings of the Transportation Research Board 2006 Annual Meeting, Paper No. 06-2696.
- Tian, Z., Vandehey, M., Robinson, B. W., Kittelson, W., Kyte, M., Troutbeck, R., Brilon, W., & Wu, N. (1999). Implementing the maximum likelihood methodology to measure a driver's critical gap. Transportation Research Part A, 33, 187-197.
- Yan X., & Radwan, E. (2007). Effect of restricted sight distances on driver behaviors during unprotected left-turn phase at signalized intersections. Transportation Research Part F, 10, 330-344.
- Yan, X., Radwan, E. & Guo, D. (2007). Effects of major-road vehicle speed and driver age and gender on left-turn gap acceptance. Accident Analysis & Prevention, 39 (4), 843-852.

## Chapter 8 - Go / No Go Decisions

### Figures

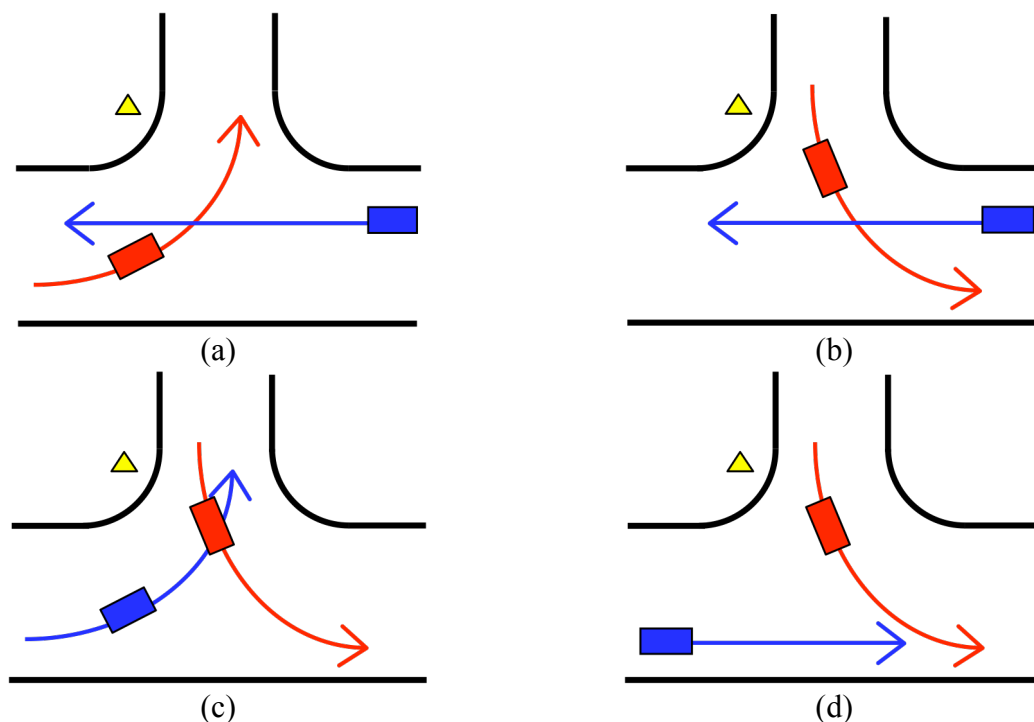


Figure 8.1 The four scenarios considered in the study of provoker decision making. The provoker, shown in red, turns in front of the blue car which has the right of way. (a) Left turn across path from the opposite direction (LTAP/OD, 3xa at Sävenäs, NLSSX and SLNSX at Jung), (b) left turn across path from the lateral direction (LTAP/LD, 4xs, ELSSX and WLNSX), (c) two crossing left turns (4xi, insufficient data at Jung), and (d) merging into path (4sm, WLSSM and ELNSM).

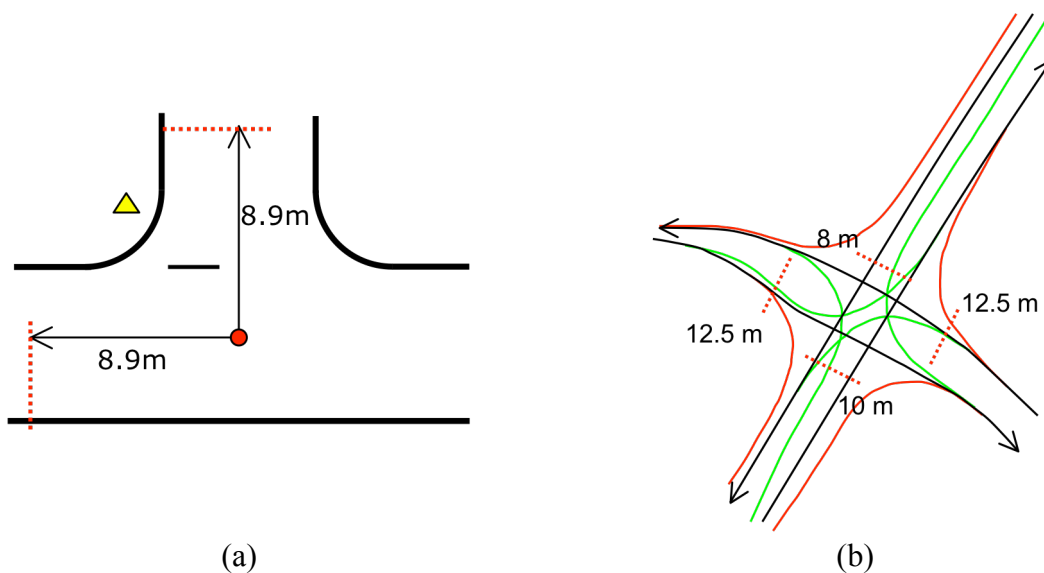


Figure 8.2 The distances to the points defined by the minimum velocities of all left-turning vehicles at (a) Sävenäs and (b) Jung. Both sketches are oriented with north up. The rotation of the sketch for Jung reflects the actual orientation of the intersection.

## Chapter 8 - Go / No Go Decisions

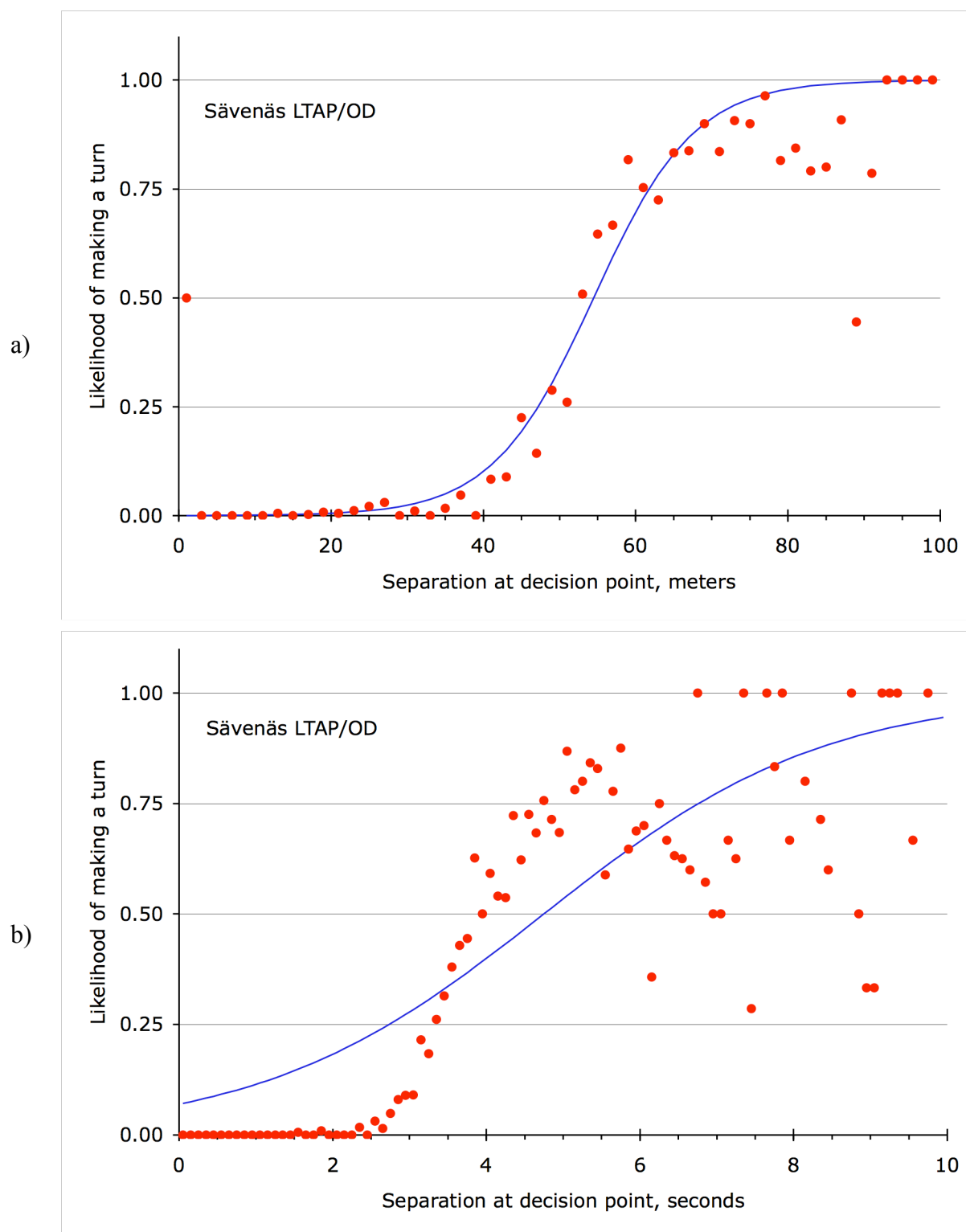


Figure 8.3 Observed percentages of Go / No Go decisions for LTAP/OD cases at Sävenäs (3xa) and best-fit logistic regression models as functions of (a) distance and (b) time at the minimum velocity point for encroaching vehicles.

## Chapter 8 - Go / No Go Decisions

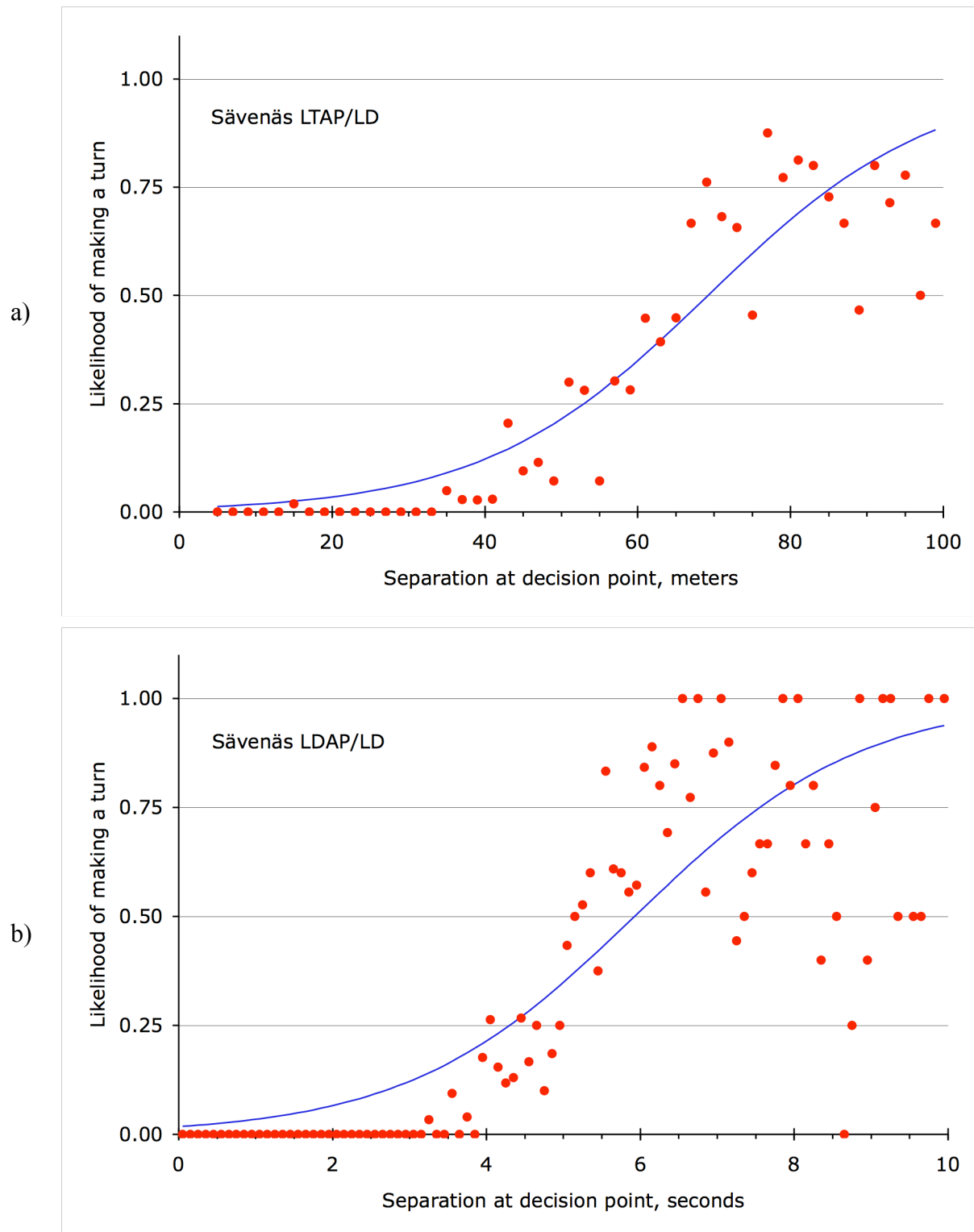


Figure 8.4 Observed percentages of Go / No Go decisions for LTAP/LD cases at Sävenäs (4xi) and best-fit logistic regression models as functions of (a) distance and (b) time at the minimum velocity point for encroaching vehicles.

## Chapter 8 - Go / No Go Decisions

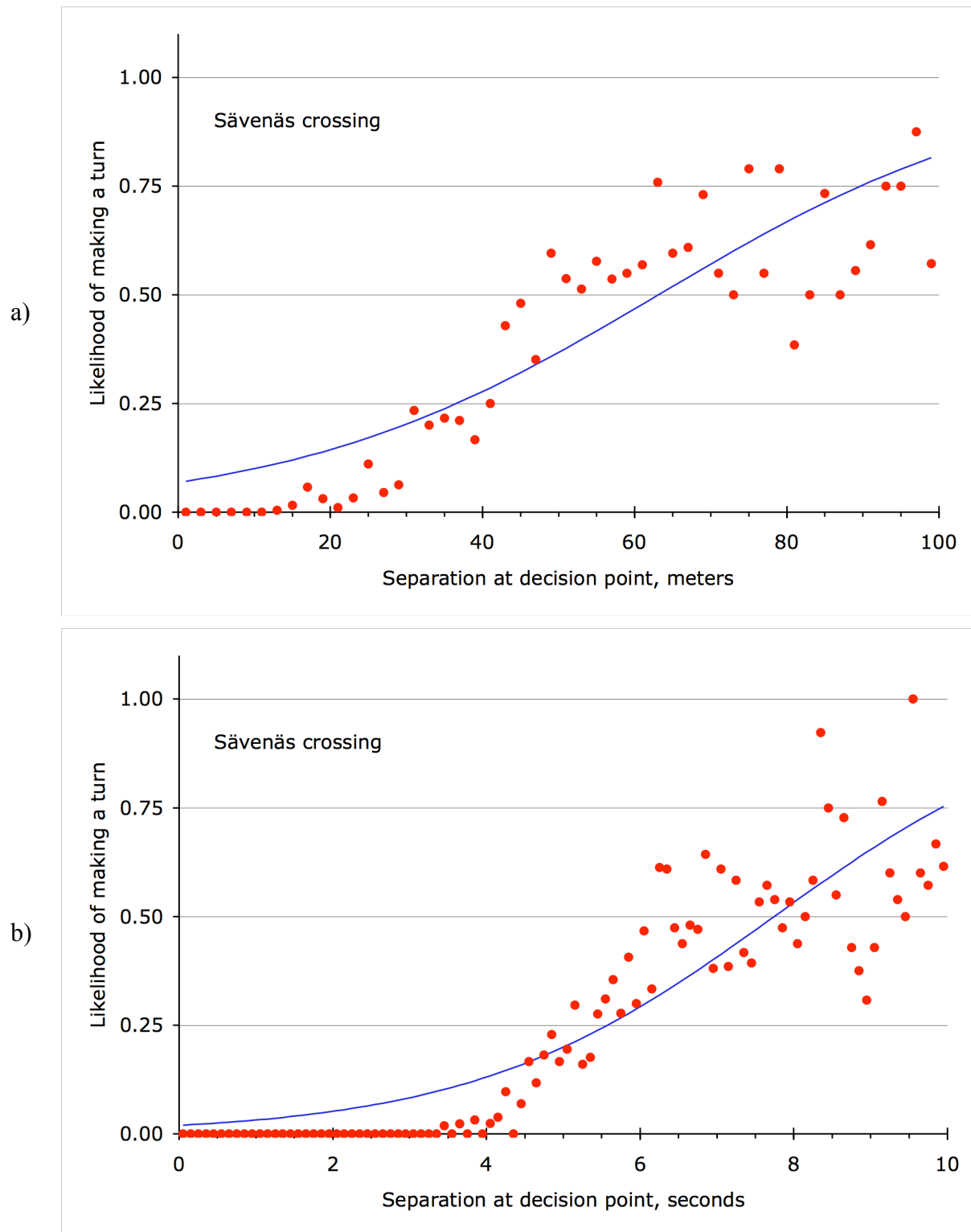


Figure 8.5 Observed percentages of Go / No Go decisions for crossing cases at Sävenäs (4xs) and best-fit logistic regression models as functions of (a) distance and (b) time at the minimum velocity point for encroaching vehicles.

## Chapter 8 - Go / No Go Decisions

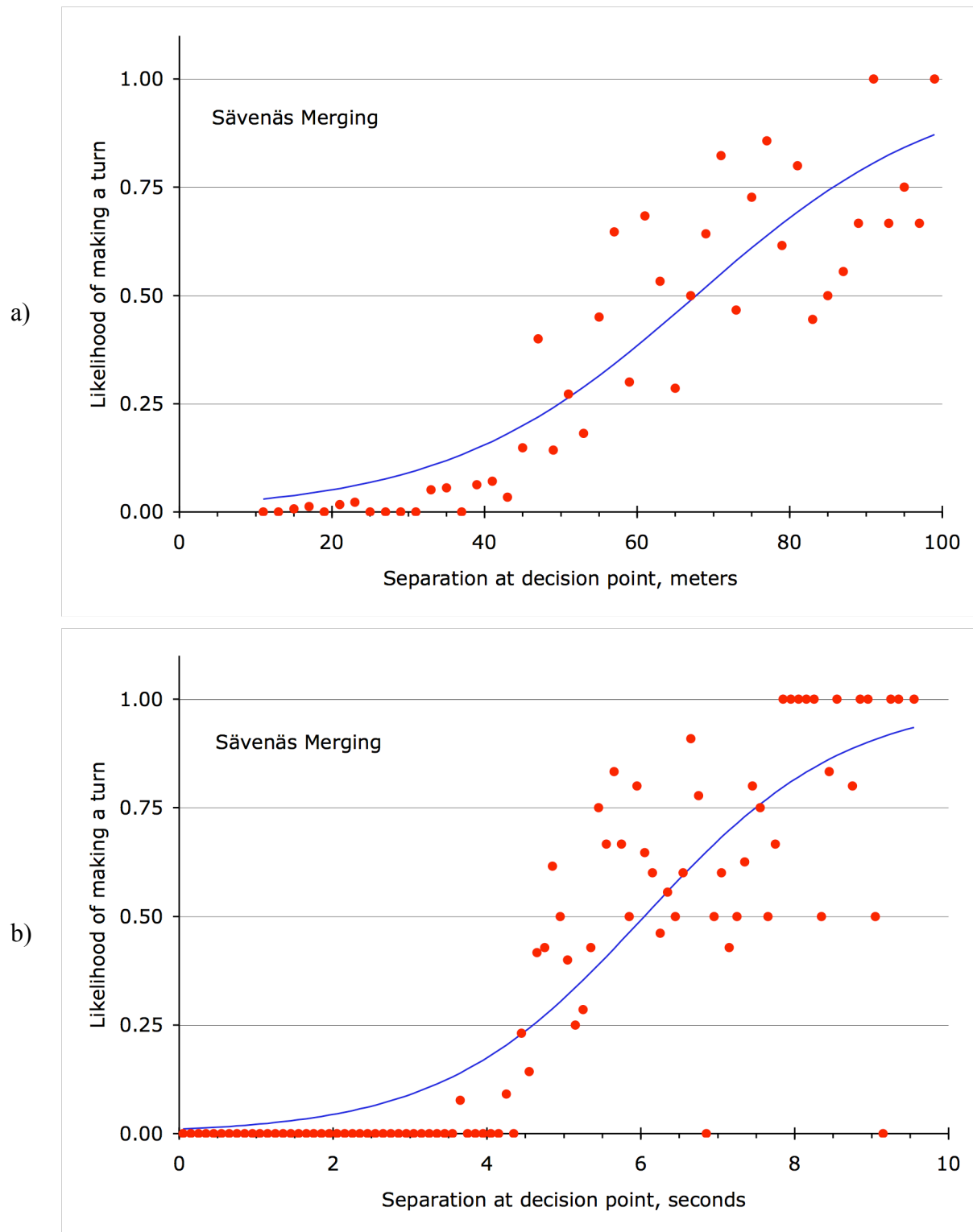


Figure 8.6 Observed percentages of Go / No Go decisions for merging cases at Sävenäs (4ms) and best-fit logistic regression models as functions of (a) distance and (b) time at the minimum velocity point for encroaching vehicles.

## Chapter 8 - Go / No Go Decisions

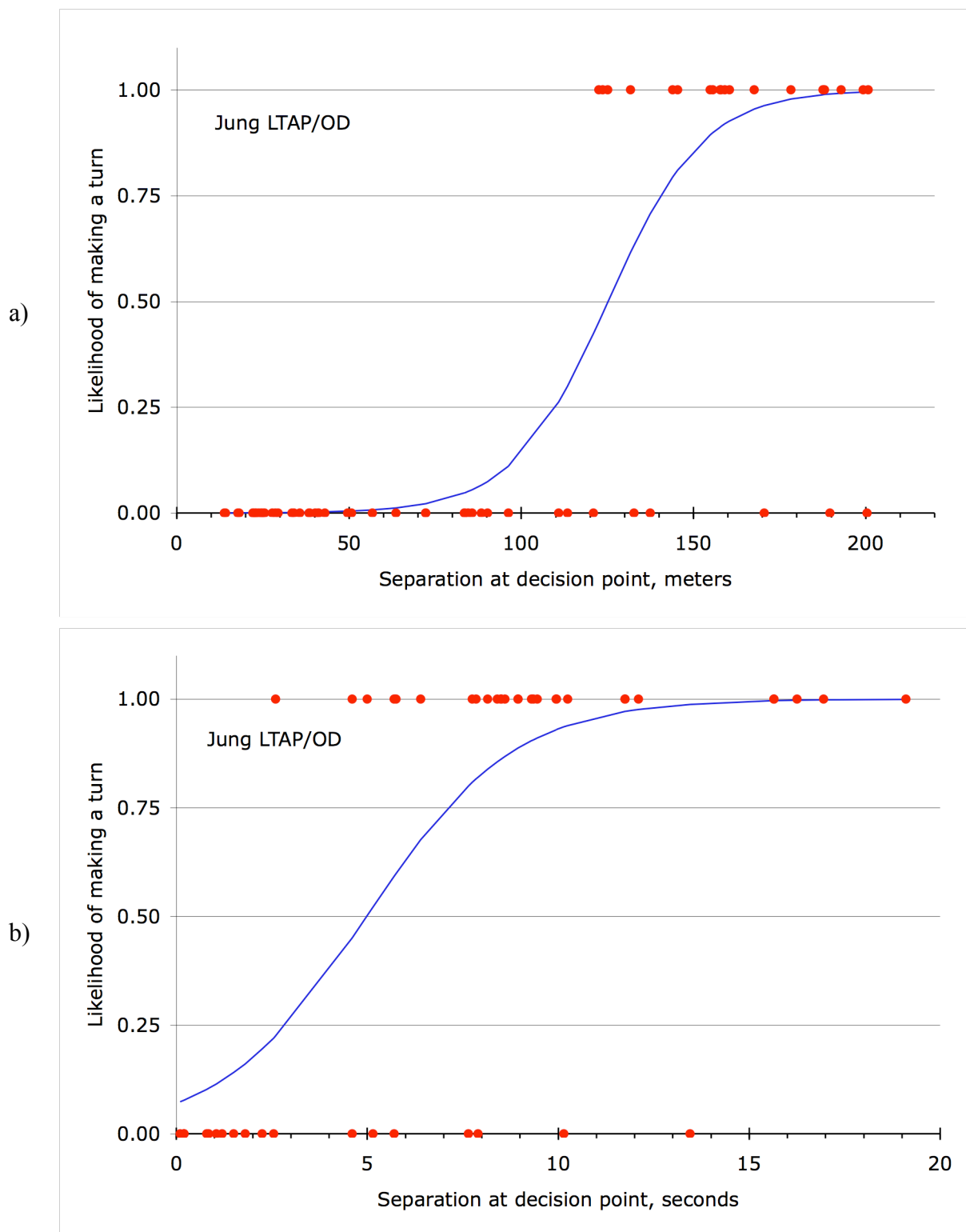


Figure 8.7 Observed percentages of Go / No Go decisions for LTAP/OD cases at Jung (NLSSX, SLNSX) and best-fit logistic regression models as functions of (a) distance and (b) time at the minimum velocity point for encroaching vehicles.

## Chapter 8 - Go / No Go Decisions

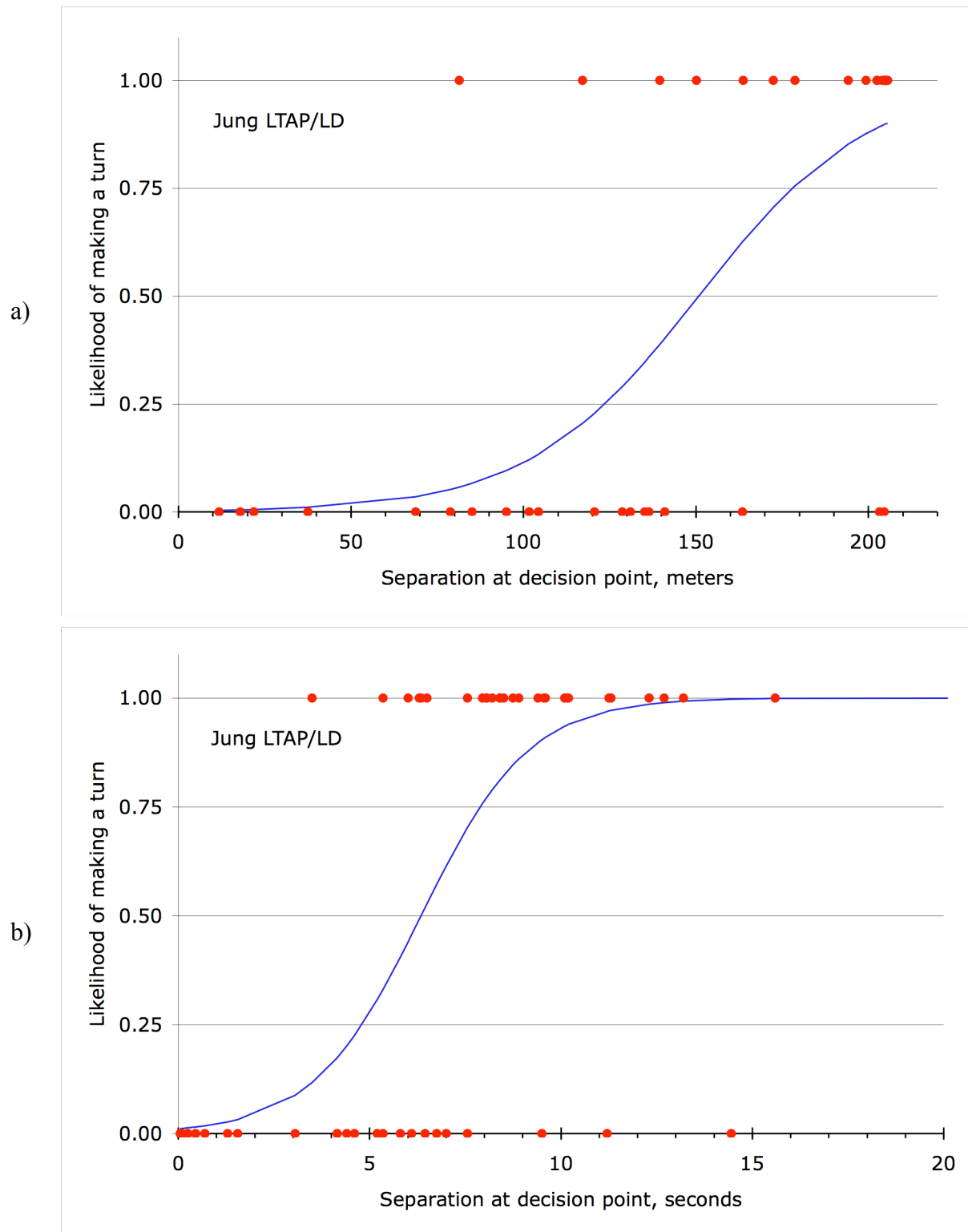


Figure 8.8 Observed percentages of Go / No Go decisions for LTAP/LD cases at Jung (ELSSX, WLNSX) and best-fit logistic regression models as functions of (a) distance and (b) time at the minimum velocity point for encroaching vehicles.



## Chapter 8 - Go / No Go Decisions

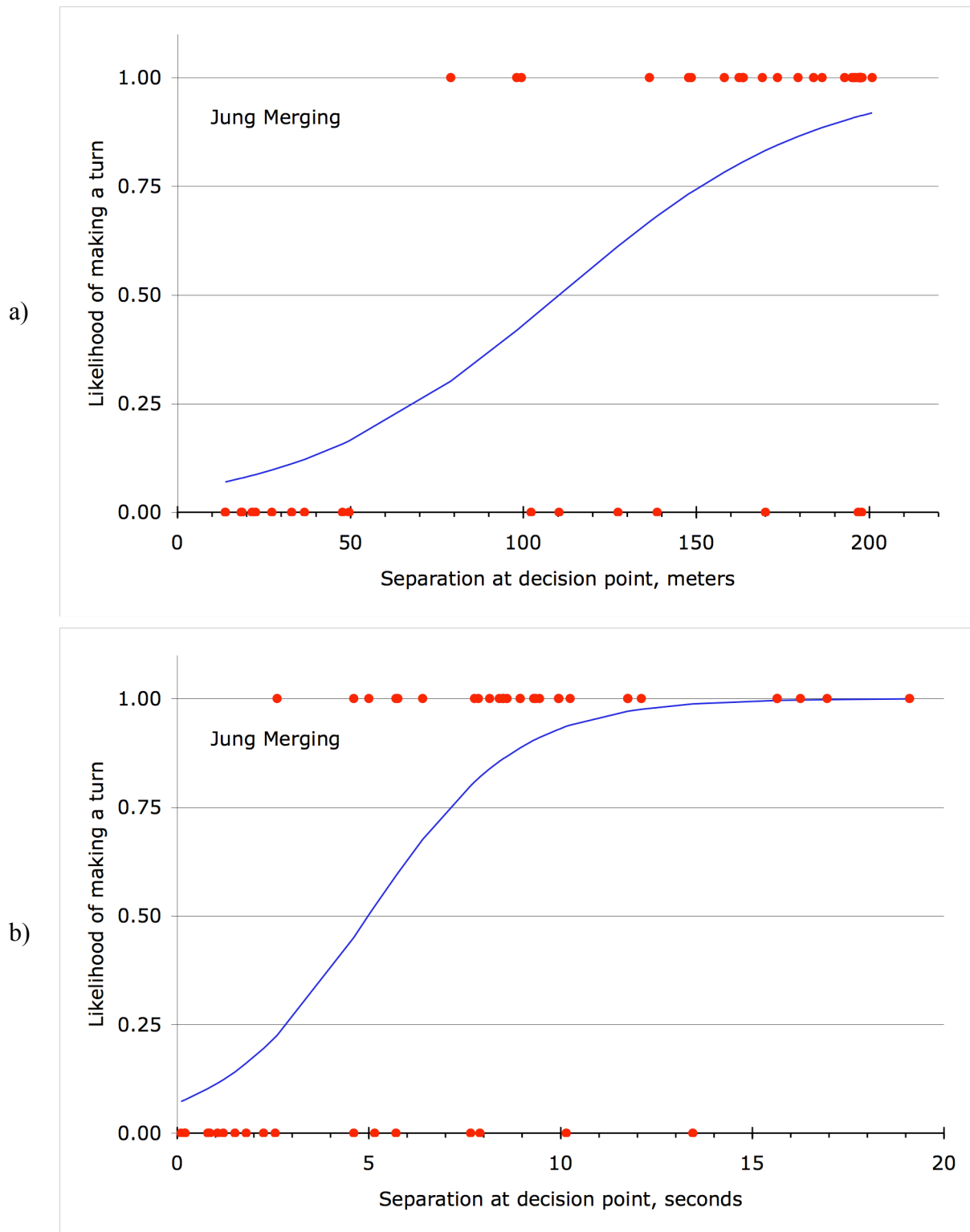


Figure 8.9 Observed percentages of Go / No Go decisions for merging cases at Jung (WLSSM, ELNSM) and best-fit logistic regression models as functions of (a) distance and (b) time at the minimum velocity point for encroaching vehicles.

## Chapter 8 - Go / No Go Decisions

### Tables

Table 8.1 Summary of logistic regression models for encroachment decisions at Sävenäs

Separation at 50/50 point	Scenario			
	LTAP/OD 3xa	LTAP/LD 4xi	Crossing 4xs	Merging 4ms
Meters	54.5	69.2	63.1	67.7
Seconds	4.75	5.93	7.75	6.05
Relative velocity (kph)	41	42	29	40
N	5125	1680	3904	1198
Trailing buffer (meters)	57.7	55.5	49.9	46.0

Table 8.2 Summary of logistic regression models for encroachment decisions at Jung

Separation at 50/50 point	Scenario		
	LTAP/OD NLSSX SLNSX	LTAP/LD ELSSX WLNSX	Merging WLSSM ELNSM
Meters	125	130	110
Seconds	5.6	6.3	5.0
Relative velocity (kph)	80	74	79
N	74	51	47
Trailing buffer (meters)	144	132	100

## Chapter 9 - Simulations of traffic scenarios at Sävenäs and Jung

### Overview of the simulator experiments

One of the goals of the IVSS Intersections project was to observe the actions taken by drivers in ‘near-crash’ situations. As described in Chapters 4 and 8, the project team settled on Post Encroachment Time (PET) as the favored metric for near-crash situations. A PET value of zero indicates a crash. Short PET values (e.g.,  $< 2$  sec) flag ‘encroachment incidents,’ our operationalization of near-crash situations.

The Driving Simulation Laboratory at the Department of Information and Computer Science at Linköping University (LiU) conducted five experiments designed to create simulated encroachments and to obtain data on drivers’ reactions to and anticipations of those encroachments. In the first four experiments, different cohorts of volunteers drove repeatedly through multiple replicas of the Sävenäs intersection. In the fifth, a new cohort drove repeatedly through a single replica of the Jung intersection.

To ascertain whether encroachment would arise naturally in realistic simulations of the Sävenäs intersection, Experiments 1 and 2 were designed to create as natural a driving environment and experience as we could in the laboratory. We constructed a realistic road circuit with intersections that replicated the Sävenäs intersection and flows of traffic that appeared natural. The optic flow of the simulated environment, the kinematics of traffic, and the handling of the drivers’ cars matched reality as well as possible. Instructions invited the groups of 4 drivers to interact and explore the simulated world.

This realism prompted fast but cautious driving by our drivers. Like the drivers on the roads at Sävenäs, few of drivers in the simulator experienced encroachments with PET values less than 2 seconds. Our interpretation of these data is that the experience of encroachment in a realistic simulator emulates driving on the road when drivers are allowed to drive naturally.

Faced with need to satisfy the project’s goal of observing encroachment and to overcome our drivers’ natural caution, we adopted a radically different approach for Experiments 3 and 4. These experiments created artificial driving conditions in which encroachment was frequent and predictable. Individual drivers (not groups of 4) drove a route in which they had the right-of-way through each of the replicas of the Sävenäs intersection. They encountered another car at most of the intersections. More often than not, that car would turn left across the driver’s path. The turns were timed to generate short PET values. We call these turning cars ‘provokers’ because we scripted their actions to provoke encroachment.

As expected, the drivers quickly learned to anticipate the starkly unrealistic behavior of the provokers and adapted their driving behavior in response. The nature of this adaptation is the data we were hoping to find. Armed with the expectation of encroachment, most drivers slowed down and waited for the provoker to pass before proceeding through the intersection. The observation that drivers modify their driving to avoid expected encroachment bodes well for the introduction of active safety systems designed to detect and alert drivers to impending encroachment.

The paradigm for Experiment 5 blended the best elements of the previous experiments. As in Experiments 1 and 2, drivers were instructed to explore the simulated world. They crossed the replica of the Jung intersection many times, in all directions, and at their own pace. As in Experiments 3 and 4, drivers occasionally encountered provokers at the intersection. Unlike the provokers in the previous experiments, the presence of provokers at Jung was unpredictable. The drivers’ responses to these encroachments were, accordingly, more likely to emulate those by drivers who experience encroachment at real intersections.

## Chapter 9 - Simulations of traffic scenarios at Sävenäs and Jung

This chapter has three parts. The first describes the experimental protocols for the five experiments. The second documents the traffic scenarios observed in the replicas of the Sävenäs and Jung intersections and compares them to the observed traffic patterns at the actual intersections, Chapter 6. The third section discusses the distribution of velocities through the simulated intersections and compares them to the those at the actual intersections, Chapter 6. These discussion provide the necessary background for Chapter 10 where we present and assess the responses of our drivers to predicable provocations with short PET values.

### Experimental Protocols

#### Experiment 1

The simulator in the LiU Driving Simulation Laboratory allows as many as four drivers to drive on the same road circuit and interact at intersections. Experiment 1 took full advantage of this ability. Groups of four volunteers drove simultaneously in the same simulated world. The road circuit, Figure 9.1, contained multiple replicas of the Sävenäs intersection, Figure 9.2. The experimental manipulations were designed to uncover which set of conditions would prove to be the most conducive to encroachments with short PET. The simulator captured and wrote to file at 10 Hz time-stamped data specifying the locations, velocities, and headings of all cars. Post-processing of these log files extracted information about (1) traffic scenarios, (2) the spontaneous occurrence of short PET, and (3) velocity distributions.

#### Drivers

Groups of four arrived at the laboratory together and drove simultaneously in the same simulated world. There were 14 groups of four, for a total of 56 drivers (21 women and 35 men). Their ages ranged from 19 to 61 with a median of 23. All but two were students at Linköping University. A valid driver's license was a requirement for participation. Each group participated in four driving sessions of 12 minutes each, producing 48 minutes of spontaneous driving data. Subject participation conformed to the ethical guidelines established by Vetenskapsrådet, the Swedish Research Council (2002).

#### Road circuit and the Sävenäs intersections

The groups of drivers drove on the same road circuit in all four sessions. The road circuit, shown in Figure 9.1, consisted of a ring road and an internal pair of secondary roads that intersected at right angles. The posted speed limit was 50 kph everywhere. The 'bumps' on each leg of the ring road and the internal roads were designed to act as speed reducers.

The four 3-way intersections along the ring road all replicated the Sävenäs intersection, Figure 9.2. Considerable effort was spent to construct a model of the Sävenäs intersection that matched the geometry, signage, and sight-lines of the actual intersection. The positions and sizes of the island in the road circuit, the buildings, and the parking lots were all faithfully reproduced. There were two elements of the actual environment that could not be reproduced. The first was the covered walking bridge over the road circuit that connects the two buildings to the west of the intersection. The second was the raised speed-bump associated with the pedestrian and bicycle crossing of the secondary road. Unlike the real Sävenäs, the entire simulated world was absolutely flat.

## Chapter 9 - Simulations of traffic scenarios at Sävenäs and Jung

Drivers on the ring road had the right-of-way. As at Sävenäs, drivers on the secondary roads had to yield to traffic on the major (ring) road. To simplify bookkeeping, the replicas of Sävenäs were distinguished by assigning them cardinal directions so that the intersection at the top of Figure 9.1 was designated the 'North' intersection, etc. It took approximately a minute to drive from one Sävenäs to the next along the ring road (e.g., from the North intersection to the East intersection). Much effort was expended to beautify the scenery along the stretches between intersections. The central 4-way intersection at the center was unregulated.

### Task and experimental design

The groups of drivers completed four 12-minute driving sessions. The instructions emphasized that the primary task driving safely and normally. If the traffic situation were to become demanding, they were to focus on their driving. The instructions also posed a secondary task - to drive through the simulated world, to find six different road signs, with one word written on each, and to use them to form a sentence. Figure 9.3 shows one of the signs. Without using a pen and paper, the driver had to assemble the sentence created by the six word. The full sentences were either a question or a request and are listed in Table 9.1. Upon deciphering the sentence, the driver answered the question and continued to explore the world.

The secondary task was intended be slightly distracting and to encourage drivers to explore the entire simulated world. We expected the task to downplay the importance of the intersections. We did not want the drivers to focus on the intersections as that focus might influence how they would act when they encountered other vehicles (each other) there.

The four drivers all drove red Volkswagen Passats. In addition to these cars, there were 24 other red Passats driving on the road circuit. All 24 were automata - computer generated cars that followed a defined route (script), stayed within their lanes, and adapted to the surrounding traffic. The only way to distinguish between the driver-driven cars and the automata was to observe a driver driving irregularly. The driveways that appear to cross the ring road, Figure 9.1, mark the locations where the automata entered the circuit.

The experimental was run using the 2x2 repeated measures (within subjects) design shown in Table 9.2. The first factor was the instructional set, the second the variability of the velocities of the automata. Fully crossing the two factors created four conditions. Each condition had the same road circuit but slightly different landscaping. In accord with the repeated measures design, assignment of conditions to the four experimental sessions was randomized and every group drove in all four conditions.

The manipulation of instructional set told the group either to adhere strictly to all rules of the road or to complete the secondary task as quickly as possible. We expected the 'competitive' condition (sessions B and D) to generate higher velocities and correspondingly more opportunities for encroachment.

The variability of the velocities of automata was set to either high or low. In the low condition, 8 of the automata drove at 45 kph, 8 adhered to the 50 kph speed limit, and 8 drove at 55 kph. In the high condition, 2 of the automata drove at 20 kph, 16 drove at 50 kph, 3 drove at 70 kph, and 3 drove at 90 kph. We expected the high variability condition (sessions A and B) to generate more opportunities for encroachment.

## Chapter 9 - Simulations of traffic scenarios at Sävenäs and Jung

### Procedure

Four drivers entered the laboratory together and were randomly assigned to workstations. The four work stations were in the same room but positioned so that the drivers could not see each other. They read the instructions to subjects as an audio recording of the instructions was broadcast by an iPod. They then signed informed consent forms and drove a 10 minute practice sessions that provided the opportunity to master the simulator hardware (steering wheel, pedals, etc.) and performance (turning, braking, etc.). During the experimental sessions, the drivers alternately drove in the simulator and completed the battery of 11 questionnaires listed in Table 9.3. Analyses of the questionnaire data are discussed in Chapter 12.

### Dependant measures

The simulator captured and recorded the time, x-position, y-position, velocity and heading of all cars (4 driver-driven cars and 24 automata) in a session. Post-processing of these log files extracted information about (1) traffic scenarios, (2) the spontaneous occurrence of short PET values, and (3) velocities.

### **Experiment 2**

Like Experiment 1, Experiment 2 asked four drivers to explore and interact in a simulated world containing replicas of the Sävenäs intersection. The road circuit was designed to overcome the two disparities in observations between Experiment 1 and the actual intersection: (1) the low density of traffic and (2) the mismatch in the relative frequencies of traffic scenarios. Much of the method and procedure was identical to that of Experiment 1. This section focuses on those aspects of the study that differed.

### Drivers

There were 12 groups of four drivers for a total of 48 drivers (10 women and 38 men). Their ages ranged from 21 to 33 with a median of 25. A valid driver's license was a requirement for participation. Years of licensure ranged from 1 to 13. Nine reported having been in a traffic accident.

### Road circuit

The major difference between Experiments 1 and 2 was the design of the road circuit. The road circuit used in Experiment 2 is shown in Figure 9.4. There was no ring road. There were only two replicas of the Sävenäs intersection and the length of the roadways between intersections was considerably shorter. The distance around the upper loop, 1100 m, was approximately the same as the distance between intersections in Experiment 1. The distance along the straight segment between the two loops was 300 m and the distance around the smaller circuit was 800 m. At 50 km/h, the times needed to complete these segments of roadway were 1min 20sec, 23 sec and 1 min, respectively. The key-shaped layout was designed to force drivers to turn at the intersections in order to explore the entire world. These changes were intended to increase the density of traffic, the frequency of drives on trajectories 2 and 3, and the number of encounters with other drivers and automata at the intersections.

## Chapter 9 - Simulations of traffic scenarios at Sävenäs and Jung

In addition, we added a traffic light midway between the two intersections. The inspiration for this change was the traffic light used by Hancock and deRidder (2003) in their landmark paper on the interaction of drivers in a simulator. The traffic light was controlled by the passage of other vehicles on the road ahead. Like Hancock and deRidder, we hoped the traffic light would force cars on different paths to arrive at the intersections at approximately the same time.

A second new manipulation was the implementation of a voice-based routing system (GPS) in each of the four cars driven by drivers. This system issued scripted instructions to turn or drive straight that were designed to increase the likelihood of two or more drivers meeting at the intersections.

### Design and task

The experiment was run using the 2x2 repeated measures design shown in Table 9.4. The first factor was the traffic light at two levels (with and without). The second factor, also at two levels, was the GPS system (with and without). Fully crossing the two factors created four conditions that were randomly assigned to sessions. Every group of four drivers drove in all four conditions. Each session was 10 minutes long.

In Experiment 2 there were eight automata plus the four cars driven by the drivers. We believed that eight automata would be sufficient to increase the density of traffic on the shorter road circuit. The automata behaved the same in all four sessions. All four sessions had the same road circuit but slightly different landscaping.

As in Experiment 1, the drivers were given a lightly distracting task that involved finding road signs and using them to form a sentence. This time the sentence was a part of a familiar song. In Experiment 1 the audio output from the other drivers' workstations could be heard. To diminish distraction, audio output was suppressed in Experiment 2.

### **Experiment 3**

Experiment 3 changed the experimental paradigm. A single driver, rather than four drivers, drove a specified route around a smaller version of the loop road used in Experiment 1, Figure 9.1. The driver had the right-of-way through each of the four replicas of the Sävenäs intersection. At the intersections, the driver frequently encountered a car that was likely to turn left directly across her path. These left turns were designed to provoke encroachments with short PET values.

### Drivers

Twenty-two students from LiU volunteered to participate in Experiment 3. Only one driver, rather than 4, drove in each experimental session.

### Road circuit, task, provokers, and projected gap times

The road circuit was a smaller version of the circuit used in Experiment 1, Figure 9.1. The 500 m x 500 m circuit contained replicas of the Sävenäs intersection at the midpoints of each side. The driver's task was to drive 7 loops in a clockwise direction around the ring road in the inner lane. This route followed a path that has the right-of-way at Sävenäs (from east to west) and crossed 28 replicas of the Sävenäs intersection. The geometry of the intersection

## Chapter 9 - Simulations of traffic scenarios at Sävenäs and Jung

makes it possible for a provoker to cross the driver's paths by making a left turn either from the opposite direction (west to north, LTAP/OD) or from the lateral direction (north to east, LTAP/LD). Figure 9.5 sketches the two provocation scenarios. The direction of provocation was a between-subjects manipulation. Half the drivers experienced provokers turning from the opposite direction and half from the lateral direction.

Three confederates drove three other cars (provokers) in the same simulated world as the driver. One confederate drove a provoking car in the north intersection. The others were provokers in the east and south intersections. There were no provokers in the west.

The provokers had two tasks. The first was to drive normally at a relatively constant and reasonable velocity (e.g., 30 kph) and to approach the intersection in a manner that adhered to all traffic laws. The second task was to arrive at the intersection at a prescribed interval of time in advance of the driver's car and to turn left across the driver's path. We call the projected time interval between the provoker's left turn and the subsequent driver's pass through the intersection the 'projected gap time'. Table 9.5 lists the projected gap times targeted by the provokers. All seven crossings of the West intersection were designed to be solo drives that would provide a baseline for comparison with the crossings with provokers. In five of the 28 crossings, the provoker was to wait. In 16, there was a scheduled provocation.

### Procedure

Drivers reported individually to the laboratory and read a paper copy of the instructions to subjects as it was read aloud to them. The confederates were already seated at their workstations making themselves look busy to make it appear they were not involved in the experiment. While there was no active deception on the part of the experimenters, deception was an integral part of the experimental design.

After signing an informed consent form, the driver drove a 10 minute practice session. There was traffic but no provokers in the practice session. After the driver reported feeling comfortable with the setting and task, he or she completed three questionnaires: the Schwartz value survey, the Driver Style Questionnaire (DSQ), and the Manchester Driving Behavior Questionnaire (DBQ). The questionnaire data are discussed in Chapter 12.

During the one 20-minute experimental session, the driver completed seven laps around the loop road in the interior lane. The confederates attempted to create 'near-crash situations' by turning left in front of the driver in a manner that would generate the 'projected gap times' listed in Table 9.5. After making a left turn in front of the driver, the confederates drove short loops using the interior roadways to return to their starting points. The locations of these points were marked on the side of the road at distances where smooth acceleration to 30 kph would put them in the intersection at the designated times.

The drivers' adaptations to the presence of the provokers complicated the confederates' task. The confederates found themselves having to decide whether to (a) adjust their velocities in response to the driver in order to achieve the projected gap times or to (b) maintain their velocity (and the realism of the situation) and execute their turns at larger than planned gap times.



## Chapter 9 - Simulations of traffic scenarios at Sävenäs and Jung

### Experiment 4

Experiment 4 improved upon the experimental paradigm of Experiment 3 by using software to drive the provokers rather than human confederates. The goal, once again, was to ascertain how drivers respond to and anticipate encroachment.

#### Drivers

Twenty-nine students (7 women and 13 men, mean age = 28.5 years) volunteered to participate. Ages ranged from 21 to 60 years. Years of licensure ranged from 1 to 32. Two reported having been in an accident.

#### Road circuit, task, provokers, and projected gap time

The road circuit used in Experiment 4 was the same as that used in Experiment 3. The driver's task was to drive four loops in a clockwise direction around the ring road in the inner lane crossing 16 replicas of the Sävenäs intersection. A provoker was scripted to turn left across the driver's path before each of the 16 intersection crossings. As shown in Table 9.6, the projected gap times for these scripted encroachments included no waiting cases and no solo cases. Nineteen drivers experienced provokers turning from the opposite direction and ten from the lateral direction.

Software drove four other cars in the same simulated world as the driver. There was one provoker at each of the four replicas of the Sävenäs intersection. The software directed the provoker to maintain its lane, to accelerate smoothly, to abide by the speed limit, and to turn left across the driver's path at a scripted gap time. In order to attain the gap time, the software modulated the velocity of the provoker in response to changes in the driver's velocity up to the point where the provoker was within 10 m of the intersection. Within the intersection itself, this 'link' between the provoker and the driver was cut. The provoker made its turn with a constant and reasonable velocity with no consideration given to the position or velocity of the driver. From the driver's perspective, the trajectories and velocity profiles of the provokers appeared realistic.

#### Procedure

The procedure was identical to that in Experiment 3 with the notable difference that there were no human confederates at the other workstations. Deception was not a part of the experiment. During the one 15-minute experimental session, the driver completed four laps around the road circuit and the software attempted to create encroachments. The software responded to but did not anticipate changes in the driver's velocity.

### Experiment 5

Experiment 5 embraced a new paradigm that was designed to blend the best of the previous four. It borrowed from the first two experiments the idea of allowing the drivers to explore the road circuit freely. It borrowed from the fourth experiment the use of automated provokers to create encroachments at specified times and on known trajectories. The goal was to make the encroachments relatively rare and unpredictable so that the drivers would not expect them and their responses would be relatively spontaneous. Ten students volunteered to participate.

## Chapter 9 - Simulations of traffic scenarios at Sävenäs and Jung

### Road circuit, task, and provokers

The road circuit used in Experiment 5 is shown in Figure 9.6. The circuit is a cloverleaf with the replica of the Jung intersection at the center. The E20 is modeled as a four-lane road that runs north-south. Traffic in the right lanes in both directions of the E20 must turn right. Both directions have dedicated left-turn pocket lanes at the intersection.

The east-west secondary road is modeled as a two lane road. Both directions of traffic on the secondary road must stop at the intersection. The west road provides access to the service station on the southwest corner of the intersection. The four large loops are one-lane, one-way roads that direct traffic back to the intersection after approximately a minute. A driver who always drives straight through the intersection cycles counterclockwise through the four direction of travel.

The driver's task was to explore the simulated world, drive safely, and heed the posted speed limits, 90 kph on the loop roads and 70 kph through the intersection. Software drove six classes of automata (red cars), two types of provokers and four types of 'random traffic'. The scripts for the of red cars are summarized in Table 9.7. There were two types of red cars for each direction of travel. Drivers on the E20 always encountered a red car that was scripted to turn left. Half of the time the red car yielded the right of way; half the time it encroached. Drivers on the secondary road encountered red cars that would not interact with the driver if the driver heeded the speed limit and drove straight through the intersection.

### Procedure and projected gap times

During one 40-minute experimental session, the driver drove freely around the road circuit, completing as many laps as time allowed. The software generated scripted encroachments, responding to but not anticipating changes in the driver's velocity. A scripted provoker maintained its lane and accelerated smoothly. The timing of its turn was designed to run directly into the driver's car (projected gap time = 0.0) if the driver maintained the speed limit and took no evasive action. If the driver drove straight through the intersection on all passes, the first encroachment would occur approximately four minutes into the session. The first encroachment was intended to be a surprise that would inform analysis of the driver's response during subsequent passes through the intersection.

## Traffic patterns at the simulated intersections

### Experiment 1

The scenario classification system developed at Chalmers, Chapter 5, was used to extract the traffic scenarios experienced by drivers in the experiment. The cells in the matrix of Table 9.8 contain the counts of cases for each of the 150 traffic scenarios at Sävenäs. The cases include all driver-driver interactions and all driver-automaton interactions but no interactions between two (or more) automata. The entries below the matrix present the sums and relative frequencies for each column. Table 9.9 presents the sums and relative frequencies by row for the 6 solo cases and the 144 cases with traffic. It also summarizes the frequencies of scenarios at Sävenäs itself (from Table 6.1) to illustrate the level of agreement between observations in the simulator and those made at the actual Sävenäs intersection.

A total of 1,710 cases were classified. The distribution of cases observed in Experiment 1 was significantly different than the distribution observed at the actual intersection  $\chi^2(10) =$

## Chapter 9 - Simulations of traffic scenarios at Sävenäs and Jung

344,  $p < .001$ . Most of the cases contribute to this disparity. As shown in Table 9.9, there were relatively too few drives on paths 2 and 3 and too many on paths 4 and 6.

There were relatively more solo drives in the simulator than on the road at Sävenäs. In 49% of the cases in the simulator, there was only one (blue) car. This is nearly 10% more than in the actual intersection. The 50 - 50% split between solo drives and drives with traffic in the simulator was observed on all 6 paths. At the actual intersection, the relative frequencies are consistently near 40 - 60%. This result suggests that we may have put too few automata on the road in Experiment 1.

Of the 150 cases in the matrix, 51 had no observations and only 6 had more than 100. Most of the cases with no counts involve waiting. It appears that the traffic density in the simulator would have to be much higher to generate the relative frequency of waiting observed at Sävenäs. Once again, this result suggests we needed to increase the density of automata to replicate conditions as Sävenäs.

Cases involving only one red car accounted for 32% of the total number of observations. This compares with 40% at the actual intersection. Relatively few of these interactions involved traffic (red cars) on paths 5 and 6, the paths with the right of way and where traffic would be expected. It appears that the predefined paths of the automata should have included more drives straight through the intersection.

Of the two-car interactions, only a small percentage involved waiting red cars. The of waiting cases, the vast majority involves drivers on path 6 and red cars on paths 3 and 4. These counts represent automata and other drivers who were respecting the driver's right-of-way in the intersection.

In sum, the patterns of traffic observed in Experiment 1 differed significantly from that observed at Sävenäs. The density of traffic was too low. The proportion of drives on the ring road was higher than on the road at Sävenäs and, correspondingly, the proportion of drives on the secondary road was lower. The road circuit in Experiment 2 was designed to overcome these disparities.

### Experiment 2

The cells in the matrix of Table 9.10 contain the counts of cases for each of the 150 traffic scenarios at Sävenäs. The entries below the matrix present the sums and relative frequencies for each column. Table 9.11 presents the sums and relative frequencies by row for the 6 solo cases and the 144 cases with traffic. It also reformats the data shown in Figure 9.2 to illustrate the level of agreement between observations in the simulator and on the road at Sävenäs.

A total of 1,179 cases were classified. Once again, the distribution of observed cases was significantly different than the distribution observed at the actual intersection,  $\chi^2(10) = 277.$ ,  $p < .001$ . Most of the cases contribute to this disparity. As shown in Table 9.11, there were relatively too few drives on paths 5 and 6 and too many on paths 2 and 4. This is nearly the inverse of the outcome of Experiment 1. It appears that the redesign of the road circuit succeeded in forcing drivers to turn. However, it had the unintended side-effect of virtually eliminating through traffic with the right-of-way.

In 58% of the cases in the simulator, there was only one (blue) car. This is 20% more than in the actual intersection. It appears that we need considerably more than 8 automata to replicate the density of traffic at Sävenäs. The 60 - 40% split between solo drives and drives with traffic was observed all tracks except track 5. In the actual intersection, the relative

## Chapter 9 - Simulations of traffic scenarios at Sävenäs and Jung

frequencies are consistently near 40 - 60%. These findings reveal that the manipulations of Experiment 2 failed to produce traffic flows like those at Sävenäs.

### Experiment 3

Data from three of the drivers in Experiment 3 were lost. As a result, there are data from only nine drivers in the LTAP/OD condition and 10 in the LTAP/LD condition. Each driver crossed 28 replicas of the Sävenäs intersection. The schedule of projected gap times, Table 9.5, is the basis for predicting the expected distribution of traffic scenarios. This distribution is shown in the bottom row of Table 9.12.

The seven crossings with no traffic were designed to be 'solo' drives categorized as Scenario 6 using the numbering scheme developed by Autoliv and Chalmers, Figure 5.1a. As all 19 drivers made these solo crossings, the expected total count is 133. The 16 crossings where the driver encountered a provoker were designed to be either case 6xa (crossing from ahead, LTAP/OD) or case 6xs (crossing from the side, LTAP/LD). The five crossings where the provoker was to wait for the driver to pass were designed to be waiting casings categorized as either 6wxa or 6wx. Nine drivers encountered scenarios 6xa and 6wxa and 10 encountered scenarios 6xs and 6wx. None of the intersection crossings was designed to involve multiple vehicles.

The top row of Table 9.12 summarizes the observed traffic scenarios. There were 27 fewer solo crossings than expected, many more provocations than expected, very few waiting cases, and a surprising number of multiple cases. Only 70% of the observed traffic scenarios were classified as expected. The difference between the observed and expected distributions is significant,  $\chi^2(4) = 113.$ ,  $p < .001$ .

The two contingency tables in Table 9.13 were constructed to shed light on the sources of disparity between the expected and observed classifications of cases in Experiment 3. The columns represent the three expected scenarios - the solo drives, the encounters with a provoker, and the cases where the provoker was to wait. The rows represent the seven scenarios captured by the automatic classification system. Had the crossings occurred as expected, all entries would be in the highlighted cells.

Table 9.13a shows the distribution of cases when provokers approached the driver from the opposite direction, the LTAP/OD scenario. There are two surprising findings. First, none of the waiting cases materialized. Most were experienced by the drivers as case 6xa - the provoker turned in front of the driver rather than wait. This is consistent with the interpretation that the confederates found themselves having to wait an unrealistically long time for the driver to cross the intersection. Rather than sit in the intersection, they opted to turn in front of the drivers.

The second surprise in the LTAP/OD data is that fewer than half of the solo cases materialized. Many were experienced by the drivers as 6xs - a provoker turned across the drivers' path from the side. Because all the solo cases were scheduled to occur at the West intersection, there is only one realistic explanation for this type of event. The confederate driving the provoker in the South intersection had to pass through the West intersection to return to position. It appears that this confederate drove faster than the driver, arrived at the West intersection before the driver, and, instead of waiting for the driver to pass, turned in front of the driver. The result is an unexpectedly large number of 6xs cases.

Table 9.13b shows the distribution of cases with provokers crossing the drivers' path from the side, the LTAP/LD scenario. The only substantial deviation from the expected pattern

## Chapter 9 - Simulations of traffic scenarios at Sävenäs and Jung

involves the waiting scenarios. Most were experienced by the drivers as case 6xs - the provoker turned in front of the driver rather than wait. Once again, it appears that the confederates opted to turn in front of the drivers rather than sit and wait unrealistically at the intersection.

The lesson to be learned from Experiment 3 is that our drivers appear to have developed expectations for the encroachments we had planned. They adapted their driving to avoid the unrealistic encroachment events by forcing the confederates to turn rather than wait at the intersection. This observation suggests that the drivers were driving rather slowly to avoid the provocations they had learned to expect. The discussion about observed velocities in the second part of this chapter supports this conclusion.

### Experiment 4

The schedule of projected gap times, Table 9.6, is the basis for predicting the expected distribution of traffic scenarios summarized in the bottom row of Table 9.14. The observed distribution is shown in the top row. Nearly all cases were classified as expected. This observation stands in marked contrast to the scoring of Experiment 3 with human confederates as provokers. The comparison suggests that actions taken by the confederates are the source of the noise in the contingency tables for Experiment 3. Software is clearly superior to human confederates at provoking simulated encroachment.

### Experiment 5

The cells in the matrix of Table 9.15 contain the counts of cases for each of the 156 traffic scenarios at Jung. The sparse nature of the entries reflects the design of the experiment. Drivers entering the intersection from the south met a car from the north that either yielded or turned left across its path. There were of these 19 LTAP/OD encroachments. Drivers entering the intersection from the north met a car from the west that either yielded or turned left across its path. There were 26 of these LTAP/LD encroachments.

More often than not, drivers entering Jung from the east met traffic from either the south or the west. Meeting the traffic from the west was expected and produced four opportunities for encroachment. Similarly, drivers entering Jung from the west met traffic from either the south or east. A left turn by the driver produced three opportunities for merging encroachments by a red car turning right. The encroachments and resulting PET values are discussed in Chapter 10.

There are insufficient data from the Jung simulator study to warrant analyses of velocity profiles.

## Velocity distributions

### Free drives at Sävenäs

In two conditions of Experiment 1 (A and C) and all four conditions of Experiment 2, drivers were encouraged to follow the rules of the road and to explore the virtual world. On average, they maintained appropriate velocities through the simulated intersections. In contrast, the variability in their velocities far exceeded that seen at the actual intersection. Some of the drivers appear to have treated the simulator like a high-speed video game.

## Chapter 9 - Simulations of traffic scenarios at Sävenäs and Jung

Table 9.16 lists the average velocities of drivers continuing straight through the center of the intersection in Experiment 1. It groups the data by experimental condition in the same format as Table 9.2. Drivers who were asked to adhere to the 50 kph speed limit did so. Drivers who were told to complete the secondary task as rapidly as possible ignored the speed limit. The encouraging observation here is that, on average, drivers in the simulator are able to adhere to the rules of the road and drive at responsible velocities.

A similar finding obtains far from the intersection. Table 9.17 presents velocity data 70 meters before the intersection in Experiment 2. Because very few drivers proceeded straight through the intersection in this experiment, the data in Table 9.17 are averages from turning cases. These are velocities well before the drivers began to negotiate their turns. On average, drivers in all conditions adhered to the speed limit.

The graphs in Figure 9.7 are plots of the average velocities observed in the simulator and at Sävenäs at 10 meter intervals starting 30 meters before the center of the intersection and ending 20 meters beyond it. The red lines represent right turns, green lines left turns, and black lines passes straight through the intersection. Odd-numbered trajectories are marked by squares and even-numbered trajectories by circles. Trajectories 1 and 3, marked by squares, are turns from the primary road to the secondary road. Trajectories 2 and 4, marked by circles, are turns from the secondary road to the primary road. The data from simulator experiments 1 (A and C) and 2 are shown in Figure 9.7a. For comparison, Figure 9.7b is a copy of Figure 6.1, the baseline data of velocities by all car captured by the image processing system at Sävenäs.

Comparison of the two graphs reveals that the velocity profiles in the simulator are systematically shifted up - drivers in the simulator drove faster than drivers in the world. While their velocities were generally below the speed limit, they were far from representative of velocities observed at Sävenäs.

The distributions of velocities in the simulator were faster than traffic in all 34 of the 34 observations plotted in Figure 9.7. A separate Kolmogorov-Smirnov test was run for each observation to compare the distributions. Of the 34 tests, only two were not significantly different. Our drivers were not representative of traffic.

The most extreme disparity occurred on trajectory 4 (north to east, from the secondary road to the primary road) 10 meters before the intersection. At the real Sävenäs, this is where drivers encounter a little speed bump where the pedestrian and bicycle paths cross the road. The speed bump accounts for the two slowest velocities plotted in Figure 9.6b. There was no speed bump in the simulated intersection. Figure 9.8 affords examination of the observed distributions of velocities at this location. The histogram in the upper graph reveals a highly normal distribution of velocity with a mean near 11 kph at the real intersection. Velocities greater than 15 kph are rare. In contrast, the histogram of data from the simulator includes more than a few velocities greater than 30 kph. The average is approximately 22 kph, twice that at the real intersection. It comes as no surprise that the Kolmogorov-Smirnov test finds these two distributions to be significantly different,  $D(4967, 160) = .57, p < .001$ .

The disparities in the distributions of velocities for the other 33 observations are less extreme but of the same kind. Compared to the data from Sävenäs, all have high variability and positive skew. Many of our drivers adhered to the speed limit. But many of those who did not broke the rules with impunity.

## Chapter 9 - Simulations of traffic scenarios at Sävenäs and Jung

### Drives at Sävenäs with provokers

We cannot expect the distributions of velocities in Experiments 3 and 4 to be representative of traffic at Sävenäs. Drivers in these experiments repeatedly experienced encroachments by provokers from either the oncoming or lateral direction. However, their velocity data are information about how they responded to those provocations. These data are plotted in Figure 9.9.

The jagged lines in both graph plot the average maximum velocities and the average minimum velocities at each of the intersections the drivers crossed. The letters on the horizontal axis represent the west, north, east and south replicas of the Sävenäs intersection. The large dots use vertical exaggeration to indicate the projected gap times of Tables 9.6 and 9.8. The exaggeration is 10x (gap time in seconds).

Both graphs reveal that the range of average velocities was well below the speed limit. Unlike the drivers in Experiments 1 and 2, these drivers were being very cautious. The inclusion of provokers appears to be a viable remedy for the excesses observed in the earlier experiments.

The data plotted in Figure 9.9a reveal that the drivers slowed during an encroachment and did not slow when there was no encroachment. Their velocities were consistently (but cautiously) higher in intersections without provokers and where the red car was supposed to wait. An encroachment at one intersection did not have a strong influence on the velocity in the next. There is no evidence in these data for autocorrelation or hysteresis in the impact of the prior provocations.

In Experiment 4, Figure 9.9b, provocations occurred at every intersection. The drivers responded by driving slower than in Experiment 3. The correlations between project gap time and average velocities are positive strong, .73 for the average minimum velocity and .62 for the average maximum velocity. 80% of the variability in velocity is explained by the projected gap times. When gap times are short, velocities are low. These drivers quickly learned that they were going to experience encroachments. They adapted by slowing and by continuing to slow as long as the provoker was present. The analysis of the resulting PET observations in Chapter 10 is a study of this adaptive slowing.

### Discussion

In the first two experiments we created a natural driving environment. We manipulated the instructions to subjects and portions of the infrastructure (e.g., GPS, traffic lights) to ascertain whether these conditions would create opportunities for drivers to meet at intersections and for incidents with short PET values. None of these manipulations was especially effective at arranging for drivers to meet at the intersections. Like Hancock and deRidder (2003), we found that modulating traffic with stop lights is not sufficient to induce encounters at an intersection down the road.

In the second two experiments, we abandoned all pretext of realism and intentionally created repeated encroachments. As expected, drivers quickly learned to anticipate the provokers and modulated their velocities in response. In Experiment 3, the interplay between the drivers' anticipatory actions and our confederates' attempts to provoke encroachment produced a distribution of traffic scenarios that was significantly different than we had planned. This disparity vanished in Experiment 4. Software proved to be much better than our confederates at adhering to the script. The distribution of traffic scenarios was exactly as

## Chapter 9 - Simulations of traffic scenarios at Sävenäs and Jung

planned and the nature of their adaptation clearer: drivers who expect encroachment slow to avoid it.

This result is highly auspicious for the development of active safety systems. Drivers who receive an appropriate alert to an impending encroachment are likely to heed it and to slow down to avoid it.

### Reference

Hancock, P. A., & deRidder, S. N. (2003). Behavioural accident avoidance science: Understanding response in collision incipient conditions. *Ergonomics*, *46*, 111-1135.



Figures

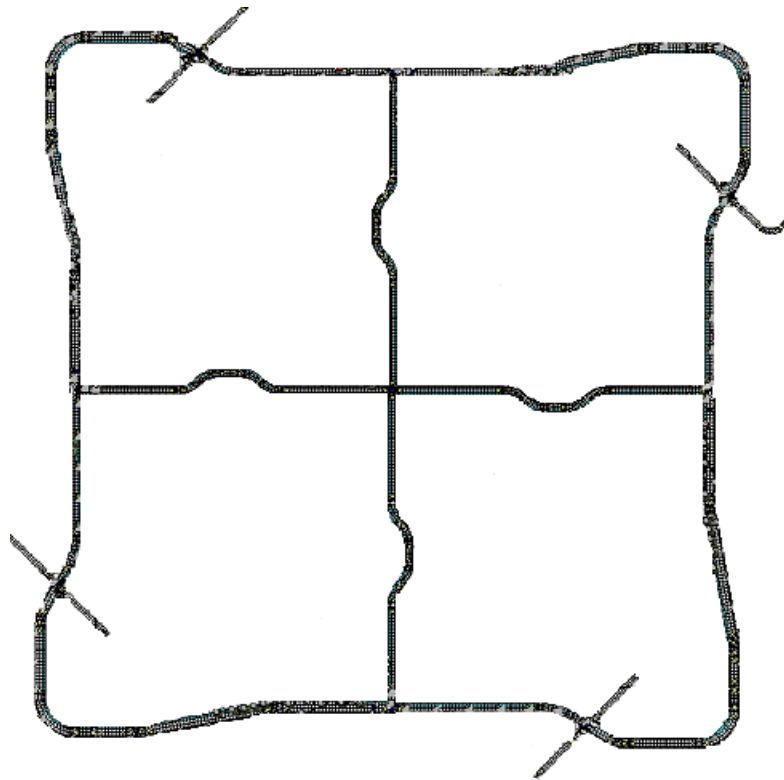


Figure 9.1 The road circuit used in the Experiment 1. The ring road contained four identical replicas of the 3-way Sävenäs intersection.



(a)



(b)

Figure 9.2 Views of the replica of the Sävenäs intersection. (a) An overhead view. (b) From the perspective of a driver approaching from the East.



Figure 9.3 One of the signs posted along the road circuit in Experiment 1.

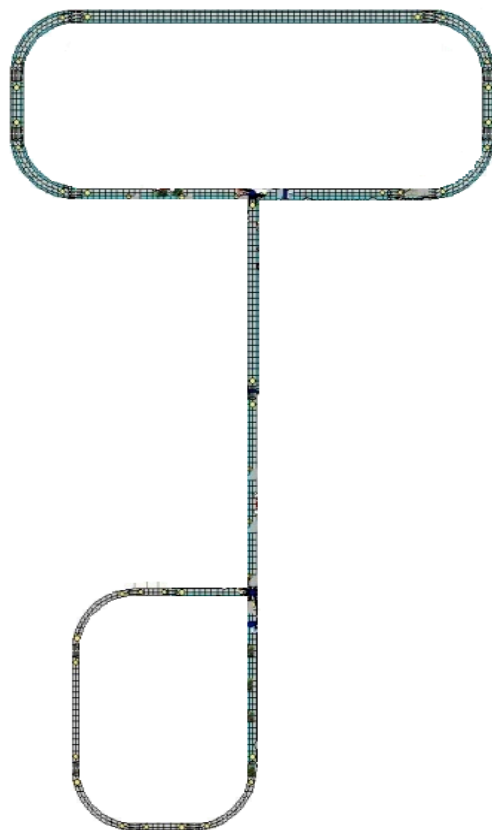


Figure 9.4 The road circuit used in the Experiment 2. The two identical replicas of the 3-way Sävenäs intersection forced drivers to make turns.

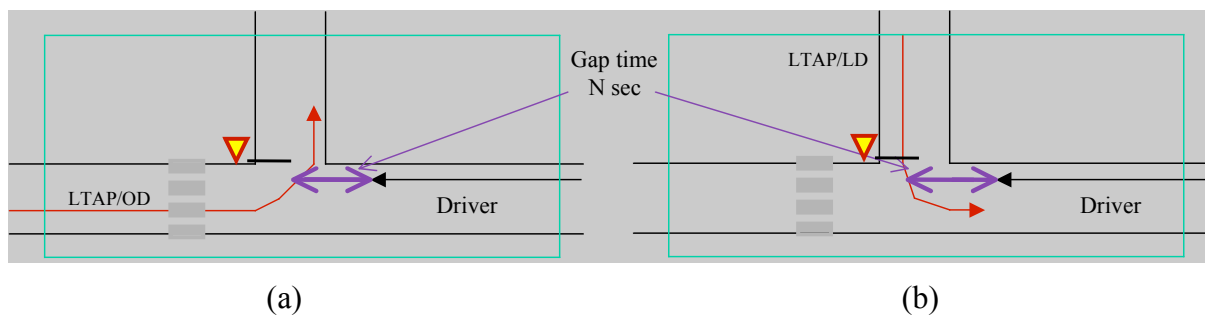


Figure 9.5 The two provocation scenarios showing the projected gap time. (a) 6xa, LTAP/OD. (b) 6xs, LTAP/LD.

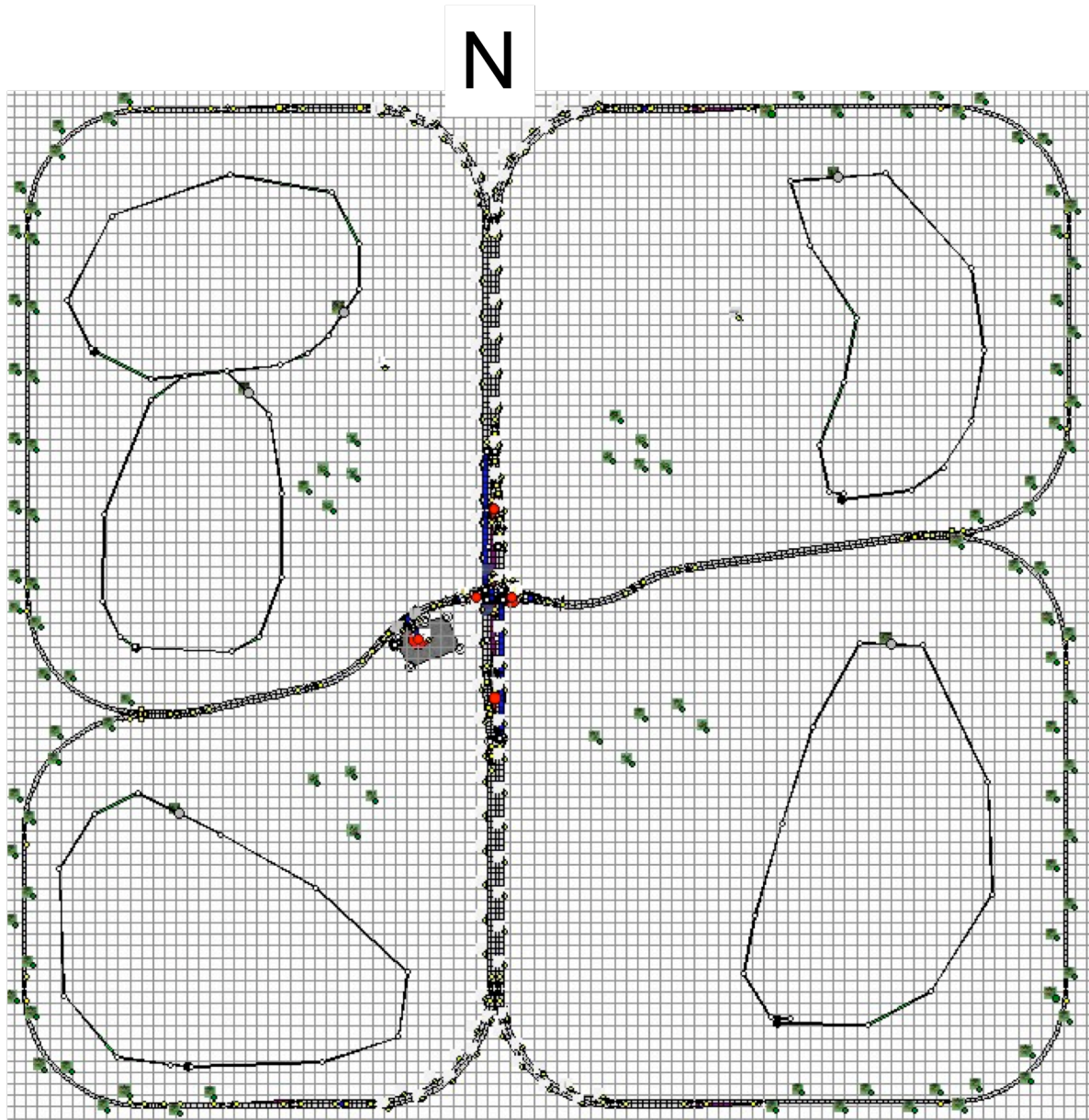


Figure 9.6 The road circuit used in Experiment 5 with its one replica of the Jung intersection. The E4 is the four-lane north-south road. The east-west secondary road has two lanes. The loop roads are one-lane, one-way. The service station sits on the southwest corner of the intersection. Within each quadrant are forested zones that block the driver's line of sight.

Chapter 9 - Simulations of traffic scenarios at Sävenäs and Jung

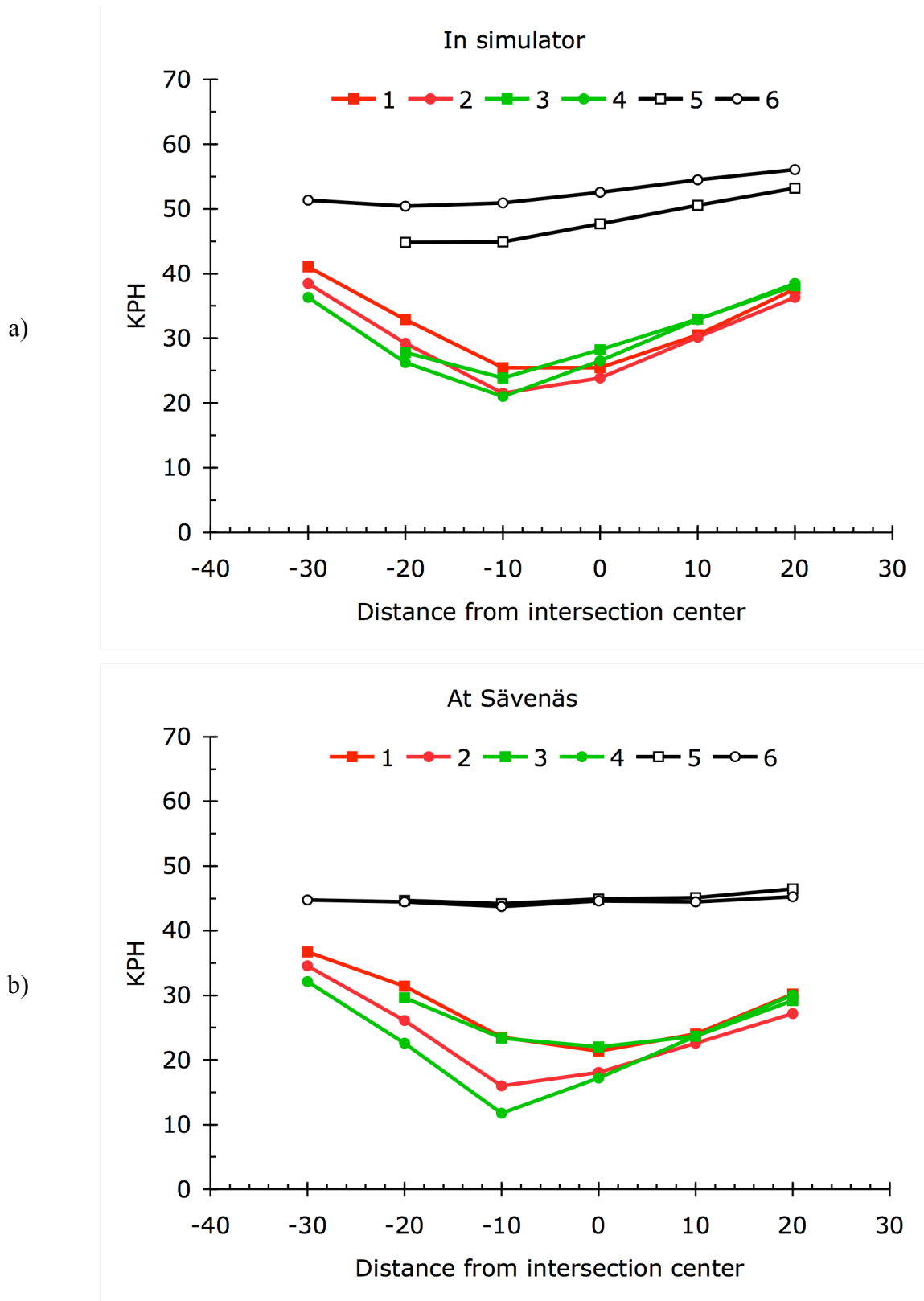


Figure 9.7 Average velocities for each trajectory (a) in the simulator when drivers were allowed to drive freely: Experiment 1, conditions A and C, and Experiment 2 and (b) at Sävenäs.

## Chapter 9 - Simulations of traffic scenarios at Sävenäs and Jung

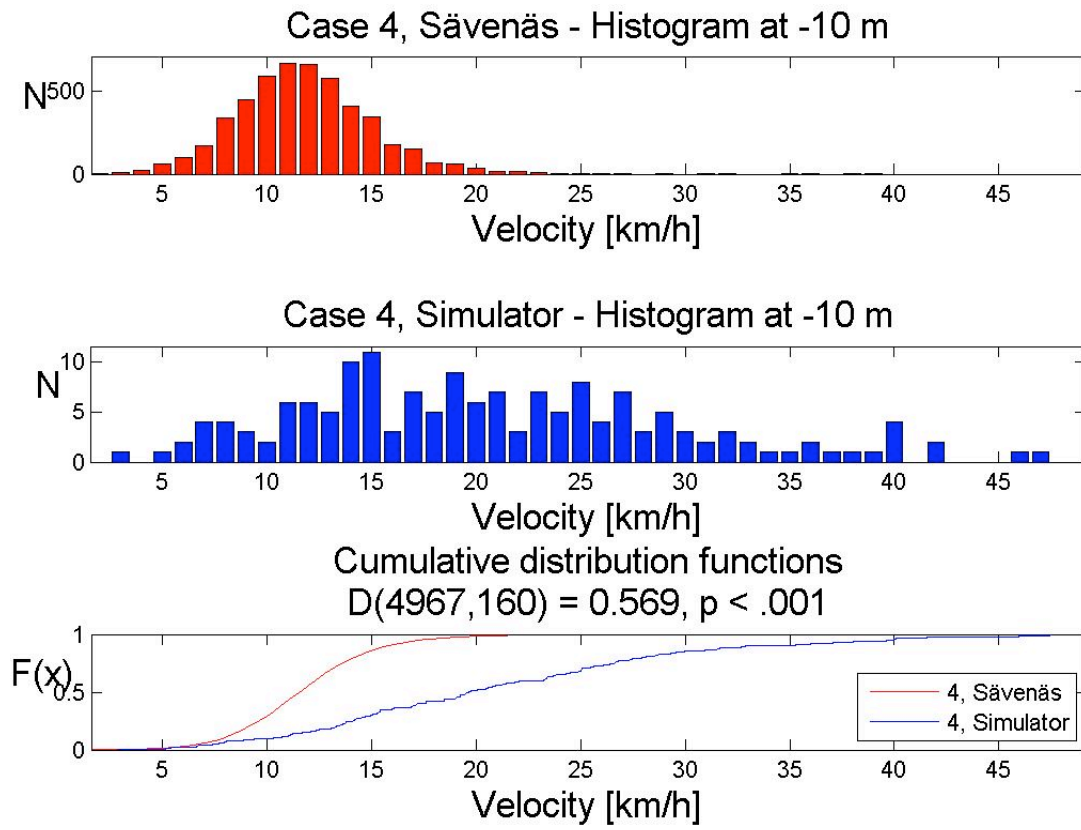


Figure 9.8 Histograms and cumulative frequency curves for the most extreme disparity in velocity distributions between the simulator and traffic at Sävenäs.

Chapter 9 - Simulations of traffic scenarios at Sävenäs and Jung

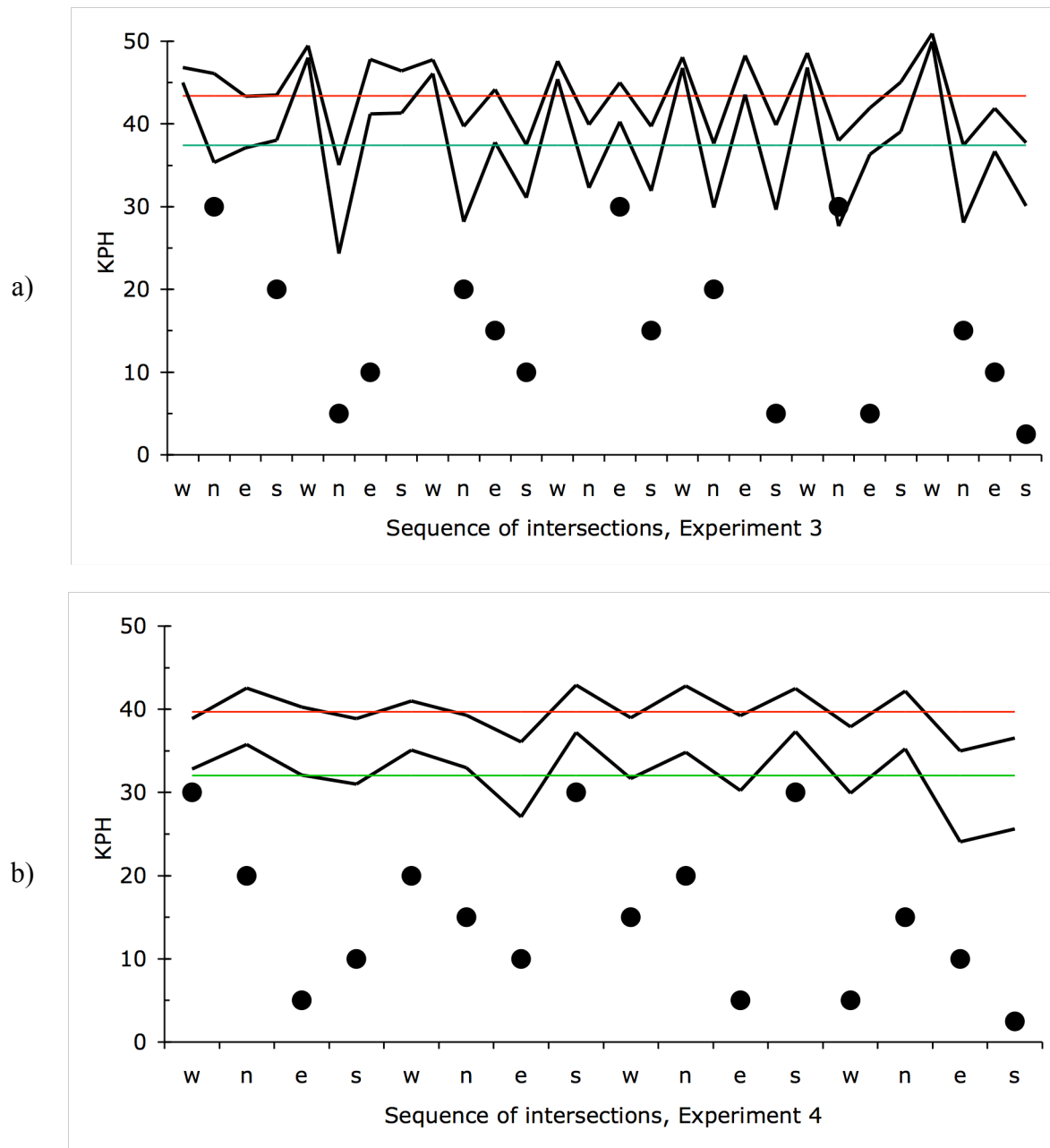


Figure 9.9 Average maximum and minimum velocities in kph while approaching the simulated intersections in (a) Experiment 3, and (b) Experiment 4. Dots represent the relative values of the projected gap times (plotted point = 10 x Gap in seconds).

## Chapter 9 - Simulations of traffic scenarios at Sävenäs and Jung

### Tables

Table 9.1 Sentences formed by the 6 signs along the road circuit in Experiment 1.

Session	Sentence	Answer
A	Vad står på skylten vid kraftverket?	SAAB
B	Hitta skylten där stadens namn står	Göteborg
C	Vilket djur bor i stadens park?	Kanin
D	Hur många korsningar finns i världen?	5

Table 9.2 The 2x2 design and assignment to labels to conditions in Experiment 1.

Speed variability	Instruction set	
	Rule following	Competition
High	A	B
Low	C	D

Table 9.3 The fixed order of questionnaire presentation in Experiments 1 and 2.

1	Demographics
2	NEO-FFI
	Training session
3	Schwartz value survey Part 1
	First session
4	Schwartz value survey Part 2
	Second session
5	Time horizon
6	Tolerance for uncertainty
	Third session
7	Conflict avoidance
8	Locus of control
	Fourth session
9	Driver style
10	Driver behavior
11	Debriefing

## Chapter 9 - Simulations of traffic scenarios at Sävenäs and Jung

Table 9.4 The 2x2 design and assignment to labels to conditions in Experiment 2.

GPS	Traffic light	
	+	-
+	A	B
-	C	D

Table 9.5 Projected gap times in seconds for the 28 crossings of the Sävenäs intersection in Experiment 3. The letter 'w' indicates the provoker was scheduled to wait for the driver to pass. There were no provocations at the west intersection.

	Sävenäs	West	North	East	South
Lap 1		-	3.0	w	2.0
2		-	0.5	1.0	w
3		-	2.0	1.5	1.0
4		-	w	3.0	1.5
5		-	2.0	w	0.5
6		-	3.0	0.5	w
7		-	1.5	1.0	0.25

Table 9.6 Projected gap times in seconds for the 16 crossings of the Sävenäs intersection in Experiment 4.

	Sävenäs	West	North	East	South
Lap 1		3.0	2.0	0.5	1.0
2		2.0	1.5	1.0	3.0
3		1.5	2.0	0.5	3.0
4		0.5	1.5	1.0	0.25

Table 9.7 Locations and occurrence of provokers (automata) in Experiment 5.

Driver arrival direction	Passes	Red car path	Designed encroachment
South	Odd	NL	None, red car yield
	Even	NL	LTAP/OD
North	Odd	WL	None, red car yield
	Even	WL	LTAP/LD
East	Odd	SS	None, red car after driver
	Even	WS	Potential crossing encroachment if driver turns left
West	Odd	SS	None, red car before driver
	Even	ER	Potential merging encroachment if driver turns left



## Chapter 9 - Simulations of traffic scenarios at Sävenäs and Jung

Table 9.8 The distribution of traffic scenarios in Experiment 1. Entries are counts of cases.

Trajectory	One red car						One waiting red car						Multiple red cars						Multiple red cars with waiting								
	Solo	1	2	3	4	5	6	1w	2w	3w	4w	5w	6w	1m	2m	3m	4m	5m	6m	1wm	2wm	3wm	4wm	5wm		6wm	
1	109	24	21	11	17	5	3	0	2	6	3	0	0	18	1	8	5	2	0	0	0	10	0	0	0	0	E to N
2	164	25	19	32	26	7	7	0	0	1	1	0	0	9	14	7	1	3	5	0	0	1	0	0	0	0	N to W
3	121	17	10	21	15	4	4	0	0	0	2	0	0	8	0	5	15	0	2	1	0	5	2	0	0	1	W to N
4	133	17	17	29	17	8	7	0	0	1	0	0	0	3	0	20	4	2	8	0	0	5	0	0	0	1	N to E
5	125	15	19	24	18	2	6	0	0	1	2	0	1	5	6	5	14	1	3	0	0	3	2	0	0	0	W to E
6	182	29	19	16	16	7	7	1	9	19	25	0	0	0	11	13	11	0	1	0	2	15	3	0	0	0	E to W
	834	127	105	133	109	33	34	1	11	28	33	0	1	43	32	58	50	8	19	1	2	39	7	0	2		
	49%	7%	6%	8%	6%	2%	2%	0%	1%	2%	2%	0%	0%	3%	2%	3%	3%	0%	1%	0%	0%	2%	0%	0%	0%		
							541						74						210						51		
							32%						4%						12%						3%		

Table 9.9 Summary of the distributions of traffic scenarios in the simulation of Sävenäs in Experiment 1 and if all traffic at Sävenäs.

Trajectory	Simulated Sävenäs						Actual Sävenäs		
	Counts			Percentages			Percentages		
	Solo	With Traffic	Total	Solo	By Case		Solo	By Case	
1	109	136	245	44	14	E to N	42	13	
2	164	158	322	51	19	N to W	40	25	
3	121	112	233	52	14	W to N	36	26	
4	133	139	272	49	16	N to E	35	9	
5	125	127	252	50	15	W to E	41	14	
6	182	204	386	47	23	E to W	45	13	
Total	834	876	1710	49	100		40	100	

## Chapter 9 - Simulations of traffic scenarios at Sävenäs and Jung

Table 9.10 The distribution traffic scenarios in Experiment 2. Entries are counts of cases.

Trajectory	Solo	One red car						One waiting red car						Multiple red cars						Multiple red cars with waiting						
		1	2	3	4	5	6	1w	2w	3w	4w	5w	6w	1m	2m	3m	4m	5m	6m	1wm	2wm	3wm	4wm	5wm	6wm	
1	107	18	7	11	10	1	1	1	0	8	1	0	0	9	1	7	0	1	0	0	1	2	0	0	0	E to N
2	222	7	62	24	5	4	3	0	1	1	0	16	0	2	13	2	2	0	0	0	0	2	0	0	0	N to W
3	203	5	26	61	5	6	0	0	0	0	0	1	0	2	2	9	12	1	2	2	0	0	1	0	1	W to N
4	101	13	4	12	39	0	0	0	0	2	2	0	1	0	0	12	7	0	1	0	0	6	0	0	0	N to E
5	10	2	2	2	2	3	0	0	0	0	0	0	1	1	0	1	2	1	0	0	0	0	0	0	0	W to E
6	40	3	4	1	1	0	4	0	0	2	1	0	0	0	4	0	0	0	0	0	0	1	0	0	0	E to W
	683 58%	48	105	111	62	14	8	1	1	13	4	17	2	14	20	31	23	3	3	2	1	11	1	0	1	
		4%	9%	9%	5%	1%	1%	0%	0%	1%	0%	1%	0%	1%	2%	3%	2%	0%	0%	0%	0%	1%	0%	0%	0%	
							348						38						94						16	
							30%						3%						8%						1%	

Table 9.11 Summary of the distribution of traffic scenarios in the simulation of Sävenäs in Experiment 2 and at Sävenäs itself.

Trajectory	Simulated Sävenäs						Actual Sävenäs	
	Counts			Percentages			Percentages	
	Solo	With Traffic	Total	Solo	By Case		Solo	By Case
1	107	79	186	58	16	E to N	42	13
2	222	144	366	61	31	N to W	40	25
3	203	136	339	60	29	W to N	36	26
4	101	99	200	51	17	N to E	35	9
5	10	17	27	37	2	W to E	41	14
6	40	21	61	66	5	E to W	45	13
Total	683	496	1179	58	100		40	100

## Chapter 9 - Simulations of traffic scenarios at Sävenäs and Jung

Table 9.12 The observed and expected distributions of traffic scenarios at in Experiment 3. Entries are counts of cases.

Case	Solo	Provoker		Waiting		Multiple	
	6	6xa	6xs	6wxa	6wxs	6mxa	6mxs
Observed	106	172	221	0	9	19	5
Expected	133	144	160	45	50	0	0

Table 9.13 Contingency tables of the expected and observed distributions of traffic scenarios in Experiment 3. (a) Provokers from the opposite direction, LTAP/OD. (b) Provokers from the lateral direction, LTAP/LD.

(a)	Expected			Total
	Solo 6	Provoker 6xa	Wait 6wxa	
Observed				
6	30	1	3	34
6xa	1	130	38	169
6wxa	0	0	0	0
6xam	1	12	4	17
6xs	28	0	0	28
6wxs	1	0	0	1
6xsm	2	1	0	3
Total	63	144	45	252

(b)	Expected			Total
	Solo 6	Provoker 6xs	Wait 6wxs	
Observed				
6	66	4	2	72
6xa	1	147	45	193
6wxs	0	6	2	8
6xsm	0	2	0	2
6xa	3	0	0	3
6wxa	0	0	0	0
6xam	0	1	1	2
Total	70	160	50	280

## Chapter 9 - Simulations of traffic scenarios at Sävenäs and Jung

Table 9.14 The observed and expected distributions of traffic scenarios at in Experiment 4. Entries are counts of cases.

Case	Solo	Provoker		Waiting		Multiple	
	6	6xa	6xs	6wxa	6wxs	6mxa	6mxs
Observed	3	234	159	3	1	0	0
Expected	0	240	160	0	0	0	0

Table 9.15 The distribution of traffic scenarios in Experiment 5, at Jung. Entries are counts of cases.

		TOTAL												SUBTOTAL		
		SOLO			L			E			N					W
		L	S	R	L	S	R	L	S	R	L	S	R			
S	L	1						5						6	4%	
	S	0						19						19	13%	
	R	0						7						7	5%	
E	L	0	2									5		7	5%	
	S	4	4									8		16	11%	
	R	1	6									6		13	9%	
N	L	0									2			2	1%	
	S	0									26			26	18%	
	R	0									12			12	8%	
W	L	0	5			2								7	5%	
	S	6	8			10								24	16%	
	R	4	0			4								8	5%	
		16	0	25	0	0	0	16	31	0	0	40	19	0	147	100%
		11%	0%	17%	0%	0%	0%	11%	21%	0%	0%	27%	13%	0%		

Table 9.16 Average velocities in kph at the center of the intersection for drivers (participants) crossing straight through (paths 5 and 6), Experiment 1, conditions A and C.

Speed variability	Instruction set		
	Rule following	Competition	
	High	46.2	66.1
Low	50.4	65.6	59.5
	48.1	65.8	57.8

Table 9.17 Average velocities in kph 70 meters before crossing the intersection, Experiment 2.

GPS	Traffic light		
	+	-	
	+	47.1	47.8
-	51.9	52.3	52.1
	49.7	50.4	50.2

## Chapter 10 - Simulated encroachments at Sävenäs and Jung

### Introduction

This chapter discusses the encroachment incidents observed in the simulator experiments at LiU. As discussed in Chapters 4 and 7, the metric used to quantify the severity of encroachment is Post Encroachment Time (PET). The first two experiments, drivers were asked to explore the simulated world with four replicas of the Sävenäs intersection. These experiments generated a total of only 8 encroachment incidents. The fifth experiment, which asked drivers to explore a simulated world with the replica of the Jung intersection, generated only 24. These are too few to support meaningful extrapolation to driver behavior in actual ‘near-crash situations.’ To meet that goal, Experiments 3 and 4 created driving conditions in which encroachment was frequent ( $N = 261, 384$ ) and predictable. Analyses of the PET data from Experiments 3 and 4 are the focus of this chapter.

In these experiments, participants drove a route in which they had the right-of-way through four replicas of the Sävenäs intersection. The road circuit is shown in Figure 9.1. Drivers encountered another car at many of these intersections and, more often than not, that car would turn left across their path. The left turns were timed to generate short PET values. We call these turning cars ‘provokers’ because they were designed to provoke encroachment.

Encroachment occurs when a car turns left across the path of another car that has the right-of-way. The experiments were designed to set up two types of encroachment, left turns across path from the lateral direction (LTAP/LD), Figure 10.1a, and left turns across path from the opposite direction (LTAP/OD), Figure 10.1b. At the Sävenäs intersection, the car with the right-of-way travels from the east to the west. At Jung, cars traveling in either direction of the E20 have the right of way. The encroaching car approaches either from the opposite direction (from the primary road) or from the side (from the secondary road). Table 10.1 lists the counts of both types of encroachment observed in the simulator experiments.

Participants quickly learned to anticipate the behavior of the provokers and adapted their driving behavior in response. The nature of this adaptation is the data we were hoping to find. Armed with the expectation of encroachment, most drivers slowed and waited for the provoker to pass before proceeding through the intersection. With each wait and pass, they defined a PET value with which they were comfortable. The median of these PET values represents an estimate of a ‘comfort zone’ for safe passage. A key finding is that the distances and times that define the comfort zone do not vary significantly across the two traffic scenarios.

The observation that drivers modify their driving to avoid expected encroachment and to create a ‘comfort zone’ for safe passage bodes well for the introduction of active safety systems designed to detect and alert drivers to impending encroachment incidents. The concept of a comfort zone in driver responses to encroachment might be useful information for the designers of active safety systems.

### Experiments 1, 2, and 5

Four participants drove cars simultaneously in Experiments 1 and 2. These experiments were designed to create opportunities for drivers to meet in the replicas of the Sävenäs intersection and for encroachment to occur spontaneously. Only 7 encroachments were observed in Experiment 1. The manipulations introduced in Experiment 2 - a new road circuit, traffic signals, and GPS guidance - were counterproductive; only 1 encroachment was observed. In Experiment 5, one driver at a time explored a cloverleaf road circuit with one replica of the

## Chapter 10 - Simulated encroachments at Sävenäs and Jung

Jung intersection, Figure 9.6. Software drove autonomous vehicles on a variety of paths designed either to provoke an encroachment, to wait for the driver to pass, or to pass through the intersection without incident. Once again, asking drivers to explore the world was counterproductive; only 24 encroachments were observed.

The lesson from these experiments is clear: drivers avoid encroachment in simulation experiments in which they are asked to drive naturally. Encroachment in realistic simulations is rare.

### Experiment 3

These results forced us to reconsider the design of the experiments. The redesign featured cars - provokers - that were intentionally driven to create encroachment. In Experiment 3, the drivers of the provokers were human confederates. Software drove the provokers in Experiment 4.

The method and procedure for Experiment 3 is discussed in Chapter 9. Drivers completed 7 laps of the road circuit and crossed replicas of the Sävenäs intersection 28 times. A provoker turned across their path at 16 of these crossings and was scheduled to wait for the driver to pass at another 5. In the remaining 7 crossings, no other cars were scripted to be present. The scripted schedule of 'projected gap times' is shown in Table 10.2. These are the target values of PET that the provoker tried to attain when turning left across the driver's path. The simulator recorded PET data for 10 drivers in the LTAP/LD condition and 9 different drivers in the LTAP/OD condition.

### Scenario 6xs, LTAP/LD

The symbols in Figure 10.2 indicate the scripted and observed PET values for the intersection crossings made by drivers who experienced provokers turning from the lateral direction (LTAP/LD). The horizontal axis shows the 7 laps and the 4 intersection crossings that were made during each lap. The solid symbols represent the 16 projected gap times. These are the values of PET that would have occurred had the driver maintained a constant speed and if the confederate had timed the arrival of the provoker according to the script. The open symbols represent the median value of PET (across the 10 drivers) for each intersection crossing. We use the median rather than the mean to filter out the effects of a few extreme values.

In the first crossing, the observed PET value is a full second shorter than the scripted value. The median PET is less than 2 seconds. The incident appears to have taken the drivers by surprise and to have been sufficiently provoking to lead them to change how they approached the intersections. For the duration of the experimental session, the observed PET values are greater than the expected values.

It appears that it took only one experience with a provoker for the drivers to expect encroachment to occur and to compensate by modifying their driving. They slowed to avoid the scripted encroachments and to cross the intersections well after the provokers.

The experimental procedure required confederates to drive provokers in three of the four replicas of the Sävenäs intersection. One confederate drove in the North intersection, a second in the East, and a third in the South. There were no encroachments at the West intersection. This design raises the possibility that the different confederates may have unintentionally influenced the drivers and their adaptation to expected encroachment. To test for that possibility, Figure 10.3 uses color codes for the different intersections (confederates)

## Chapter 10 - Simulated encroachments at Sävenäs and Jung

and plots the difference between the observed and expected PET values across the 16 scripted provocations from the lateral direction. There is no evidence in these data for a systematic bias that might have been introduced by the confederates.

### Scenario 6xa, LTAP/OD

The solid symbols in Figure 10.4 indicate the projected gap times for each of the 28 drives through the simulated intersections when the provoker encroached from the opposite direction (LTAP/OD). The open symbols represent the median observed PET values. Once again, the first observed value is well below the scripted. The median is less than 1 second. This incident appears to have taken the drivers by surprise. For the remainder of the experimental sessions, they modified their driving to cross the intersection after the provoker.

Once again, the experimental procedure required three different confederates to drive the provokers. Figure 10.5 uses color codes for the different intersections (confederates) to test for unintentional interactions with the drivers. Values above the horizontal axis indicate the driver slowed to allow more time to pass before crossing the intersection. Values below the axis indicate the driver sped up to cross the intersection before the provoker arrived.

On average, the drivers tended to slow down enough to give themselves an extra second of headway time. However, there are two patterns of divergence from this general trend. Drivers tended to speed up at the north intersection, shown in yellow in Figure 10.5, and slow down in the east intersection, shown in blue. The specificity of these patterns to particular intersections is consistent with the interpretation that the drivers were responding to the provokers in systematic but diametrically opposite ways. The most likely explanation for the patterns shown in Figure 10.5 is that each the two confederates unintentionally but consistently signaled the intent to provoke and that these signals prompted different adaptive responses from the drivers. This interpretation is supported by a comment by one of the confederates:

I know that in the opposite direction we as provokers could not avoid interacting with the driver. We could always see him. Although we knew what to do, it was difficult to do it. I believe we interacted.

### The influence of encroachment context

The bar chart of Figure 10.6a plots the median observed PET values for all encroachments except the first and compares the data from the two encroachment conditions. The data plotted in Figure 10.6b convert the times shown in Figure 10.6a into meters traveled at the posted speed limit at Sävenäs (and in the simulator), 50 kph. The error bars show the standard error of the mean of the medians across the 15 expected encroachments.

These are the PET values observed when the drivers expected an encroachment. They represent the ‘comfort zones’ that drivers create when they know an encroachment is likely. The median PET values are significantly different,  $t(14) = 4.18$ ,  $p < .001$  and are longer for encroachment from the lateral direction (LD) than from the opposite direction (OD). If these data are replicable, they suggest that the comfort zone for encroachment from the lateral direction is a full second longer than it is for encroachment from the opposite direction. However, interpretation of these results must be tempered by acknowledging the likelihood that our human confederates unintentionally influenced driver responses.

## Chapter 10 - Simulated encroachments at Sävenäs and Jung

### Experiment 4

As discussed in Chapter 9, Experiment 4 improved upon the experimental paradigm of Experiment 3 by using software to drive the provokers rather than human confederates. The goal, once again, was to ascertain how drivers respond to and anticipate encroachment. Twenty-nine students participated in the experiment. Ten drove in the LTAP/LD condition and 19 in the LTAP/OD condition. Each driver drove four laps. The script for the projected gaps time is shown in Table 10.3. There were scripted encroachments at every intersection. The discussion parallels that for Experiment 3.

#### Scenario 6xs, LTAP/LD

The symbols in Figure 10.7 indicate the scripted and observed PET values for the LTAP/LD scenario. The horizontal axis shows the 4 laps and the 4 intersection crossings that were made during each lap. The solid symbols represent the 16 the values of PET that would have occurred had the driver maintained a constant speed at the posted limit, 50 kph. The open symbols represent the median observed value of PET (across the 10 drivers) for each intersection crossing.

Most but not all of the observed PET values are greater than the expected values. This result suggests that, as in Experiment 3, the drivers often slowed to avoid the scripted encroachments. The salient finding, however, is that the driver-defined PET values define a floor. The minimum observed median PET value is 1.3 seconds (18 meters at 50 kph). On average, the drivers appear to have worked at ensuring that they got no closer to the provoker. This limit suggests that the comfort zone for lateral encroachment is substantially shorter than observed in Experiment 3.

Figure 10.8 uses color codes for the different intersections and plots the difference between the observed and expected PET values across the 16 scripted provocations. The data raise the possibility that the software implementation in the north and south intersections may have systematically missed the scripted gap times and crossed the driver's path approximately 0.5 seconds later (closer) than planned.

#### Scenario 6xa, LTAP/OD

The symbols in Figure 10.9 indicate the scripted and observed PET values for the LTAP/OD scenario. The open symbols represent the median value of PET (across the 19 drivers) for each intersection crossing.

All but three of the observed PET values are greater than the expected values. Those that are shorter are less than 0.2 seconds less. This result suggests that, as in Experiment 3, the drivers slowed to avoid the scripted encroachments. Once again, the salient finding is the driver-defined floor for the PET values. The minimum observed median PET value is 1.6 seconds (22 meters at 50 kph). On average, the drivers appear to have worked at ensuring that they got no closer to the provoker. This comfort zone is similar to and better defined than that observed in Experiment 3.

Figure 10.10 uses color codes for the different intersections and plots the difference between the observed and expected PET values across the 16 scripted provocations. There is no evidence in these data for a systematic bias in the scripted gap times.



## Chapter 10 - Simulated encroachments at Sävenäs and Jung

### The influence of encroachment context

The bar charts of Figure 10.11 plots the median observed PET values (and associated separation distances at 50 kph) for all encroachments except the first. These are the PET values observed when the drivers expected an encroachment. The data are not significantly different,  $t(15) = 1.78$ ,  $p = .10$ . This result is consistent with the interpretation that drivers in our simulation of the Sävenäs intersection were comfortable with a 2 second (30 meter) gap with a provoker. It appears that that the significant difference observed in Experiment 3 may have been due to unintended interactions between our confederates and the drivers.

### The comfort zone

The two graphs of Figure 10.12 summarize the PET data from the simulator experiments. The data are the means of the median PET values observed at each intersection. There are two striking findings.

First, the mean PET value for the LD condition with human confederates is a full second longer than the other three means. A two-way fully between-subjects ANOVA was run to assess the significance of this disparity, Table 10.4. Both main effects and their interaction were found to be significant. The Tukey post-hoc test indicates that the confederate-LD condition is indeed significantly different from the other three and that the other three do not differ from each other. This finding, coupled with the likelihood of confederate interaction with the drivers, suggests the LD results from Experiment 3 are suspect.

Second, the data are in substantial agreement in the other three cases. The drivers appear to have been able, on average, to establish and maintain a comfortable level of PET. The comfort zone in the simulator appears to have been  $2.15 \pm 0.2$  seconds (30 meters). This value stands as our best estimate for the minimum separation that drivers are willing to tolerate when they expect an encroachment.

The unexpected finding is that there is no pragmatic difference in the size of the comfort zone across encroachment directions. If these results are replicated, it would appear that the influence of contextual sensitivity on expected encroachment is minimal.

### Figures

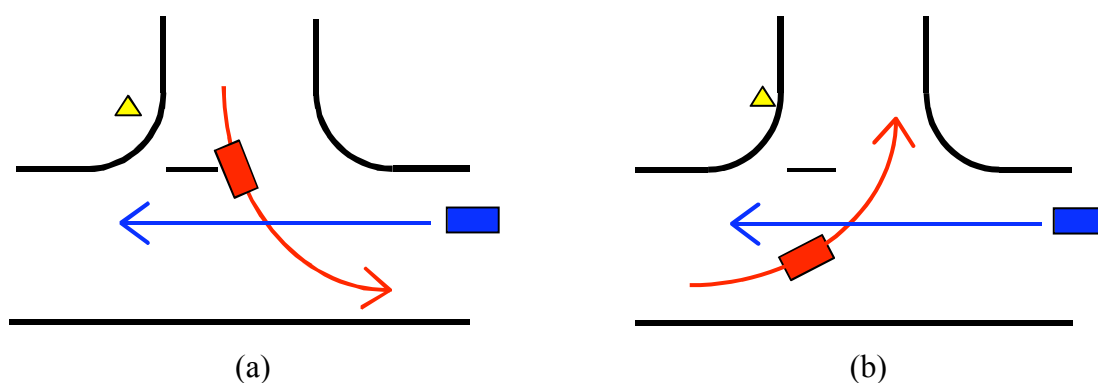


Figure 10.1 The two types of encroachment incidents investigated in the simulator experiments. Both involve a provoker, shown in red, that turns left across the path (LTAP) of car with the right-of-way, shown in blue. (a) Scenario 6xs, left turn from the lateral direction, (LTAP/LD). (b) Scenario 6xa, left turn from the opposite direction (LTAP/OD).

## Chapter 10 - Simulated encroachments at Sävenäs and Jung

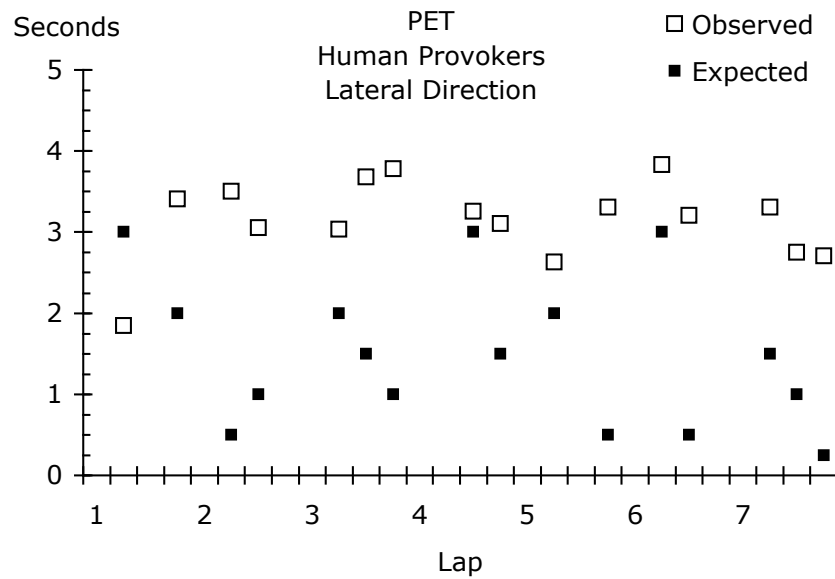


Figure 10.2 Observed PET values and expected gap times for Scenario 6xs, LTAP/LD in Experiment 3.

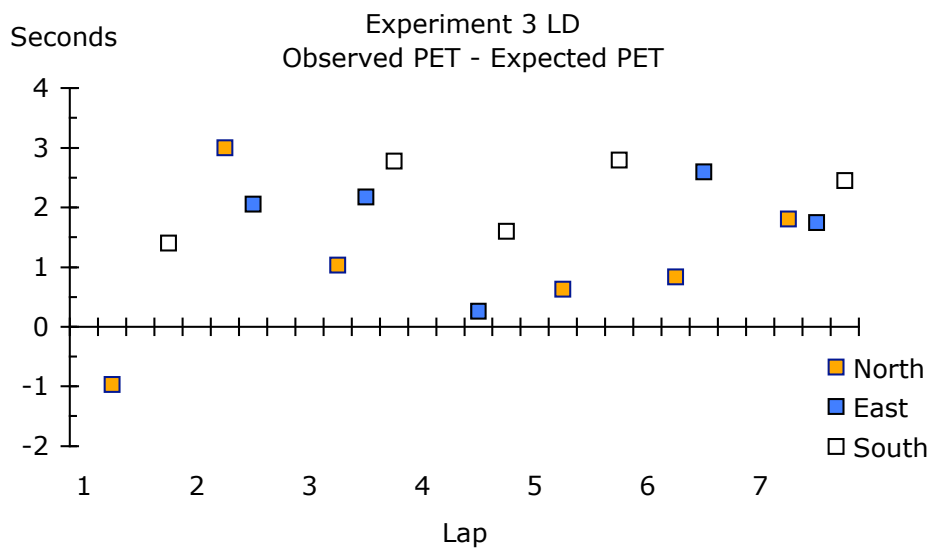


Figure 10.3 Extra headway achieved by the drivers when the provokers crossed from the side in Experiment 3. Provokers encroached on the driver at the north, east, and south replicas of the Sävenäs intersection. Different confederates drove the provokers in the different intersections.

## Chapter 10 - Simulated encroachments at Sävenäs and Jung

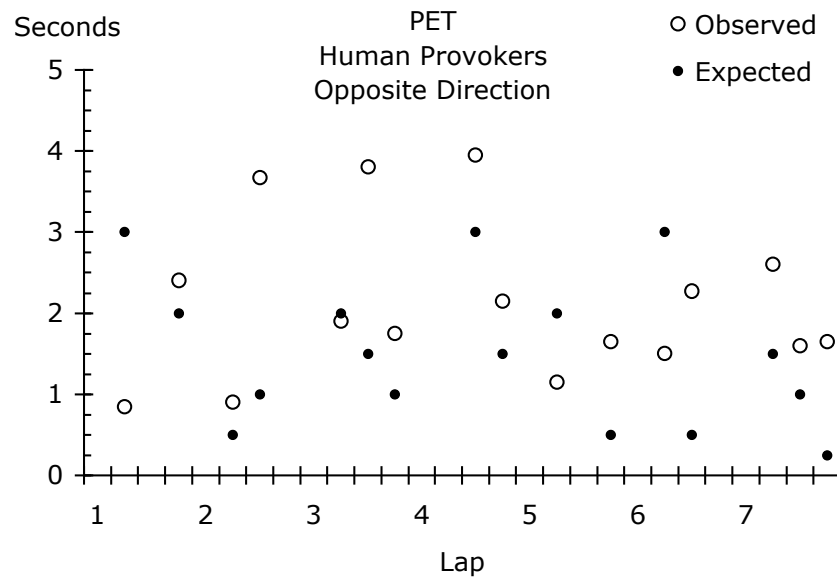


Figure 10.4 Observed PET values and expected gap times for Scenario 6xa, LTAP/OD in Experiment 3.

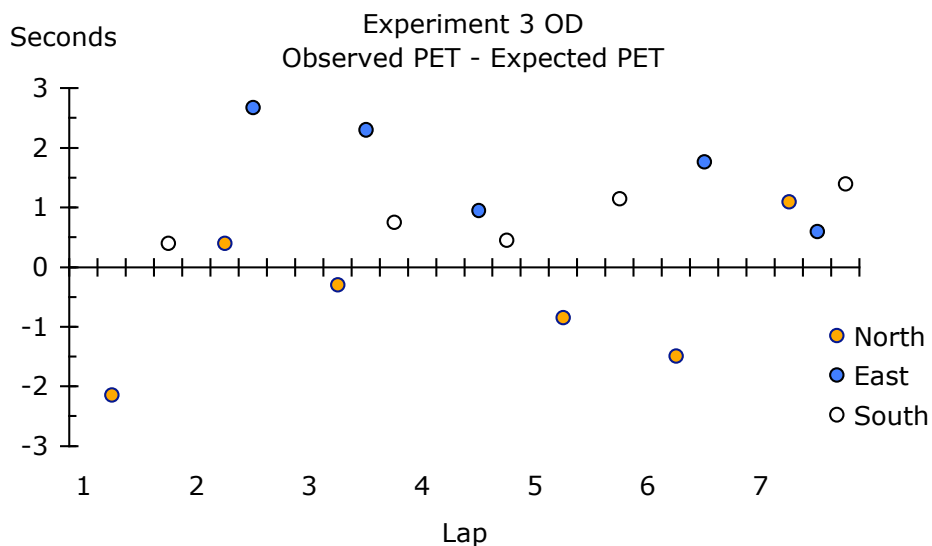


Figure 10.5 Extra headway achieved by the drivers when the provokers crossed from the opposite direction in Experiment 3. Provokers encroached on the driver at the north, east, and south replicas of the Sävenäs intersection. Different confederates drove the provokers in the different intersections.

## Chapter 10 - Simulated encroachments at Sävenäs and Jung

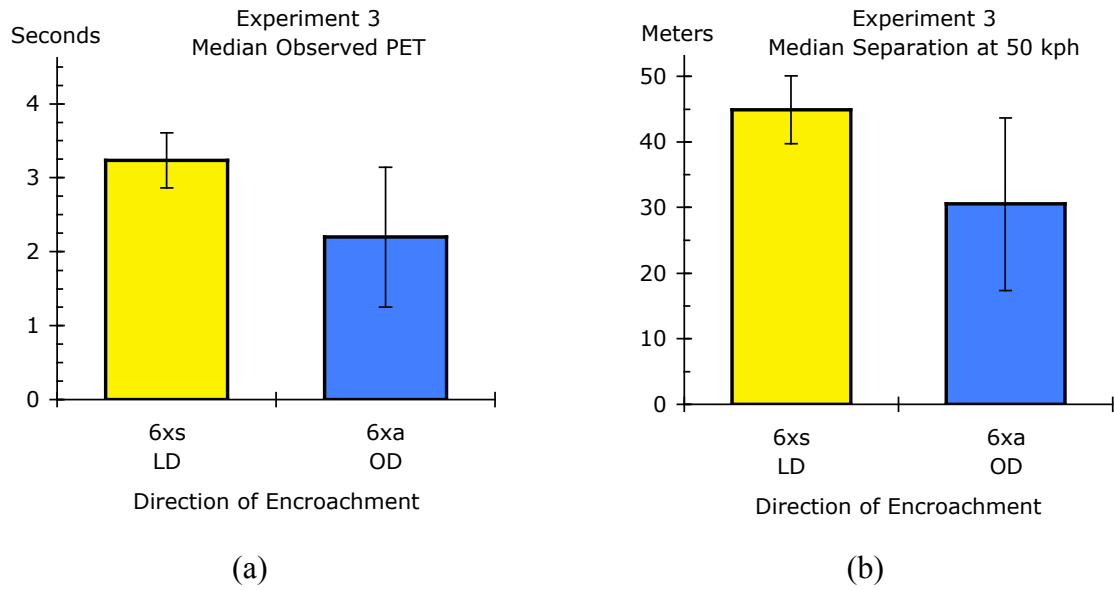


Figure 10.6 Plots comparing median observed PET values for LTAP/LD and LTAP/OD cases in Experiment 3. (a) Observed PET values in seconds. (b) The distance traveled during that time at 50 kph.

## Chapter 10 - Simulated encroachments at Sävenäs and Jung

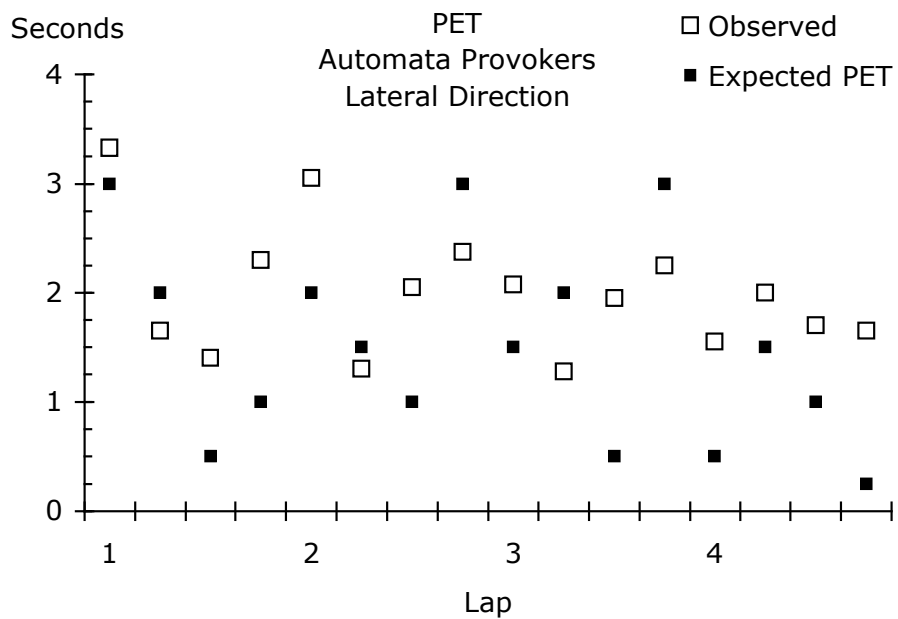


Figure 10.7 Observed PET values and expected gap times for Scenario 6xs, LTAP/LD in Experiment 4.

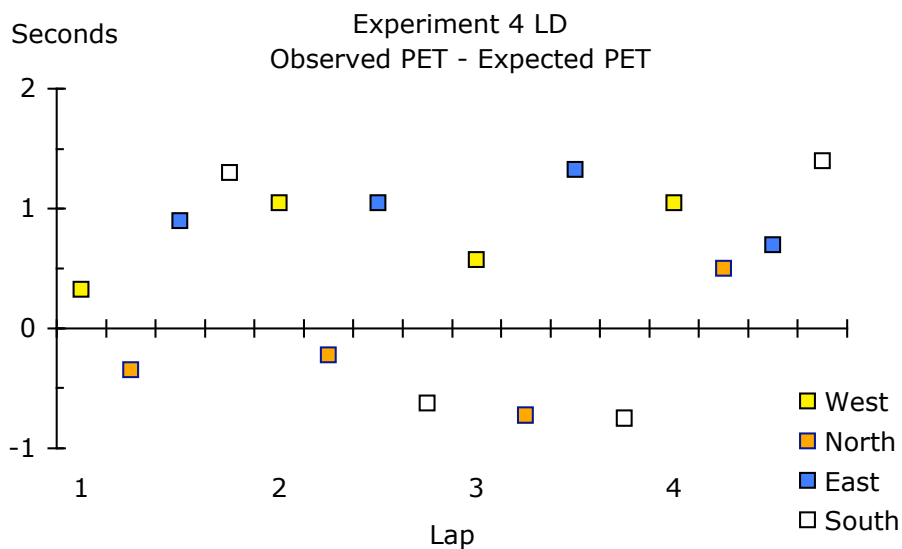


Figure 10.8 Extra headway achieved by the drivers when the provokers crossed from the side in Experiment 4.

## Chapter 10 - Simulated encroachments at Sävenäs and Jung

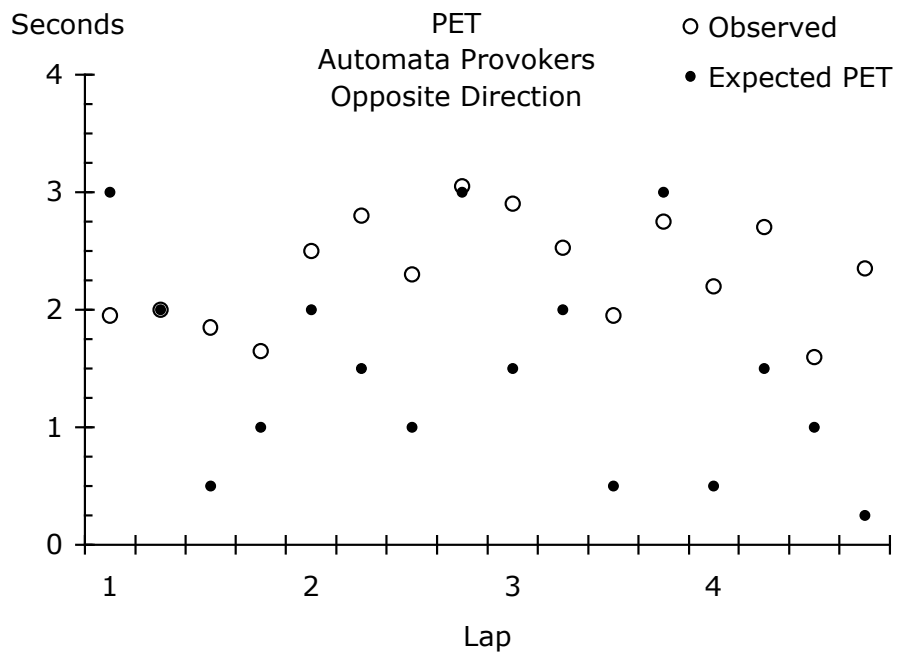


Figure 10.9 Observed PET values and expected gap times for Scenario 6xa, LTAP/OD in Experiment 4.

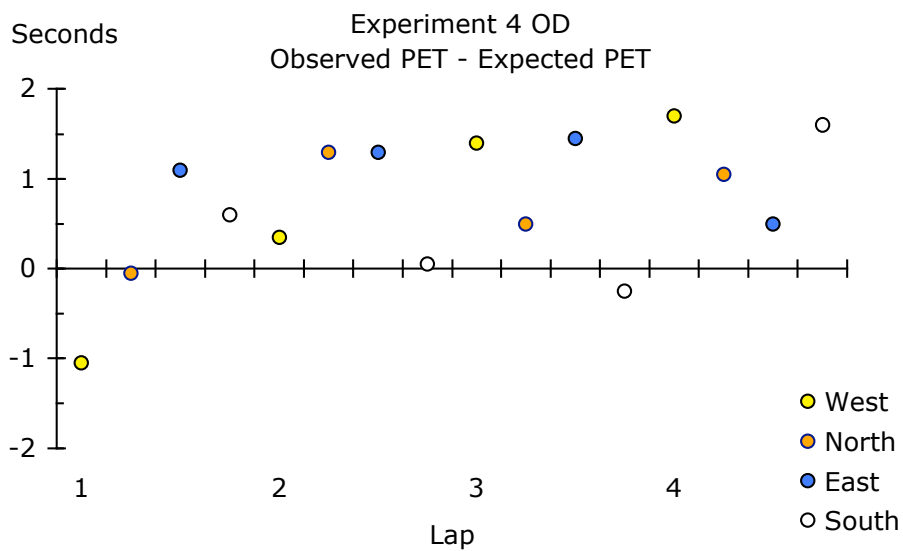


Figure 10.10 Extra headway achieved by the drivers when the provokers crossed from the opposite direction in Experiment 4.

## Chapter 10 - Simulated encroachments at Sävenäs and Jung

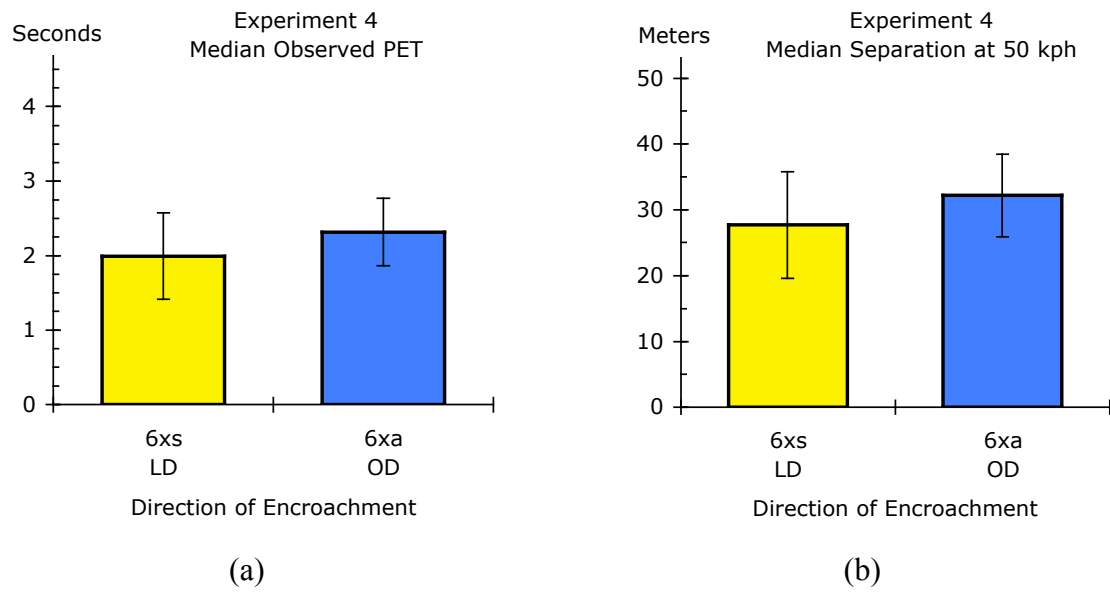


Figure 10.11 Plots comparing median observed PET values for LTAP/LD and LTAP/OD cases in Experiment 4. (a) Observed PET values in seconds. (b) The distance traveled during that time at 50 kph.

## Chapter 10 - Simulated encroachments at Sävenäs and Jung

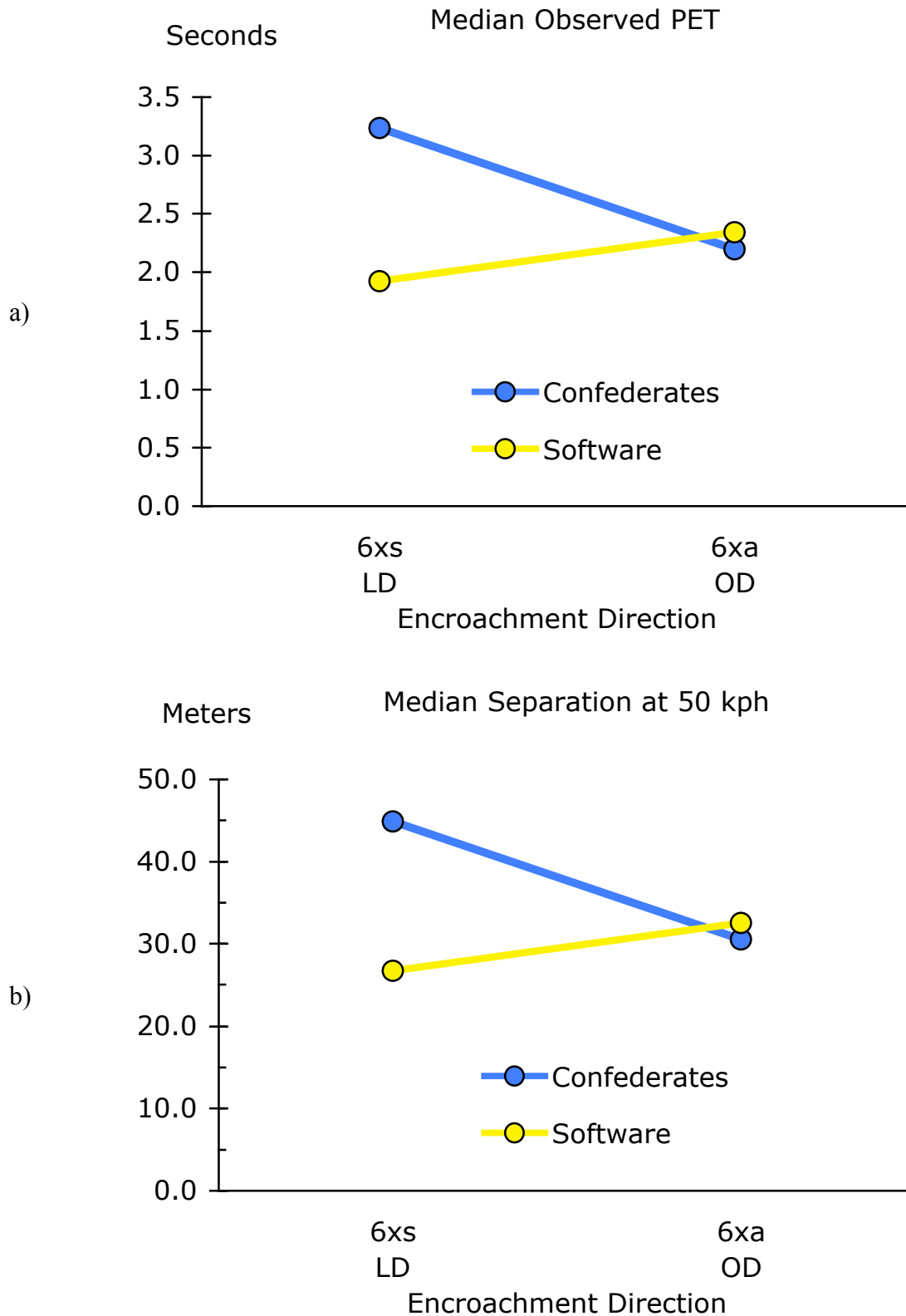


Figure 10.12 Comparison of average observed encroachment times across experimental conditions and experiments.



## Chapter 10 - Simulated encroachments at Sävenäs and Jung

### Tables

Table 10.1 Counts of encroachment incidents in the LiU simulator experiments.

Experiment	Traffic scenario	
	6xs LTAP/LD	6xa LTAP/OD
1	3	4
2	1	0
3	130	131
4	157	227
5	16	8
Total	307	370

Table 10.2 Projected gap times in seconds for the 28 crossings of the Sävenäs intersection in Experiment 3. The letter 'w' indicates the provoker was scheduled to wait for the driver to pass. There were no provocations at the west intersection.

Sävenäs	West	North	East	South
Lap 1	-	3.0	w	2.0
2	-	0.5	1.0	w
3	-	2.0	1.5	1.0
4	-	w	3.0	1.5
5	-	2.0	w	0.5
6	-	3.0	0.5	w
7	-	1.5	1.0	0.25

Table 10.3 Projected gap times in seconds for the 16 crossings of the Sävenäs intersection in Experiment 4.

Sävenäs	West	North	East	South
Lap 1	3.0	2.0	0.5	1.0
2	2.0	1.5	1.0	3.0
3	1.5	2.0	0.5	3.0
4	0.5	1.5	1.0	0.25

Table 10.4 Analysis of variance for observed Post Encroachment Times

Comparison	F(1, 56)
Experiment (humans vs. automata as provokers)	11.3**
Encroachment direction (lateral vs. opposing)	5.1*
Interaction	16.6***

\* $p < .05$ . \*\* $p < .005$ . \*\*\* $p < .001$ .

## Chapter 11 - Driver ratings of simulated encroachment incidents

### Summary

Seventy-one experienced drivers participated in an experiment in a fixed-based driving simulator with a 220° viewing angle that presented simulated encroachment incidents in an intersection. In each of the 36 trials, an encroaching vehicle (the ‘provoker’) turned left across the path of a vehicle that had the right-of-way as it drove straight through the intersection. After each trial, participants rated the welcomeness of hypothetical alerts to the incident they had just experienced.

The experiment was run using a 2x2x9 repeated-measures design. The first factor was participant Point-of-View. The participant viewed simulated encroachment incidents both from the vehicle with right-of-way and from the provoker. The second factor was Provoker Direction. The provoker approached the right-of-way vehicle either from the opposite direction (LTAP/OD) or from the side (LTAP/LD). The third factor, Post-Encroachment Time (PET), was manipulated at nine levels ranging from 0.2 to 4.5 seconds. There were 18 unique traffic scenarios, 9 with the provoker approaching from the opposite direction and 9 with the provoker approaching from the side. Every participant saw each scenario twice, once from each point-of-view.

Each experimental trial had two parts. First, participants passively viewed a simulated encroachment incident. They could not operate the vehicle’s control systems (e.g., braking and steering) to ensure that the incident unfolded with the desired PET. Then, using the method introduced by Källhammer, Smith, Karlsson, and Hollnagel (2007), they rated the welcomeness of an alert to that incident on a scale ranging from 0 to 10 with unit intervals. Participants also completed self-report questionnaires on driving style and behavior.

None of the self-report dimensions of driving style or behavior correlated significantly with the welcomeness ratings. These personality variables do not appear to have influenced the participants’ assessment of hypothetical alerts to the simulated encroachment incidents. This result suggests that the designers of active safety systems that would alert drivers to encroachments in intersections may not need to be especially concerned with the influence of individual differences in driving style or behavior on the welcomeness of those alerts.

Repeated measures ANOVA revealed significant differences in welcomeness for all three factors and their interactions at the .005 level. As expected, welcomeness increased monotonically as PET decreased. Alerts to traffic that encroached from the side were more welcome than alerts to traffic that encroached from directly ahead. Participants welcomed alerts more when they were in the vehicle with the right-of-way than when they were in the provoker.

The significant interaction between driver point-of-view and encroachment direction may have implications for the design of active safety systems. The analysis indicated that an alert was welcomed significantly less when participants were sitting in a provoking vehicle that turns in front of a vehicle that can be seen by looking straight ahead. Unfortunately, it appears that an alert may be least welcome when may do the most good.

## Chapter 11 - Driver ratings of simulated encroachment incidents

### Introduction

Since drivers play an important role in the pre-crash phase of an encroachment incident, driver acceptance of warning to an impending incident becomes an important design goal when developing active safety systems. Accordingly, knowledge of how drivers and vehicle systems function together is critical in achieving a successful design. One hallmark of this interaction is the human dislike for false alarms. When false alarms are the rule, drivers may either ignore them or disable the system. Indeed, the rate of false alarms may be a key factor for driver acceptance of novel active safety systems.

Unfortunately, because even highly accurate systems are likely to have a high rate of false alarms (Parasuraman, Hancock, & Olufinboba, 1997), they are likely to encounter driver resistance. This resistance poses a dilemma for the designers and developers of novel active safety systems: How to design the system so that drivers and society can reap their benefits while minimizing the likelihood of rejection due to the human dislike for false alarms? One approach to overcoming the dilemma is to focus on driver expectations and to design systems to issue alarms only for conditions where the driver is likely to accept them. The current study adopts one such approach.

Farber and Paley (1993, cited in Parasuraman et al., 1997) speculate that the ideal detection algorithm may provide alarms in conditions that may lead to collision, even though the driver will probably avoid the crash. A warning only for situations leading to a crash will however be very rare. In the US during 2004 there were 38,253 fatal police reported motor vehicle traffic crashes, 1,862,000 crashes with injuries and 4,281,000 crashes with property damages only (NHTSA, 2005). Given that the total vehicle miles traveled was 2,962 billion with almost 199 million licensed drivers, a fatal motor vehicle traffic crash would be expected once every 5,200 driver years. Similarly, a crash resulting in an injury would be expected once every 107 driver years and property damage crashes once every 46 driver years. A warning *only* in situations leading to any of these crashes would therefore be so rare that it would likely exacerbate the already critical situation and make the driver's reactions hard to predict. As intersection related accidents are only a fraction of the total accident rate, it follows that the rate of intersections related accidents will be even less frequent. Thus, we need to accept warnings in situations that do not always lead to a crash.

Instead of a traditional engineering performance criteria such as receiver operating characteristics curves (ROC), the goal may equally well be to match the driver's expectations of when the system should become active. By conforming to driver expectations, the system should be able to achieve a relatively high level of user acceptance and become an effective partner in the driver-vehicle system. Following this approach, we should strive to identify those situations in which drivers would expect alerts and therefore also accept them as relevant and appropriate.

In this paper we describe an empirical approach to quantifying how the relative level with which drivers are likely to welcome an alarm or intervention from an active safety system varies across situations. The current study asked drivers to watch a range of simulated intersection encroachment incidents and to rate the welcomeness of an alert to them. The study addressed two pragmatic questions. Is there a threshold of distance or time at which an alert become highly acceptable? What factors should be considered when designing active safety systems to alert drivers to impending encroachment incidents in intersections? The results point to thresholds in time and identify a significant interaction between driver point-of-view and encroachment direction that may have implications for the design of active safety systems.

## Chapter 11 - Driver ratings of simulated encroachment incidents

### Method

#### Participants

Participants were 19 women and 52 men (age: M 39 yr, range 20 - 60). Mean age among the women was 36 years and among the men 41 years. Summaries of their responses to two self-report measures of driving experience are listed in Table 11.1. There was no noticeable difference in driving experience between older and younger participants. Subject participation conformed to the ethical guidelines established by Vetenskapsrådet, the Swedish Research Council (2002).

#### Apparatus

The fixed base driving simulator used in the experiment is shown in Figure 11.1. It presents the driver of a Saab 9-3 with 220° view angle. Four projectors created a continuous panoramic view on a cylindrical screen. The eye-point of the driver of the car was located 240 cm from the screen. The car contained a touch screen in the center stack that enabled the display of a wide variety of information and the testing of interfaces.

#### Stimuli

The stimuli were 36 trials in which two simulated vehicles reached the center of a replica of the Sävenäs intersection at approximately the same time. Sävenäs is a 3 way intersection where traffic on a two-lane secondary road must yield to through traffic on the two-lane major road. For a discussion of the Sävenäs intersection, see Chapters 2, 6 and 7.

In all 36 trials, the vehicle with the right-of-way drove straight through the intersection on the main road from east to west. The direction of its travel put the secondary road on the right-of-way vehicle's near side (to the right). The second vehicle, the 'provoker', turned left across the path of the vehicle with the right-of-way. The turns by the provoker are instances of a left-turn-across-path (LTAP) encroachment. In every trial, traffic law would dictate that the provoker yield the right of way.

Participants were passengers - not drivers - of one of the two vehicles. They had no control over the vehicle and no way to influence the scene that unfolded in the simulated intersection. The reason for preventing them from controlling their vehicles was to ensure that the incident would unfold with the scripted level of PET.

The experiment used a 2x2x9 completely-crossed repeated-measures design. The first factor was the participant's vehicle, either the vehicle with the right-of-way or the provoker. The second factor was encroachment direction. This factor manipulated the relative direction of travel of the two vehicles. In half the scenarios, the provoker approached the right-of-way vehicle from the opposite direction (LTAP/OD), Figure 11.2a. In the other half, the provoker approached from the secondary road, that is, from the lateral direction (LTAP/LD), Figure 11.2b. Participants observed the incident from the perspective of the right-of-way vehicle in half the scenarios and from the provoker in the other half. They saw each traffic scenario twice, once from each point of view. The final factor was post-encroachment time at 9 levels (0.2, 0.5, 1.0, 1.5, 2.2, 2.6, 3.3, 4.0, 4.5 seconds). Participants experienced 4 incidents at each level of PET. Each trial was 30 seconds long, starting 18 to 25 seconds prior to crossing the center of the intersection.

## Chapter 11 - Driver ratings of simulated encroachment incidents

The paths taken by the vehicles adhered to three of the principal trajectories (Chapters 3 and 5) observed at Sävenäs. The path taken by the right-of-way vehicle followed the principal trajectory for traffic driving from east-to-west (path 6). The provoker from the opposite direction followed the principal trajectory for traffic driving from west to north (path 3). The provoker from the lateral direction followed the principal trajectory for traffic driving from north to east (path 4). The starting positions of the vehicles were shifted along the principal trajectories to create incidents within the intersection with the specified post-encroachment times.

### Task

The participant's task was to rate the welcomeness of a hypothetical alert to a simulated intersection encroachment incident. The nature and modality of the alert was not specified. Each participant individually viewed a series of 36 simulated incidents. Immediately after viewing each incident, the participant rated the degree with which he or she would welcome an alert to it. The rating used a scale ranging from 0 to 10 with unit intervals and the procedure introduced by Källhammer, Smith, Karlsson, and Hollnagel (2007).

### Procedure

The participants were SAAB employees and contractors working in Trollhättan, Sweden. They applied voluntarily to the study, some by answering advertisements in the SAAB internal newsletter, others spontaneously. The majority of the volunteers were contacted for a brief interview about driving experience and motion sickness. Those who indicated a history of motion-sickness were advised not to participate in the study. Those who still wished to participate were assigned a time to come to the simulator facility.

Upon arrival, a participant received information about the objective of the study and the IVSS project in general. The instructions covered the experimental procedure, the voluntary basis of participation, and some details about the simulator. All were given the opportunity to ask questions before the experiment started and were told that they could quit or pause the experiment at any time for any reason at all including motion sickness. They then signed a consent form and answered self-report questionnaires about driver style and behavior. Only one person did not complete the full set of trials due to motion sickness.

Once in the simulator, the participant was introduced to the car and to the touch screen shown in Figure 11.3. The screen was mounted in the center console. To start a trial the participant pressed 'Next scenario'. The tool then hid (went dark) while the scenario was running. When the scenario finished, the rating tool reappeared on the screen and prompted the participant to rate the degree of welcomeness to a warning to the situation just shown. The buttons numbered 0 to 10 represented ordinal levels of welcomeness, with 0 representing the lowest degree of welcomeness and 10 the highest. Pressing 'Next scenario' stored the selected value in the log file and started the next scenario. The participants was also able to watch the scenarios again by pressing 'Repeat' on the touch screen. As it was the participant who started the scenarios by pressing a button, the experiment was self-paced and afforded opportunities to have breaks in-between in case of simulator sickness etc.

Participants completed three practice trials while the experiment leader sat in the passenger seat. For the 36 experimental trails, the participants sat alone in the driver's seat but were monitored from a control station located in separate room. When all 36 scenarios were rated,

## Chapter 11 - Driver ratings of simulated encroachment incidents

the participant was asked to exit the car. A short debriefing was conducted to assess how they felt well and to gather spontaneous reactions to the experience.

### Questionnaires

Participants answered two questionnaires, the Driving Style Questionnaire (French, West, Elander, & Wilding, 1993) and a version of the Driving Behavior Questionnaire (Lajunen & Summala, 2003; Reason, Manstead, Stradling, Baxter, & Campbell, 1990) provided by LeBlanc, et al. (2006). The DSQ is a 15 item self-report instrument using a six point Likert scale. The 15 questions probe the extent to which drivers exhibit behaviors consistent with the first six dimensions in Table 11.2 (West, Elander, & French, 1992). The DBQ is a 24 item self-report instrument using a six point Likert scale. The 24 questions probe the extent to which drivers exhibit behaviors consistent with the last four dimensions in Table 11.2 (Lajunen & Summala, 2003).

## Results

### Ratings and driving

The purpose of asking participants to complete the DSQ and DBQ was to ascertain whether the way that they reported that they drive correlated with their ratings of the hypothetical alerts. If the ratings were found to be strongly correlated with one or several of the dimensions tapped by the questionnaires, then it could be argued that the ratings were more sensitive to personality variables than to the simulated encroachment incidents. Such a finding would diminish the utility of the rating procedure to the goals of the project. If, on the other hand, the correlation between the ratings and the personality variables were low, it would eliminate these possible sources of confound. Such a finding would lend credence to our assumption that the ratings are valid indicators of drivers' responses to encroachment incidents in intersections.

Table 11.3 shows the observed correlations and their significance levels. Of the 10 dimensions, only Focus from the DSQ and Deviance from the DBQ approached the .05 level of significance. Both correlated negatively with the welcomeness of ratings. Neither finding is surprising. Ratings tend to be less welcomed by individuals who report they are able to ignore distractions (e.g., noisy children in the back seat) and by individuals who report they break traffic rules with relative impunity. These two subsets of the driving population may prefer alerting systems set to a more tolerant threshold than the population at large.

As none of the dimensions of driving behavior or style correlate strongly with the welcomeness ratings, we can be confident that the ratings methodology is relatively uninfluenced by individual differences.

### Ratings = F(PET)

The first analysis of the ratings data collapsed across the four conditions of point-of-view and provoker direction. The aggregated data are plotted in Figure 11.4. As expected, ratings vary inversely and monotonically with PET. The relationship is not linear. There is a suggestion of a floor effect at long intervals of PET. The best-fit model to the data, Equation 10.1, is a simple quadratic function with no linear component.

$$Rating = 1.56 + 0.35(4.5 - PET)^2 \quad 10.1$$

## Chapter 11 - Driver ratings of simulated encroachment incidents

### Main effects, aggregated data

To assess the statistical significance of the main effects and their interaction, a 2 (Point-of-view: Right-of-way vs. provoker) x 2 (Provoker direction: Oncoming vs. lateral) x 9 (PET) repeated measures ANOVA was performed on the average ratings for each of the 36 experimental trials. As expected, the main effect of PET was highly significant  $F(8, 560) = 236.$ ,  $MSE = 6.61$ ,  $p < .001$ ,  $\eta^2 = .33$ . The Tukey HSD procedure, adjusting for multiple comparisons at  $p < .05$ , indicated that all adjacent pairs of ratings were significantly different.

The bottom row of Table 11.4 shows the grand mean of all ratings and the F-test and their levels of significance for the main effects and their interaction. The corresponding data are shown in Figure 11.5. Both main effects and their interaction are highly significant. Participants welcomed alerts less when they were sitting in the provoking vehicle than in the vehicle with the right-of-way. They welcomed alerts more when the provoker turned left across traffic from the lateral direction than from the oncoming direction. The graph of the interaction reveals that alerts were significantly less welcome when the participants were sitting in the provoker in an oncoming traffic scenario (LTAP/OD). This result suggests that drivers who decide to turn in front of a vehicle that can be seen by looking straight ahead will resist alerts that second-guess their decision. It appears that an alert may be least welcome when is likely to do the most good.

### Differential effects across the range of PET

Nine additional 2 x 2 (Point-of-view and Provoker-direction ) repeated measures ANOVA were performed to assess the influence of PET on the ratings. The results are summarized in Table 11.4.

The analyses reveal two distinct modes of responding to the hypothetical alerts. At PET intervals less than 2.2 s, one or both of the main effects and their interaction was statistically significant. The influence of PET was stronger on Point-of-view than it was on Provoker direction. As shown in Figure 11.6, participants were more likely to welcome alerts when sitting in vehicles with the right-of-way than when sitting in a provoker. The interaction effect noted in the aggregate data, Figure 11.5, applies when encroachment time is less than 2.2 s, Figure 11.6.

In contrast, at PET intervals greater than 2.2 s, only the main effect of Provoker direction was statistically significant. The interaction was no longer significant. As shown in Figure 11.7, at relatively long PET intervals, alerts were more welcome in the lateral scenario than in the oncoming scenario.

In sum, the factors that influenced the welcomeness of an alert changed across the range of PET intervals studied in this experiment. At relatively short intervals, the point-of-view is the dominant factor. At relatively long intervals, provoker direction is the dominant factor.

No effects reached significance at the 2.2 s and 4.5 s PET intervals. The former is likely to reflect a transition between the two modes of responding. In the latter, the time to encroachment is likely to be too long to be considered worthy of an alert in any condition.

### Critical values of PET

To estimate the values of PET at which 50% of our subjects would accept an alert from an active safety system for intersection encroachment incidents, we reduced the ratings to binary outcomes: accept or reject the alert. Ratings between 1 and 5 inclusive were categorized as rejecting the alert and ratings between 6 and 10 inclusive were categorized as accepting the alert. We counted the number of acceptances for each of the 36 trials and used that sum to compute the percentage of participants who accepted the alert in that trial.

## Chapter 11 - Driver ratings of simulated encroachment incidents

Figure 11.8 shows the percentage of drivers who would accept an alert in each of the four experimental manipulations. We used logistic regression to compute the best-fit least squares model to the data for the two points of view and two encroachment direction. The best-fit parameters can be used to estimate the '50/50 point' - the critical value of PET at which half the participants indicated they would accept an alert. These values represent threshold values of PET that could be used to guide the design of active safety systems.

The 50/50 acceptance times for the regression models are listed in Table 11.5 and illustrated in Figure 11.9. The figure highlights the contextual sensitivity of driver acceptance of alerts. Drivers accept alerts at longer values of PET when they have the right-of-way than when they are provokers. The effect of encroachment direction is dichotomous. In an oncoming scenario, the driver with the right of way welcomes an alert at substantially longer values of PET than the provoker. In a lateral encroachment scenario, the difference in acceptance across driver point of view is minimal. Building these contextual factors into the design of in-vehicle active safety systems may improve the likelihood of driver acceptance.

### Implications for the design of active safety systems

The method used in this study identified the PET values at which most drivers would likely accept an alert. These values appear to vary across the direction of the encroachment and the driver's point of view. They stand as criteria that could inform the specification of warning thresholds for the first generation of active safety systems for intersection encroachment incidents.

The results provide evidence of a significant interaction between driver point-of-view and the direction of encroachment. An alert was welcomed significantly less when participants were sitting in a vehicle that turned in front of another vehicle that could be seen by looking straight ahead. This finding may inform the design of active safety systems that would provide the driver with warnings to impending encroachment incidents: If the system were designed to fit the expectations of the drivers in this study, it would adapt to both the right-of-way in the intersection and the encroachment direction.

False alarms will be more accepted when the driver has the right-of-way and is being encroached upon than when the driver does not have the right-of-way and is doing the encroaching. Further, false alarms will be more accepted when vehicles encroach from the side than from the oncoming direction. It is indeed unfortunate that these findings imply that an alert is least welcome when it is likely to be the most needed: when the driver is turning left across the path of an oncoming vehicle.

The study did not distinguish between intentional and unintentional encroachments. A driver who intentionally provokes an incident with a small PET value by turning left across another's path may be less prone to accept an alert than a driver who mistakenly provokes an incident. As the results in this study are derived from a simulator study in which all participants were aware of the artificiality of the setting, we must assume that they responded as if all the encroachments were deliberate. Future work could readily address this issue by crafting instructions to subjects that specify the intent of the encroaching driver.

A well-designed active safety system might induce positive driver adaptation. Drivers may modify their behavior to reduce the rate of unwelcome alerts if those alerts are issued in situations they realize could have been dangerous. A poorly designed system that issues an alert either too early or too often or both would likely become annoying and could push the drivers to ignore them or, perhaps, to disable the system. On the other hand, if the warning threshold were set too high, the driver might infer that the system is prone to miss



## Chapter 11 - Driver ratings of simulated encroachment incidents

incidents that it should detect. The findings reported here are among the first to inform designers how to set the thresholds for an active safety system that will match driver's expectations for warnings to encroachment incidents in intersections.

### References

Farber, E. & Paley, M. (1993). Using freeway traffic data to estimate the effectiveness of rear end collision countermeasures. Paper presented at the *Third Annual IVHS America Meeting, IVHS America*, Washington DC.

French, D. J., West, R. J., Elander, J. & Wilding, J. M. (1993). Decision-making style, driving style, and self-reported involvement in road traffic accidents. *Ergonomics* 36, 557-567.

Källhammer, J. E., Smith, K., Karlsson, J., & Hollnagel, E. (2007). Shouldn't the car react as the driver expects? *Proceedings of the 4th International Driving Symposium on Human Factors in Driver Assessment, Training, and Vehicle Design*. Stevenson, WA.

Lajunen, T., & Summala, H. (2003). Can we trust self-reports of driving? Effects of impression management on driver behaviour questionnaire responses. *Transportation Research F* 6, 97-107.

LeBlanc, D., Sayer, J., Winkler, C., Ervin, R., Bogard, S., Devonshire, J. Mefford, M., Hagan, M., Bareket, Z., Goodsell, R., and Gordon, T. (2006). Road departure crash warning system field operational test: Methodology and results. *University of Michigan Transportation Research Institute Report 2006-9-2*, Vol. 2, Appendix E.

NHTSA [National Highway Traffic Safety Administration]. (2005). *Traffic Safety Facts 2004*. Washington, D.C.: U.S. DOT.

Parasuraman, R., Hancock, P.A., & Olufinboba, O. (1997). Alarm effectiveness in driver centered collision-warning systems. *Ergonomics* 40, 3, 390 - 399.

Reason, J., Manstead, A., Stradling, S., Baxter, J., & Campbell, K. (1990). Errors and violations on the roads: a real distinction? *Ergonomics* 33, 1315-1332.

Vetenskapsrådet (2002). *Forskningsetiska principer inom humanistisk-samhällsvetenskaplig forskning*. Vetenskapsrådet, Sverige.

Figures



Figure 11.1 (a) The simulator. (b) The participant's view from the vehicle.

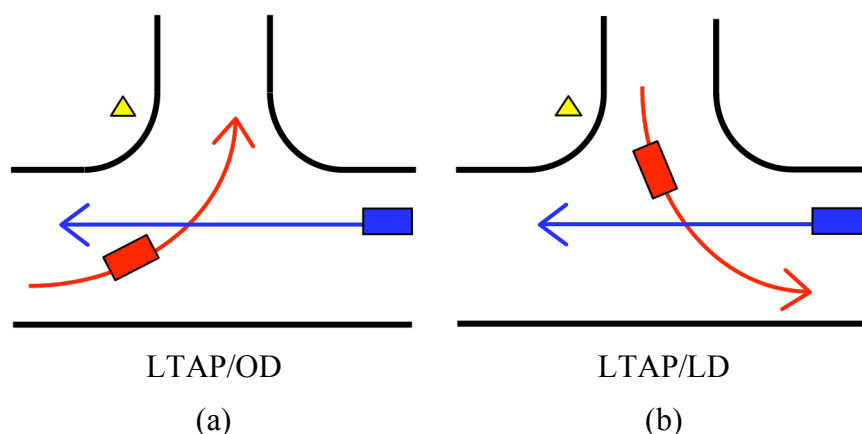


Figure 11.2. Schematic diagram of the two left-turn across path traffic scenarios: (a) from the opposite direction, and (b) from the lateral direction. The car that enters the intersection from the right on the major road (east at Sävenäs) has the right of way.

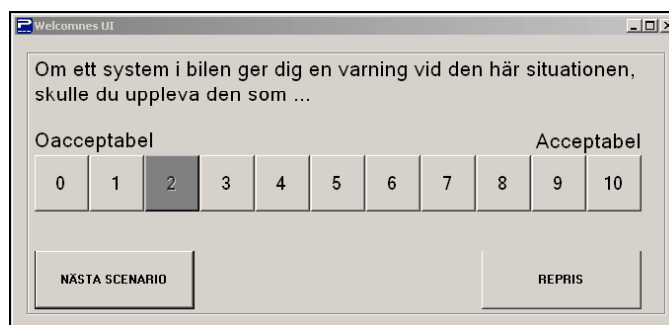


Figure 11.3 The tool used to provide ratings and (re)start a scenario. The prompt asks “If a system in the car gave you a warning about this situation, you would find it ...”

## Chapter 11 - Driver ratings of simulated encroachment incidents

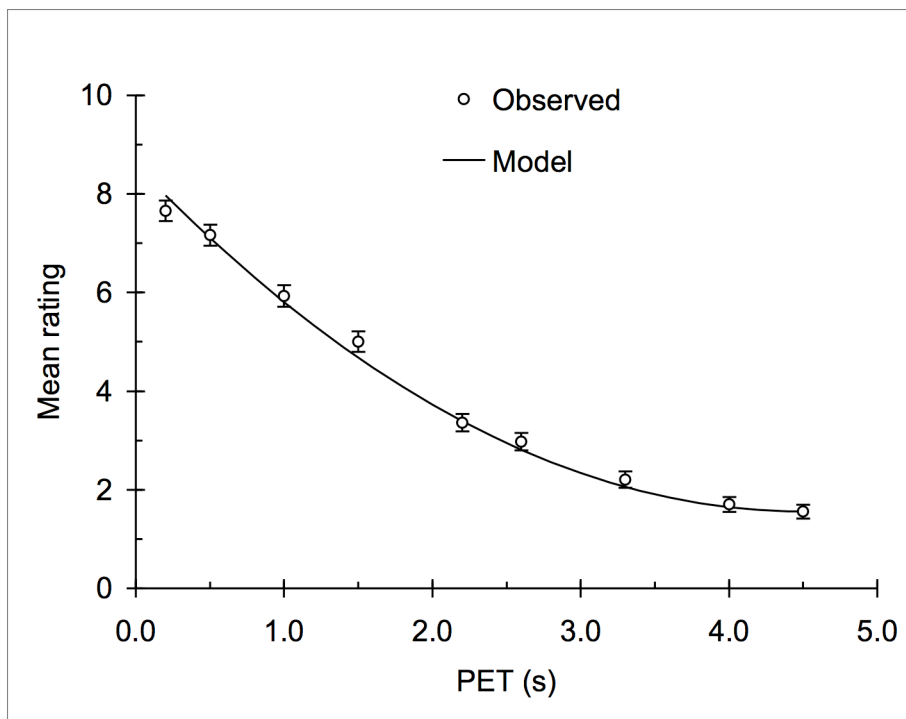


Figure 11.4 Welcomeness ratings averaged across all conditions as a function of Post encroachment time (PET).

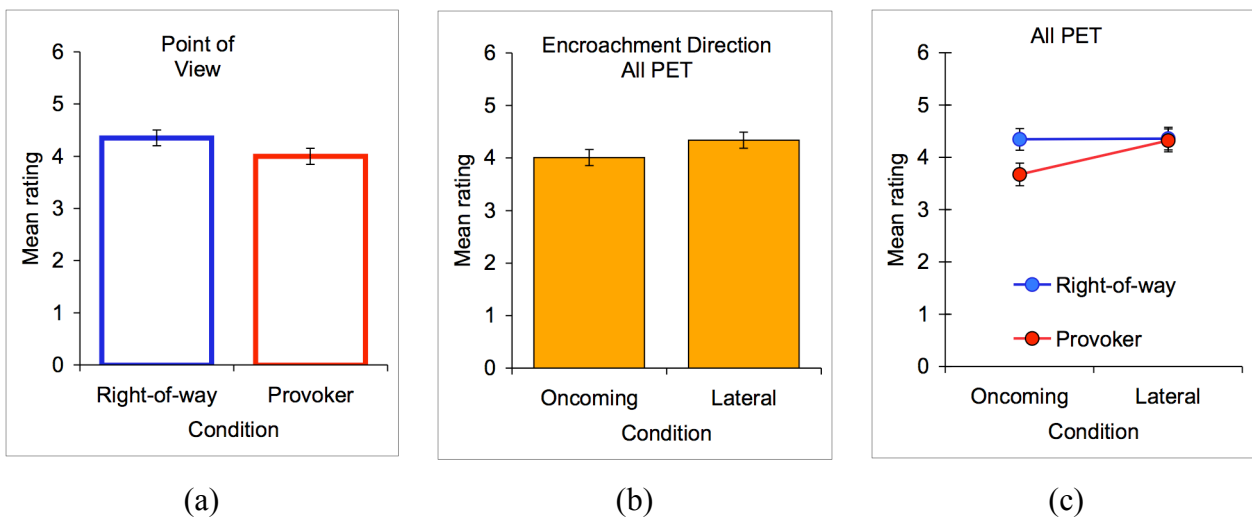


Figure 11.5 Graphs showing the average and standard errors of ratings aggregated across all 9 intervals of PET and for (a) point-of-view, (b) encroachment direction, and (c) their interaction.

## Chapter 11 - Driver ratings of simulated encroachment incidents

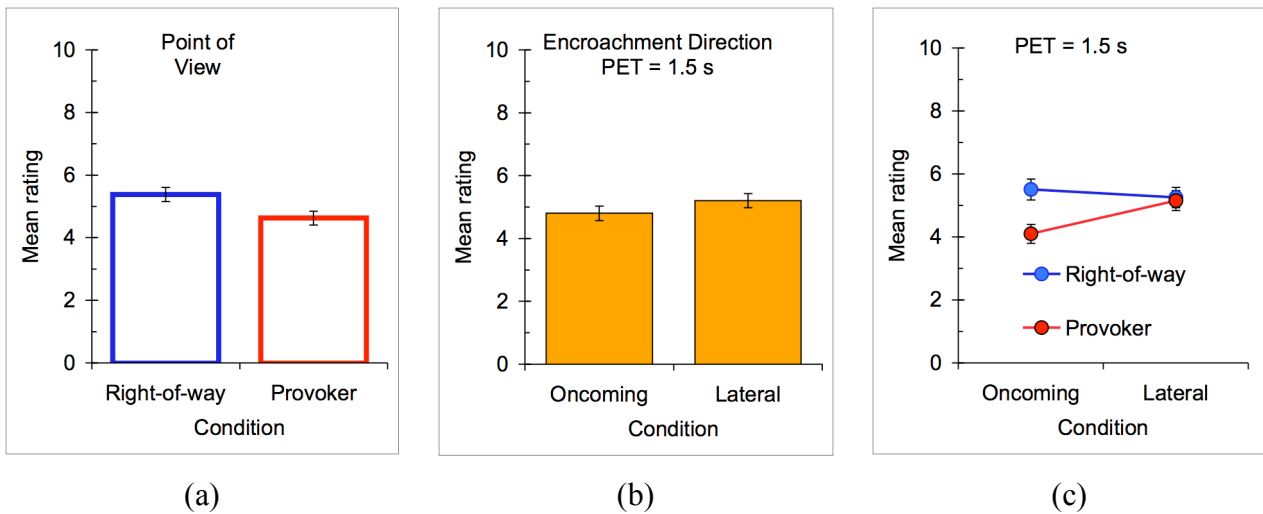


Figure 11.6 Graphs showing the average ratings and standard errors of ratings at PET = 1.5 s for (a) point-of-view, (b) encroachment direction, and (c) their interaction.

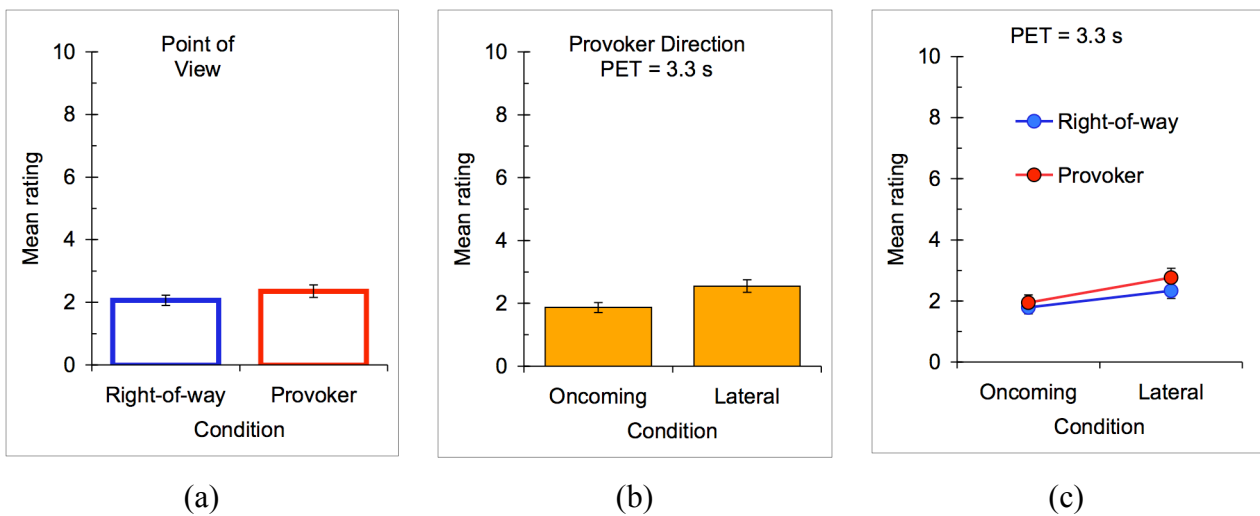


Figure 11.7 Graphs showing the average ratings and standard errors of ratings at PET = 3.3 s for (a) point-of-view, (b) encroachment direction, and (c) their interaction.

## Chapter 11 - Driver ratings of simulated encroachment incidents

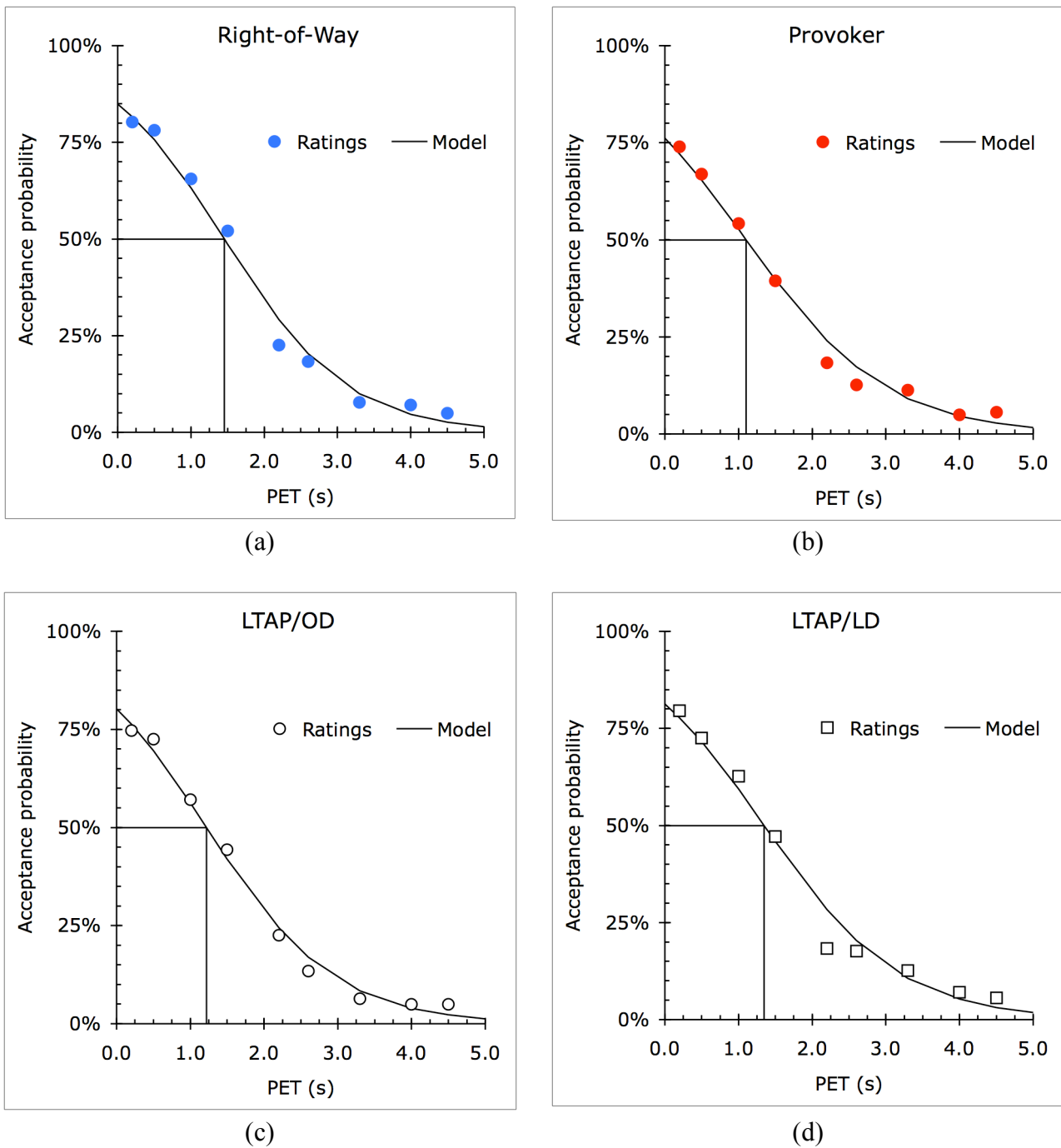


Figure 11.8 Graphs showing the percentage of participants who would accept an alert across experimental conditions: (a) drivers with the right-of-way, (b) provokers, (c) encroachment from the opposite direction, LTAP/OD, (d) encroachment from the side, LTAP/LD.

## Chapter 11 - Driver ratings of simulated encroachment incidents

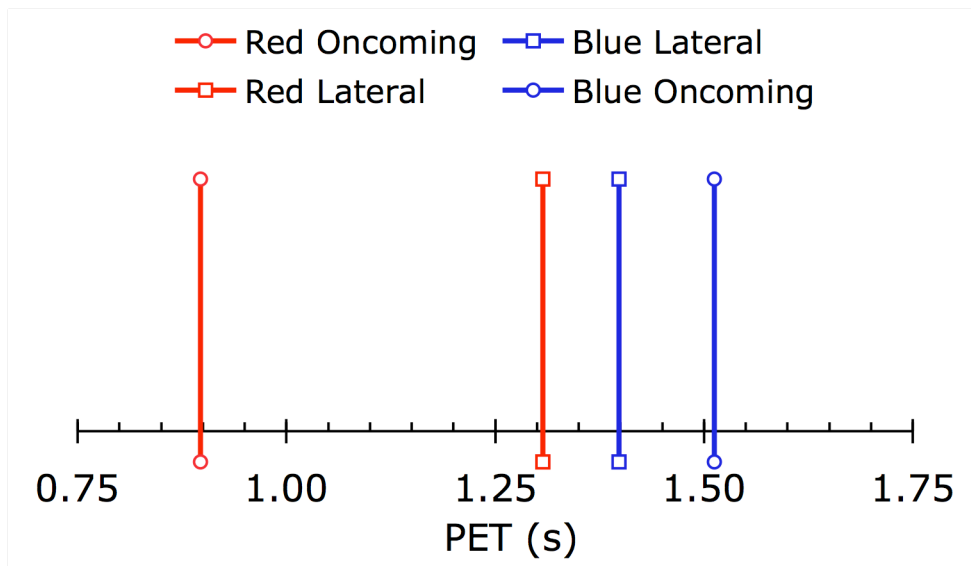


Figure 11.9 Graph illustrating the contextual sensitivity of the PET values at which 50% of participants indicated they would accept an alert.

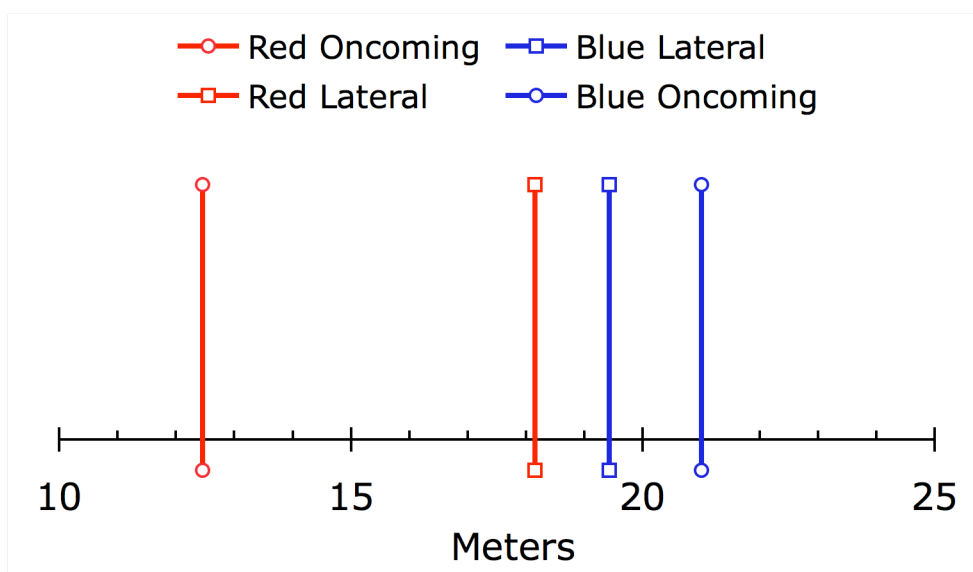


Figure 11.10 Inferred ranges (m) at which 50% of drivers would accept an alert.

## Chapter 11 - Driver ratings of simulated encroachment incidents

### Tables

Table 11.1 Self-reported driving experience.

Km/Year		Days/Week	
Range	N	Range	N
0 - 5,000	4	< 1	1
5,001 - 10,000	14	1 - 3	11
10,001 - 15,000	18	4 - 6	22
> 15,001	36	7	37

Table 11.2 The dimensions of driving style and behavior tapped by the questionnaires. DSQ = Drive Style Questionnaire. DBQ = Driver Behavior Questionnaire.

Source	Dimension	Sample question
DSQ		How frequently ...
	Speed	Do you exceed the 70 mph limit during a motorway journey?
	Calmness	Do you become flustered when faced with sudden dangers while driving?
	Social resistance	Is your driving affected by pressure from other motorists?
	Focus	Do you find it easy to ignore distractions while driving?
	Planning	Do you plan long journeys in advance, including places to stop and rest?
	Deviance	Do you ever drive through a traffic light after it has turned to red?
DBQ		How frequently ...
	Lapse	Do you forget where you left your car in a parking lot?
	Error	Do you misread the signs and turn the wrong direction on a one-way street?
	Violation	Do you disregard the speed limit?
	Aggression	Do you show hostility to other drivers?

## Chapter 11 - Driver ratings of simulated encroachment incidents

Table 11.3 Partial correlation coefficient (r), the value of the significance test (t, df = 69), and the two-sided probability of that test for the 10 dimensions of driving style and behavior.

Dimension	r	t	p
Speed	.00	0.04	.97
Calmness	-.04	0.35	.73
Social resistance	.10	0.82	.41
Focus	-.19	1.61	.11
Planning	.01	0.08	.93
Deviance	-.21	1.78	.08
Lapse	-.12	1.00	.32
Error	.09	0.79	.43
Violation	.06	0.46	.64
Aggression	-.01	0.07	.94

Table 11.4 Summary of the 2x2 ANOVA showing the changing influence of the main effects and their interaction across intervals of PET.

PET (s)	Average Rating	Point of View E(1, 70)	Provoker Direction E(1, 70)	Interaction E(1, 70)
0.2	7.65	19.07***	0.63	7.44**
0.5	7.15	41.59***	1.10	8.75**
1.0	5.91	6.62*	4.73*	9.14**
1.5	5.00	13.97***	4.26*	17.50***
2.2	3.32	3.61	0.27	1.17
2.6	2.72	0.09	29.29***	0.09
3.3	2.21	2.97	19.63***	0.84
4.0	1.69	0.02	6.67*	0.07
4.5	1.56	2.15	1.32	0.23
All	4.71	12.01***	11.62**	20.69***

\*p < .05. \*\* p < .01. \*\*\*p < .001.

Table 11.5 Critical values of PET in seconds at which 50% of participants indicated they would accept an alert to an encroachment.

		50 / 50 point
	All data	1.29
Point-of-view	Blue	1.45
	Red	1.10
Encroachment direction	Oncoming	1.22
	Lateral	1.35



## **Chapter 12 - Cultural determinants of individual differences in driving style**

The Driving Simulation Laboratory at IDA conducted four experiments that asked participants to drive repeatedly through simulations of the Sävenäs intersection. In addition to driving, participants completed a battery of self-report questionnaires. This chapter discusses correlation analyses of their self-reports for indications of factors that might influence the acceptance of active safety systems.

### **Materials**

Participants answered a trio of questionnaires that focused on personal values and driving.

#### **Schwartz value survey**

The Schwartz Value Survey is a 57 item questionnaire that asks respondents to rate 57 values “As a guiding principle in my life,” using a nine-point scale. The 57 values have been found to define the 10 ‘value types’ listed in Table 12.1 (Schwartz, 1992, 1994). The value types are recognized by people from diverse cultures and walks of life but are consistently rated differently by people from different cultures. We used it here to ascertain whether driving style and behavior is sensitive to differences in life’s guiding principles.

The 57 values are presented in two lists: the first contains nouns (e.g., equality, freedom, excitement in life); the second contains adjectives (e.g., humble, helpful, curious). This splits the survey into two manageable parts. Prior to rating the values on each list, respondents are instructed to read the whole list, and to chose and rate the value most important to them, and then to chose and rate the value they most oppose. This procedure serves to anchor the 9-point scale and to encourage introspection when rating the values.

#### **Driver style questionnaire**

The Driving Style Questionnaire (DSQ, French, West, Elander, & Wilding, 1993) is a self-report instrument using a six point Likert scale. The 15 items probe the extent to which drivers exhibit behaviors consistent with six dimensions of driving style: (1) speed, (2) calmness, (3) social resistance, (4) focus, (5) planning, and (5) deviance (West, Elander, & French, 1992). The version of the DSQ we used was taken from LeBlanc, et al. (2006).

#### **Driver behavior questionnaire**

The Manchester Driving Behavior Questionnaire (DBQ, Lajunen & Summala, 2003; Lajunen, Parker, & Summala, 2004; Reason, Manstead, Stradling, Baxter, & Campbell, 1990) is a 24 item self-report instrument using a six point Likert scale. Based on Reason’s (1990) model of human error, it probes the extent to which drivers exhibit behaviors consistent with four dimensions of driving behavior: (1) lapses, (2) errors, (3) violations, and (4) aggression. The version of the DBQ we used was taken from LeBlanc, et al. (2006).

### **Correlation Analysis**

The primary tool for data analysis is the partial correlation between responses to the Schwartz Value Survey (1992, 1994) and to the other questionnaires. All correlations and their significance levels are listed in the Table 12.2. The partial correlation procedure minimizes the impact of individual differences by taking into account each individual’s mean scale use.

## Chapter 12 - Cultural determinants of individual differences in driving style

The resulting pattern of partial correlations more accurately reflects relationships between variables.

The graph used to display the pattern of correlations between one variable and several others is the correlogram. The correlograms of Figure 12.1 show the patterns of correlations between four of the six dimensions of the DSQ and the 10 value types. None of the correlations in the other two dimensions, Social Resistance and Planning, reached the .05 level of significance.

Figure 12.1a shows the correlations between the responses made by all participants to the Speed dimension of the DSQ and the 10 value types of the Schwartz Value Survey. The horizontal axis shows the 10 value types; the acronyms are listed in Table 12.1. The vertical axis is the value of the partial correlation between the scores for Speed and the value types. The filled dots reveal the two statistically significant correlations. The correlation between Speed and Stimulation (ST) is positive ( $r = .17$ ,  $p = .042$ ); the correlation between Speed and Universalism (UN) is negative and strong ( $r = -.23$ ,  $p = .006$ ).

These correlations make sense. The positive correlation indicates that participants who admit to driving fast tend to report that excitement and challenge are important in their lives. The negative correlation indicates that those who admit to driving fast tend to find little value in tolerance and the welfare of others. It should come as no surprise that the data reveal that speeders crave excitement and tend to discount pedestrians and cyclists and other road users. The intuitive good sense behind this finding reveals that the self-report instruments and the analyses are likely to be reliable and insightful.

Figure 12.1b shows the pattern of correlations between the Calmness dimension of the DSQ and the 10 value types. The negative correlation between Calmness and Tradition (TR) is significant ( $r = -.20$ ,  $p = .017$ ). The values associated with tradition - 'moderate', 'humble', 'devout', and 'accepting my portion in life' - appear to be antithetical to the ability to remain calm in the face of unexpected and potentially hazardous driving situations (e.g., an encroachment incident). Indeed, the resignation and fatalism associated with 'accepting my portion in life' may work against developing the resolve and steeliness required to maintain poised equanimity in a moment of crisis.

Figure 12.1c is the correlogram for the Focus dimension of the DSQ. The pattern of correlations is a subdued replica of that for Speed. The positive correlation between Focus and Stimulation (ST,  $r = .19$ ,  $p = .023$ ) indicates that participants who claim they are not easily distracted tend to seek excitement and challenge. It may also indicate that drivers who admit to distraction are not open to unnecessary and extraneous stimuli.

The Deviance dimension of the DSQ refers to the propensity or willingness to break the traffic laws with impunity. The pattern of correlations for Deviance, shown in Figure 12.1d, is nearly the inverse of that for Calmness, Figure 12.1b. A willingness to break the law appears to invert the relationships found for Calmness. There are three statistically significant correlations which we address in ascending order of significance. On the right side of Figure 12.1d, the positive correlation between Deviance and Power (PO,  $r = .21$ ,  $p = .011$ ) indicates that drivers who seek to obtain and maintain social esteem are relatively likely to be scofflaws. Perhaps they break the law because they believe they deserve to get away with it. This finding is consistent with the unwillingness of diplomats to pay their parking tickets.

The correlation between Deviance and Benevolence (BE) is negative and strong ( $r = -.24$ ,  $p = .004$ ). Benevolence values the welfare of others. Deviance scorns the concern of others. That they are negatively correlated comes as no a surprise. In contrast, the basis for the

## Chapter 12 - Cultural determinants of individual differences in driving style

strong positive correlation between Deviance and Tradition (TR,  $r = -.27$ ,  $p = .001$ ) is less intuitive. A major element in the value type Tradition is the fatalism associated with resignation to one's lot in life. Perhaps this fatalism provides a rationale for breaking traffic laws. If something goes wrong, it was fated and, hence, the driver may in some sense feel exonerated. People from non-fatalistic cultures may find the flip side of the positive correlation between Deviance and Tradition easier for to understand. Drivers who are not traditional and who are, accordingly, relatively self-directed may tend to heed traffic laws.

Indeed, it is likely that our sample of drivers elicits responses on both sides of this correlation. Our participants can be partitioned into three broad classes based on nationality. Many were students from nations where tradition and fatalism are fundamental parts of the culture (e.g., Pakistan and Iran). Others were from a variety of nations on the European continent. A third group was from Sweden. Tradition and fatalism are known to play a far less central role in Europe (including Sweden) than in Pakistan and Iran (Schwartz, 1992, 1994). A between-group ANOVA on responses to Tradition found a significant difference across the three national groups,  $F(2, 49) = 13.9$ ,  $p < .001$ . Post-hoc comparison indicates the Swedish group was significantly different than the other Europeans and that both groups were significantly different than the Pakistanis and Iranians. The Swedes valued Tradition much less than the other two groups. A second between-group ANOVA on responses to Deviance found the parallel difference,  $F(2, 49) = 6.7$ ,  $p < .005$ . Here, the Swedes admitted to much less law breaking than either of the other two groups. These results suggest that our sample of Swedes was relatively averse to both Tradition and Deviance but that our sample from more fatalistic cultures valued Tradition much more than heeding traffic laws.

The correlograms of Figure 12.2 show the patterns of correlations between all four dimensions of the DBQ and the 10 value types. The patterns are similar for all four dimensions. The similarity across all four dimensions of the DBQ suggests that all four sources of error are supported by the same value structure. Our data do not support Reason's (1990) argument that Lapses, Errors, and Violations are distinguishable.

The pattern of correlations for the dimensions of the DBQ is similar to that for Deviance, Figure 12.1d. There are peaks at Tradition (TR) and Power (PO) and a trough at Universalism (UN) and/or Benevolence (BE). Participants who admitted to making Lapses, Errors, Violations, and to being Aggressive drivers tended to value respect and control and to downplay the value of the welfare of others. This is a value structure that is fundamentally self-serving. The data support the inference that drivers who seek dominance and the respect of others are willing to bend the rules to reach their goals (or destinations).

Once again, it may be easier to appreciate the flip side of this value structure. Participants who claimed to make relatively few errors tended to value the welfare of others more than the goals of status and adherence to custom. This is a value structure that seeks the common good. The data support the inference that drivers who claim to bend the rules only rarely heed the law because they value its role in assuring social harmony.

### Implications for the design of active safety systems

The data in Figures 12.1a and 12.1c are consistent with the interpretation that speeders and drivers who are not easily distracted are open to excitement and challenge. This type of individual may even find it exciting to 'game the system' by pushing an active safety system to the limit where it issues an alert. Alerts may need to be implemented in a manner that precludes their transformation into a behavioral reward for thrill-seekers.

## Chapter 12 - Cultural determinants of individual differences in driving style

The pattern of correlations in Figure 12.1b indicates that people from traditional cultures may be relatively unlikely to be able to remain calm in a moment of crisis. It is possible that a loud or unnerving alarm might only exacerbate their inability to cope. This type of individual would likely be more open to an alert that issues guidance than to an alarm.

The similarity of the four correlograms for the dimensions of the DBQ, Figure 12.2, reveals the action of antithetical value structures. One is fundamentally self-serving; the other seeks the common good. It is unlikely that the same design of an active safety system would satisfy both types of driver. The former might treat such systems with disdain. The latter would surely welcome them.

The radically different responses to the dimensions Tradition and Deviance by participants from Sweden and from traditional, fatalistic nations may portend the need for cultural sensitivity in the design and implementation of active safety systems. Drivers in traditional, fatalistic cultures may find such systems relatively superfluous or frivolous. In contrast, drivers in law-abiding non-traditional cultures (e.g., Sweden) may be relatively welcoming to the introduction of active safety systems. It behooves Swedish designers of automotive systems to take into account their cultural bias and not to assume that drivers from in other cultures will think as they do.

### References

- French D. J., West R. J., Elander J., Wilding, J. M. (1993). Decision-making style, driving style, and self-reported involvement, in road traffic accidents. *Ergonomics* 36, 627-644.
- Lajunen, T., & Summala, H. (2003). Can we trust self-reports of driving? Effects of impression management on driver behaviour questionnaire responses. *Transportation Research F* 6, 97-107.
- Lajunen, T., Parker, D., & Summala, H. (2004). The Manchester Driver Behaviour Questionnaire: a cross-cultural study. *Accident Analysis & Prevention* 36, 231-238.
- LeBlanc, D., Sayer, J., Winkler, C., Ervin, R., Bogard, S., Devonshire, J. Mefford, M., Hagan, M., Bareket, Z., Goodsell, R., and Gordon, T. (2006). Road departure crash warning system field operational test: Methodology and results. *University of Michigan Transportation Research Institute Report 2006-9-2*, Vol. 2, Appendix E.
- Reason J. (1990). *Human error*. New York: Cambridge University Press.
- Reason, J. T., Manstead, A. S. R., Stradling, S. G., Baxter, J. S., & Campbell, K. (1990). Errors and violations on the road: a real distinction? *Ergonomics* 33, 1315-1332.
- Schwartz, S. H. (1992). Universals in the content and structure of values: theoretical advances and empirical tests in 20 countries. *Advances in Experimental Social Psychology* 25, 1-65.
- Schwartz, S. H. (1994). Are there universal aspects in the structure and contents of human values? *Journal of Social Issues* 40, 19-45.
- Smith, K., Lindgren, I., & Granlund, R. (in press). Exploring cultural differences in team collaboration. *Journal of Cross-Cultural Psychology*.

## Chapter 12 - Cultural determinants of individual differences in driving style

### Figures and Tables

Table 12.1 Schwartz's 10 value types.

Value type	Acronym	Description
Self direction	SD	Independent thoughts and actions; autonomy and independence.
Stimulation	ST	The organismic need for variety, excitement, novelty, and challenge.
Hedonism	HE	Pleasure or sensuous gratification for oneself.
Achievement	AC	Demonstrating competence to obtain social approval; the focus is social esteem.
Power	PO	Attainment of social status and prestige, and control or dominance over people and resources; the focus is social esteem.
Security	SE	Safety, harmony, and stability of society, of relationships, and of self.
Conformity	CO	Self-restraint in everyday interaction; restraint of actions, inclinations, and impulses likely to upset or harm others and violate social expectations or norms.
Tradition	TR	Respect, commitment, and acceptance of the customs and ideas that one's culture or religion imposes on the individual.
Benevolence	BE	Concern for the welfare of close others.
Universalism	UN	Understanding, appreciation, tolerance and protection of the welfare of all people and for nature.

Note: Definitions from Schwartz (1994)

## Chapter 12 - Cultural determinants of individual differences in driving style

Table 12.2 Summary of the correlation analyses showing the relationships between the ten Value Types of the Schwartz Value Survey and the six dimensions of driving style from the DSQ and the four dimensions of driving behavior from the DBQ.

Dimension	Value Type									
	CO	TR	BE	UN	SD	ST	HE	AC	PO	SE
Speed	-0.09	-0.15	-0.13	-0.23**	0.00	0.17*	0.04	-0.02	0.10	0.06
Calmness	-0.16	-0.20*	0.16	0.02	0.10	-0.08	0.03	-0.10	-0.09	0.01
Social Resistance	-0.10	-0.02	-0.03	0.12	0.05	0.09	0.03	0.09	-0.03	0.10
Focus	-0.05	-0.02	-0.11	-0.12	0.06	0.19*	-0.01	-0.03	-0.06	0.04
Planning	0.04	-0.07	0.01	0.14	-0.01	-0.08	-0.14	0.10	0.01	0.04
Deviance	0.05	0.27**	-0.24**	-0.02	-0.11	0.00	-0.13	-0.04	0.21*	0.03
Lapses	0.03	0.17*	-0.04	-0.12	0.01	0.05	-0.10	-0.03	0.11	-0.11
Errors	0.14	0.19*	-0.21*	-0.11	0.02	0.04	-0.08	-0.11	0.20*	-0.01
Violations	0.01	0.10	-0.14	-0.15	-0.14	0.08	0.07	-0.02	0.17*	0.17*
Aggression	0.12	0.19*	-0.10	-0.09	-0.06	0.06	-0.02	-0.13	0.13	0.13

\* $p < .05$ . \*\* $p < .01$ .

## Chapter 12 - Cultural determinants of individual differences in driving style

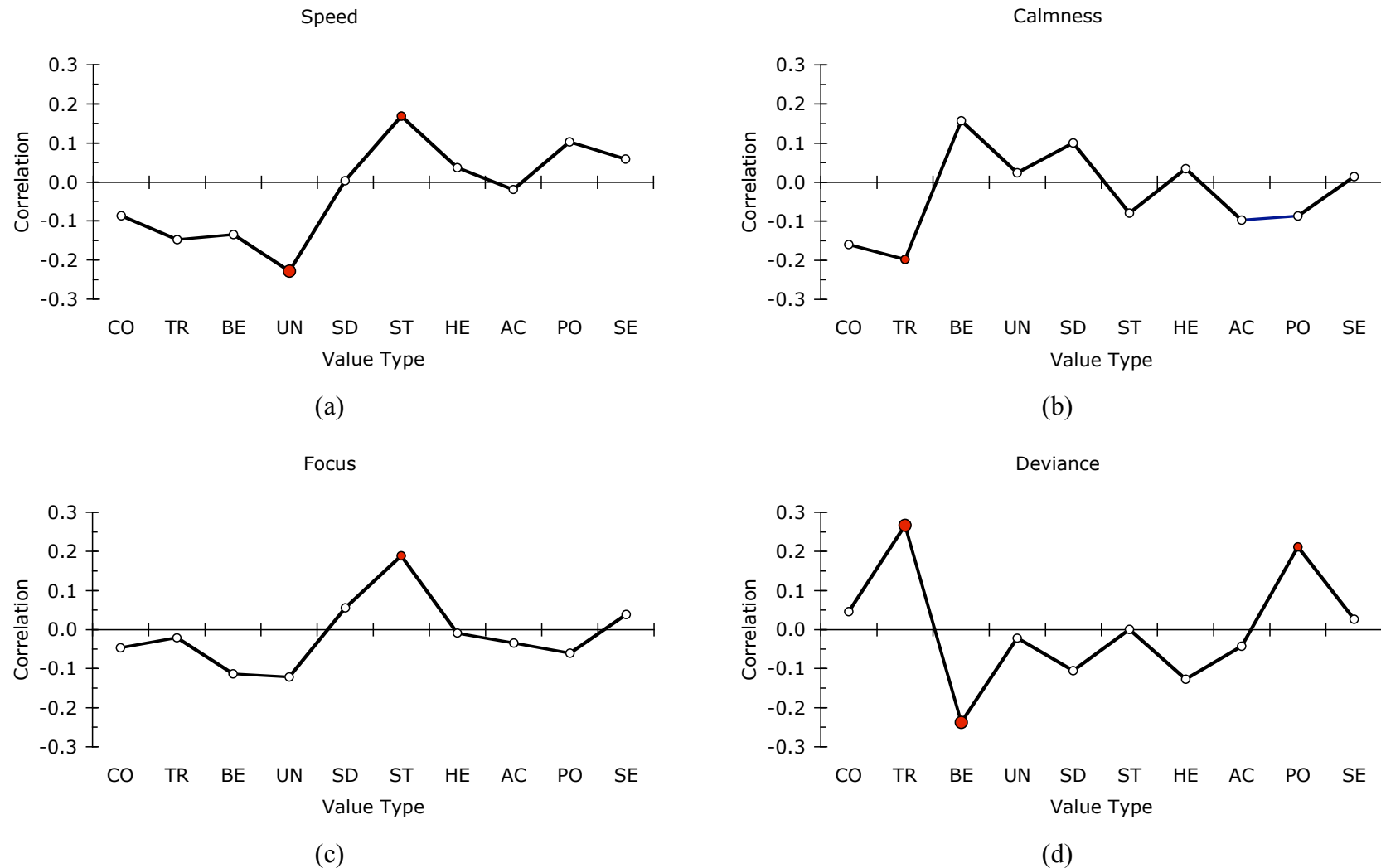


Figure 12.1 Correlagrams showing the relationships between the 10 Value Types and the 4 (out of 6) dimensions of Driving Style from the DSQ with statistically significant correlations. The color and size of dots signify levels of statistical significance: large filled dots  $p < .01$ , small filled dots  $p < .05$ , open dots  $p > .05$ .

## Chapter 12 - Cultural determinants of individual differences in driving style

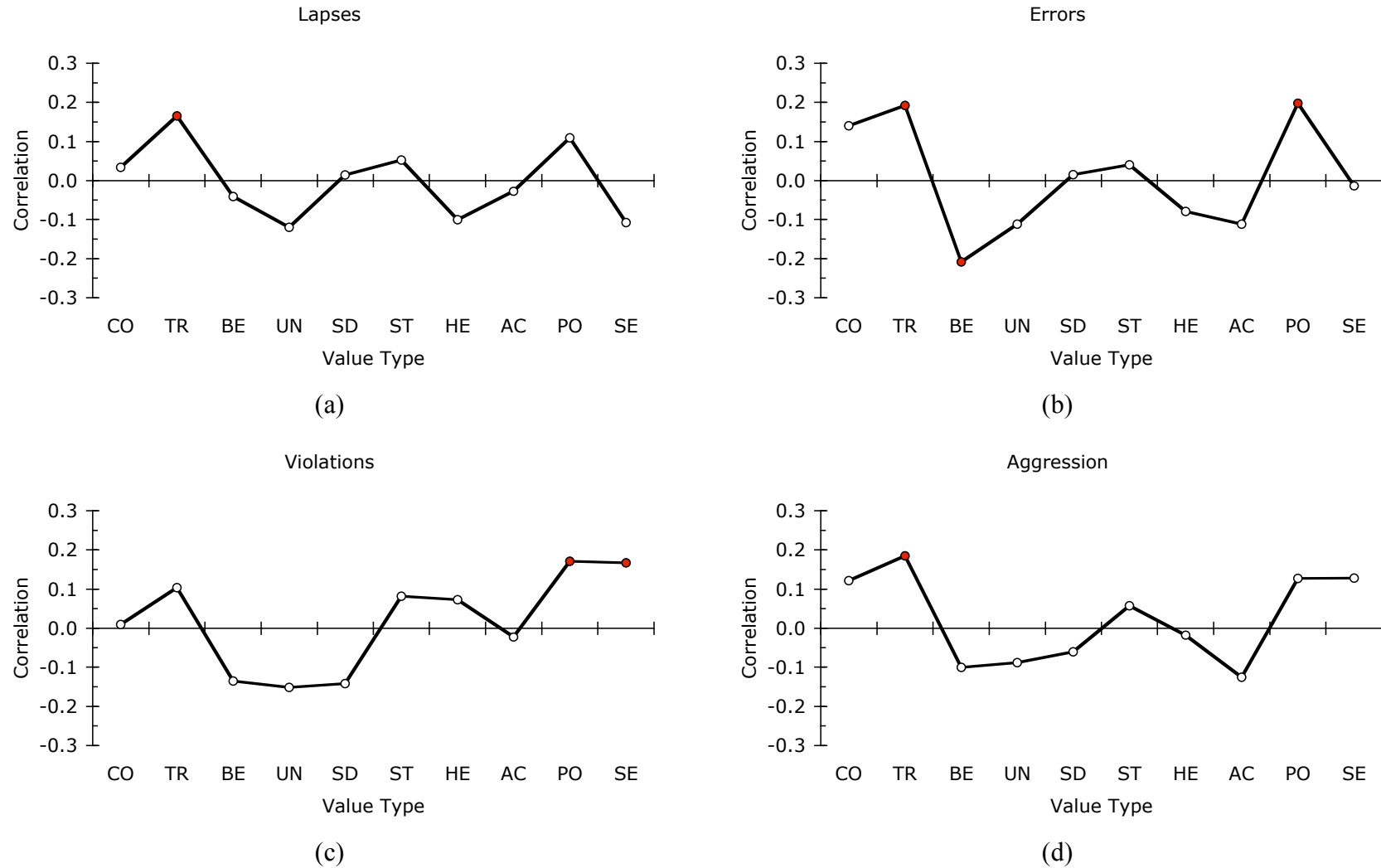


Figure 12.2 Correlograms showing the relationships between the 10 Value Types and the 4 dimensions of Driving Behavior from the DBQ. All 4 dimensions achieved statistical significance. The color and size of dots signify levels of statistical significance. Large filled dots  $p < .01$ . Small filled dots  $p < .05$ . Open dots  $p > .05$ .



## Chapter 13 - Traffic experienced by the test vehicle

The third leg of the IVSS Intersection project consists of the data collected by equipment in Autoliv's instrumented test vehicle. This chapter reviews the case study and the representativeness of the passes made by the test vehicle through the Sävenäs intersection and describes the one encroachment it encountered. The analysis of Chapter 15 develops a five-zone model of the characteristic patterns of actions taken by the driver during repeated crossings of the Sävenäs intersection.

### The case study

The data from the test vehicle came from repeated drives made over several days by one driver, a 33 year-old female. This case study was not intended to be representative of the population of drivers. It was, however, intended to be representative of the traffic and the distribution of traffic cases observed at the Sävenäs intersection. This chapter documents the degree to which we achieved that representativeness.

The driver followed a predetermined circuit that took her through the intersection on all six possible paths, Figure 5.1a. She drove the circuit a total of 37 times for a total of 222 passes through the intersection. It was expected that every trajectory would be observed by the camera and extracted by the image processing system.

### On the extraction of observations by the image processing system

The analysis used the classification system developed by Chalmers that extracts the traffic context from the driver's point of view. The counts of the scenarios captured by the system are shown in the cells of the matrix of Table 13.1. The entries below the matrix of scenarios present the sums and relative frequencies for each column. Table 13.2 summarizes the totals and relative frequencies by row for the 6 solo cases and the 144 cases with traffic. It also summarizes the data shown in Table 6.1 to illustrate the representativeness of the traffic experienced by the driver of the test vehicle.

A total of 193 scenarios were extracted by the image processing system and classified by the Chalmers software. This is 87% of the expected total of 222. The loss of observations indicates that the image processing / trajectory extraction system, for one reason or another (e.g., the presence of a truck), did not categorize a scenario 13% of the time. This figure is our best estimate of the percentage of traffic cases discarded by the automated system.

The expected total number of scenarios for each trajectory is 37. A comparison of the distributions of the expected and the extracted counts reveals that they are not significantly different,  $\chi^2(5) = 8.78$ ,  $p > .10$ . Nevertheless, of the 37 passes made by the test vehicle along trajectory 4, the left turn from the secondary road to the main road (north to east), only 21 (57%) were classified as such by the automated software. Similarly, the system accounted for only 30 of the 37 (81%) passes on trajectory 2, the left turn from the north to the west. These findings suggest that traffic from the north posed the greatest challenge to the image processing system. We can expect these percentages to obtain for all traffic through the intersection. Accordingly, the counts presented in Chapter 6 are likely to underestimate the actual flow of traffic by approximately 19% on trajectory 2 and 43% on trajectory 4.

It is not possible to infer from these data those factors that contributed to the loss of data about traffic arriving at the Sävenäs intersection from the north. A likely factor is the need for traffic on the secondary road to stop while yielding the right-of-way. The image processing system is known to have had trouble with motionless vehicles. A trajectory may terminate when a vehicle stops and a second one may appear when the vehicle starts to move.

## Chapter 13 - Traffic experienced by the test vehicle

Linking these two segments may be a weak link in the automated system. If that were the case, it may explain the high percentage of ‘lost passes’ by the test vehicle when it entered the intersection from the north.

### Representativeness of the passes

Of the 193 observations shown in Table 13.1, 34% were solo drives and 66% involved other cars. These percentages do not differ significantly from the 40 / 60% split observed in the complete Sävenäs data set (Chapter 6),  $\chi^2(1) = 2.36$ ,  $p > .10$ . The driver of the test vehicle encountered other road users with the expected frequency.

The same conclusion cannot be drawn about all six trajectories. Table 13.2 shows the frequencies for the test vehicle and the complete data set. Using the complete data set as the standard for comparison, the trajectories taken by the test vehicle differ significantly from those taken by the population of drivers at Sävenäs,  $\chi^2(5) = 22.9$ ,  $p < .001$ . The circuit taken by the driver of the test vehicle produced more observations than expected on trajectories 1, 5, and 6 and fewer than expected on trajectories 2 and 3. Trajectories 2 and 3 combine for more than 50% of the complete data and only 35% of the data involving the test vehicle.

The over-representation of trajectories 5 and 6 at the expense of trajectories 2 and 3 reflects our focus on the actions of drivers (of blue cars) who are encroached upon in encroachment incidents and other near-crash situations. Vehicles on trajectories 5 and 6 have the right-of-way and are, accordingly, those who would be encroached upon in an encroachment incident. This overrepresentation at the expense of mirroring the flow of traffic at Sävenäs is a worthy trade-off that reflects the purpose of the IVSS project. By emphasizing driving with the right-of-way, we held true to our focus on informing the development of active safety systems that alert drivers to impending encroachment incidents.

### Velocity of the test vehicle

Figure 13.1 shows the average velocity of the test vehicle as it crossed the intersection on all six trajectories. Data were captured at 10 meter intervals starting 30 meters before the center of the intersection and ending 20 meters beyond it. The red lines represent right turns, green lines left turns, and black lines passes straight through the intersection. Odd-numbered trajectories are marked by squares and even-numbered trajectories by circles. Trajectories 1 and 3, marked by squares, are turns from the primary road to the secondary road. Trajectories 2 and 4, marked by circles, are turns from the secondary road to the primary road. The baseline data of velocities by all cars captured by the image processing system is shown in Figure 7.1.

The data shown in Figure 13.2 supplement the average velocity data shown in Figure 13.1. Each of the 36 small graphs contains two ‘box plots’. A box plot is a graphic representation of three key descriptive statistics. The red horizontal line is the average. The box shows the range of the upper and lower quartiles. 50% of observations plot within the box. The wings above and below mark the extreme observations. The box plot on the right side of each graph presents the data for the driver of the test vehicle. The plot on the left side presents data extracted by the video processing software from all solo trajectories at Sävenäs. The horizontal axis of the grid of graphs is distance from the center of the Sävenäs intersection. The vertical axis is the scenario type.

Comparison of the box plots reveals that the test vehicle was slower than traffic in 28 of the 34 scenarios for which there are data. It appears that the driver of the test vehicle was more

## Chapter 13 - Traffic experienced by the test vehicle

cautious than the average driver. A Kolmogorov-Smirnov test was run for each scenario to compare the distributions of velocities by the test vehicle and by the baseline for traffic. Of the 34 tests, only one was significantly different (Scenario 6, at -10 m, bottom row, column 3).

Thus, while our driver was more cautious than most, her driving was fully representative of traffic. These findings lend credence to the model that was developed on the basis of these drives, Chapter 15

### The encroachment incident

The driver of the test vehicle experienced one and only one salient encroachment incident with a short PET value. This incident is the focus of the demonstration video that highlights all three programs in the project. In her words:

“I came from the direction of Stockholm and headed to Göteborg and was just about to pass the intersection in Sävenås from east to west when a little truck unexpectedly drove out in front of me.

“I was on the primary road and intended to continue straight ahead and checked the surrounding traffic as I normally do. As I approached the intersection I passed a car going the opposite direction and saw two other cars close to the intersection. One was the little truck. It came from the west on the primary road and was slowing down, almost to a stand still. I thought it would wait for me to get through the intersection and then turn left onto the secondary road. The second car came from the secondary road and slowed down to turn right. I saw nothing strange and continued on my path as planned. My speed was approximately 40 km/h.

“Suddenly, the little truck that had been slowing down turned left onto the secondary road just in front of me. I did not see that coming since, according to my judgment, he should have let me pass before he turned left. I had to brake, hard.

“I guess that we judged the gap between us differently. There was no real danger so in that way the other driver made a correct judgment. However, from my point of view, it was an incorrect judgment since I it made me very uncomfortable. I also felt annoyed since he did not behave as I expected him to and forced me to make this unplanned breaking.”

The incident was a case of LTAP/OD (6xam) with other vehicles present, Figure 13.). The PET value was 1.05 seconds. Figure 13.4 shows the view captured by the cameras on the test vehicle at the time of minimum separation, after the driver had applied the brakes. This incident stands as an exemplar of an encroachment where most drivers would likely welcome an alert by an in-vehicle active safety system.

## Chapter 13 - Traffic experienced by the test vehicle

### Figures

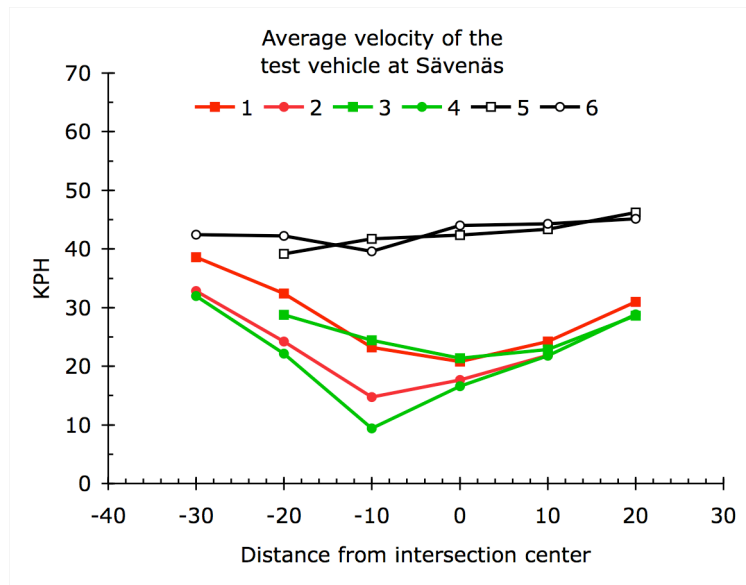


Figure 13.1 Average velocity of the test vehicle at Sävenäs.

### Chapter 13 - Traffic experienced by the test vehicle

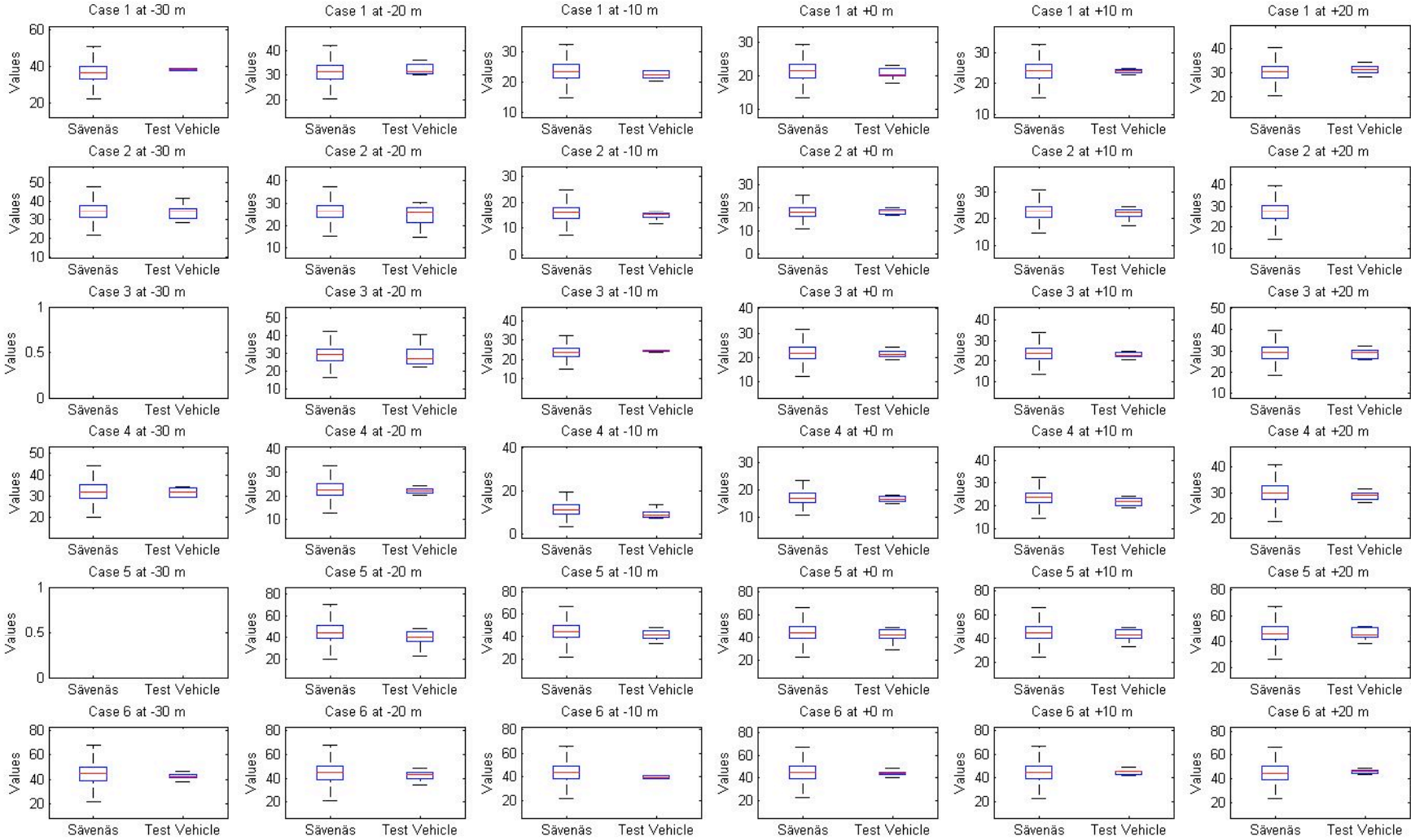


Figure 13.2 Grid of 36 graphs, each containing two ‘box plots’ of velocities. The box plots plot the mean, standard deviations, and extreme values of velocity extracted by the video processing software at Sävenäs (left) and driven by the test vehicle (right). The horizontal axis of the grid is distance from the center of the Sävenäs intersection. The vertical axis is the scenario type.

## Chapter 13 - Traffic experienced by the test vehicle

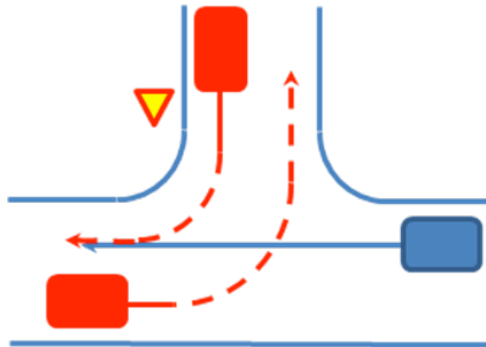


Figure 13.3 The 6xam scenario (LTAP/OD with other traffic) that describes the one encroachment experienced by the driver of the test vehicle.



Figure 13.4 The view from the test vehicle of the “little truck” that encroached by turning left from the opposite direction.

## Chapter 13 - Traffic experienced by the test vehicle

### Tables

Table 13.1 The distribution traffic scenarios encountered by the driver of the test vehicle. Entries are counts of cases.

Counts		Red						Waiting						Multiples						Waiting Multiples						
Blue	Solo	1	2	3	4	5	6	1w	2w	3w	4w	5w	6w	1m	2m	3m	4m	5m	6m	1wm	2wm	3wm	4wm	5wm	6wm	
1	11		8	4		3				1	1				1	4	1	1					2			E to N
2	9	2	2	2	3	1	2					1		3	1	1		1	2						N to W	
3	10		3	8			4									7		1	3				1		W to N	
4	5	1	1	1			3				1					4		2	3						N to E	
5	13	1	4	1		3	2								2	5	1	1							W to E	
6	18		1	6		1	2		2	2	1					1							1		E to W	
	66	4	19	22	3	8	13	0	2	3	3	1	0	3	4	22	2	6	8	0	0	3	1	0	0	
	34%	2%	10%	11%	2%	4%	7%	0%	1%	2%	2%	1%	0%	2%	2%	11%	1%	3%	4%	0%	0%	2%	1%	0%	0%	
							69						9						45						4	
							36%						5%						23%						2%	

Table 13.2 Summary of the distributions of traffic scenarios encountered by the driver of the test vehicle and of all traffic at Sävenäs.

Blue	Test Vehicle at Sävenäs						All Sävenäs	
	Counts			Percentages			Percentages	
	Solo	With Traffic	Total	Solo	By Case		Solo	By Case
1	11	26	37	30	19	E to N	42	13
2	9	21	30	30	16	N to W	40	25
3	10	27	37	27	19	W to N	36	26
4	5	16	21	24	11	N to E	35	9
5	13	20	33	39	17	W to E	41	14
6	18	17	35	51	18	E to W	45	13
Total	66	127	193	34	100		40	100

## Chapter 14 - A multi-zone model of expected driver actions in intersections

This chapter is an excerpt from an article to be submitted for publication as part of the requirements for a Licentiate degree at Chalmers (Bjelkemyr, 2009). The student received support from the IVSS Intersections project.

The chapter develops a model of driver behavior while driving through an intersection. The model is a template of how we can expect the driver-vehicle system to act in intersections and identifies characteristic sequences of actions that define spatial zones. The basis for the model is a semi-naturalistic study of one driver who drove the Autoliv test vehicle through the Sävenäs intersection 181 times. She entered the intersection from each direction and made all possible maneuvers: driving straight, turning left, and turning right. The test vehicle recorded the vehicle dynamics and position using GPS coordinates, the driver's eye and head movements, and continuous video of the outside scene.

The model suggests that there are more similarities across traffic scenarios with the same sequence of road types (e.g., primary to secondary road or secondary to primary road) than across scenarios with the same driver intent (e.g., turning right).

### Introduction

Conducting research on 'normal' driver behavior in intersections can play an important role in the work of preventing intersection accidents and in finding new solutions to support drivers in their driving task. A fuller understanding of normal driving behavior is a prerequisite for understanding irregular driver behavior. Without a deeper understanding of driver behavior and the contextual cues that influence that behavior, any remedial action, e.g. changing traffic rules, reconstructing the infrastructure, and developing active safety systems designed to support drivers through tricky situations, can be nothing more than guesswork.

The approach taken in this study was to define the range of driver behavior that defines a 'normal' pass through an intersection for the six paths at Sävenäs. This approach builds upon the recommendation by Ranney (1994) in his review article on theories and models of driver behavior. Ranney argued that research should focus on the interaction between the driver and the driving situation rather than on the driver in isolation.

A common approach for many studies of driver behavior is the correlation between eye and head movements, vehicle trajectory, and steering actions (Chattington, Wilson, Ashford, & Marple-Horvat, 2007; Land & Lee, 1994; Robertshaw & Wilkie, 2008) and their contextual dependence (Janssen, van der Horst, Bakker, & ten Broeke, 1988). A non-exclusive alternative is to study acceleration patterns (Fugger, Wobrock, Randles, Stein, & Whiting, 2001). Previous studies have found that the onset of the deceleration is dependent on the traffic situation (Sato & Akamatsu, 2008) and rules of yielding (Helmert & Åberg, 1978). This study follows both traditions to develop a model of the relationship between eye and head movements, vehicle heading, and acceleration while approaching and passing through an intersection.

The model is developed using data from one driver participant in a semi-naturalistic scenario study at a T-intersection in the Sävenäs industrial area near Göteborg, Sweden. The analyzed data are a subset of a larger data set. The analyses were restricted to traffic scenarios in which there were no other road users (e.g., 'solo' drives). This approach was taken to minimize sources of variability due to traffic. It is anticipated that the validity of the model developed here will be tested in a second paper that will analyze data that includes traffic and/or vulnerable road users.



## Chapter 14 - A multi-zone model of expected driver actions in intersections

The model is informed by an analysis of the basic physics of a vehicle making a turn at an intersection. A top-view of a 90° right turn in a T-intersection and graphs of the corresponding ideal vehicle heading and its derivative as a function of distance are shown in Figure 14.1. Changes in the derivative define five zones. The first zone is characterized by straight ahead driving, that is, a constant vehicle heading. In the second zone, the absolute value of the derivative of heading increases. This is followed by the third zone where the derivative of heading is constant but different than zero. In the fourth zone, the absolute value of the derivative of heading decreases. In the final zone, the pass through the intersection ends with a constant vehicle heading in a new direction.

Following Land (2006), the model postulates that there are characteristic correlations between the driver's gaze and head movements and the vehicle heading. Land described the correlation during a near-side turn (left turn in the UK). When entering the turn, the driver's head starts to rotate to the side before the vehicle begins to change heading. During the turn, the head starts to counter-rotate until the head and the heading are aligned straight ahead. During the counter-rotation, the head rotates with approximately the same velocity as the vehicle but in the opposite direction. Land suggested that these coordination actions keep the fixation point in a relatively constant location at the exit of the turn.

We borrow from Land the principle that the head anticipates the vehicle when entering an intersection. We extend it to the entire crossing of the intersection and to the five zones. We hypothesize here that each of the five zones can be defined by a characteristic movement of the gaze and/or the head followed by a characteristic range of vehicle headings. The idea is thus that vehicle heading, its derivative, and driver gaze and head angles are sufficient to characterize the actions of the driver-vehicle system in the intersection. In general terms, the gaze and/or head initiates its activity before the vehicle begins its corresponding activity throughout all five zones of the turn.

When the vehicle passes straight through the intersection, the variation in vehicle heading is typically limited. Accordingly, the model for straight ahead scenarios model is defined purely by characteristic gaze and/or head movements.

### Method

#### Participant

A 33 year old female was the driver in the scenario study. She was an experienced driver (>15,000 kilometers/year), did not wear glasses, and was familiar with the Sävenäs industrial area and the intersection.

#### Vehicle

As discussed in Chapter 2, the vehicle used in the scenario study was equipped with several data capture systems. Vehicle velocity and acceleration were available from the internal CAN-bus system already in the vehicle. A GPS transmitter and three front-view cameras covering approximately 200° of view were mounted on the roof. A non-intrusive 4 camera eye tracker device (SmartEye Pro 3.5) was mounted in the vehicle cockpit. The backseat contained a screen for managing the data logging by computers secured in the luggage boot.

## Chapter 14 - A multi-zone model of expected driver actions in intersections

### Route

The choice of the Sävenäs intersection was based on the demands of having high traffic intensity, accessibility, and a velocity limitation of 50 km/h. The two lane primary road runs east west. A two lane secondary road with a yield sign connects to the primary road from the north. A dead end road to the south leads to a small parking area with an entrance gate. As shown in Figure 14.2, there are six possible paths through the intersection: two right turns (traffic scenarios 1 and 2, Chapter 5), two left turns (scenarios 3 and 4), and straight ahead passes (scenarios 5 and 6). Right of way rules for each scenario are listed in Table 14.1.

### Procedure

To calibrate the eye-tracker system, a profile was created by having the driver look from side to side at targets with known locations.

The study was carried out during two sunny summertime weekdays between 11:00 and 14:00. The driver collected the vehicle in Vårgårda and drove to Göteborg, a distance of 70 kilometers. When she arrived at the intersection, she booted up the vehicle's data logging system. The driver was alone in the vehicle and followed a predetermined driving circuit. Each circuit included all six possible passes through the intersection starting with scenario 1 followed by scenarios 2, 3, 4, 6 and 5. Data were collected continuously throughout the driving circuit.

The driver made 15 circuits each day. The task took approximately three hours including a break after half of the circuits had been completed. After completing the final circuit, the driver shut down the data logging system and returned to Vårgårda. The planned number of drives through the intersection was 180 (2 days \* 15 circuits \* 6 passes).

### Dependent variables

Velocity and acceleration were measured by the vehicle's CAN-bus system at 50 Hz. A GPS provided an independent estimate of velocity as well as the absolute position and heading of the vehicle relative to the Swedish RT90 coordinate system at 10 Hz. The front-view camera system had a frame rate of 25 Hz. The Smart-Eye eye tracker system determined the gaze and head direction relative to the axis of the vehicle at 60 Hz.

The test vehicle collected time-stamped data continuously for three hours. Only data in the close vicinity of the intersection were needed for analysis. The data set was filtered and only segments within a radius of 70 m from the center of the intersection were retained.

Accordingly, data are presented as a function of distance to the center of the intersection. Zero distance axis is defined as the point on the trajectory that is closest to the center of the intersection. A negative sign corresponds to the approach to the intersection and a positive sign to exiting the intersection.

### Heading

The raw vehicle heading data were measured using to the world coordinate system (with west defined as +83.5°, north as 173.5°, east as 263.5° and south as 353.5°). Straight ahead when entering the intersection was defined as the mean value of observed headings between -70 m and -50 m. To facilitate comparison across scenarios, the heading while entering the intersection is used to define 0° for each of the 6 scenarios. A turn to the right (left) generates positive (negative) heading angles.

## Chapter 14 - A multi-zone model of expected driver actions in intersections

### Gaze and head angles

The eye-tracking system measures gaze and head angles using an in-vehicle coordinate system where an angle equal to  $0^\circ$  corresponds to the vehicle heading (e.g., straight ahead). A turn to the right (left) generates positive (negative) heading angles. To facilitate comparison with the vehicle heading, the gaze and head angles are summed with the heading angle to define their orientation in world coordinates.

### **Analyses**

To identify changes in the driver-vehicle system, a mutually exclusive and exhaustive set of possible actions were assembled for each dependent variable. The actions and rules for classifying them are listed in Table 14.3. The rules define five action categories of vehicle heading, five for gaze and head angles, two for the difference between the gaze and head angles, and three for vehicle acceleration.

### Heading

In Table 14.3, the five categories of vehicle heading are listed in sequence as a function of distance to the intersection. These categories are defined by inspection of ideal curves for vehicle heading and its spatial derivative, Figure 14.1. The first and last are both straight ahead driving where the heading is essentially constant. When making a  $90^\circ$  turn, this occurs twice, at approximately  $0^\circ$  and at approximately  $+90^\circ$  or  $-90^\circ$ . Three categories are defined by the derivative of the vehicle heading: zones with increasing, constant and decreasing derivatives.

The boundaries between the five categories are determined from the derivative of vehicle heading. The limits on straight ahead driving when entering the intersection are set to be  $\pm 1^\circ$  of the average heading between -70 m and -50 m. An analogous definition is used for exiting the intersection: the average vehicle heading between +25 m and +30 m  $\pm 1^\circ$ . The boundaries for the third category where the rate of heading change is essentially constant is defined by the value of the derivative of heading at the apex of the turn (the inflection point)  $\pm 10\%$ . The boundaries automatically generate the limits for the categories where the heading derivative either increases or decreases.

### Gaze and head angles

Straight ahead gaze and head directions are defined to be equal to  $0^\circ \pm 5^\circ$ . The rules define four additional categories with distinct gaze and/or head movements. Two are categories for increasing and decreasing angles. A third category is defined by a 'steady' gaze and/or head direction to the side. The final category is reserved for sequences of two or more glances or head movements from side to side without stopping in the middle.

### Difference between gaze and head angles

The absolute value of the difference between the gaze angle and the head angle at given point is calculated to differentiate alternative methods for visual search. The differences are classified into two categories, greater than or less than  $5.5^\circ$ . Twenty percent of the complete data set have values greater than this threshold.

### Acceleration

Acceleration data are partitioned three categories, acceleration and two types of deceleration. The first deceleration category includes increasing and steady-state deceleration. The second is a decreasing deceleration.

## Chapter 14 - A multi-zone model of expected driver actions in intersections

### Results

The driver crossed the intersection a total number of 181 times, the planned 30 passes on each path plus an additional pass from east to west. Twenty passes were lost during data collection. To eliminate confounds due to other vehicles and vulnerable road users, 109 data segments with traffic or vulnerable road users were set aside for later analysis. The remaining 52 passes are solo drives as defined in Chapter 5. These data segments were automatically assigned to the six solo scenarios using the software developed by Autoliv and Chalmers. Table 14.2 shows the number of the drives available for analysis for each scenario. As discussed in Chapter 13, there was a significant loss of data for scenario 4 (north to east from the secondary to the primary road) which may have been associated with the give-way rule on the secondary road.

### Scenario 1: A right turn from the primary road

#### Data

In scenario 1, the driver's intention is to turn right at the intersection from the road with the right of way to the secondary road. The five curves in Figure 14.3a plot the mean values of the vehicle heading in world coordinates and head and gaze angles in both in-vehicle and world coordinates. The vertical axis is in degrees where zero represents straight-ahead vehicle motion and gaze and head orientation. Positive values indicate a movement to the right and negative values movement to the left. Zero on the horizontal axis is the point where the vehicle's trajectory was closest to the intersection center. Negative values indicate the entrance road and positive values the exit road. The single curve in Figure 14.3b plots the derivative of the mean vehicle heading as a function of distance to the center of the intersection. The vertical axis of Figure 14.3b is positive down so that changes in heading to the right plot in the same direction as the corresponding headings in Figure 14.3a.

Reading the graphs of Figure 14.3 from left to right corresponds to the sequence of actions during the drive - approaching, crossing and exiting the intersection. The rules in Table 14.3 were applied point by point to each curve separately to select the appropriate category of action for that parameter. As the analysis moves to the right, a change in category defines a boundary. A sequence of boundaries are defined for each parameter. Alignments of boundaries across parameters define zones that characterize patterns of actions made by the driver and vehicle as they approach the intersection, turn right, and continue down the road.

#### Heading

The analysis of the data from scenario 1 begins with the vehicle heading and its derivative. The data define five zones. The boundaries between the zones are listed in the first row of Table 14.4. Between 70 and 20 m before the intersection (-70 to and -20 m), the vehicle enters the intersection with a heading near  $0^\circ$  and derivative near  $0^\circ/\text{m}$ . It starts to turn right at -19 m; the derivative increases. Between -6 m and +5 m the derivative is non-zero but essentially constant. The turn continues until +17 m where the derivative returns to near  $0^\circ/\text{m}$ . As the vehicle exits the intersection, the heading is near  $90^\circ$  and the derivative remains near  $0^\circ/\text{m}$ .

#### Gaze and head angles

A similar analysis follows the driver's gaze and head movements to produce the boundaries shown in the second row of Table 14.4. Changes in the gaze angle define five zones as do

## Chapter 14 - A multi-zone model of expected driver actions in intersections

changes in the head angle. The gaze and head start to rotate to the right at -29 m and continue this movement until the gaze and the head reach a constant angle at -13 m and -15 m respectively. At +3 and +4 m respectively, the gaze and the head start to counter-rotate back until they are once again directed straight ahead.

Plotting the orientation of gaze and head in world coordinates, Figure 14.3a, illustrates several key points: the two curves have the same shape as the vehicle heading but are offset in a characteristic and diagnostic manner. The gaze angle anticipates the head angle which, in turn, anticipates the vehicle heading. Setting the threshold for the difference between the gaze and head angles at  $5.5^\circ$  defines three zones. In the first and last zones, the difference is less than  $5.5^\circ$ . Between -14 m and +4 m, the differences is greater than  $5.5^\circ$ .

### Acceleration

The acceleration profiles for all six scenarios are plotted as a function of distance from the center of the intersection in Figure 14.4. Values on the vertical axis below 0 indicate deceleration. The acceleration data for scenario 1 define three zones. On approach, the vehicle decelerates. The deceleration defines two zones. In the first, the rate of deceleration increases. In the second, between -21 m and -3 m, the vehicle continues to slow but less abruptly. The third zone is characterized by acceleration away from the intersection.

### Synthesis, the 5 zone model

The zones defined by vehicle heading, gaze and head angles, the difference between the gaze and head angles, and acceleration are shown in Figure 14.5. The zones are color-coded to reveal commonalities across the sources of data. Red indicates straight ahead, orange represents increasing or decreasing rates of change, and yellow indicates a constant change in heading or a steady gaze or head angle to the side.

The color codes in Figure 14.5 can be clustered to define five zones, each with a characteristic gaze and/or head movements followed by a characteristic vehicle heading and acceleration profile. The boundaries overlap because the gaze and head anticipate the vehicle dynamics. The overlapping zones are numbered sequentially.

The first red zone, Zone 1, is characterized by straight ahead deceleration. The deceleration suggests that in Zone 1 the driver is preparing to negotiate the intersection. The straight ahead gaze and head angles suggest the driver has yet to interact with the intersection. Zone 1 is thus a zone of 'preparing to turn'.

In Zone 2 the vehicle decelerates and the driver inspects the road to the right. At -29 m, the driver's gaze and head transit from a straight ahead direction to the right. Between -29 m and -20 m the gaze and head move together to the side. At -19 m the gaze begins to lead the head. This transition coincides with the change in vehicle heading. In this zone, the gaze and head anticipate the change in the vehicle trajectory by a full 10 m, actions consistent with 'anticipating the turn and initiating the turning maneuver'.

After initiating the turning maneuver, the driver reaches Zone 3, the zone of "making the turn". The head angle, gaze angle and heading are all relatively constant and directed to the right. The difference between the gaze and head angles is uniformly high. The vehicle executes the turn with a constant curvature radius and acceleration begins at the inflection point in the vehicle trajectory.

Zone 4 begins at +3 m with counter-rotations of both gaze and head. At +4 m the difference between gaze and head is again low. The head leads the counter-rotation up to +7 m when the gaze and head begin to counter-rotate together towards straight ahead. At +6 m the

## Chapter 14 - A multi-zone model of expected driver actions in intersections

vehicle starts to counter-rotate to align with road ahead. The counter-rotations, led by the head and gaze, are characteristic of Zone 4, 'completing the turn'.

Zone 5 is straight ahead acceleration. By +11 m the gaze and head are directed straight ahead. By +18 m the vehicle is heading down the new road.

### Scenarios 2 - 6

Similar graphs were constructed and analyses conducted for the other five paths through the intersection (Bjelkemyr, 2009). Driver-vehicle behavior for all six drives can be described using the same set of five zones. The locations of the boundaries between the five zones are listed in Table 14.4.

To illustrate commonalities and differences across traffic scenarios, the analyses are grouped five ways: right turns (scenarios 1 and 2), left turns (3 and 4), straight ahead passes (5 and 6), passes from the primary road to the secondary road (1 and 3), and passes from the secondary road to the primary road (2 and 4). These groupings reveal characteristic sequences of actions that apply across scenarios.

### Right turns (Scenarios 1 and 2)

Scenarios 1 and 2 are both right turns, scenario 1 from the primary to the secondary road and scenario 2 from the secondary road to the primary road. Both sets of heading, gaze and head data are plotted in Figure 14.6. Inspection of the graph reveals few similarities. In scenario 1, the driver looks steadily to the right between -39 m and -9 m. In contrast, at -15 m in scenario 2, the gaze abruptly turns to the left. This leftward look persists until -7 m where it returns to the right. The difference in gaze and head angle widens earlier in scenario 2.

The vehicle begins to turn earlier in scenario 1 which may be explained by a broader lane on the primary road than on the secondary road. The onset of acceleration occurs earlier in scenario 2 than in scenario 1 (not shown). In sum, the sequences of actions are quite different across the two right turns.

### Left turns (scenarios 3 and 4)

The data for the two left turns, scenarios 3 and 4, are shown in Figure 14.7. Scenario 3 is the left turn from the primary road to the secondary road; scenario 4 is the left turn from the secondary road to the primary road. In scenario 3 the driver starts to look to the left at -48 m and continues to look to the left up to -8 m where she turns her head back to straight ahead. In contrast, in scenario 2 the driver looks straight ahead much longer and then turns her head to the right. The first look to the left in scenario 4 is a large excursion at -17 m that is rapidly followed by an excursion to the right and a second to the left.

The vehicle begins the turn earlier in scenario 3 but begins to decelerate earlier in scenario 4. Other than the S-shaped vehicle heading curve that is characteristic of a left turn, the data from the two left turns are remarkably different. Further, it appears that making a left turn generally involves a more complex patterns of gaze and head movements than right turns.

## Chapter 14 - A multi-zone model of expected driver actions in intersections

### **Straight ahead passes (scenarios 5 and 6)**

Scenarios 5 and 6 are straight ahead passes characterized by a relatively constant and near-zero vehicle heading. The difference between these scenarios is the relative position of the secondary road, to the left in scenario 5 and to the right in scenario 6. The data shown in Figure 14.8, reveal that in both scenarios the eyes and head turn to the side with the secondary road between -50 m and -13 m as the vehicle approaches the intersection. This directed look to one and only one side may be explained by the T-shape of the intersection. The driver knew not to expect traffic from the other side.

Common characteristics for these two scenarios are the constant, near-zero vehicle heading, gaze and head angles less than  $22^\circ$ , and the glance to the side with of the secondary road while approaching the intersection. This glance begins and ends earlier than in the turns, suggesting that the driver has finished the intersection task and is satisfied with the results of her actions before the vehicle passes the secondary road.

### **Turns from the primary road to the secondary road (Scenarios 1 and 3)**

Scenarios 1 and 3 are passes from the primary road to the secondary road. The two sets of data are plotted in Figure 14.9. The curves are mirror images indicating that the turns are made in opposite directions. In both scenarios there is a straight ahead look until -41 m where the gaze begins to turn to the side. The eyes and head turn in the same direction as the vehicle heading. The steady look to the side persists through both turns. The only difference between the two data sets is the larger amplitude of the maximum gaze and head angles for the left turn, scenario 3. In sum, the actions taken by the driver in these scenarios are quite similar.

### **Turns from the secondary road to the primary road (Scenarios 2 and 4)**

Similarly, the actions taken while making turns from the secondary road to the primary road have much in common. The relevant data are shown in Figure 14.10. Once again, the shapes of the curves of vehicle heading are mirror images. In both scenarios there is a straight ahead look until -28 m where the gaze turns to the right. In scenario 2 this corresponds to the side of the intended turn but in scenario 4 it corresponds to the opposite side.

The gaze and head movements have similarly large and rapid excursions in both directions. In scenario 4 there are three large excursions between -17 m -11 m. The first is directed to the left and is followed by a rapid changes to the right and again to the left. In this same span in scenario 2, there are two large excursions, first to the left followed by a rapid changes to the right side. As the vehicle exits the intersection, the two scenarios are virtually identical as gaze and head counter-rotate back to straight ahead.

## **Discussion**

### **Characteristic sequences of actions**

The data support the conclusion that there are more similarities across scenarios with the same sequence of road types (e.g., primary to secondary road or secondary to primary road) than there are similarities across scenarios with the same driver intent (e.g., turning right). Turns from the primary road to the secondary road are characterized by similar velocities and acceleration curves. Vehicle headings and gaze and head angles in these two scenarios are

## Chapter 14 - A multi-zone model of expected driver actions in intersections

similar but mirrored. Eye and head movements are in the same directions as is the vehicle heading.

Turns from the secondary road onto the primary road are also characterized by similar velocity and acceleration curves and mirrored curves of vehicle heading. In Zones 2 and 3 the gaze and head angles are characterized by two or more eye and head movements to both the right and left.

This analysis suggests a common model for all intersection crossings with three variants in Zones 2 through 4. The model, shown in Table 14.5, outlines the characteristic sequence of actions that describe driver behavior approaching, entering and exiting an intersection. It is a detailed explanation how we can expect the driver-vehicle system to act in intersections.

### Future work

One limitation of this study is that it is a case study of a single driver. The question of generality across drivers is important and needs to be addressed. A study of driver behavior in intersections that compares several drivers would test the findings in this paper.

A second limitation is selective subset of passes considered. The data reported here were collected during solo drives. Driving through an intersection without traffic is probable less complicated than when there is traffic. This study of driver actions in intersections without traffic provides a baseline for comparison. The logical following step is to analyze how drivers act when there is traffic in the intersection.

A third issue that needs testing is the generality of the model across intersection types. The level of complexity differs across intersections and there are several variables in intersections that could be studied, including traffic and velocity rules, different road user, intersection design, etc.

The first two studies are in progress and will address two questions. The first is whether the model presented here generalizes across drivers and traffic complexity. The second is whether individual differences in driver behavior in different traffic situations are so large that they swamp the signal of characteristic patterns of driver-vehicle behavior that may be useful for developers of traffic safety systems.

### Implications for the design of active safety systems

This semi-naturalistic study of driver behavior in intersections was conducted in a technically advanced instrumented vehicle. Eye-tracking, GPS and camera surveillance are examples of devices in this vehicle that produced useful data about the evolving traffic situation and the driver's anticipation of it and responses to it. A combination of these two types of devices may be considered for the design of active safety systems.

The first type of device defines and may predict where the vehicle is in the world relative to paths through the intersection and other road users, etc. By combining positioning technologies (e.g., GPS systems) with technologies that map the traffic, it may be possible to identify and predict the unfolding traffic situation. This information could be combined with information from other devices that tap how the driver anticipates and responds to traffic situations. The combined information might be compared with expectations specified by the model presented here. Deviations from expectations might be treated as a trigger to an active safety system.



## Chapter 14 - A multi-zone model of expected driver actions in intersections

### References

- Bjelkemyr, A. (2009). Manuscript in preparation for a Licentiate Degree, Chalmers University of Technology.
- Chattington, M., Wilson, M., Ashford, D., & Marple-Horvat, D. E. (2007). Eye-steering coordination in natural driving. Experimental Brain Research, 1-14.
- Fugger, T. F., Wobrock, J. J., Randles, B. C., Stein, A. C., & Whiting, W. C. (2001). Driver characteristics at signal-controlled intersections. (Report no. 2001-01-0045). SAE.
- Helmers, G., & Åberg, L. (1978). Driver behaviour in intersections as related to priority rules and road design. An exploratory study. (Report no. 167). Linköping, Sweden: Swedish Road & Traffic Research Institute (VTI).
- Janssen, W., van der Horst, R., Bakker, P., & ten Broeke, W. (1988). Auto-auto and auto-bicycle interactions in priority situations. In T. Rothgatter, & R. de Bruin (eds.), Road user behaviour: theory and research. (pp. 639-644). Netherlands: Van Gorcum.
- Kulmala, R. (1990). Driver behaviour at urban junctions with the right hand rule. In Draskóczy, M. (Ed.) International cooperation on theories and concepts in traffic safety. (pp. 137-147).
- Land, M. F. (2006). Eye movements and the control of actions in everyday life. Progress in Retinal and Eye Research, 296-324.
- Land, M. F., & Lee, D. N. (1994). Where we look when we steer. Nature, 742-744.
- Ranney, T. A. (1994). Models of driving behaviour: A review of their evolution. Accident Analysis & Prevention, 733-750.
- Robertshaw, K. D., & Wilkie, R. M. (2008). Does gaze influence steering around bend? Journal of Vision, 1-13.
- Sato, T., & Akamatsu, M. (2008). Modeling and prediction of driver preparations for making a right turn based on vehicle velocity and traffic conditions while approaching an intersection. Transportation Research Part F, 242-258.

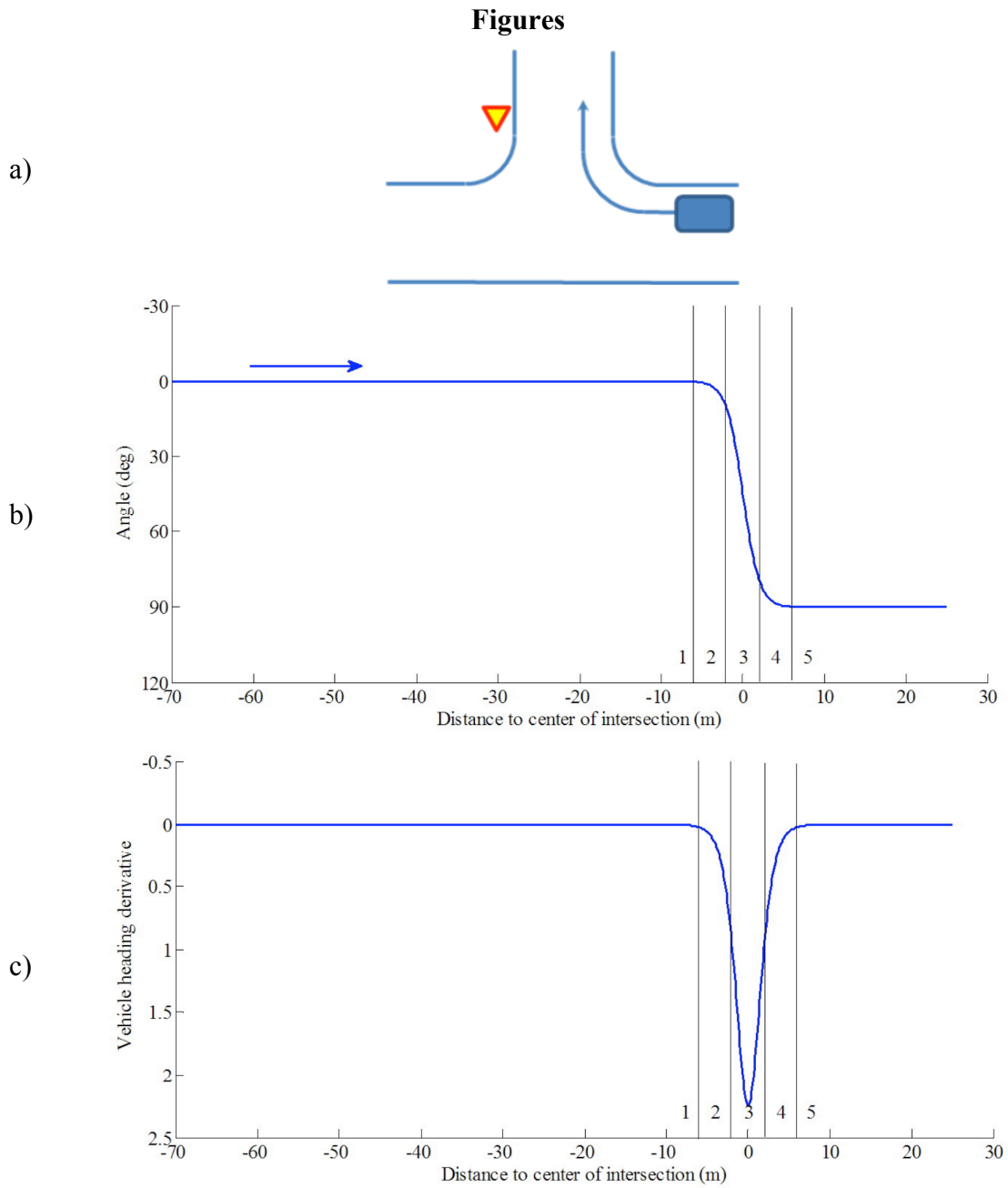


Figure 14.1 (a) Scenario 1, a right turn from the primary road to the secondary road. (b) The corresponding ideal vehicle trajectory, and (c) its derivative.

Chapter 14 - A multi-zone model of expected driver actions in intersections

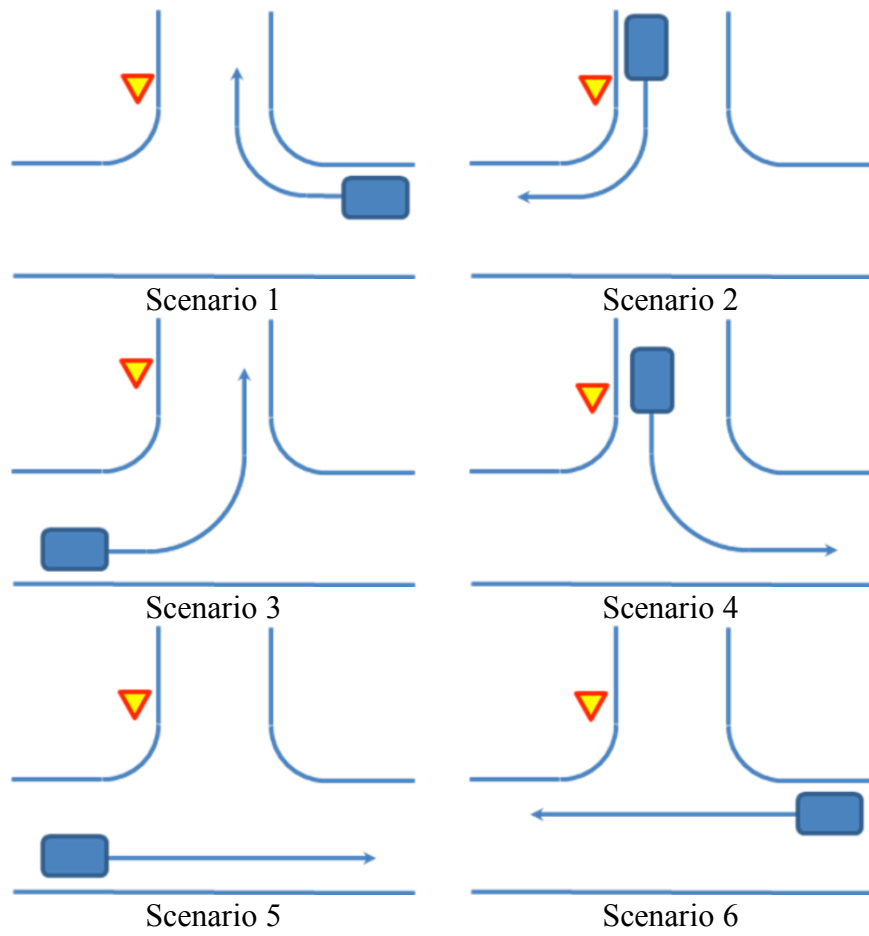


Figure 14.2 The six possible passes through the three-way intersection.

## Chapter 14 - A multi-zone model of expected driver actions in intersections

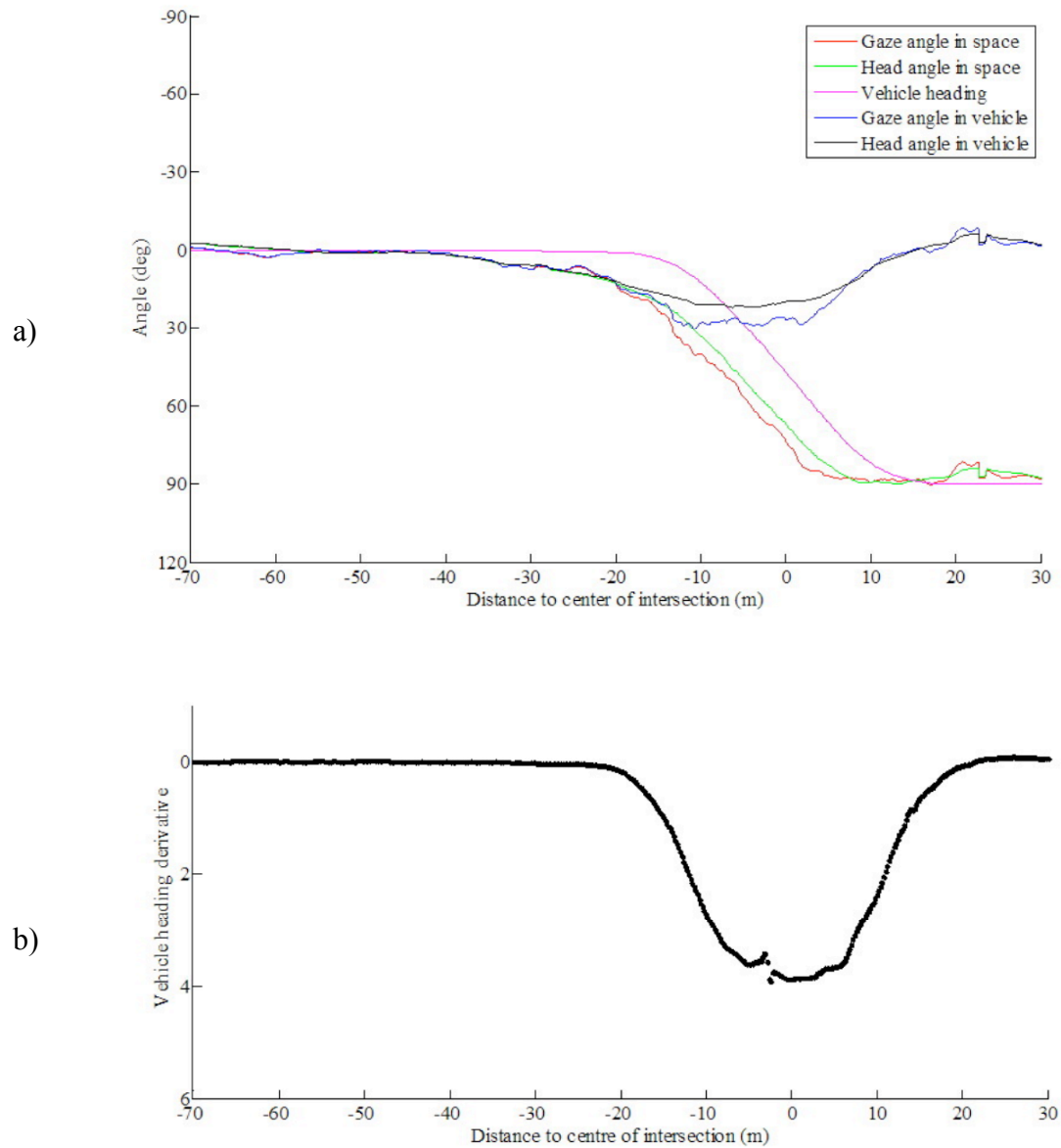


Figure 14.3 Scenario 1 (a) Mean (N=8) values of gaze and head angle and vehicle heading as functions of the distance from the center of the intersection. (b) The derivative of heading.

## Chapter 14 - A multi-zone model of expected driver actions in intersections

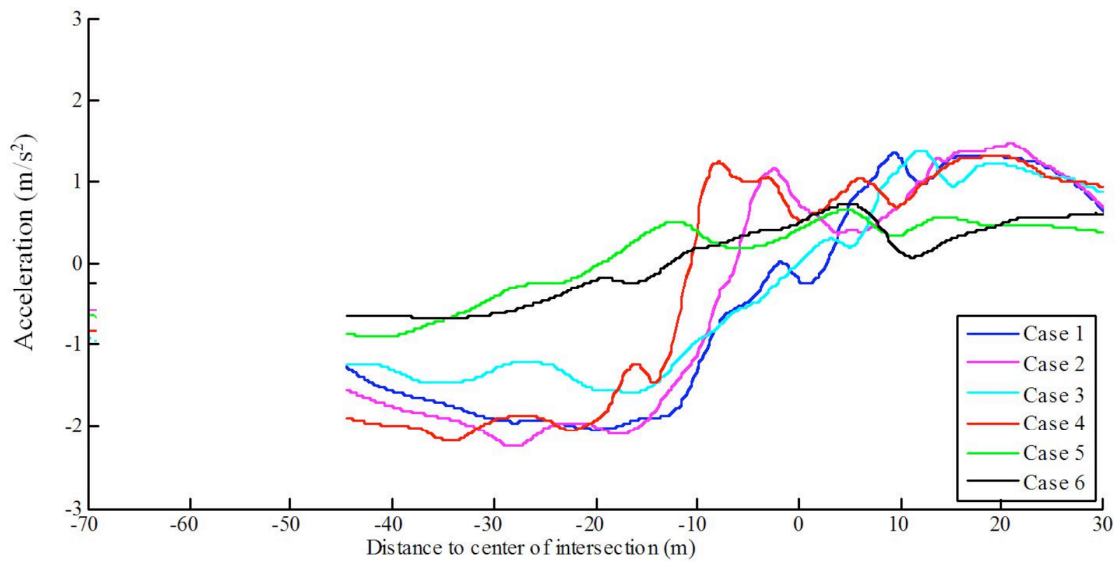


Figure 14.4 Mean values for acceleration for the six scenarios.

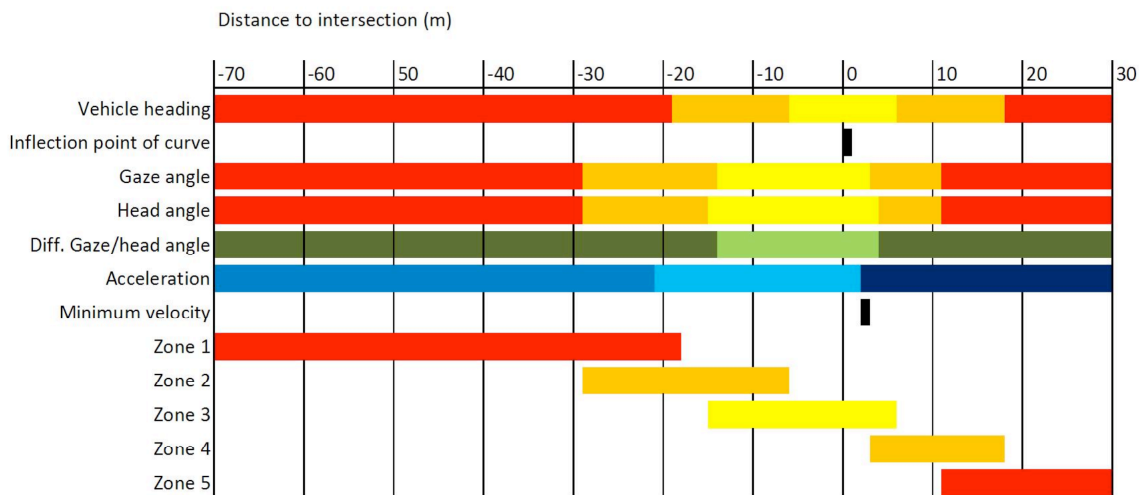


Figure 14.5 The 5 zone model for Scenario 1.

## Chapter 14 - A multi-zone model of expected driver actions in intersections

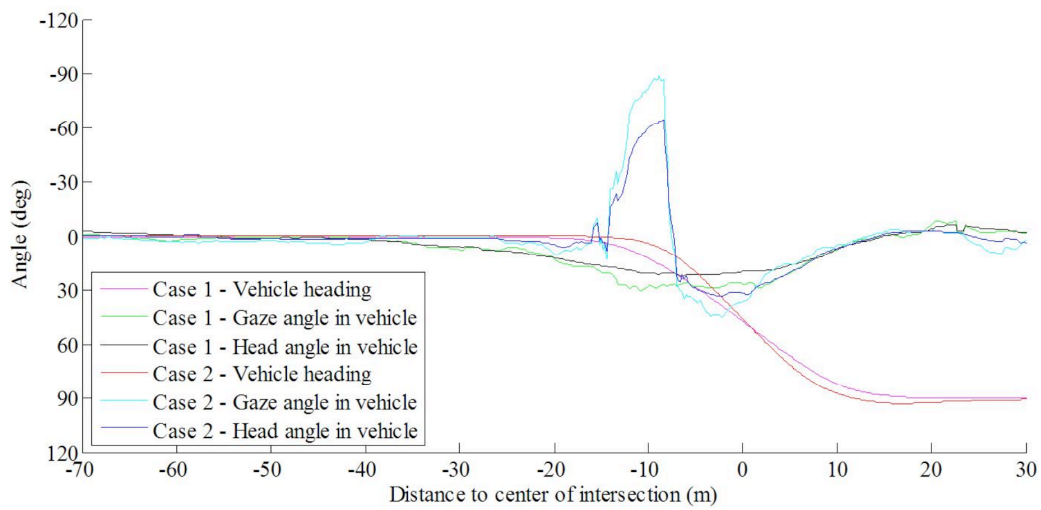


Figure 14.6 Gaze, head, and heading data for Scenarios 1 and 2, right turns

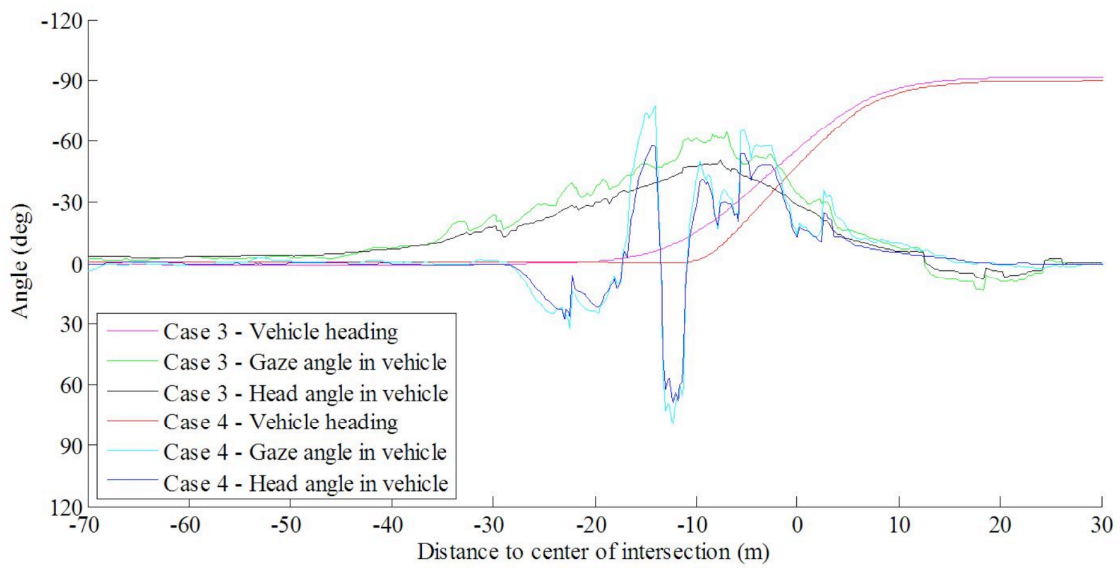


Figure 14.7 Gaze, head, and heading data for Scenarios 3 and 4, left turns

## Chapter 14 - A multi-zone model of expected driver actions in intersections

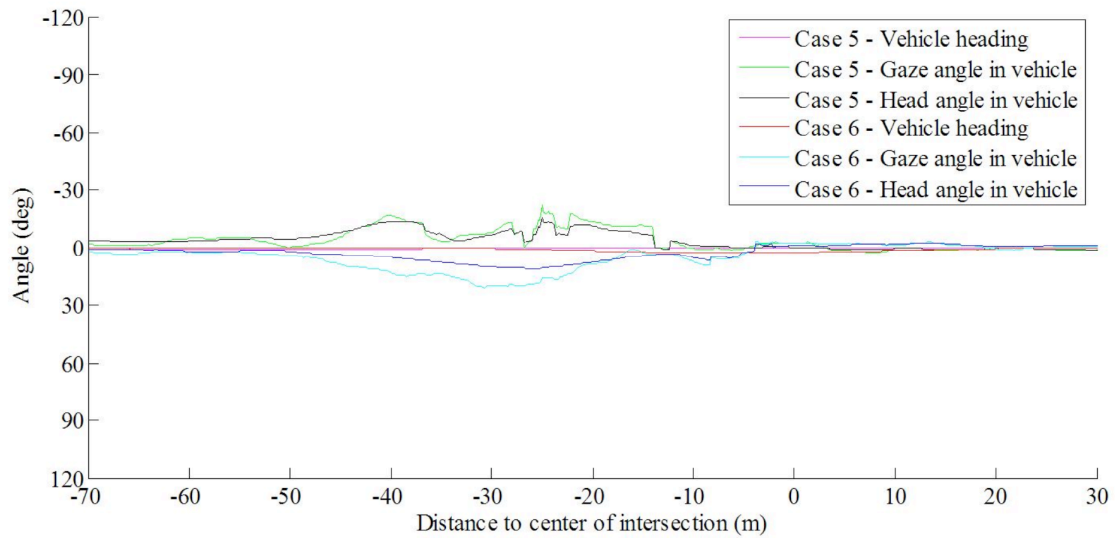


Figure 14.8 Gaze, head, and heading data for Scenarios 5 and 6, straight passes

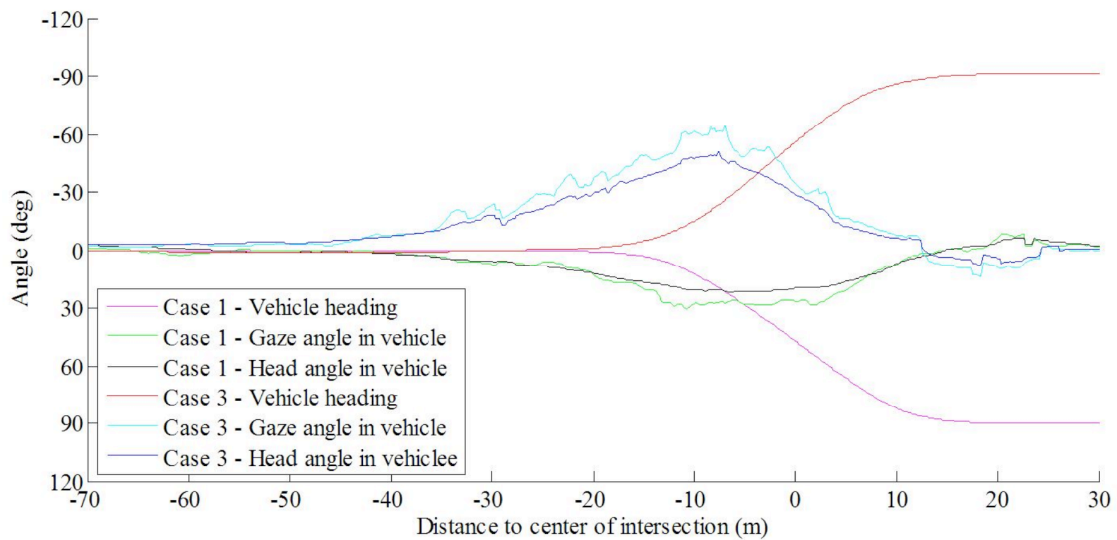


Figure 14.9 Gaze, head, and heading data for Scenarios 1 and 3, turns from the primary road to the secondary road

## Chapter 14 - A multi-zone model of expected driver actions in intersections

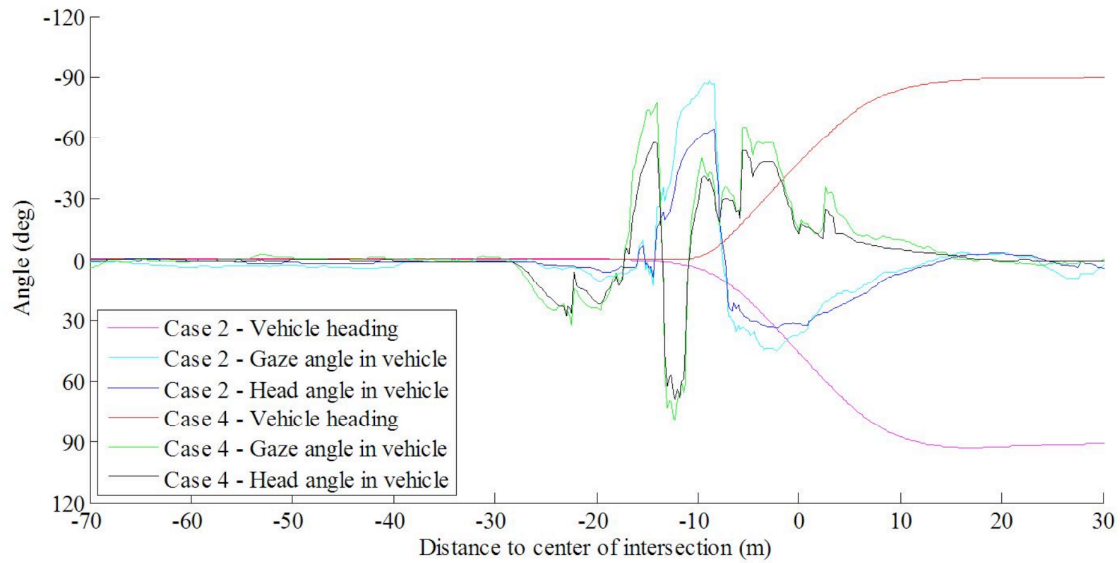


Figure 14.10 Gaze, head, and heading data for Scenarios 2 and 4, turns from the secondary road to the primary road

### Tables

Table 14.1 Characteristics of the six scenarios at the Sävenäs three-way intersection.

Scenario	Pass type	Entering direction	Exiting direction	Priority rule
1	Right turn	East	North	Right of way
2	Right turn	North	West	Give way to 6
3	Left turn	West	North	Give way to 1, 6
4	Left turn	North	East	Give way to 3, 5, 6
5	Straight ahead	West	East	Right of way
6	Straight ahead	East	West	Right of way

Table 14.2 The numbers of drives through the intersection and of solo drives used in the analyses.

Passes	Scenario						Total
	1	2	3	4	5	6	
Driven	30	30	30	30	30	31	181
Solo drives	8	7	9	4	11	13	52



## Chapter 14 - A multi-zone model of expected driver actions in intersections

Table 14.3 Categories of actions and the corresponding rules for scoring the data.

Parameter	Action	Explanatory rule
Vehicle heading, $\theta_{VH}$	Straight ahead entering	Mean $\theta_{-.70 - .50} \pm 1^\circ$
	Increasing turning	$ d\theta /ds$ increasing
	Constant turning	$ d\theta /ds > 90\% * d\theta/ds_{\text{inflection point}}$
	Decreasing turning	$ d\theta /ds$ decreasing
	Straight ahead exiting	Mean $\theta_{+.25 - +30} \pm 1^\circ$
Gaze angle in vehicle, $\theta_G$	Straight ahead eye direction	$0^\circ \pm 5^\circ$
	Gaze rotates to the side	$d \theta_G /ds$ increasing
	Steady gaze to the side	$\theta_G >  \theta_{G\max}  - 5^\circ$
	Gaze movements from one side to another	$\geq 2$ looks in both directions
	Gaze counter-rotates (from the side to the centre)	$d \theta_G /ds$ decreasing
Head angle in vehicle, $\theta_H$	Straight ahead head direction	$0^\circ \pm 5^\circ$
	Head rotates to the side	$d \theta_H /ds$ increasing
	Steady head to the side	$\theta_H >  \theta_{H\max}  - 5^\circ$
	Head movements from one side to another	$\geq 2$ looks in both directions
	Head counter-rotates (from the side to the centre)	$d \theta_H /ds$ decreasing
Diff. gaze/head, $\theta_{\Delta GH}$	Low difference gaze/head angle	No $\theta_{\Delta GH} > 5,5^\circ$
	High difference gaze/head angle	$\theta_{\Delta GH} > 5,5^\circ$
Acceleration, $a$	Increasing or constant deceleration	$a < 0$ and $da/ds \leq 0$
	Decreasing deceleration	$a < 0$ and $da/ds > 0$
	Acceleration	$a > 0$

## Chapter 14 - A multi-zone model of expected driver actions in intersections

Table 14.4 The five zones of characteristic actions for the six scenarios.

Zone	Action	Boundary	Scenario					
			1	2	3	4	5	6
1	Preparing for the intersection	Start (m)	-	-	-	-	-	-
		End (m)	-20	-15	-22	-11	-48	-38
2	Anticipating the turn/pass	Start (m)	-31	-21	-43	-28	-47	-48
		End (m)	-7	-6	-8	-8	-43	-35
3	Making the turn/pass	Start (m)	-15	-7	-12	-9	-44	-38
		End (m)	+5	+2	+1	+1	-20	-20
4	Completing the turn/pass	Start (m)	+3	-1	-7	-3	-21	-23
		End (m)	+17	+15	+18	+15	+5	+8
5	Exiting the intersection	Start (m)	+11	+8	+10	+10	-14	-9
		End (m)	-	-	-	-	-	-

## Chapter 14 - A multi-zone model of expected driver actions in intersections

Table 14.5 Characteristics patterns of driver-vehicle actions approaching, crossing, and exiting and intersection.

Zone	Action	Driver - gaze and head	Vehicle heading
1	Preparing for the intersection	Straight ahead	Straight ahead
2	Anticipating the turn/pass	Primary to secondary: Rotation to side of turn Secondary to primary: Rotation from side to side Straight passes: Rotation toward the secondary road	Turns: Increasing angle Straight passes: Straight ahead
3	Making the turn/pass	Primary to secondary: Constant to side of turn Secondary to primary: Rotation from side to side Straight passes: Rotation toward the secondary road	Constant derivative
4	Completing the turn/pass	Counter-rotation	Turns: Decreasing angle Straight passes: Straight ahead
5	Exiting the intersection	Straight ahead	Straight ahead

## Chapter 15 - The driver's gaze and the monitoring of encroachment

### Introduction

One of the goals of driving is to safely navigate through complex environments. Part of safe passage is the detection and avoidance of encroachment incidents. The field of safe travel is a hypothetical and unspecified construct that nevertheless is aptly descriptive (Gibson and Crooks, 1938). Encroachments are violations of the field. Part of safe passage is the detection and avoidance of encroachment. Indeed, observations of actions taken to avoid encroachment may be the only way to ascertain where a point on the boundary of a driver's field of safe travel was at that time.

In the exercise of safe passage, drivers invoke two complementary modes of control, anticipatory and compensatory (feedforward and feedback control). Anticipatory control is an ongoing cyclic activity (e.g., Neisser, 1976) that invokes a suite of expectancies about objects and events to predict if and when the field of safe travel may be violated and to develop compensatory strategies. Examples of items for which drivers are likely to form expectancies include the flow of traffic, the roadway, the (future) status of traffic signals, the driver's vehicle, and the tracks to be taken by specific other vehicles, among others. In contrast, compensatory control is an episodic activity that kicks in whenever the field of safe travel is compromised. Activities associated with compensatory control include harsh braking, swerving, and frantic acceleration.

Visual search and monitoring the traffic environment are actions that inform both modes of control. The search is done to evaluate the situation and assess it from both an anticipatory and a compensatory control perspective. Is it safe to continue on the current path? Do I need to make an immediate action to avoid a threat? The gaze activity is the scanning of the scene using the eyes and rotation of the head (Land & Lee, 1994). The traffic environment consists of all parts of the environment that are relevant to driving a vehicle. This includes vehicles, pedestrians, bicyclists, as well as road and roadside layout and design. In the development of active safety systems it is important to understand how, when, and why drivers direct their gazes to monitor the traffic environment and the evolving traffic situation.

The scientific aim of this study is to improve our understanding of how drivers direct their gazes in the exercise of anticipatory and compensatory control as they approach and traverse an intersection and how this search is influenced by the presence of traffic. The pragmatic aim of this study is to inform the design and development of active safety systems specifically aimed at enhancing the anticipation of encroachments in intersections and, as a consequence, reducing the need for compensatory actions.

### Visual search while driving

Vision is a driver's main source of information about traffic, the roadway, other vehicles, and most everything else in the scene (e.g., Gibson and Crooks, 1938; Moray, 1990; Walker and Brosnan, 2007). While the cognitive and neurological aspects of vision are complex and beyond the scope of this essay, a basic physiologic constraint drives the patterns of gazes we investigate here. The primary locus of detailed information gathering occurs at a small part of the retina called the fovea. Foveal vision covers only a few degrees of the visual scene. The pick up of information elsewhere on the retina is much less precise. This physical limitation of the eye forces the driver to search the scene in order to gather information relevant to safe passage.

The motion of the eye during visual search is customarily divided into fixations and saccades. A fixation focuses foveal vision on a certain area in a scene. Saccades are the rapid eye

## Chapter 15 - The driver's gaze and the monitoring of encroachment

movements necessary to change the focus of successive fixations. Little of the information that falls on the fovea during a saccade is picked up and acted upon. Indeed, blinks often occur during saccades. A fixation on the other hand can rest on a static object in a static scene or can follow a moving object (smooth pursuit). The time spent fixating on a specific object is called onset duration or dwell time.

The context for most of the research on drivers' vision has been driving on straight roads. As expected, it has been found that the modal direction of a driver's gaze is directly ahead, straight down the road. Deviations from that norm tend to occur when the driver diverts attention to a secondary task or to the sides of the road. Indeed, the issue that drives much of the research on driver vision is the interaction and interference between scans on the scene that serve the goal of safe passage (e.g., eyes on the road) and scans directed at supporting secondary tasks within the vehicle (Caird et. al, 2008).

An issue that is more relevant to this essay is documentation of the strategies drivers adopt for visual search. For example, Victor (2005) identified into two distinct strategies, vision-for-action and vision-for-identification. Vision-for-action is a real time process that handles the immediate interpretation of the surrounding and transforms this into actions. In locomotion it uses precise and absolute positions of yourself and the surrounding as information in the non-conscious vision-action process. In contrast, vision-for-identification is a conscious process, where object identification, classification, and the goals for the vision-for action are set (Goodale and Milner, 2004; Milner and Goodale, 1995). Both vision-for-action and vision-for-identification apply to straight-road-driving, negotiating an intersection, determining the position and (relative) velocity of other vehicles, and assessing the risk for encroachment and other potentially hazardous situations in intersections.

In a departure from the context of straight-road driving, Land and Lee (1996) studied the directions of drivers' heads and gazes relative to the roadway as they negotiated a curve. They found that drivers tend to keep their eyes on the tangent of the curve and not the roadway itself. The study presented in this paper builds upon the methodology of Land and Lee. The participants in our case study are drivers with the right of way as they approach and negotiate an intersection. We study their head motions and the directions of their gazes as a function of the proximity of an intersection to gain insight into how visual search informs their anticipatory and compensatory control. We also briefly investigate brake and accelerator pedal usage as actions coupled to the visual search.

### Previous work on visual search in intersections

A study by Moray (1990) found that drivers can focus effectively on only one object at a time and on no more than three objects per second. Crundall and Underwood (1998) investigated differences in onset durations between novice and experienced drivers. They found that a novice driver has significantly longer onset times than experienced drivers. Theeuwes (1996) used video recordings of drivers approaching an intersection to determine the time they needed to identify static objects (traffic signs) in the traffic scene. He found that signs in expected locations were identified faster than signs in unexpected locations. The time pick up information was a function of both the conspicuity of an object and the driver's expectation for its location. This finding led Theeuwes (1991) to challenge the view that conspicuous objects capture visual attention automatically. He claimed that conspicuous but irrelevant objects if may be ignored, while relevant but less conspicuous may be identified faster.

## Chapter 15 - The driver's gaze and the monitoring of encroachment

### A task analysis of visual search at a non-signalized intersection

In this section we present an analysis of the driver's visual search for information while approaching and crossing a non-signalized intersection with the right-of-way. Driving through an intersection lasts only a few seconds but often requires relatively large head and gaze motions to pick up the elements in the scene that inform the driver's assessment of the situation. The time constraint limits the search to only a few fixations. The goals of the search are to assess the dynamic situation (anticipatory control) and to take adaptive action as necessary (compensatory control). Because the flow of activity will widely across intersections and traffic situations, we restrict our analysis to situations where the driver has the right-of-way and has a limited line-of-sight onto the crossing road.

To pass safely through an intersection, the driver must understand the traffic rules and assess the intentions of other road users. This knowledge informs the inference of whether the others may or may not pose potential hazards. One common hazard is encroachment, defined as the passage of a vehicle across the path of a vehicle that has the right of way. Part of anticipatory control while approaching an intersection is assessing the possibility of an encroachment or other provocation. This assessment is informed by scanning the intersection for oncoming vehicles and judging whether they are likely to encroach. The assessment involves making tacit, heuristic estimates of the other vehicle's distance and velocity and may inform the selection of a compensatory tactics to avoid or mitigate the potential encroachment before the situation becomes critical. A tacit decision must be made to discount the risk or to keep a close watch on the developing situation. Factors that influence the decision include (but are not limited to) familiarity with the intersection, the traffic situation, the appearance of the provoking vehicle, and the assessed severity of the threat. The weights assigned to different factors are likely to differ across drivers but to reflect relatively stable traits for a particular driver. Vehicles (or objects) that a driver judges to be potential hazards are likely to receive additional visual attention until the assessment of their status changes or other vehicles become more salient. When a potential encroachment is detected, compensatory control kicks in, taking action (brake, accelerator pedal or steering angle) to modify the vehicles' dynamics. This unfolding of events is an example of vision-for-action (Victor, 2005).

In an intersection there are several possible encroachments, both merge encroachments and path crossing encroachments. In the merge, the encroaching vehicle enters the same lane as the right of way vehicle, and stays there, while in path crossing the encroaching vehicle passes in front of the right of way vehicle. Collision can occur when the encroaching vehicle occupies the path of the right of way vehicle. In the path crossing encroachment, the encroaching vehicle can either come from the opposite direction (OD), or from a side road on either the left or right (lateral direction, LD). From a visual point of view, the OD case requires very little or no deviation from straight road driving to get the potentially encroaching vehicle in the visual fovea, to be able to identify, classify and assess the vehicles intentions. For the LD cases, depending on the sight-line to the crossing roads, the needed search strategies to assess the situation differ significantly from those used in the OD case. For example, in urban environments with buildings, like the intersection in this study, there is often a limited line of sight. The need for large head and eye movements are significantly greater from in the OD case. In this study the focus is on the intersection situation that differs the most from straight road driving – the lateral direction case in an intersection with a limited line of sight.

In addition to the differences in situation (SD, LD and line of sight), the traffic rules for the specific intersection plays a significant role in the way the intersection is negotiated and how

## Chapter 15 - The driver's gaze and the monitoring of encroachment

other vehicles are likely to act. When a driver has the right of way, there is little need to check and assess if other traffic is going to encroach if it can be assumed that they will all heed the law. In contrast, when a driver does not have the right of way, it is essential to check and assess the traffic situation on the right of way road. The presence of traffic signals reinforces the expectation of rule-following and may relax the need to consider (however tacitly) the likelihood of others crossing against the red light or suddenly swerving into the field of safe travel.

When having the right of way, a limited line-of-sight often precludes monitoring vehicles that might encroach. Because an occluded vehicle could readily trigger an encroachment, a driver with the right-of-way and a limited line-of-sight must make a tacit assessment of the likelihood of that encroachment (take a calculated risk). The assessment invokes expectations about others' propensity to heed traffic laws and experience with the intersection and roadway. The situation and assessment (including visual search) of occluded traffic is likely to be different than that encountered when driving with a clear line-of-sight.

When developing active safety systems and warning strategies, it is important to understand how drivers pick up information and respond to potential threats. Drivers who perceive a vehicle as a potential threat are more likely to accept a warning or indication of the potential provoker. The level of acceptance is likely to rise if the driver has yet to see that the vehicle may encroach. Our approach to assessing how drivers gather information relevant to safe passage through an intersection and to the detection and response to potential encroachments is to measure how and where drivers turn their heads and direct their gazes to look at the crossing road and vehicles on it.

### **Hypotheses regarding the decision about lateral encroachment**

When driving straight through a non-signalized intersection with the right of way, there is a time when the driver makes the tacit decision that the other vehicles are not likely to enter the intersection and provoke an encroachment. In this section we outline hypotheses that link three readily observable metrics and the time that the driver acts upon the decision about lateral encroachment. The first metric is the location where the driver's gaze returns to the roadway ahead. The second is the location where the driver's head returns to the roadway ahead. The calculations are the same as for the gaze, but using head angle instead of gaze angle. The third is the location where the driver puts his foot above or on the brake pedal. We propose that these measures vary systematically with traffic conditions. The reason for including the head as well as the gaze is that head movements are easier to obtain using in-vehicle sensors that are integral parts of an active safety system.

#### Intersection release distance – Gaze

We propose that changes in the direction of the driver's gaze and head provide information about the time when he acts upon the decision about lateral encroachment. This section describes this approach from a gaze perspective, and the next from a head rotation perspective. Our analysis of the task suggests that a driver who is assessing the potential for encroachment searches the crossing roadway for information about the locations and velocities of other vehicles. Gazes and head rotations directed away from the driver's lane and toward the crossing roadway are diagnostic of an ongoing search.

The decision that an encroachment is not imminent is revealed by a shift in gaze/head direction away from the crossing roadway and back to the roadway ahead. By releasing the gaze/head from the crossing road and returning to straight-road driving, the driver reveals that actions associated with intersection negotiation and encroachment assessment have been

## Chapter 15 - The driver's gaze and the monitoring of encroachment

completed. We call the time of this diagnostic transition the 'Intersection Release Time' and the vehicle's position at that time the 'Intersection Release Distance' (IRD). For convenience, we measure the IRD with reference to the center of the intersection. In discussions of detailed analyses, we use notation IRDG for gaze and IRDH for head. In general discussions, we use IRD to refer to both measures.

IRD is determined by the time and place where the driver returns to straight road driving. Accordingly, we define straight road driving as occurring when the horizontal component of gaze falls within  $\pm 10$  degrees of the modal direction of the driver's gaze (Victor, 2005, pp 35).

We use IRD as our metric for the diagnostic transition in gaze/head direction for two reasons. First, future in-vehicle systems can reasonably be expected to be able to estimate IRD continuously and precisely. Second, we use distance instead of time because estimates of the time to the center of the intersection require untenable assumptions about the constancy of velocity.

'Baseline IRD' is defined during 'solo' passes through the intersection, that is, by the driver's pattern of gazes/head rotations when there is no crossing traffic. We propose that the dwell time of a driver's gaze and head rotation on the crossing road will be longer when there is a vehicle on the crossing road than in the baseline case. It is possible that the dwell time will be longer yet when the driver judges that the vehicle may be on a track consistent with an encroachment. These extended dwell times can be captured by an in-vehicle camera and the distance to the center of the intersection captured from GPS data. The prediction is that the IRD will be closer to the center of the intersection when a vehicle is present on the crossing road than when it is not. Equation 15.1 formalizes this one-sided hypothesis; the inequality represents 'is closer to the center of the intersection.'

$$\text{IRD}_{\text{other vehicle}} < \text{IRD}_{\text{baseline}} \quad 15.1$$

This study considers only cases where the vehicle with the potential to encroach was waiting on the crossing road and yielding the right of way to the participant's vehicle. The reason for this choice was to eliminate moving vehicles that are a potential source of individual differences in the assessment of time/distance/velocity.

Reformulated, the main hypothesis is that drivers with the right of way will return their gaze/head back to straight road driving closer to the intersection center if a vehicle is yielding than if no vehicle is present on the crossing road. This is formalized in equation 15.2.

$$\text{IRD}_{\text{yielding vehicle}} < \text{IRD}_{\text{baseline}} \quad 15.2$$

It is also reasonable to expect that many drivers may never direct their gaze/head far down the crossing road while making a solo pass through an intersection. These 'no-look' passes may reveal distraction or complacency or experience that supports the judgment that encroachment is unlikely. Whatever the reason for not looking, these drivers' pattern of gazes will remain on the road ahead and the IRD will be undefined. We treat passes with an undefined IRD as an end-member of a continuum and bin them in the  $\text{IRD}_{\text{no vehicle}}$  category.

### Intersection release distance - Head

Head rotation is a slower process than using the eyes to conduct a search. However, head rotation is activated automatically for searches that require horizontal rotations greater than  $\pm 15$  degrees from straight ahead driving (Victor, 2005). The interaction between head and eyes are complex and will not be investigated further in this essay. For a detailed discussion, see Land and Lee (1994).



## Chapter 15 - The driver's gaze and the monitoring of encroachment

In this study we test and show results using two alternative thresholds for horizontal head rotations believed to be diagnostic of straight ahead driving,  $\pm 10$  degrees, the same as for gaze, and  $\pm 6$  degrees. Both of these thresholds are centered around mode of the drivers head rotation.

### Brake readiness

Brake readiness is a third measure that may be informative about the driver's assessment of the level of threat in a situation. Moving the foot from the accelerator pedal to the brake pedal can be viewed as diagnostic of anticipatory control – preparation for actions to intervene in a potentially threatening situation. At an intersection, this action could either slow the vehicle down to increase the available time to react or prepare for a potential need to brake. The time when the decision is made to move the foot away from the brake pedal and back to the accelerator pedal can be viewed as the time when the driver reverts to straight ahead driving.

We measure brake pedal usage as a function of distance to the center of the intersection. In this study, brake readiness is defined as having any part of the foot over (within 60mm) or on the brake pedal. A binary classification of on-brake-pedal and off-brake-pedal is used. We define the 'Brake Readiness Release Distance' (BRRD) as the point where the driver makes the last transition away from the brake pedal before 5 m past the intersection center.

In the same way as for IRD, it would be anticipated that the BRRD for the case with a waiting/yielding vehicle on the crossing road would be closer to the intersection, compared with the case of no vehicle on the crossing road. This line of reasoning motivates equation 15.3, a one-sided hypothesis; the inequality represents 'is closer to the center of the intersection.'

$$\text{BRRD}_{\text{yielding vehicle}} < \text{BRRD}_{\text{baseline}} \quad 15.3$$

The BRRD is independent measure of the IRD and could be used by in-vehicle systems alone or together with the IRD. In on-market vehicles today, neither eye trackers or pedal proximity sensors are commonly available, but the information about brake pedal activity (indicating when brake pedal is depressed) is available in many vehicles already. The two measures could be used in a sensor fusion approach.

### **Logic**

To test these hypotheses we conducted a quasi-experiment. We observed and recorded the gazes, head rotation and brake usage by 11 drivers, as they repeatedly drove through the Sävenäs and Jung intersections. We systematically varied the drivers' route through the intersections but had no control over the presence or actions of traffic. Accordingly, the positions, velocities and headings of other vehicles are organismic variables.

To simplify the analyses and to test our methodology, we restricted our study to situations where the driver had the right-of-way and to two traffic scenarios: the baseline case with no crossing vehicles and the yielding case where a single vehicle was waiting at the intersection on the right-side crossing road. We also culled the data to eliminate four suspected sources of variability unrelated to our goal of understanding driver actions in the face of encroachment. First, we removed from the data set all traffic situations that included pedestrians and other vulnerable road users. Second, we dropped all cases in which the driver was following another vehicle into the intersection. Third, we considered only drives made between 09:00 and 15:00 to avoid rush hour traffic. Finally, we eliminated cases with a moving vehicle approaching the intersection to avoid having to evaluate individual differences in the assessment of the relationship between time, distance, and velocity. In ongoing work we have

## Chapter 15 - The driver's gaze and the monitoring of encroachment

relaxed these restrictions and are evaluating the influence of pedestrians and approaching vehicles on our metrics of the monitoring of encroachment.

### Method

#### Drivers

Ten volunteers drove a test vehicle repeatedly through an intersection that was equipped with an infrastructure-based vehicle tracking system. Of the 10 drivers, two were singled out for the detailed analysis presented here (drivers 1 and 3). Driver 1 drove in Sävenäs and driver 2 drove in Jung. The other 8 drivers drove at Sävenäs.

Driver 1 was a 33 year old female with 16 yrs of driving experience who drives 25,000 km per year. She was a PhD. student part working on a different part of the IVSS project. Driver 2 was a 35-yr old male with 18 years of driving experience who drives 20,000 km per year and is an employee of one of the partners in the project. The additional 9 drivers drove significantly less than drivers 1 and 2. They were primarily graduate students from the Universities involved in the project. All drivers were remunerated for their time and knew that intersection driving was the focus of the study. They were, however, blind to the research questions or hypotheses being addressed in this paper.

#### Task and setting

The main location of the study was the intersection at Sävenäs, 5 km east of Göteborg, Sweden. A to-scale sketch of the intersection is shown in Figure 15.1. While technically a four-way intersection, the southern roadway ends immediately in a private, industrial-area parking lot. Traffic into and out of the lot is rare. Accordingly, we treat the intersection as a three-way 'T' with 6 possible tracks, Figure 15.2. The one and only track that we consider here is shown with the bold arrow in Figure 15.1. Traffic from the east and west have the right-of-way. The road from the north has a yield sign. The primary traffic flow is from the north (a residential neighborhood) to the west (toward Göteborg) and the return from west to north.

The second location was a rural 4-way, 70 km/h intersection on the E20 near Jung, 130 km northeast of Göteborg. A to-scale sketch of the intersection is shown in Figure 15.3. The bold arrows in Figure 15.3 show the directions of the traffic with the right of way on the E20 (and the two paths taken repeatedly by driver 2).

Driver 1 crossed the Sävenäs intersection from a total of 180 times, taking each of the 6 possible tracks 30 times. The tours were driven in 1.5 hour sets, two sets per day, over three days. Prior to these tours, driver 1 had driven the test vehicle through the intersection more than 50 times to become familiar with the vehicle, the intersection, and the traffic. Her instructions were to follow a specific sequences of crossings.

Driver 2 made one 2.5-hour tour of the Jung intersection. His instructions were to obtain as many crossings as possible by driving back and forth on the right of way road. Driver 2 made a total of 71 passes through the intersection.

#### Apparatus

The study used two independent sources of data that were synchronized in time. The first data source was an instrumented test vehicle equipped with a non-obtrusive eye tracking

## Chapter 15 - The driver's gaze and the monitoring of encroachment

system (SmartEye Pro), roof-mounted video cameras, an internal-bus capturing system, and inertial navigation sensors. All data were time-stamped with millisecond accuracy using a GPS-based time stamping card (Hopf).

The second source is the infrastructure-based vehicle tracking system described in Chapter 3. On-site equipment consisted of a video camera mounted 20 m above the southwest corner of the Sävenäs intersection. The image capture rate was 20 Hz and was time stamped using a GPS time synchronization card. The off-site portion of the tracking system applied image processing algorithms to extract vehicle trajectories from the 2D image pixel coordinates of the video files. The trajectory data uses the Swedish National Grid to record the locations on the road directly below the center of the vehicle at 20 Hz. The trajectory data also specify the positions and velocities of all vehicles in the intersection as functions of the time and distance to the center of the intersection. The Jung installation consisted of 4-cameras, but in all other aspects the setup was the same as for Sävenäs.

Synchronizing the trajectories from the image-processing system with the time-stamped data from the test vehicle makes it possible to classify the traffic situation encountered by the test vehicle each time it approached and passed through the intersection.

As a backup system, a sensor fusion algorithm was implemented to extract the position (velocity, etc.) of the test vehicle during periods of GPS data dropouts. The algorithm used a fiber optic gyro, and the internal-bus velocity and acceleration sensors. This implementation is explained by Ardeshiri et. al. (2005).

### Procedure

#### Synchronizing trajectories

Both data sets contain considerably more data than were used in this study. The test vehicle records the entire driving tour. The video cameras record continuously during daylight hours. The time stamping of each both data sets made it possible to extract from both data sets those periods covering the 100 m before and 100 m after the test vehicle crossed the center of the intersection. Because the Jung intersection is much larger and the cameras had clear lines of sight, the distance was increased to 300 m at Jung.

#### Dependant variables

The data extracted for analysis were gaze direction, head direction and position, brake readiness and use, vehicle location, heading, yaw rate, acceleration and velocity. All data except for GPS information was extracted relative to the vehicle coordinate system.

In addition, the image processing system provided the trajectories of all other vehicles that were in the intersection during the period when the test vehicle was present. The result was a complete description of the positions, headings, and velocities of all vehicles in the vicinity while the test vehicle crossed the intersection.

#### Gazes and time

Commercial software and hardware (SmartEye Pro) captured images at 60 Hz and calculated measures of the driver's head and eye position and motion. The calculations are based on a face/head model from the four cameras, together with user-marked features of the face and head prior to the test. The main measures used here are head and gaze direction. Both gaze and head directions are defined relative to the vehicle coordinate system with straight ahead driving set at 0 degrees. Only the horizontal component of the gaze and head information from the eye tracker was used. A low pass 13-point median filter was used to remove noise in

## Chapter 15 - The driver's gaze and the monitoring of encroachment

the gaze data (Victor, 2005). The accuracy of the system is  $\pm 3^\circ$  centrally and approximately  $\pm 6^\circ$ ,  $90^\circ$  of center.

The gaze data were used to find the time when and the distance where the driver released his or her gaze/head from the intersection to the road ahead (IRT and IRD, respectively) for each pass through the intersection. The baseline IRD is defined during 'solo' passes through the intersection, that is, by the driver's pattern of gazes and head rotations when there was no traffic on the road to the right. 'Yielding IRD' is defined during passes when a vehicle on the road to the right appears to be yielding the right-of-way.

### Brake readiness

A proximity sensor was mounted on both the brake and accelerator pedal. The sensor used a light source and a photo sensor (integrated in the same sensing unit with the size of about 10mm) and produced a binary signal if an object came within 60mm of the sensor (in the direction of the emitted light). The sensors were mounted on the side of the pedal closest to the other pedal (brake/accelerator). Foot proximity data were synchronized with the gaze and head data with an accuracy of 50 ms.

## Results

### Driver 1

Driver 1 crossed the intersection from east to west a total of 31 times. Of these 31, 20 were identified by the image processing system as baseline cases and 4 as yielding cases. We omit the other 7 cases as they all contained vehicles moving on the right crossing road or vulnerable road users that would introduce uncontrollable sources of variance in the analyses.

### Intersection release distance - Gaze

To test whether the presence of a yielding vehicle influenced the distance where Driver 1 reverted to straight ahead driving, we counted the number of cases in two bins, greater than or less than 15 meters. The two bins and the IRDGs for the 22 cases with defined IRDGs are shown in Figure 15.4. Of the 20 baseline cases, 3 had IRDG values less than 15 m, 15 had IRDG values greater than 15 m, and 2 had undefined IRDs (and are plotted at 0 meters). In the two undefined cases, the driver never appears to gaze at the crossing road. The undefined cases can be viewed as an infinitely high IRD, thus, these are included in the greater than 15 m bin. Of the 4 yielding cases, 3 had IRDG less than 15 m and only 1 greater than 15 m. The Fisher Exact Test found a significant difference between these distributions,  $F = 0.98$ ,  $p < .05$ . Thus the presence of a yielding vehicle appears to strongly influence when Driver 1 returned her gaze to the road ahead.

### Focal distance of gazes on the crossing road

To ascertain how far down the road Driver 1 looked, we extracted the last 25 gaze angle data points (approximately 400 ms) prior to the IRDG for each of the 22 cases where Driver 1 looked down the crossing road. These data form the line segments shown in the upper graph of Figure 15.5. The horizontal axis is the distance to the intersection. The vertical axis is the gaze angle. Each segment has a flat top and then drops off. The drop represents the decision to move the eyes back on the road, while the flat top represents keeping the eyes on the crossing road. A slowly increasing value instead of a flat top would be expected if the driver adjusted the gaze to get as much view of the crossing road as possible. Such a pattern would be diagnostic of a smooth pursuit "around" a static object.

## Chapter 15 - The driver's gaze and the monitoring of encroachment

The fact that all segments contain flat tops rather than sloped tops could indicate that the time is too short for a smooth pursuit (<400 ms). The small X's in the upper graph of Figure 15.5 highlight the maximum value of the gaze angle during these 400 ms. They define the 'Maximum Gaze Before IRDG' (MGBIRDG). MGBIRDG increases as a function of proximity to intersection. This may reveal the driver's line-of-sight onto the crossing road. That is, the closer to the intersection, the further "around the corner" the driver can see. This produces a steadily increasing MGBIRDG.

The lower graph in Figure 15.5 shows the projections of the gaze angles at the points highlighted by the X's in the upper graph. The vertical axis represents distance down the road rather than gaze angle from the test vehicle. The distances were determined by projecting the driver's gaze onto the crossing road, with the gaze angle and the distance from the intersection at MGBIRDG. The projected distances cluster between 15 and 20 m. This finding suggests that Driver 1 considers vehicles further away than 15-20m on the crossing road (in this particular intersection) to be relatively unimportant or unthreatening. The distance down the road of the gazes is independent of the IRD.

### Expected velocity of traffic

The distance data of Figure 15.5 represent the distance down the side road that the driver looks to detect potential encroachment. By combining this distance with the velocity of the driver's vehicle, we can estimate how fast a vehicle at that distance on the side road would have to go to produce a crash with the test vehicle. This velocity is an estimate of Driver 1's expectation for the velocity of the traffic she sought to avoid. The calculation is shown in equation 15.4.

$$V_{OV\_MGBIRDG} = D_{OV\_MGBIRDG} * V_{SV\_MGBIRDG} / D_{SV\_MGBIRDG} \quad 15.4$$

Where  $V_{OV\_MGBIRDG}$  is the velocity needed for a vehicle on the side road to create a crash if both were to continue on their current paths and velocities,  $D_{OV\_MGBIRDG}$  is the distance of driver 1's vehicle to the intersection at MGBIRDG,  $V_{SV\_MGBIRDG}$  is the velocity of driver 1's vehicle, and  $D_{SV\_MGBIRDG}$  is the distance to the intersection center for the vehicle on the side road at MGBIRDG.

Figure 15.6 is a graph showing the  $V_{OV\_MGBIRDG}$ , the velocity needed for a vehicle on the side road to create a crash. These velocities are all less than 40 kph, the average velocity taken by driver 1 through the intersection. This suggests that driver 1 expects traffic on the side road to be slowing and yielding as it approaches the intersection. Thus, the analyses support an inference about a fundamental assumption the driver makes when monitoring encroachment.

### Intersection release distance – Head

Initially the IRDH was run with a 10 deg threshold. The results of this analysis are shown in Figure 15.7. Of the 20 baseline cases, 4 had IRDH values less than 15 m, 7 had IRDH values greater than 15 m, and 8 had undefined IRDHs. In the undefined cases, the driver never appears to gaze at the crossing road. Of the four yielding cases, one was undefined and three had IRDH less than 15m. None were greater than 15 m. Due to the large number of undefined cases and the fact that for small gaze angles, no head movement is necessary, a lower threshold, 6°, was adopted. The results with this threshold are shown in Figure 15.8. There is only one undefined case rather than 8. The Fisher Exact Test found no significant difference between these distributions. It appears that head angle and a bin threshold of 15 meters do not discriminate the presence of yielding vehicles.

## Chapter 15 - The driver's gaze and the monitoring of encroachment

### Brake readiness

Data for Brake Readiness Release Distance (BRRD) are shown in Figure 15.9. The results of the analysis of BRRD show no significant differences between cases with and without a yielding vehicle. In 10 of the 20 drives with no other vehicle, the driver never moved her foot to the brake readiness position as she approached and crossed the intersection. In these cases, she kept her foot on the accelerator pedal (or at least not above the brake pedal). In the 10 cases where BRRD can be calculated, the values are clustered 15-30 m from the intersection. This clustering is similar to the IRDG values shown in Figure 15.4. For the four drives with yielding/waiting vehicles, in one case the driver never prepared to brake, one BRRD was below the 15 m threshold and two were above it. Thus, the presence of a yielding vehicle does not appear to influence the direction and timing of driver 1's BRRD. The findings suggest that the BRRD metric can be a diagnostic measure if and only if the driver reliably moves the foot in the presence of a yielding vehicle.

### **Driver 2**

A second driver drove repeatedly through the Jung intersection. The IRDG values for the 25 no-other-vehicle cases are shown in Figure 15.10. Of these 25, 13 were below the 30m IRDG bin threshold and 12 above. Of the five waiting cases, 4 were below 30m and 1 above. The Fisher Exact Test found no significant difference between these distributions.

The corresponding IRDH data are shown in Figure 15.11. Of the 26 no-other-vehicle cases, 15 were above 30m, 4 below, and 7 were undefined. For the yielding cases, 1 was below 30m, and 4 were above. Once again, the Fisher Exact Test did not find significant differences between these distributions.

### **Other drivers**

Drivers 3 through 10 made a total of 21 passes though the Sävenäs intersection. The IRDG data are plotted in Figure 15.12 and the IRDH data in Figure 15.13. Of 18 no-other-vehicle cases, 2 were undefined, 5 were greater than 15 meters and 11 less than 15 meters. Three cases had yielding vehicles and 1 was undefined. One of the yielding cases was greater than 15 meters and one less. The Fisher Exact Test did not find significant difference between these distributions.

## **Discussion**

This study focused on driver actions when approaching an intersection with right of way. It presents evidence of the sequence of actions is a function of the context (e.g., the presence of other vehicles).

At Sävenäs the IRDG was diagnostic of the presence of yielding traffic. At Jung it was not. This difference may reveal contextual factors that influence the need the direct the gaze toward the side road. The Jung intersection is in a rural setting with a completely clear field of view. The driver rarely decides not to look for crossing traffic, In contrast, at the urban and smaller Sävenäs intersection, the field of view is partially occluded and the driver had to look to ascertain whether their was traffic on the side road.

Neither the IRDH or BRRD proved to be useful metrics at either the Sävenäs or Jung intersections. However, the similarities between the BRRD and the IRDs (for driver 1)

## Chapter 15 - The driver's gaze and the monitoring of encroachment

indicates that about the time of the last check of a potentially crossing vehicle on the road, the driver also tended to move from brake readiness to straight ahead driving. The convergence of results suggests that the BRRD might be a useful complement to the IRDG in a fused sensor application.

All metrics used in this study were calculated post-hoc, since the distance to intersection center is based on the vehicle trajectory. For an active safety application, this should be changed to relative position to the intersection, and probably relative to a store map of the specific intersection layout. The intersection release distance could then be used in a real time implementation and thus used directly in an active safety system.

One potential challenge to the design of the study is the use of the same driver to make many passes through the same intersection. Like all case studies, it is vulnerable to critiques of irreproducibility and lack of generality. Our motive here is more to test the utility of a novel method and metrics than to define driver behavior at the two intersections.

This method has the potential to be applied on a wider scale. There are several projects currently ongoing where infrastructure vehicle tracking is being used or will be used. Conducting studies with highly instrumented test vehicles through these intersections could potentially generate quantitative insights into the use of gaze for anticipatory and compensatory control while negotiating intersections. A follow up study could focus on the influence of the location and velocity of vehicles on the side road.

For active safety applications this research could be interesting in several ways. One aspect is the cues that drivers use to assess the intent of other drivers and their potential for encroachment when the distance between vehicles precludes eye contact. In these situations, the assessment of the other driver's intent has to be made using information about vehicle dynamics and location in the intersection. These data should be possible to acquire using sufficiently sophisticated sensors and high-resolution map information. The task would then be to apply research like this to identify the cues used by drivers to assess the likelihood of encroachment.

### References

Ardeshiri, T., Kharrazi, S., Sjöberg, J., Bärgran, J., & Lidberg, M. (2005). Sensor fusion for vehicle positioning: Intersection active safety applications. *8th International Symposium on Advanced Vehicle Control*. Taipei: Taiwan.

Caird, J., Willness, C., Steel P., Scialfa, Chip., (2008). A meta-analysis of the effects of cell phones on driver performance. *Accident analysis and prevention*. 40 (4), 1282-93.

Crundall, D.E., & Underwood, G. (1998). Effects of experience and processing demands on visual information acquisition in drivers. *Ergonomics* 41 (4), 448 – 458

Fletcher, L., Loy, .G., Barnes, N., & Zelinsky, A. (2005). Correlating driver gaze with the road scene for driver assistance systems. *Robotics and Autonomous Systems* 52, 71-84

Gibson, J. J. & Crooks, L. E. (1938). A theoretical field-analysis of automobile driving. *The American Journal of Psychology*, 51 (3).

Goodale, M.A. and Milner M.D. (2004). *Sight unseen: An exploration of conscious and unconscious vision*. Oxford: Oxford University Press.

Hopf, 6039 GPS, hopf Elektronik GmbH, Nottebohmstr. 41, D-58511 Lüdenscheid

Neisser, U. (1976). *Cognition and reality*. New York, Freeman

## Chapter 15 - The driver's gaze and the monitoring of encroachment

Land M.F. & Lee, D.N.. (1994). Where we look when we steer. *Nature* 369, 742-744

Milner, M D and Goodale, M A. (1995) *The visual brain in action*, Oxford, Oxford University Press

Moray, N. (1990). Designing for transportation safety in the light of perception, attention and mental models. *Ergonomics* 33, 1201-1213.

Theeuwes, J. (1996). Visual search at intersections: An eye movement analysis. *Vision in Vehicles*.

Victor, T. (2005). *Keeping eye and mind on the road*. Ph. Dissertation, Uppsala Universitet

Walker, I. & Brosnan, M. (2007). Drivers' gaze fixations during judgement about bicyclist's intentions. *Transportation Research F*, 90-98



Figures



Figure 15.1 The Sävenäs intersection with driving direction of test vehicle

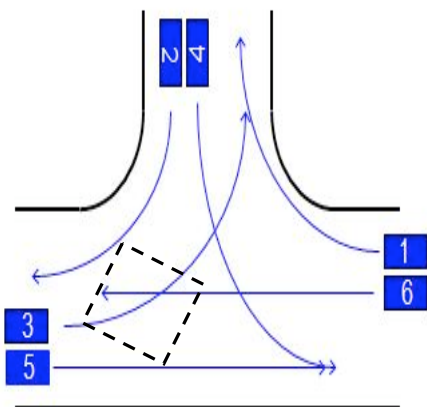


Figure 15.2 The 6 possible tracks through the Sävenäs intersection with driving direction of test vehicle (full arrow) and the potential waiting vehicle cases (dashed box)

## Chapter 15 - The driver's gaze and the monitoring of encroachment



Figure 15.3: The Jung intersection with the directions of travel of the test vehicle in the cases analyzed with respect to Intersection Release Distance.

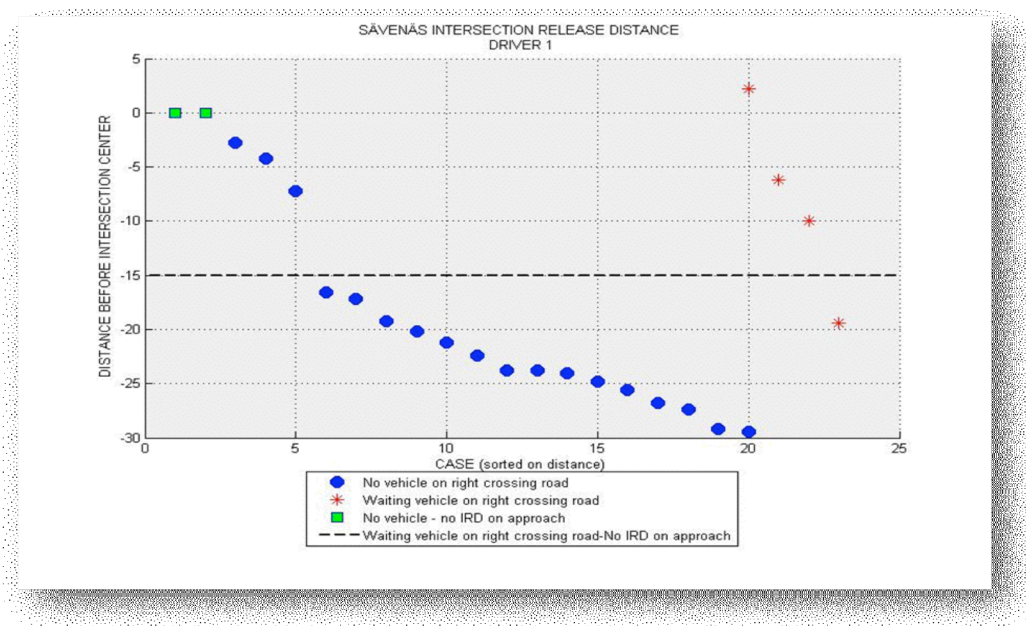


Figure 15.4: Intersection Release Distance (gaze) for driver 1. A total of 24 passes.

## Chapter 15 - The driver's gaze and the monitoring of encroachment

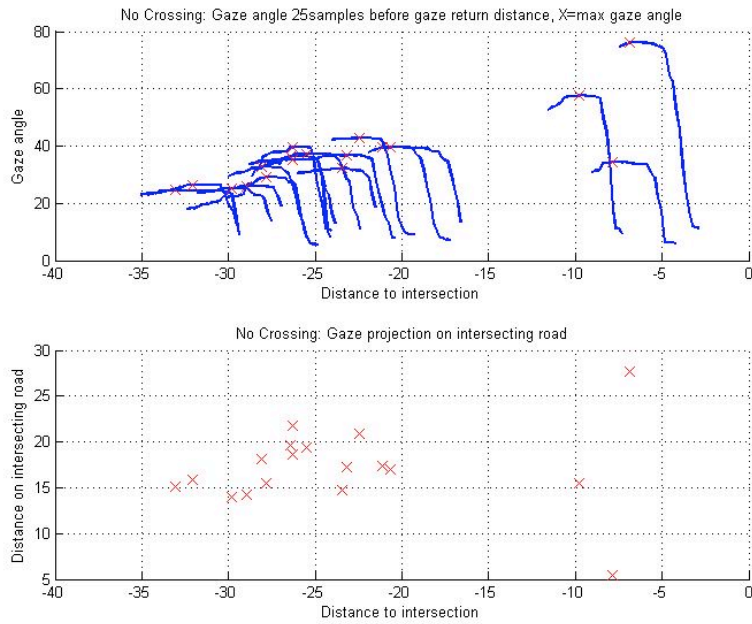


Figure 15.5: Top: Gaze angle 25 samples before IRD with the maximum marked with an X. Bottom: The projection of the angle at the maximums in the top graph onto the crossing roads. That is, how far down the road did the driver look at the maximum point closest to the intersection. Driver 1.

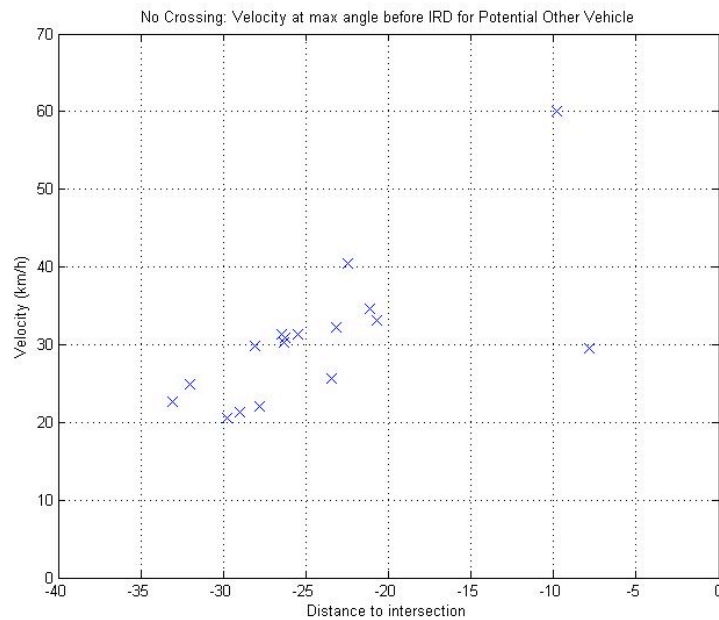


Figure 15.6: Needed velocity of other vehicle to create a crash, at the positions of maximum gazing onto crossing road.

## Chapter 15 - The driver's gaze and the monitoring of encroachment

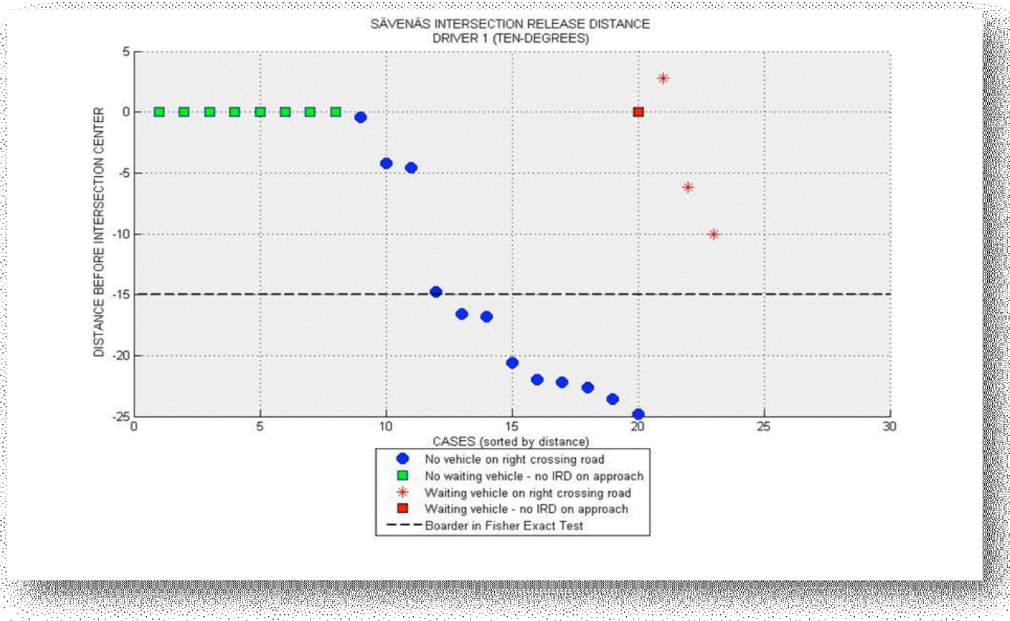


Figure 15.7: Intersection Release Distance (head) for driver 1 calculated with head rotation instead of gaze as raw data. Using 10 deg threshold.

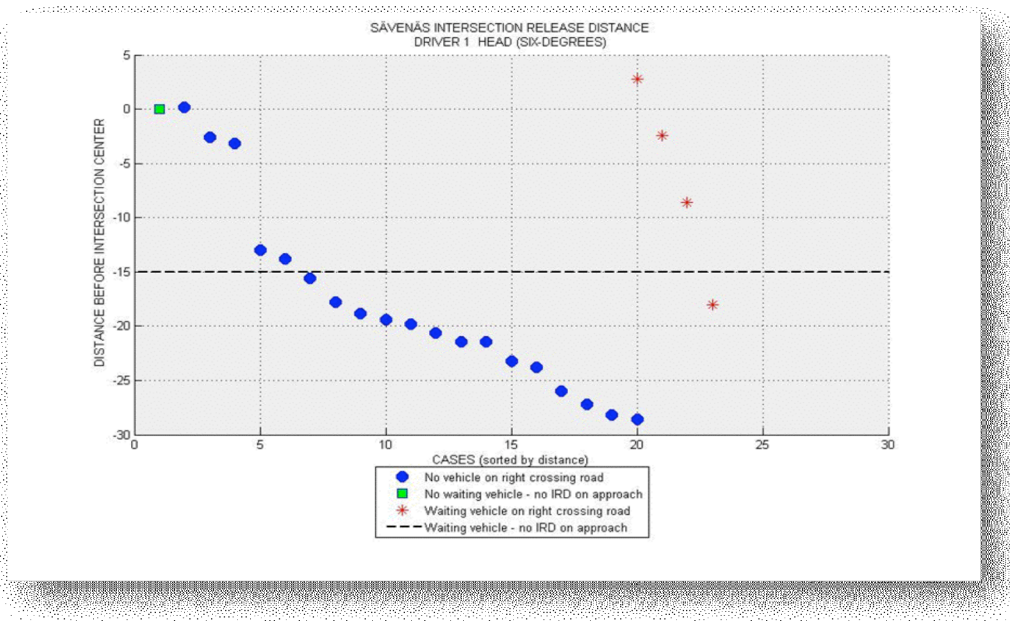


Figure 15.8: Intersection Release Distance (head) for driver 1 calculated with head rotation instead of gaze as raw data. Using 6 deg threshold.



## Chapter 15 - The driver's gaze and the monitoring of encroachment

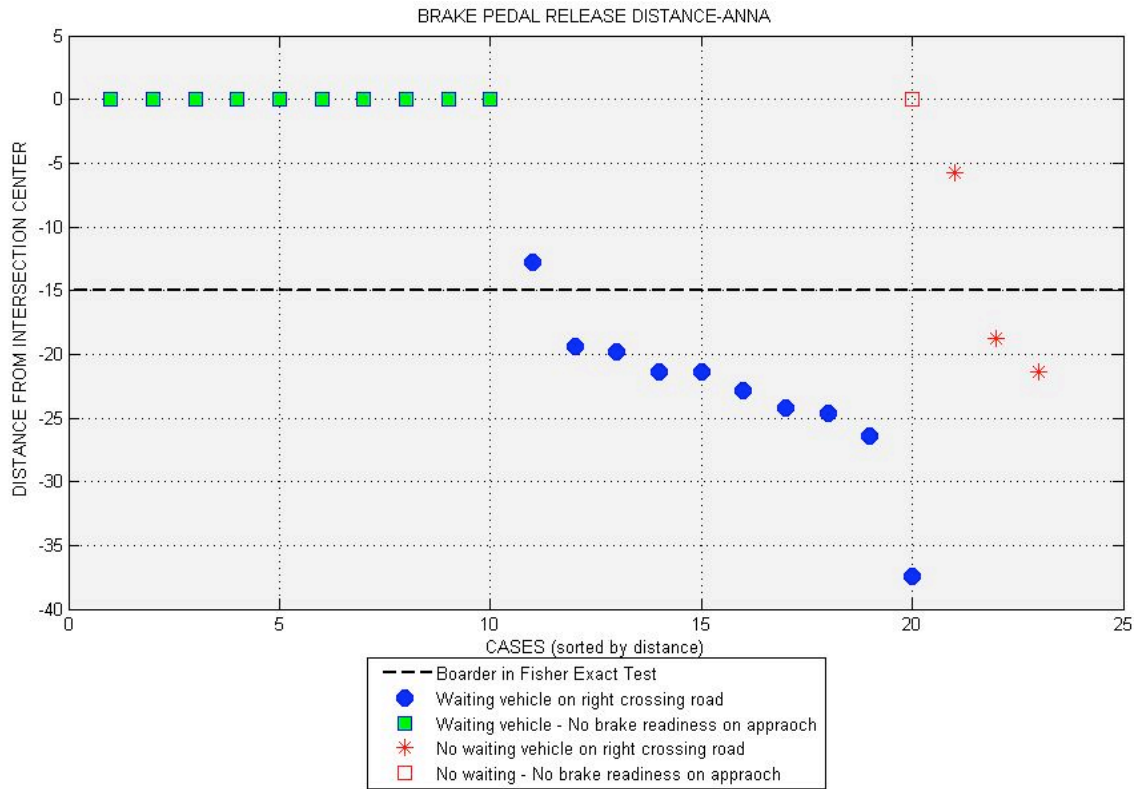


Figure 15.9: Brake pedal release distance (BPRD) for driver 1.

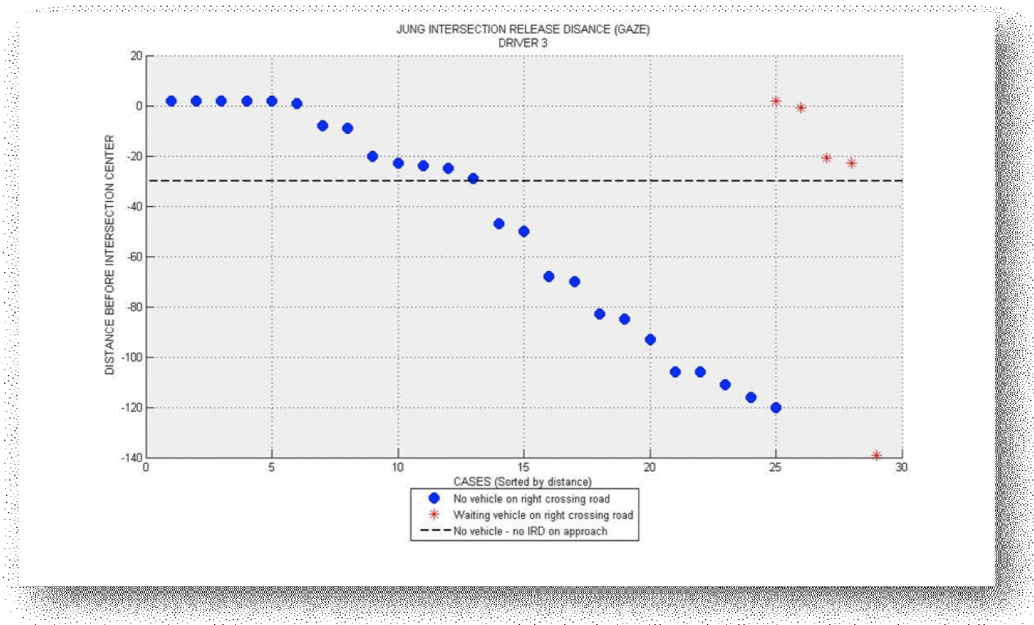


Figure 15.10: Intersection Release Distance (gaze) for driver 2 in the Jung intersection.

## Chapter 15 - The driver's gaze and the monitoring of encroachment

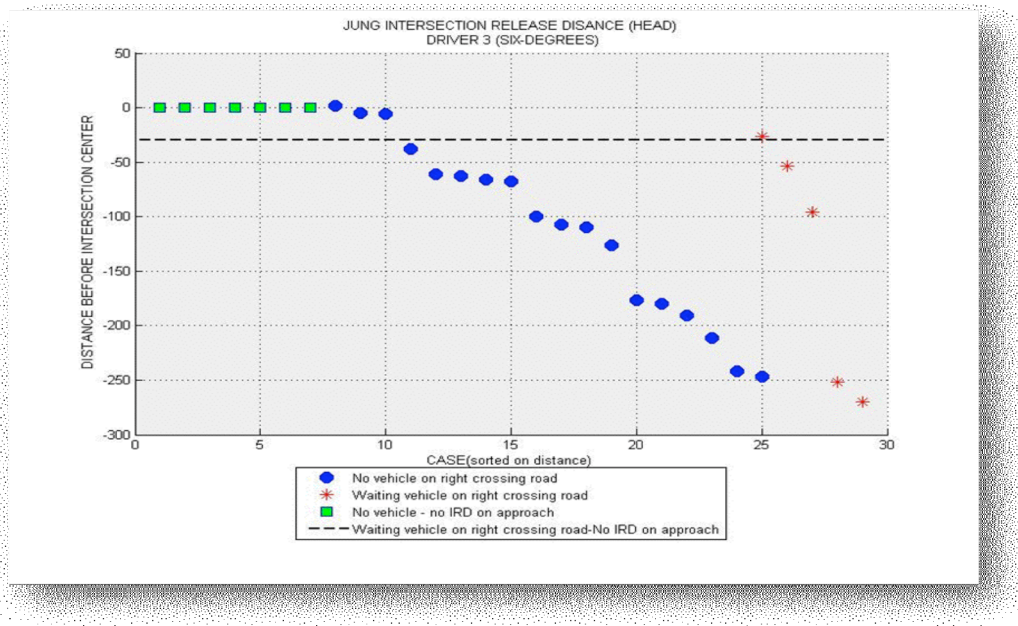


Figure 15.11: Intersection Release Distance (head) for driver 2 in the Sävenäs intersection.

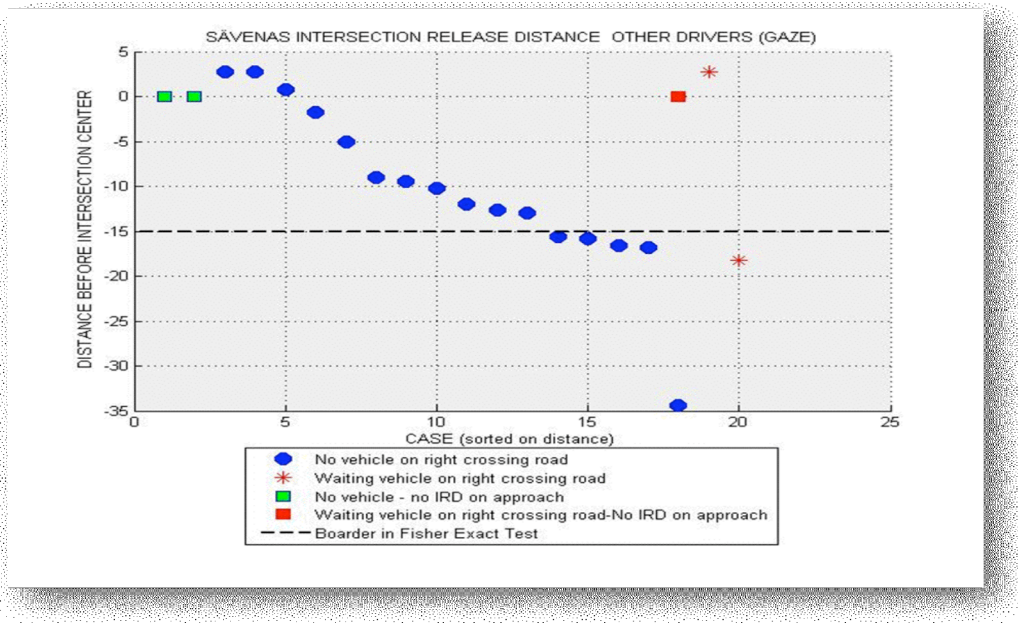


Figure 15.12: Intersection Release Distance (gaze) for 8 drivers in the Sävenäs intersection.

## Chapter 15 - The driver's gaze and the monitoring of encroachment

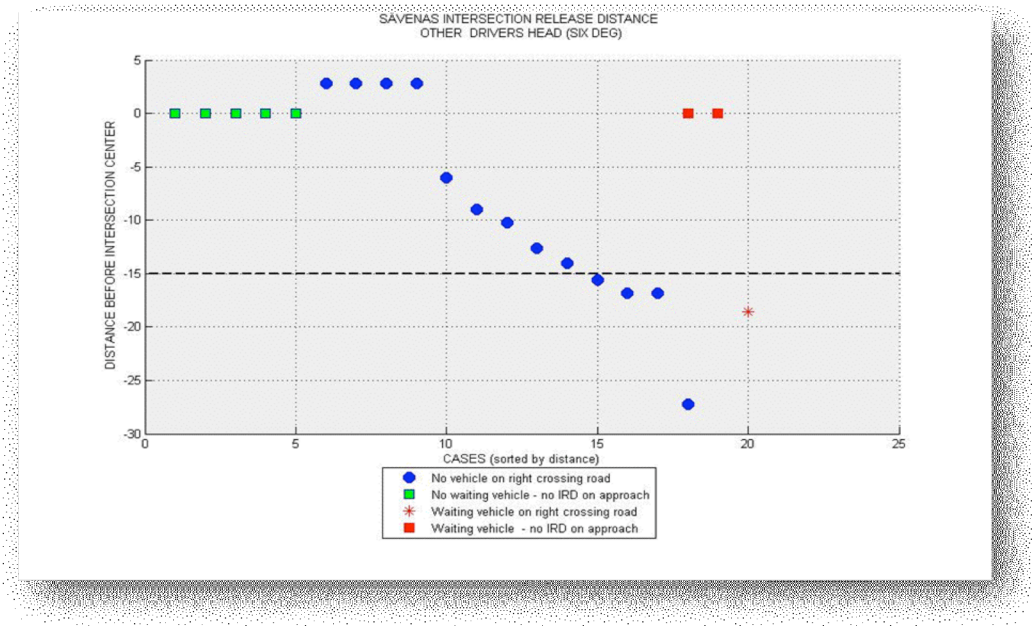


Figure 15.13: Intersection Release Distance (head, 6degrees) for 8 drivers in the Sävenäs intersection.

## **Chapter 16 - Synthesis of results that may inform the design of active safety systems**

### **Introduction**

The mission of the IVSS Intersection project has been to develop an understanding of driver actions and behavior in intersection situations and to contribute to the future of the Swedish automotive industry. The focus has been on encroachments - situations where one car crosses the path of another that has the right of way - and its metric, post-encroachment time (PET). The aim has been to develop guidelines that could be used to inform the design and development of active safety systems that issue alerts to impending encroachment or directly intervene (e.g., auto-braking) or both.

This chapter summarizes many of the findings in the context of active safety system development and design specification. The first section highlights a key finding - the contextual dependence of driver behavior in intersections. The context is largely defined by factors that differ across traffic scenarios. The second section presents a preliminary template for the functionality for an active safety system tailored for intersections. The template highlights schemata associated with traffic scenarios. The third section relates our findings to the draft template of system functionality. The final section develops tables that we offer as guidelines for setting system parameters that designers may choose to consider when developing active safety systems.

### **Disclaimer**

The material in this chapter is offered as a possible source of guidelines for the specification of system functionality. By no means is it intended to be interpreted as a description of how an active safety system should be designed. Further, this chapter is not an attempt to compile all the results from this project - the chapters discussing the data and results contain vastly more information for system developers to consider.

A final note of caution concerns the generality of the results. The project obtained data at only two intersections, Sävenäs and Jung. Traffic at these intersection may or may not be truly representative of intersections at large. The data set is limited in many ways, e.g., the elimination of large trucks from the analyses. Logical directions for future work include testing the generality of the results reported here at a wider variety of intersections, considering all road users, and studying several intersections of the same kind.

### **Contextual factors that may inform the design of active safety systems**

The project has identified three different types of contextual information about driver behavior at intersections that could be critical in the design of active safety systems.

#### **Identification of traffic scenarios**

Several of the chapters have pointed out the influence of traffic scenarios on drivers' behavior and on how they are likely (a) to respond to an encroachment and (b) to welcome an alert from an active safety system when experiencing encroachment. Key factors that appear to influence driver expectations, behavior, and the welcomeness of an alert include, but are not necessarily limited to:

- The location and number of other vehicles
- The apparent intent (e.g., the path to be taken, yielding) of the drivers of those vehicles
- Whether or not the driver has the right of way



## Chapter 16 - Synthesis of results that may inform the design of active safety systems

- The base rate of the traffic scenario

We believe that systems will be better accepted by drivers if they behave as drivers expect them to. Designers of some active safety systems may find a need to adapt system behavior to take these and other contextual factors into account.

### Velocity as a function of traffic scenarios

In several traffic scenarios at both Sävenäs and Jung, the average velocity was influenced by the number of other vehicles in the intersection. Velocities were different on solo drives, when only one other car was present and when multiple cars were present. These findings suggest that it may be beneficial for an active safety to take into account information about the number and distribution of other vehicles and their expected velocity profiles. The practicality of doing so is beyond the scope of this project.

### Frequency of encroachments as a function of scenarios

The data from both Sävenäs and Jung identified trajectories that had relatively little traffic but a disproportionate frequency of encroachment. If this finding were to generalize, it would appear that paths that are rarely traveled may be preferential loci for encroachment. If so, the design of active safety systems might benefit from incorporating information about the base-rate of traffic scenarios and encroachments in intersections.

## A template for active safety system functionality

### System functionality

In this section we characterize a set of functions that might be performed by active safety systems designed to (a) detect impending encroachments and to (b) decide whether or not to issue an alert or intervention. Our purpose here is to illustrate the complexity and variety of the factors that must be considered during the design and development of such systems. The template is not presented as and should not be interpreted as the specification of a product. It may be incomplete or may not be operational. It is, however, a template for evaluating and synthesizing the results of the IVSS Intersections project.

We assume that active safety systems for encroachment in intersections may possess the following functionality:

- 1) Sensors identify the locations and velocities of traffic, the presence of static objects, and the driver's intended path through the intersection.
- 2) The sensor data is linked to stored information about the intersection geometry, layout, and the rules of the road.
- 3) The system feeds this information to an automated traffic classification scheme that specifies the traffic scenario for the impending passage through the intersection. The traffic scenario is (linked to) an information-rich schema for expectations and actions.
- 4) The schema provides the traffic context - expectations for locations and velocities of other vehicles, for how the event will unfold, and for the factors that are likely to influence the driver's acceptance of an alert or intervention.
- 5) The system monitors traffic for deviations from the expected locations and velocities of other vehicles.

## Chapter 16 - Synthesis of results that may inform the design of active safety systems

- 6) The system monitors the driver for deviations from the expected patterns of control actions.
- 7) The system applies an algorithm that fuses the multiple streams of information and compares them to expectations.
- 8) The system issues an alert or intervention if and only if the data fail to adhere to expectations and the driver is likely to accept it.

### The relevance of our work to the template

- 1) The first of the functions - using sensor data to identify the locations and velocities of traffic and the presence of static objects - was explicitly excluded from the scope of the project. However, our experience with the test vehicle provided insights into the limitations and capabilities of current technology. The primary source of data about traffic in this study was infrastructure-mounted cameras and a post-processing by an image processing system that extracted vehicle trajectories (Chapter 3).
- 2) Sensor fusion was not part of the project. However, we found commercially available navigation maps for in-vehicle use to be insufficiently accurate for reliable guidance in the intersections we studied. We had to gather the data ourselves in order to characterize the geometry and layout of the intersections and the rules of the road (Chapter 2).
- 3) The geometric traffic scenario method appears to be robust (Chapters 4, 5, 6, 9, 13). In this study we used the method to classify the different ways that drivers interact in intersections. The classification system could readily be extended to incorporate information about how drivers expect the scenario to unfold.
- 4) Among the expectations to be associated with the schema linked to a traffic scenario are
  - its relative frequency (Chapter 6),
  - the velocity profiles of the driver's car and the other cars (Chapter 6, 9, 13),
  - the likelihood of encroachment (Chapter 7),
  - the 50/50% point for encroachment (Chapter 8),
  - the distance at which most drivers would welcome an alert to encroachment (Chapter 11), and
  - the intersection release distance (Chapter 15).
- 5) The system continuously monitors the unfolding of the traffic situation and the driver's actions for deviations from expected patterns (Chapter 8).
- 6) The system monitors the driver's actions for evidence of deviations from expected patterns (Chapters 14, 15).
- 7) The system applies an algorithm that fuses the multiple streams of information and compares them to contextually sensitive thresholds (Chapters 7, 8, 10, 11, 12, 14, 15). This type of algorithm will likely be developed as proprietary work by industry partners and is beyond the scope of the project.
- 8) The system issues an alert or intervention if and only if the data are over (or under) the thresholds and the driver is likely to accept it. The design of the human-machine interface and the decision algorithm will also be proprietary work by industry partners and is beyond the scope of the project.

## **Chapter 16 - Synthesis of results that may inform the design of active safety systems**

### **Specific results that can be used for preliminary specification of system parameters**

The findings presented in this report can be used to establish preliminary boundary conditions on the specifications of sensing systems and decision algorithms for active safety systems for intersections. These conditions could be applied to systems designed to issue warnings to the driver of (a) the vehicle with the right of way or (b) the provoker. To facilitate presentation, only the LTAP/OD and the LTAP/LD scenarios are covered here. The chapters provide data that support similar analysis of other scenarios.

Table 16.1 lists four sources of information that could inform system design. Tables 16.2 and 16.3 list the values of the corresponding boundary conditions for Sävenäs and Jung, respectively. The tables differentiate between sources of information relevant to drivers with the right of way and to provokers. Entries in the tables are times and distances presented in this report and do not take into account the additional time (and distance) needed for the detection, identification, and tracking of objects by a sensing system or for driver-in-the-loop responses. The four sources of information are discussed in turn.

### **Probability of PET < 5%**

Throughout this study, PET has been our principal metric for quantifying encroachment. Unfortunately, PET is a post-hoc measure and cannot be used directly in an active safety system. As a result, information about expected PET values, etc., will have to be modified in active system design to become a more predictive measure. It is not within the scope of this project to define that measure or to develop the requisite information fusion and decision algorithms.

The PET analyses found that encroachments are unexpectedly common but that short values of PET are rare. The entries in Row 1 of Tables 16.2 and 16.3 are the PET values that define the 5% tail at the low end of the cumulative distribution functions of PET for LTAP/OD and LTAP/LD at Sävenäs and Jung. We expect that these limits define encroachments for which most drivers would likely accept an alert from an active safety system.

### **Buffer distances**

The simulator studies with human confederates and automatic provokers (Chapter 10) yielded a set of PET times and distances that are the levels to which the drivers adjusted their velocity and approach strategy. These values could be considered buffers in distance/time - the 'comfort zone' - below which the drivers may feel uncomfortable with an encroaching vehicle. Below the values shown in Row 2, the encroachment is just too close for the driver with the right of way.

### **Ratings of the welcomeness of warnings**

The simulator study at SAAB, Chapter 11, revealed the times and distances at which drivers would welcome a hypothetical warning to encroachment. The modality and nature of the warnings were not specified. Such specification is beyond the scope of this project. We offer the values shown in Row 3 of the tables as starting points for the initial design of warning systems.

## Chapter 16 - Synthesis of results that may inform the design of active safety systems

### Go/No-Go decisions

The Go/No-Go analysis of the image processing data generated a set of sigmoid distributions representing the percentage of drivers who decided (not) to encroach at a range of times and distances for four left-turn-across-path scenarios. The data presented in Row 4 of the tables corresponds to the points where 50% of potential provokers decided (not) to encroach on a driver with the right of way.

In addition to the decision times, the distance between the vehicles at time of PET calculation was extracted. This corresponds to the distance between the vehicles when the provoker has just left the critical PET-encroachment area.

### Tables

Table 16.1 Examples of measures found in this project that can be used implicitly or explicitly for active safety system design.

	<b>Chapter</b>	<b>Right Of Way</b>	<b>Provoker</b>
1	7	5% tail on PET	
2	10	Buffer distances	
3	11	50/50 points for ratings of welcomeness of warnings as a function of PET.	50/50 points for ratings of welcomeness of warnings as a function of PET.
4	8		Go/No-Go decision boundaries (50/50 points), and resulting minimum critical separations.

## Chapter 16 - Synthesis of results that may inform the design of active safety systems

Table 16.2 Numerical values for the fields in Table 16.1 for the Sävenäs intersection

	<b>Chapter</b>	<b>Right Of Way</b>	<b>Provoker</b>
1	7	LTAP/OD 1.10 s 15.2 m LTAP/LD 1.15 s 16.0 m	
2	10	LTAP/OD 2.32 s 32.2 m LTAP/LD 1.99 s 27.6 m	
3	11	LTAP/OD 1.51 s 21.0 m LTAP/LD 1.40 s 19.4 m	LTAP/OD 0.90 s 12.4 m LTAP/LD 1.31 s 18.2 m
4	8		LTAP/OD 4.75 s 54.5 m Min. separation 57.7 m LTAP/LD 5.93 s 69.2 m Min. separation 55.5 m

Table 16.3 Numerical values for the fields in Table 16.1 for the Jung intersection

	<b>Chapter</b>	<b>Right Of Way</b>	<b>Provoker</b>
1	7	LTAP/OD 2.70 s 52.5 m LTAP/LD 2.91 s 56.6 m	
2	10	-	
3	11	-	-
4	8		LTAP/OD 5.6 s 125 m Min. separation 144 m LTAP/LD 6.3 s 130 m Min. separation 131 m



**CHALMERS**

**Linköping University**

